UNIVERSITY OF CALIFORNIA

Lawrence Berkeley Laboratory
Berkeley, California

DEVELOPMENT OF A FEASIBLE PROCESS FOR THE SIMULTANEOUS REMOVAL OF NITROGEN OXIDES AND SULFUR OXIDES FROM FOSSIL FUEL BURNING POWER PLANTS.

David T. Clay* and Scott Lynn

Energy and Environment Division
Lawrence Berkeley Laboratory
and
Department of Chemical Engineering
University of California, Berkeley

June 1974

* PhD Thesis

TO

Glenda whose love, encouragement and assistance is entwined throughout this work.

ACKNOWLEDGEMENTS

This Dissertation is more than a record of the work of one individual on a specific problem. Many different inputs were given during its progression. Each of these greatly aided the author by providing new insight into the problem. Professor Lynn provided many practical suggestions and very effective guidance throughout the course of the project. Professors King and Sawyer contributed significantly in the project review and evaluation sessions. Discussions with Derk Vermeer and Stuart Simpson were helpful in dealing with day to day problems.

I am indebted to the staff at Lawrence Berkeley Laboratory for the help in the production of this thesis. I wish to especially thank Ms. Ruth Lewis and Mrs. Evelyn Grant for their efforts in this regard.

Financial support for the author was received from the National Science Foundation, the Environmental Protection Agency, the Department of Chemical Engineering, and the Lawrence Berkeley Laboratory during the course of this work.

Development of a Feasible Process for the Simultaneous Removal of Nitrogen Oxides and Sulfur Oxides from Fossil Fuel Burning Power Plants.

ABSTRACT

David T. Clay* and Scott Lynn

A dry solids process has been developed for the simultaneous removal of NO and SO_2 from power plant stack gases. A catalyst/absorbent in a net reducing flue gas effects the removal of SO_2 by absorption as ferrous sulfide or sulfate and the removal of NO by reduction to nitrogen or ammonia. The solid is regenerable; reaction with air produces a rich stream of SO_2 and ferric oxide. The SO_2 may be converted to saleable H_2SO_4 and the solid is recycled to the process.

The process is capable of greater than 90% removal of SO_2 and NO. The emissions of H_2, CO, and NH_3 are well below acceptable emissions levels. The concentration of the solids in the effluent stream is not significantly increased over normal flyash levels. There is no significant increase in the quantity of solids which must be disposed of. No flue gas cooling or reheating is required. There are no large storage vessels or slurry transport lines within the process. The regeneration process is thermally self-sufficient.

Experiments in a flow-through fixed-bed reactor between 370-540°C have confirmed that the process reactions are feasible. Known

* PhD Thesis

calculational techniques were used to extrapolate the fixed-bed rate data to dispersed-phase contactor conditions. The rapid rates result in a relatively short contact time for the highly dilute dispersed-phase contactor. Similar experimental and calculational techniques were used to confirm that regeneration would be feasible at 680°C in a fluidized bed.

An economic analysis of the process for a 1000-Mw coal-fired power plant showed that it is quite competitive with currently existing wet-scrubbing processes which remove only SO_2. The process costs, including the H_2SO_4 plant, are $18.5/kw for the capital investment and 0.91 mills/kw-hr for the operating cost, with no credit taken for the H_2SO_4.

TABLE OF CONTENTS

Chapter I. Introduction and Background — Page

A. Problem Statement . . . 1

B. Objectives

1. Foreseeable government regulations on emission levels of NO_x and SO_x must be met . . . 2
2. No other type of pollution problem should be created by installation of the process . . . 4
3. The removal mechanism for one component should not depend upon the presence or absence of the other . . . 5
4. Furnace operation should be independent of the process operation . . . 5
5. The process should be adaptable to both new and existing power plants . . . 6
6. The economics should be an improvement over the best currently known processes . . . 7

C. Literature Review

1. Sulfur dioxide control technology
   a. Existing technology . . . 8
   b. Selection of absorbent for SO_2 removal . . . 11
   c. Sulfide formation reactions . . . 15
2. Nitric oxide control technology
   a. Combustion modification . . . 16
      i. Oil-fired units . . . 17
      ii. Coal-fired units . . . 18
      iii. Acceptable excess oxygen firing levels . . . 19
      iv. Minimum NO with combustion modification . . . 19

Page

b. Dry NO removal processes 21

i. Solid-gas chemisorption 21

ii. Heterogeneous catalytic decomposition . 23

iii. Heterogeneous catalytic reduction

(a) Initial catalyst screening 24

(b) Reduction products and reducing agents 26

(c) Reduction kinetics 28

3. Simultaneous SO_x and NO_x Dry Process Control Technology. 30

4. CO and H_2 Removal by Catalyst/Absorbent Oxidation. . 32

5. Regeneration of Catalyst/Absorbent 33

D. Conceptual Design of Proposed Process 35

Chapter II. Experimental Program

A. Summary of Phases Planned

1. Process Chemistry

a. Overall process confirmation. 39

b. Detailed removal studies 39

c. Detailed regeneration studies. 40

2. Process kinetic studies

a. Temperature, residence time, particle-size considerations 41

b. Catalyst/absorbent deactivation 42

B. Experimental Equipment

1. Overall system 43

2. Reactor/furnace 43

Page

a. Fixed-bed reactor 43

b. Reactor furnace 46

c. Fixed-bed temperature measurement 48

3. Heat-traced flow lines

a. Reactor exit line 48

b. Outlet and inlet lines 50

4. Constant-temperature water bath. 51

5. Gas feed system 51

6. Condensers

a. Removal/regeneration condenser 53

b. Water collection condenser 54

7. Outlet line apparatus

a. Capillary flow restriction 54

b. Gas scrubber 54

Chapter III. Analytical system

A. Gas Analysis

1. Detector selection. 55

2. Column selection 56

3. Column performance 58

4. Column preparation and treatment 61

5. Chromatographic, recording, and integration equipment 66

6. Gas sampling 70

7. Calibration and detection limits for gas chromatographic analysis 70

8. Interaction of gases in chromatographic columns . . . 72

Page

B. Wet Chemical Gas Analysis

1. Ammonia collection 76

2. Sulfur dioxide collection 77

C. Catalyst/Absorbent Analysis

1. Qualitative tests 77

2. Quantitative tests 77

D. Precipitate Analysis 79

E. Experimental Error

1. Gas chromatographic analysis 80

2. Integration of effluent gas profiles 81

3. Catalyst weight measurements 81

4. Capillary gas flowmeters 82

5. Condensate and precipitate in gas lines 83

6. Effluent gas scrubbing with either HCl or NaOH solutions. 84

Chapter IV. Experimental Results

A. Initial Process Studies

1. Reduction of NO with CO over Iron Oxide 85

2. Simultaneous Removal of NO and H_2S with CO 87

3. Reduction of NO with CO over Iron Sulfide. 88

4. Oxidation of CO and H_2 with Iron Oxide 88

5. Oxidation of FeS to Iron Oxide and SO_2 88

6. Summary of Initial Studies 90

B. Removal of Sulfur Compounds

1. Removal of H_2S with Iron Oxide 91

2. Removal of COS with Iron Oxide 93

Page

3. Formation and Removal of Sulfur Vapor 95

4. Removal of SO_2

a. Removal with Iron Oxide 96

b. Removal with CO or H_2 over Iron Oxide . . . 96

c. Removal with CO and H_2 over Iron Oxide . . . 102

5. Reduced Catalytic Activity 104

6. Summary of Sulfur Compound Removal 106

7. Sulfur Compound Distribution in a Net Reducing Flue Gas

a. Thermodynamic Equilibria of Sulfur Compounds in Reduced Flue Gas. 107

b. Homogeneous Kinetics of SO_2 Reduction . . . 109

C. Removal of Nitric Oxide

1. Reduction of NC with Iron Oxide 112

2. Reduction of NO with Iron Sulfide 115

3. Reduction of NO with H_2 over Iron Oxide 117

4. Reduction of NO with H_2 over Iron Sulfide 119

5. Reaction of NO and H_2O with Iron Oxide or Iron Sulfide 119

6. Reduction of NO with CO and H_2O over Iron Sulfide 121

7. Summary of Nitric Oxide Removal Reactions 123

D. Simultaneous Removal of Sulfur Compounds and Nitric Oxides at Low Temperatures 123

1. Reduction of NO with H_2S over Iron Sulfide 124

2. Removal of NO and H_2S with H_2 over Iron Oxide . . . 125

3. Removal of NO and H_2S with both CO and H_2 over Iron Oxide 128

Page

4. Removal of NO and H_2S with CO over Iron Sulfide . . . 128

5. Removal of NO and COS over Iron Sulfide 130

6. Removal of NO and SO_2 with CO and H_2 over Iron Oxide 130

7. Removal of NO, H_2S, and O_2 with CO and H_2 over Iron Oxide 132

8. Removal of NO, SO_2, and O_2 with CO and H_2 over Iron Oxide 134

9. Summary of Simultaneous Removal of Nitric Oxide and Sulfur Compounds 136

E. Simultaneous Removal of SO_2 and NO at High Temperatures

1. Removal of NO, SO_2, and H_2O over Iron Oxide

a. Long residence time runs 139

b. Short residence time runs 140

2. Removal-Regeneration Cycles for NO, SO_2, and O_2 with CO over Iron Oxide 146

F. Ammonia Generation 152

G. Simultaneous Removal of SO_2, NO, and O_2 with Copper Oxide and Nickel Oxide 152

1. Removal with Copper Oxide 154

2. Removal with Nickel Oxide 156

3. Summary of Copper and Nickel Runs 156

H. Oxidation of CO and H_2

1. CO Oxidation 159

2. H_2 Oxidation 164

I. Other Reactions Studies

1. Water-gas Shift Reaction 164

2. High Temperature Short Residence Time Sulfidization 167

Page

3. NH_3 Oxidation 167

4. Activity of Activated Alumina 169

J. Iron Sulfide Oxidation

1. High Temperature, Low O_2 Concentration 169

a. Large Pellets 170

b. Small particles 171

2. Low Temperature, Low O_2 Concentration 172

3. Summary of Regeneration Results 173

Chapter V. Process Design

A. Overall Rate Analysis

1. Removal process

a. Defining equation for reactors 174

b. Key process variables 175

2. Regeneration process

a. Defining equation for regenerator 175

b. Key process variables 176

B. Discussion of variable ranges

1. Removal reactions

a. Reaction temperature 176

b. Kinetic and mass transfer effects

i. Fixed-bed contactor 177

(a) Required residence time 177

(b) External mass transfer rate 179

(c) Reaction rate estimation 181

ii. Dispersed-bed contactor

(a) External mass transfer rate 183

Page

(b) Reaction rate estimation. 184

(c) Solids density 188

(d) Residence time. 191

(e) Particle size 192

(f) Gas concentration 195

(g) Gas and solid composition 196

2. Regeneration reactions

a. Regeneration temperature 198

b. Kinetic and mass transfer effects

i. Fixed-bed regenerator

(a) Required residence time. 199

(b) Mass transfer and solids rate estimation . 199

ii. Fluid bed regenerator 200

C. CO and H_2 Generator

1. Practical considerations 203

2. Type of generator 203

D. Design Bases

1. Process flow sheet 205

2. Material flows 209

3. Heat balance 211

4. Equipment description 216

E. Economic Analysis

1. General discussion 223

2. Cost basis 227

3. Process costs 229

Page

Chapter VI. Discussion and Recommendations

A. Process Evaluation

1. Description of the process 232

2. Comparison with other processes 233

3. Reasons for economy

a. Equipment size and complexity 235

b. Improved thermal efficiency 236

c. Make-up cost 237

B. Potential Process Problems

1. Ammonia emissions 237

2. Accuracy of process design 238

3. Flyash separation from catalyst/absorbent 239

C. Recommendations 240

Nomenclature 242

References 245

Appendix: Part 1. Experimental Data 258

Part 2. Removal Reaction Analysis 268

Part 3. Regeneration Reaction Analysis. 271

Part 4. Design Bases 273

Part 5. Heat Effects in Removal and Regeneration Reactions. 276

CHAPTER I

Introduction and Background

A. Problem Statement.

In the middle of the last decade a concentrated effort was begun by government, industry, and university groups to develop technology for control of the emissions of sulfur dioxide from stationary sources. The work concentrated on electrical power generating plants, since at that time, this source accounted for about 45% of the total SO_2 emissions in the US (USDHEW, 1969). SO_2 emissions from US power plants, assuming no control, are expected to increase 270% between 1967 and 1980 (Chilton, 1971). With no SO_2 abatement, by 1980 power plants would emit about 65% of the total SO_2 emissions.

Another important polutant which was identified as coming from power plants was nitric oxide. When work began in 1968 electrical generating plants emitted about 20% of the total nitric oxide emissions in the US and about 40% of all NO from stationary sources (USDHEW, 1970). Between 1968 and 1980 NO emissions from power plants are expected to increase by 220%, assuming no controls. Bartok (1969) has estimated that, with completely uncontrolled NO emissions, by 1980 the amount of total NO coming from electric utilities will increase to 25% of the total NO emissions. This percent increase is expected to continue in the future, particularly because of emphasis on NO control from mobile sources.

Although both of these pollutants are generated from the same

source, separate control technology was developed for each. This is evidenced by the publication of two separate control documents by DHEW, one in 1965 and the other in 1970 for NO.

In December, 1971, the EPA promulgated Standards of Performance for New Stationary Sources which included limits on the emissions of both SO_x and NO_x from power plants. This clearly identified the need to develop processes which controlled both SO_2 and NO emissions. To date there have been only a few processes developed to meet this double goal. An evaluation of these processes (Section D) shows them to be either inefficient or difficult to operate. The broad objective of this study then is the development of a feasible process for the simultaneous removal of nitrogen oxides and sulfur oxides from the effluent gases of fossil-fuel burning power plants.

B. Objectives.

In order to achieve this overall objective, criteria were established for evaluating potential process alternates. These criteria, which should be satisfied by any acceptable process, are described below.

1. Foreseeable government regulations on emission levels of NO_x and SO_x must be met.

   The proposed 1971 emission standards from EPA have set these

levels at 0.2 lb $NO_x/10^6$ BTU (210 ppm)* for gas-fired units, 0.3 lb $NO_x/10^6$ BTU (310 ppm)* and 0.8 lb $SO_2/10^6$ BTU (390 ppm)* for oil-fired units, and 0.7 lb $NO_x/10^6$ BTU (672 ppm)* and 1.2 lb $SO_2/10^6$ BTU (540 ppm)* for coal-fired units (EST, 1971). Even tighter restrictions can be expected in the future since the majority of new plants built will burn either coal or oil.

The desired process should have the potential of lowering the NO_x and SO_x concentrations to less than 100 ppm. The currently accepted technique for lowering NO_x is by combustion modification (See Section D.2.a). It is generally agreed that the present state-of-the-art in combustion techniques for oil- and coal-fired units only permits the concentration of NO to be reduced to between 300 to 400 ppm. NO itself does not dissolve appreciably in water or basic solutions and its oxidation to the soluble N_2O_3 is too slow to be practical for large flows. The only feasible method of obtaining NO_x levels below 100 ppm appears to be by the reduction of NO with CO or H_2 over a solid catalyst. SO_2, however, reacts quite readily with numerous substances and could be removed by reaction with the NO_x reduction catalyst. The key to the proposed process is a solid catalyst/absorbent which retains its activity for NO reduction reactions while reacting with and removing the sulfur compounds in the flue gas.

---

* NO_x is expressed as NO_2 and the ppm values are based on:

coal - 0.7 lb C/lb coal, 12,000 BTU/lb coal, 14% CO_2
oil - 0.865 lb C/lb oil, No. 0.6 fuel oil, 12% CO_2
gas - 0.97 ft^3 CO_2/ft^3 gas, 873 BTU/ft^3, 9.1% CO_2

2. No other type of pollution problem should be created by installation of the process.

This requires that NO_x and SO_x either be rendered innocuous or converted to saleable by-products. In the case of NO_x the latter alternative is highly improbable, and conversion to innocuous products must be achieved. The reduction of NO_x by CO or H_2 mentioned in the previous section leads to the formation of N_2 or NH_3. The extent and significance of NH_3 emission from the proposed process is discussed in Chapter VI. On the other hand, there is no compound of sulfur which does not pollute if released on a large enough scale. Saleable by-products worth considering are elemental sulfur and concentrated sulfuric acid.

Sulfur removal schemes are numerous (Davis, 1972). Dry limestone injection was reported as the least expensive SO_x control technique but was found ineffective for adequate sulfur removal (EPA, 1973). It has the added disadvantage that large amounts of unreacted sulfur-laden solids are discharged. This results in both particulate pollution and solid waste pollution. Wet limestone scrubbing, although it has much higher SO_2 removal rates, has similar problems. It discharges an aqueous stream high in sulfate and calcium ions. The Chemico Magnesium Oxide process (Shah, 1972) has potential for recovering sulfur as concentrated sulfuric acid, but it is ineffective for NO_x removal. The proposed process has the potential of both effective NO_x removal and recovering either elemental sulfur or concentrated sulfuric acid without producing other waste products.

3. The removal mechanism for one component should not depend upon the presence or absence of the other.

The nitrogen fixed as NO comes from both the fuel and the air. The significance of the two sources varies, since the extent of NO formation from air N and fuel N depends upon the burning conditions and the composition of the fuel. The NO_x concentration in the stack gas ranges from 200 to 1400 ppm, most frequently being in the range of 350 to 600 ppm. The source of sulfur oxides, however, is only from the fossil fuel itself. The concentration of SO_x has no significant dependence on the design of the combustion installation. There is essentially no sulfur in the natural gas received at power stations, but oil and coal have sulfur levels which generate SO_2 concentrations ranging from 130 to 4000 ppm SO_2.

Obviously, no correlation is to be expected between the concentrations of NO_x and SO_2 in the stack gas since they are generated by unrelated mechanisms. Hence a viable control process for both should not depend on the presence or absence of either for it to achieve satisfactory operation.

4. Furnace operation should be independent of the process operation.

The economy of power production is highly dependent upon the operation of the furnace. Large costs can result from a pollution-control process which necessitates suboptimal furnace operation, regardless of other aspects of the process which may be attractive.

The most widely accepted method for reducing the concentration of NO_x has been combustion modification (Bagwell, 1971; Bartok, 1969).

Included are such techniques as two-stage combustion, low-excess air firing, flue-gas recirculation, burner redesign, some combination of these first four, and water injection. All of these techniques are applied directly in the furnace region of the boiler, where the need to achieve complete and efficient combustion is generally given a higher priority. In order to operate to obtain both high combustion efficiency and low pollution, compromises must be made resulting in neither goal being fully reached.

Combustion modification in addition to being the best way to reduce the bulk of the NO_x, has been shown to increase furnace efficiency when properly used (Bartok, 1969). The lower limit achievable in this manner, however, is about 300 ppm NO_x for coal-fueled furnaces. This level is still too high to be acceptable. Removal of the remaining NO_x can be effected by the proposed catalytic process downstream of the furnace section of the boiler. The catalyst/absorbent is used in a dispersed phase after the superheat section so that no problems of slagging, increased system pressure drop, or loss of plume buoyancy will occur.

5. The process should be adaptable to both new and existing power plants.

Two regions in the flue gas path generally accepted as the best points for removing pollutants are either the region between the superheater and the air preheater or the region between the air preheater and the stack. Since solid removal agents react more rapidly at higher temperatures the first position would be preferable. Tempera-

tures in this region are between 370° and 540°C, with residence times of the order of 0.5 second. Longer residence times could be designed into new units or provided in older units by simple duct extentions.

6. The economics should be an improvement over the best currently known processes.

Bartok (1969) shows that investment costs for combustion control of NO_x for new furnaces range from $0.25/kw for low-excess air firing in 750-mw oil or gas units up to $2.08/kw for 2-stage combustion in 750-mw oil, gas, or coal units. The cost for modifications to existing units would be 20 to 25% higher. Operating costs range from +0.05 mills/kwh (expense) for 2-stage combustion with coal to -0.05 mills/kwh (credit) with low-excess air and 2-stage combustion for oil-fired units.

The most widely applied control for SO_2 is the use of low-sulfur fuel. Fuel oil with 0.3% sulfur sells for roughly $1/bbl higher than its higher sulfur competitors (Shah, 1972). For a 1000-Mw plant this corresponds to roughly 1.6 mills/kwh for the additional fuel expense. Another SO_2 control process which is increasing in its application is Wet Limestone Scrubbing. Reported costs for this technique are about $30-40/kw for installation costs and 2.0-2.5 mills/kwh for operating costs, depending on plant size, operating factors and other variables (Burchard, 1972). Both of these process alternates, when operated properly, can meet the EPA's SO_2 requirements stated earlier.

In comparison with the low cost Dry Limestone Injection Process the proposed process will have the added cost of catalyst/absorbent regeneration, but none of the costs associated with limestone acquisition, crushing, grinding, and disposal. In addition, some credit for sulfur recovery may be obtained. On balance, the costs are expected to be comparable to dry limestone injection. Details of the cost analysis are given in Chapter V.

C. Literature Review

1. Sulfur dioxide control technology.

a. Existing technology.

Flue gas desulfurization processes have traditionally been grouped as either wet or dry systems. The wet processes contact the main flue gas stream with a clear solution or an aqueous slurry which absorbs the SO_2 from the gas stream. The liquid composition and type of contactor vary with the process. The dry processes contact the main flue gas stream with a porous solid which either absorbs or adsorbs the SO_2. The solid and the type of contactor vary with the process. Slack (1973) has evaluated all of the major process alternatives, both wet and dry systems. Table i-1 summarizes his evaluation.

Table i-1 EVALUATION OF WET AND DRY SO_2 REMOVAL PROCESS. (Slack, 1973)

	WET	DRY
Advantages:	1. SO_2 removals are consistently high when unit is operating.	1. Gas in not cooled.
	2. In regenerable processes the ratio $SO_4^=/SO_3^=$ is much lower than in dry systems	2. No water pollution problem.
Disadvantages:	1. Flue gas cooling/reheat required.	1. Temperature cycling of absorbent or expensive dampering systems
	2. Scaling.	2. High surface area requirement may mean high attrition.
	3. Slurry transport.	3. Full oxidation generally occurs in solid.
	4. High pressure drops.	4. Potential solid pollution problem.
	5. Potential water pollution problem	

Although a reliable dry process would be preferrable, from the operational point of view, Slack concludes that because of as-yet-unsolved disadvantages of present dry processes the wet systems may be superior. In a recent publication, EPA (Princiotta, 1974) lists six SO_2 control processes that are considered the most important for the near-term future. Five of the six processes are wet, concurring with the evaluation of Slack. The sixth is catalytic oxidation, which does not fit well in either group. These processes are grouped according to the type of sulfur product produced.

Table i-2 LEADING SO_2 CONTROL PROCESSES. (Princiotta, 1974).

Throwaway Products	Saleable Products
Lime Scrubbing	Magnesium Oxide Scrubbing
Limestone Scrubbing	Sodium Sulfite Scrubbing
Double Alkali	Catalytic Oxidation

The original approach taken for the development of a dry process was first to find a metal oxide which when reacted with SO_2 would produce a stable metal sulfite under typical flue gas conditions. The metal sulfite would then decompose in a regeneration step to the metal oxide and SO_2. Unfortunately, under typical flue gas conditions metal sulfate instead of sulfite was the predominate product. This necessitated higher regeneration temperatures than would be practical if strongly alkaline solids were used, i.e., Ca or Na. Metals such as Fe and Mn could be regenerated at pratical temperatures but had high equilibrium partial pressures of SO_2 over the solid at typical reaction temperatures, producing low removals (Welty, 1971). The result of this dilemma was to select a process with a solid which could be thrown away. The solid selected was $CaCO_3$.

This original dry process, Dry Limestone Injection (DLIP), had great apparent potential because of its simplicity and low cost. Captial investment and operating costs for this system are approximately half that of the wet processes listed above. Extensive full-scale tests of the DLIP revealed, however, that its major disadvantages were low SO_2 removals(20 - 30%) and solids deposition in the superheater portion of the boiler. Despite the simplicity and low cost, the process has been de-emphasized because of these unsolved

problems.

If a solid could be found which would increase the SO_2 removal without substantially increasing the process cost or complexity, this dry system would be competitive with the wet processes. A key to keeping the process cost low is to have an absorbent which absorbs SO_2 at about the same temperature as it can be regenerated. Welty (1971) showed that such an absorbent cannot be found when both the absorption and regeneration steps are carried out under oxidizing conditions. If the absorption step were net reducing, forming a metal sulfide, and the regeneration step, net oxidizing, forming metal oxide and SO_2, temperature cycling would be minimized. A potential sorbent for such a process would be iron. At 650°C it forms a stable sulfide and an unstable sulfate.

b. Selection of absorbent for SO_2 removal.

Thomas (1969), (Also reported in Lowell, 1971), has made an extensive study of the applicablity of metal oxides for removing SO_2. The basic removal mechanism for a metal oxide system was the formation of metal sulfate in the removal step and the decomposition of metal sulfate in the regeneration step. The oxides of 47 elements were evaluated based on the following criteria:

1. Stable oxidation states at $P_{O_2} = 0.02$ atm.
2. Sulfate decomposition temperatures below 750°C.
3. Decomposition (below 750°C) must yield oxide from sulfate.
4. Low toxicity level of the compound.
5. High P_{SO_2} at elevated temperature over the oxide.
6. Low cost of material.

Based on the evaluation of the compiled data Thomas reported that

oxides of Al, Bi, Ce, Co, Cr, Cu, Fe, Hf, Ni, Sn, Th, Ti, V, U, Zn, and Zr were the most promising.

The formation of sulfate in both the DLIP and the above mentioned process creates a potential diffusion resistance when the outer layer of sulfate forms around the unreacted core of metal oxide. This effect is believed to be one of the reasons for the low SO_2 removal in the DLIP. If the sulfur were absorbed as the metal sulfide, less surface expansion would occur and the center core would be more accessible. Decreasing the amount of surface change would also cut down on particle attrition. Sulfide formation rather than sulfate formation would occur if the flue gas were made slightly reducing.

Potential metals were screened for sulfide formation with the work of Thomas as a guide. Since the sulfides are more stable than the sulfates in an inert atmosphere, elimination of those oxides which have too unstable a sulfate will be a conservative screening of potentially unstable sulfides. Therefore, the starting point for this screening was the top 16 metals given by Thomas. Table i-3 lists the oxides of these 16 metals with the evaluation data. Ten metals were eliminated for the following reasons.

Bi_2O_3 -- Cost too high
Cr_2O_3, CrO -- Toxicity high
Ce_2O_3, CeO_2 -- +3 valence decomposes with ignition
HfO_2, ThO_2 -- Radiation danger, no valence change
UO_2, U_3O_8, UO_3 -- Toxicity
V_2O_5, VO_2 -- Melting point low or ignites
Al_2O_3, ZrO_2, ZnO -- No valence change

The remaining potential metals are Fe, Cu, Ni, Co, Ti, and Sn. The sulfides of Ti and Sn are thermodynamically unstable in the presence of H_2O at 1000°K. They hydrolyze to the oxide and H_2S. Since the costs of Fe, Cu, and Ni were significantly less than Co, these three metals were selected as the best potential sorbents for the process.

Table i-3. METAL OXIDE EVALUATION

METAL OXIDE	DECOMP. T OXIDE (°C)	METAL SULFIDE	DECOMP. T SULFIDE (°C)	METAL SULFATE	DECOMP. T SULFATE (°C)	COST $/lb	TOXICITY* a	b	c	d	REFERENCES
Al_2O_3	2045 mp	Al_2S_3	1100 mp	$Al_2(SO_4)_3$	770 d	0.14	1	0	2	0	Thomas, 1969
Bi_2O_3	820 mp	BiS	680 mp	$Bi_2(SO_4)_3$	405 d	4.75 (metal)	1	2	U	1	Sax, 1968
Bi_2O_5	150 mp	---	---	---	---		1	2	U	1	Oil, Paint & Drug
CeO_2	2600	---	---	---	---	---	U	1	U	1	Reporter, 1971
Ce_2O_3	200(ignites)	Ce_2S_3	2100 d	$Ce_2(SO_4)_3$	920	---	U	1	U	1	
Co_2O_3	895 d	Co_2S_3	---	---	---	2.20 (metal)	1	1	1	1	*Toxicity given
Co_3O_4	900 d	---	---	$CoSO_4$	735 d		1	1	1	1	on basis of:
CoO	1935 mp	CoS	>1116 mp	---	---	"	1	1	1	1	a. acute local
Cr_2O_3	2435 mp	Cr_2S_3	1350 d	$Cr_2(SO_4)_3$	460-640	1.83	3	U	3	3	b. Acute systematic
CrO	---	CrS	1550 mp	---		"	3	U	3	3	c. Chronic local
CrO_2	300 d	---	---	---			3	U	3	3	d. Chronic systematic
CuO	1325 mp	CuS	220 d	$CuSO_4$	840-935	0.67	1	2	1	1	Where:
Cu_2O	1235 mp	Cu_2S	1100 mp	$Cu_2(SO_4)$	840-935	"	1	2	1	1	0 - No toxicity
Fe_2O_3	1565 mp	Fe_2S_3	d	$Fe_2(SO_4)_3$	781-810	0.08-0.20	1	0	0	0	1 - Slightly toxic
FeO	1420 d	FeS	1196	$FeSO_4$	603-810	"	1	0	0	0	2 - Moderate Toxicity
Fe_3O_4	1538 d	FeS_2	1171 mp	---		"	1	0	0	0	3 - Severe Toxicity
HfO_2	2812 mp	---	---	$Hf(SO_4)_2$	550-650	---	U	R			U - Unknown Toxicity
NiO	1990 mp	NiS, Ni_3S_2	mp 790, 797	$NiSO_4$	848 d	1.33	1	1	2	2	R - Radiation

Table i-3 METAL OXIDE EVALUATION (Con't)

METAL OXIDE	DECOMP. T OXIDE (°C)	METAL SULFIDE	DECOMP. T SULFIDE(°C)	METAL SULFATE	DECOMP. T SULFATE(°C)	COST $/lb	TOXICITY* a b c d	REFERENCES
SnO	1080 d	SnS	882 mp	$SnSO_4$	>360	2.11	---	
SnO_2	1127 mp	SnS_2	600 d	$Sn(SO_4)_2$	300-587	1.97	---	
ThO_2	3050 mp	ThS_2	1925 mp	$Th(SO_4)_2$	---		U R	
TiO	1750	TiS	---	$Ti(SO_4)_2$	150	---	1 U U U	
TiO_2	---	TiS_2	---	---	---	---	1 U U U	
Ti_2O_3	2130 d	Ti_2S_3	---	$Ti_2(SO_4)_3$	---	---	I U U U	
V_2O_5	690 mp	V_2S_5	d			2.21	U	
V_2O_4	1970 mp		---			"	U	
V_2O_3	---	V_2S_3	d>600	$V_2(SO_4)_3$	380-408	"	U	
VO	(ignites)	VS	D			"	U	
U_3O_8	1300 d	U_3S_3	ignites				U	
UO_2	2500 mp	US_2	>1100	$U(SO_4)_2$			U	
UO_3	d	US	>2000 mp				U	
ZnO	1975 mp	ZnS	1850 mp	$ZnSO_4$	600 d	0.15	U	
ZrO_2	2700 mp	ZrS_2	1550 mp	$Zr(SO_4)_2$	410 d	"	U U U U	

c. Sulfide formation reactions.

Ryason (1967) reported the catalytic reduction of SO_2 with CO over a copper oxide/alumina catalyst to give S_2. The reaction was

$$2CO + SO_2 \longrightarrow 2CO_2 + \tfrac{1}{2}S_2 \qquad \text{i-1}$$

Qualitative evaluation of the catalyst after reaction suggested that copper sulfide was formed. Since COS was also formed, the sulfidation may have occurred by

$$CuO + COS \longrightarrow CuS + CO_2 \qquad \text{i-2}$$

Khalafalla (1971) studied the same SO_2 reduction reaction over an iron oxide/alumina catalyst. In a later and more definitive study, Haas and Khalafalla (1973) definitely confirmed the presence of both FeS and FeS_2. They suggested that these sulfides were formed during the initial phases of testing when CO and SO_2 were passed over Fe_2O_3. An important observation made by Haas (1971) was that O_2 above 0.5% poisoned SO_2 reduction to sulfur.

Kasaoka (1973) tested copper oxide/alumina, iron oxide/alumina, nickel oxide/alumina, cobalt oxide/alumina, and iron oxide/chromium oxide/alumina catalysts for reaction i-1 in the presence and absence of water. Traces of COS and H_2S were measured. No discussion of the catalyst composition was given but it would be expected that all of the metals formed a sulfide before there was total sulfur compound elution. The presence of H_2S suggests that H_2, formed probably by the water-gas shift reaction, can also act as a reducer for SO_2. Kasaoka

(1973) also reported that SO_2 reduction decreased when O_2 was in the gas stream. The reduced activity was attributed to the formation of a sulfite or sulfate layer on the catalyst. At 2% O_2 the catalyst was inactive.

Querido (1973) has reported extensive work on reaction i-1 with a copper oxide catalyst. Although he outlined a process to remove SO_2 and maximize S_2 production relative to COS production, no clear discussion of the catalyst composition is given. Based on the work of Haas (1973) and Kasaoka (1973) the active solid is probably copper sulfide.

All of the studies mentioned above reduce SO_2 primarily to S_2 with either COS or H_2S being produced in varying degrees. Since there is no removal mechanism for either COS or H_2S after the metal oxide has been sulfided, the potential for total sulfur compound conversion to S_2 is low. Nonhebel (1972), Hopton (1956), and Jordan (1935) discuss the reactions for removing H_2S from coal gas streams by reaction with iron oxide to give iron sulfide at low temperatures, 55°C. By maintaining an excess of iron oxide in contact with the flue gas the sulfur formation reactions would be supressed and the sulfide formation reactions enhanced. All forms of reduced sulfur COS, H_2S, SO_2, and S_2, would then be removed from the exit gas stream.

2. Nitric oxide control technology.

a. Combustion modification.

An extensive study was done by the Esso Research and Engineering

Company (Bartok, 1969) on methods for the control of NO from stationary sources. The study concluded that the primary NO removal technique for large power plants was combustion modification. This technology can be applied to existing plants as well as new plants at low cost or in some cases at a credit to the plant. Table i-4 lists the techniques discussed and the amount of NO removal expected.

Table i-4 ESTIMATED %NO_x REDUCTION BY COMBUSTION MODIFICATION 1000-Mw UNIT. (Bartok, 1969)

	OIL	COAL
Low-excess air firing (LEA)	33	25
Two-stage combustion (2SC)	40	35
LEA + 2SC	73	60
Flue gas recirculation (FGR)	33	33
LEA + FGR	70	55
Water Injection	10	10

Low-excess air firing in combination with two-stage combustion appears to offer the greatest potential for NO removal.

i. Oil-fired units.

Bagwell (1971) reports that with fuel-oil firing on a 175-Mw face-fired unit almost 50% NO removal was achieved with two-stage combustion. The furnace burner design permitted the O_2 concentration to be decreased to 2.6% before smoke formation began. Tomany (1971) reported recent coaxial burner designs for gaseous and liquid fuels which permit a closer approach to stoichiometric firing before the onset of smoking and excessive CO formation. Reman (1963)

claims a burner design that allows liquid fuels to be burned with stoichiometric air without smoking. Bartok (1969) and Turner (1972) report that tangentially-fired oil furnaces have lower NO emissions than horizontally-fired units.

Low-excess air firing on oil units has been commercially demonstrated. Glaubitz (1960, 1961, 1962) reported that a boiler furnace equivalent to approximately a 25-Mw unit was operated satisfactorily for 4 years at 0.2% O_2. Reese (1965) reported an oil-fired, 185-Mw tangential unit that was operated at 0.5% O_2 while still maintaining acceptable carbon levels (99.9% carbon combustion efficiency, CCE) in the flyash.

ii. Coal-fired units.

Limited work has been done on low-excess air firing with pulverized coal-fired units. Bienstock (1966) reported on NO removal and soot formation in a small laboratory coal-fired furnace (1 to 4 lb/hr). When 1% O_2 concentration was maintained in the furnace zone followed by a later injection of 3.4% O_2 (two-stage combustion), 62% NO removal was achieved. The carbon in the ash increased from 2% (99.8% CCE) at 4.4% O_2 to 6.6% (99.2% CCE) with the two-stage combustion. McCann (1970) reports a 70% NO reduction when the O_2 concentration is decreased from 5% to 0.3% in a 500 lb/hr pulverized coal-fired furnace. At the low excess air levels there was 7.8% carbon in the ash (99.0% CCE). This relatively low ash level was achieved by using a 370°C air preheat and a stable air/fuel ratio.

Bartok (1972) reports that two-stage combustion was tested in

three coal units: a 175-Mw front-fired, a 480-Mw tangential-fired, and a 820-Mw horizontally opposed. In the front-fired unit an overall O_2 concentration of about 2% was used. It was reported in all cases that the modifications did not produce unacceptable levels smoke, CO, or hydrocarbons. These short term tests demonstrate the possibility but have not demonstrated the long term practicality of low-excess air firing in coal-fired furnaces.

iii. Acceptable excess-oxygen firing levels

Industry practice has been to maintain between 1 to 4% O_2 in oil-fired units and 3 to 7% O_2 in coal-fired units (Steam, 1969). The previous paragraphs indicate that commercial oil-fired units have been operated successfully at 0.2% O_2 with the aid of new firing patterns, new burner designs and higher controls. In a similar manner, research on these variables should enable the minimum O_2 level in coal firing to be decreased to about 2% O_2 (Hazard, 1974).

iv. Minimum NO with combustion modification.

Nitrogen oxide is formed in the combustion process from nitrogen in the air and nitrogen in the fuel. Lange (1971) reports that to achieve significant thermal fixation of gaseous N_2 as NO in utility boiler furnaces the temperature must be in the range 1500 - 1900°C. Hammons (1971) reported that fixation of fuel nitrogen in coal to NO can occur between 760 - 870°C. The temperature minimum for the conversion of fuel nitrogen in oil to NO is also expected to be in this range. Since the combustion temperatures for both coal and oil are equal to or above this lower limit, the minimum NO at low excess air will closely correspond to the fraction of fuel N con-

verted to NO. Martin (1972) and Turner (1972) report that the fraction of fuel N converted to NO varies with the level of N in the fuel and the amount of excess O_2 used for combustion. Turner (1972) gives a typical range of fuel N conversion to NO as 30 - 60% for oil-firing. Jonke (1969) reports a typical range of fuel N conversion to NO of 18 - 25% for a fluidized bed of coal. The N content of typical fuel oils ranges between 0.07% (light distillates) and 1.4% (heavy oils). The US crude average is estimated at 0.148% (Ball, 1962). Coal N ranges between 0.8% (Anthracite) and 1.9% (Sub-bituminous A). Most coals average around 1.5% N. Table i-5 lists the expected NO flue gas concentration resulting from the fuel N, given the listed assumptions.

Table i-5 CALCULATED MINIMUM NO EMISSIONS EXPECTED FROM OIL AND COAL FIRED UNITS.

	OIL	COAL
Wgt % Carbon in Fuel	86	72
Wgt % Nitrogen	1.4	1.5
Vol % CO_2 in flue gas	13	15
% Conversion fuel N to NO	30	18
Concentration NO (ppm)	540	480

Bartok (1972) reports that NO concentrations in commercial oil-fired and coal-fired units have been lowered to around 150 ppm to 250 ppm with two-stage combustion and low excess air. A 15 - 20% de-rating of the unit capacity was needed in all cases. The lack of % fuel N data in this study does not allow direct comparison with the NO levels reported in Table i-5. It would appear, however,

that commercial units may have lower NO values than laboratory furnaces. It is clear from Bartok (1972) that not all units operated acceptably at the extremes of these modifications. A reasonable estimate of minimum NO emissions under acceptable combustion modification operations appears to be 300 - 400 ppm for both oil and coal at the average N values listed in Table i-5. Therefore, in planning for future emission standards that may limit the NO concentration below 100 ppm, processing techniques in addition to combustion modification need to be developed.

b. Dry NO Removal Processes.

Although combustion modification techniques are effective for removing 60%-80% of the NO formed during combustion, further removal must be accomplished by flue gas treatment processes that are efficient at low NO concentrations. As was the case with SO_2, both wet and dry processes have been proposed for NO removal. Section B.1. discussed the ineffectiveness of wet systems for NO removal. Section C.1. concluded that for SO_2 removal an effective dry system would be preferrable to existing wet processes. This leads to evaluating the potential of dry NO removal processes. These are grouped into three categories.

Solid-gas chemisorption
Heterogeneous catalytic decomposition
Heterogeneous catalytic reduction

i. Solid-gas chemisorption.

Shelef (1971) has given an extensive review of the physical and chemical adsorption of NO on metals. Several different types of bonding

are described ranging from purely ionic to covalent. Ruthenium was the element which gave the largest variety of NO complexes. Iron was the common metal which showed the greatest affinity toward NO. Copper and nickel were other common metals which formed NO complexes.

Otto (1970) studied NO adsorption on supported iron oxides between 26 - 150°C and 1 to 200 Torr. He found the NO adsorption ability of iron oxides to rank: Fe_3O_4 > FeO > Fe_2O_3. With Fe_3O_4 at 26°C and 200 Torr the NO equilibrium loading corresponded to 750 mmoles/m^2 Fe_3O_4. Similar measurements for supported nickel oxide reported by Gandhi (1972) were 1650 mmoles NO/m^2 NiO. Gandhi (1973) also reported NO adsorption on supported copper oxide. A maximum of 100 mmoles NO/m^2 CuO was measured. In contrast to the iron, the more oxidized species, CuO, adsorbs NO more readily than does Cu_2O. A comparison of the chemisorption rates of NO on these three metals shows the ranking to be: iron oxide > nickel oxide > copper oxide.

Otto (1970) reported the initial NO adsorption rate on Fe_3O_4, at 90°C 3.5 Torr, as 1.09 x 10^{-3} mmoles/m^2 Fe_3O_4-sec. Since he reported 16% reduction of NO to N_2O over Fe_3O_4 at 150°C, 90°C is assumed to be the upper limit for reversible adsorption on Fe_3O_4. Calculations show that if a one-second contact time between a 700 ppm NO flue gas stream and Fe_3O_4 is assumed in a typical power plant, an adsorbant flow rate at least 8 times that of the coal would be required just to remove the NO. This assumes that the flue gas is cooled to 90°C from 150°C and that the presence of

sulfur does not inhibit the adsorption rate. First, cooling the flue gas to 90°C is undesirable since this either results in decreased plume buoyancy or added equipment. Second, Lunsford (1968) has shown by comparing NO adsorption on ZnO and ZnS that placing sulfur on the surface does inhibit NO adsorption. Gidaspow (1972), in contrast, reported NO adsorption rates on platinized $FeSO_4$ with 780 ppm NO and 82°C after 1 minute of 1.17 mmoles NO/m^2 ads.-sec (270 mmoles NO/g ads.-sec.). If this was in fact true adsorption, the adsorbent-to-coal flow rates would be reasonable, around 0.001. Since 2% H_2 in N_2 at 200°C had to be used in regeneration and no NO was measured in the outlet gases, it is apparent that reduction of NO instead of adsorption of NO was occurring at these higher rates.

In summary, adsorption of NO on solids for NO removal from flue gases appears impractical because of the following limitations:

-- Flue gas cooling required.
-- Large adsorbent-to-coal flow rates are required just for NO removal
-- Possible inhibiting interaction between sulfur and NO adsorption.

ii. Heterogeneous catalytic decomposition.

Nitric oxide is thermodynamically unstable relative to the elements in an atomosphere containing 75% N_2 and 1% O_2 below 730°C (Shelef, 1971). At 730°C(75%N_2, 1%O_2) the equilibrium concentration of NO is 7.23 ppm. The presence of NO in power plant exit flue gases (typically 150°C) is a result of kinetically freezing the NO decomposition reaction. Bartok (1969) reports that under typical combustion conditions homogeneous NO decomposition is kinetically

frozen below 1260°C.

Shelef (1969) tested the heterogeneous catalytic decomposition of NO over platinum and five base metal oxide catalysts. Even at 500°C NO decomposition kinetics were not rapid enough for practical application. Winter (1971) tested 40 metal oxides for NO decomposition. He measured rates comparable to those of Shelef. Riesz (1957) performed an extensive screening of 21 commercial and 17 laboratory-prepared catalysts. Platinum, palladium, base metal oxides and base metal sulfides were tested. The general conclusion was also that none of these catalysts produced a sufficiently high decomposition rate to be of importance.

The results of Riesz (1957) work on base metal sulfides as potential catalysts warrants further discussion since this is a system which includes both sulfur and nitrogen oxides. Sulfided iron oxide, sulfided cobalt molybdate, molybdenum sulfide, and molybdenum sulfide activated with potassium carbonate were tested. A stream of 2000 ppm NO in N_2 was passed over a fixed-bed of catalysts.

Table i-6. DECOMPOSITION OF NO BY SULFIDE CATALYSTS. (Riesz, 1957).

Catalyst	Residence Time (second)	Temperature (°C)	NO Removal (%)
Iron Sulfide	0.052	500	17
	0.041	700	24
Cobalt-Molybdenum Sulfide	0.032	500	17
	0.030	700	4
Molybdenum Sulfide	0.032	500	17
	0.030	700	4
Molybdenum Sulfide + 15% K_2CO_3	0.029	500	28
	0.030	700	17

Although NO removal is relatively high, Riesz found that the catalyst lost activity after extended use. Concurrent with the decreased activity was a loss of sulfur from the surface in the form of SO_2. Riesz, as well as later investigators, eliminated sulfides as potential catalysts because of what they thought would be an unavoidable SO_2 pollution problem. As noted in Section C.1.c., the presence of a reducing agent, CO or H_2, would prevent evolution of SO_2 from FeS.

iii. Hetergeneous catalytic reduction.

(a.) Initial catalytic screening.

The most effective means for NO removal from gas streams is heterogeneous catalytic reduction. Shelef (1971) has reviewed all of the early studies on these reactions. He concludes that, under reducing conditions, a variety of catalysts as well as a variety of reducing agents can be employed to remove NO from gas streams at low gas residence times and relatively low temperatures. Evaluation of these data showed that supported precious metals and supported copper oxide or copper chromite were the catalysts with the most promise. Typical reducing agents were CO, H_2 or a hydrocarbon.

Shelef (1971) emphasized that in addition to the reaction rates between NO and a reducing agent, the competetive reactions between other oxidizing species and the reducing agent are important. Shelef (1968) reported on the competetive oxidation of CO by NO or O_2 over various catalysts. He found that the CO-O_2 reaction proceeded more rapidly over the earlier selected Cu_2O and $CuCr_2O_4$

catalysts than did the CO-NO reaction. The reverse was found true for Fe_2O_3 and Cr_2O_3 catalysts. In his study, Fe_2O_3 catalyst showed the highest rate for the CO-NO reaction, and it was therefore viewed as a potential catalyst.

This preference for the CO-NO reaction terminated when O_2 was added to the Cr_2O_3 system. Only when the gas stream was slightly reducing relative to both NO and O_2 reduction was there complete removal of both NO and O_2. It was assumed that the Fe_2O_3 system would act similarly. In laboratory tests Jones (1971) demonstrated that neither supported $CuCr_2O_4$ nor Fe_2O_3 catalysts were effective in promoting the NO-H_2 reaction in preference to the O_2-H_2 reaction. Some improvement in reaction selectivity was found with supported Pt-Pd below 205°C. These metals are too expensive and the temperatures too low for practical considerations on power plant flue gases. From this initial screening, the best NO reduction catalysts for application on power plants would be copper oxides, copper chromite, or iron oxide, all of which should be supported.

(b.) Reduction products and reducing agents.

Kokes (1966) showed that the reduction of NO by H_2 on a Pt catalyst led to N_2O, NH_3 or N_2. Shelef (1968) reported the appearance of both N_2 and N_2O when NO was reduced by CO over Pt and copper chromite catalysts. Jones (1971) and Klimisch (1972) reported on the formation of both N_2 and NH_3 when NO is reduced by CO in the presence of H_2O over both noble and base metal catalysts.

Shelef (1968) reported that N_2O is primarily a low-temperature

product over active Fe_2O_3, $CuCr_2O_4$, and Cu_2O supported catalysts. The temperature for maximum N_2O formation for the NO-CO reaction ranges between 180°C - 220°C when the residence time is about 0.75 sec. Above 300°C there was essentially no N_2O. Decreasing the residence time to about 0.07 seconds at 273°C increased N_2O formation over supported Fe_2O_3 catalyst. This suggested that N_2O is a possible gas-phase intermediate for the NO-CO reaction.

An extensive study of NH_3 formation in the NO-H_2 reaction over base metal oxide catalysts was reported by Shelef (1972). He also studied the effect of CO in the NO-H_2 system. NH_3, N_2O and N_2 were assumed to be the reduction products in the sytem with about a 0.18 second residence time. The relative amounts of NH_3 and N_2 produced varied with the catalyst, temperature, the reducing agent, and the amount of oxygen. Table i-7 shows the effect of different catalysts and temperatures on the percent reduced nitrogen product which is NH_3 (this is referred to as the ammonia selectivity).

Table i-7 AMMONIA SELECTIVITY AS A FUNCTION OF THE CATALYST AND TEMPERATURE. (Shelef, 1972)

Inlet: NO, 0.10 - 0.12%
H_2, 1.4%
θ, 0.18 sec.

Catalyst	370°C	578°C
Nickel Oxide	20%	20%
Copper Oxide	88%	80%
Iron Oxide	16%	80%
Copper Chromite	95%	90%

Although nickel oxide has the lowest NH_3 selectivity at both extremes, at an intermediate temperature of 420°C the NH_3 selectivity is 65%. The low selectivity at the higher temperature is caused by NH_3 catalytically being decomposed by NiO (Klimisch, 1973). All of these catalysts will decompose NH_3 to the elements but at higher temperatures (greater than 600°C) than the nickel. Shelef (1972) found that in all cases the addition of CO to the NO-H_2 system resulted in an increase in both the NO removal and in the NH_3 selectivity. The addition of 0.25% O_2 to the 1.4% H_2 - 0.12% NO system decreased both the NO removal and the NH_3 selectivity at a given temperature. A significant finding was that when both O_2 and NO were present, CO reacted preferentially with O_2 while H_2 reacted to the same extent with both NO and O_2.

Klimisch (1972) also noted the higher reactivity in the NO-H_2 system. He demonstrated that the presence of both CO and H_2O in the system allowed the water-gas shift reaction to proceed, producing a more reactive H than molecular H_2 for NO reduction and NH_3 formation. The effect of O_2 on both NO removal and NH_3 selectivity was also confirmed.

Over base metal oxide catalysts the two main reduction products will be NH_3 and N_2. At very low residence times, when neither H_2O nor H_2 is present, N_2O may also be generated. The amounts of NH_3 and N_2 produced will vary depending upon the reducing agent, the temperature, the catalyst, and the amount of O_2 in the gas stream.

(c.) Reduction kinetics.

Shelef(1972) has presented data comparing the kinetics of NO

reduction catalysts. Table i-8 compares the three potential catalysts plus nickel oxide on the basis of the temperature at which 90% NO conversion occurs.

Table i-8. TEMPERATURE OF 90% NO CONVERSION IN NO-H_2-CO SYSTEMS, °C. (Shelef, 1972)

Inlet: NO, 0.10 - 0.12%
H_2, 1.4%
CO, 1.4%
θ, 0.18 sec.

Catalyst	NO-H_2	NO-H_2-CO	NO-CO
Copper Chromite	275	275	320
Copper Oxide	280	270	350
Nickel Oxide	425	420	470
Iron Oxide	480	430	510

In this study the copper catalysts showed the fastest kinetics and the iron the slowest. In all cases the combined H_2-CO system either accelerated the kinetic rate or kept it at a high value. All of the temperatures listed are below the upper process limit of 540°C, which is the temperature at which the flue gas leaves the superheater section. The 0.18-second residence time of the gas in the catalyst bed is less than the available 0.50-second residence time between the economizer and air preheater in a power plant. These facts imply that catalysts exist which have potential for at least 90% NO removal in flue gas streams.

Since no detailed discussion of the catalyst treatment or oxidation state was given it is not possible to select a catayst simply. At best it can be said that copper, nickel, and iron oxide catalysts

have potential for sufficiently rapid kinetics for power plant application. Studies under flue gas conditions are needed to confirm each catalysts reactivity.

3. Simultaneous SO_x and NO_x dry process control technology.

Jordan (1955) reported that at 105°C iron oxide removed both H_2S and NO from commercial gas streams. Iron sulfide formed and NO was adsorbed on the solid. The simultaneous removal declined rapidly as the solid became loaded with NO, the atmosphere became oxidizing, or the temperature was raised.

Pierce (1929) reported that the reaction of H_2S and NO proceeded at 27° to 100°C over silica gel and glass wool to give S, N_2, and H_2O. Princeton Chemical Research (1968) has studied a process using this reaction for simultaneous SO_2 and NO removal. They propose to recycle a stream of H_2S to an alumina or molecular sieve catalyst where it reacts with the SO_2 and NO by the following reactions:

$$SO_2 + 2H_2S \longrightarrow 3S + 2H_2O \qquad i\text{-}3$$

$$NO + H_2S \longrightarrow S + \tfrac{1}{2}N_2 + H_2O \qquad i\text{-}4$$

The sulfur condenses on the catalyst and must be stripped off at high temperature. Preliminary tests confirm acceptable sulfur removal but the catalyst was poisoned when NO was present. In addition to the poisoning problem the large H_2S recycle stream causes added problems of control.

Bartok (1969) has proposed a dry process that sequentially removes SO_x and NO_x. The SO_x in dust-free flue gas is first oxidized to SO_3 over a catalyst such as V_2O_5 at 455°C. NH_3 is injected forming

$(NH_4)_2SO_4$ which precipitates from the gas at 400°C. A second injection of NH_3 is made prior to the flue gas passing over a Pt catalyst at 200°C. The NH_3 reduces the NO, forming N_2 and H_2O. Two catalyst systems are required in this process, the second being an expensive catalyst easily poisoned by sulfur.

Ryason (1967) reported the simultaneous removal of SO_2 and NO over a copper oxide catalyst when the net gas stream was reducing. The SO_2 was reduced to sulfur, which condensed in the reactor outlet and NO was assumed to be reduced to N_2. The catalyst appeared to be copper sulfide at the end of the run. Traces of COS were also measured. Additional work on a process utilizing this concept is reported by University of Massachusetts workers, Querido (1973), Okay (1973), and Quinlan (1973). Three catalyst beds in series are used to reduce SO_2 to sulfur and NO to N_2 with an excess of CO in the flue gas stream. The original catalyst charged to each bed is copper oxide on supported alumina. The first bed catalyzes the oxidation of CO with O_2 to remove all of the O_2 which could poison the remaining catalyst beds. The flue gas is split into two streams after the first bed. The main flow enters the second bed where SO_2 is reduced to S_2 and COS and NO to N_2. The secondary flow bypasses the second bed and goes directly to the third bed. In the third bed COS and SO_2 react to produce S_2 and CO_2.

The reactions for SO_2 removal were first studied at 430 - 540°C with residence times of 0.07 - 0.22 seconds. They reported greater than 90% removal of SO_2 in less than 0.20 seconds. The addition of NO to the system decreased the SO_2 removal slightly. NO removals

were always greater than 90%. The assumed reduction product for NO in these experiments was N_2. The simultaneous reduction was studied between 400 - 430°C with residence times around 0.20 seconds. Okay (1973) reported that H_2O had an adverse effect on the SO_2 reduction in the CO-SO_2 system but that the water-gas shift reaction did not proceed. Based on this fact, Quinlan (1973) assumed that in the simultaneous removal of NO_x and SO_x no H-containing species such as H_2S or NH_3 would form. In Chapter IV, Section G.1., experimental work is reported in which it was found that both H_2S and NH_3 are formed when NO and SO_2 are reduced with CO in the presence of H_2O over copper catalyst. The H_2S would probably react like COS with the bypassed SO_2 to form sulfur. The NH_3, like the product N_2, would elute.

Even if the basic process chemistry is feasible, the University of Massachusetts process has several practical drawbacks. First, three beds in series will create a large system pressure drop. Second, the bypass stream must be very accurately controlled to provide stoichiometric COS and SO_2. Third, the amount of CO required for the reduction must be closely controlled since only reactions with O_2, SO_2 and NO remove it. Fourth, the flue gas would have to be cooled and then reheated after the bed to insure complete precipitation of the sulfur.

In summary no acceptable dry process for simultaneously removing sulfur compounds and NO has previously been developed.

4. CO and H_2 removal by catalyst/absorbent oxidation.

The removal of SO_2 and NO by the proposed process requires the

presence of a reducing agent, either CO or H_2. By necessity, an excess of CO and H_2 needs to be maintained to insure complete reaction with SO_2 and NO. If this excess CO and H_2 were emitted, it would constitute a pollution problem. Both CO and H_2 can be removed by contacting the gas stream with an excess of Fe_2O_3.

Feinman (1961, 1964) reported on the reduction of Fe_2O_3 with H_2 at temperatures between 540°C and 700°C. The iron was reportedly reduced to both Fe_3O_4 and FeO. O_2 and H_2O were found to retard the rate. A more highly reduced iron was produced at the lower temperature.

Fast (1965) discusses the reduction of iron oxide with CO or H_2 between 560 and 1000°C. This discussion is mainly about equilibrium considerations. Otto (1970) uses the work of Fast as a basis for selecting a CO/CO_2 ratio to give a reduced iron oxide for his adsorption studies.

Baranski (1972) studied the reduction kinetics of an iron catalyst with H_2 in the temperature range of 450° - 550°C. As in the case of the other investigators cited, the major concern was the solid reduction instead of CO or H_2 oxidation. All of these investigators have reported reaction at typical process temperatures but have used much higher CO or H_2 concentrations than would be present in stack gas. Experiments at low concentration will be important in the experimental study which follows.

5. Regeneration of catalyst/absorbent.

The oxidation of metal sulfides at high temperatures (700 - 900°C) to give metal oxides and SO_2 has long been a standard process for removal of sulfur from metal ores. Stollery (1964) reports on the

exothermic oxidation of iron, copper, and zinc ores in fluidized-bed roasters. Less than 0.1% sulfide remained after oxidation in a fluid bed with only 2% O_2 in the exit stream. This represented approximately 99.7% oxidation of the sulfides.

With a regeneration process which produces a rich stream of SO_2, a second process step is needed to obtain a saleable sulfur product. This could be either a sulfur plant or a sulfuric acid plant. It would be preferable for sulfur to be directly produced in the regeneration step. Guha (1972) reports on a high temperature decomposition (500 - 830°C) of FeS_2 to give S_2 and FeS. Since it is necessary to regenerate not only FeS_2, but also FeS, this technique is not applicable. A more realistic approach to producing sulfur directly is the use of low temperatures. Beavon (1968) reports that when a regeneration gas of SO_2 and/or O_2 at 200° to 400°C was passed over iron sulfide, sulfur was produced. The heated regeneration gas vaporizes the sulfur and removes it from the solid. The O_2 content is reportedly between 1% and 3%. No level of SO_2 was given. It is not clear from the patent application whether confirming experiments have actually been run. Thermodynamic considerations (presented in Chapter IV, eqns. iv - 42, 43, 44) show that at 227°C only the reactions of FeS with SO_2 to produce solid sulfur and Fe_2O_3 and that of FeS with O_2 to produce gaseous sulfur and Fe_2O_3 are favored. The reactions of SO_2 with FeS to give gaseous sulfur and Fe_2O_3 is thermodynamically unfavorable at these conditions. In order for a low temperature reaction to proceed, producing gaseous sulfur, only O_2 can be used as the oxidizing agent.

D. Conceptual Design of the Proposed Process.

The literature review presented in the previous section shows that a feasible process for simultaneous SO_2 and NO removal is to absorb SO_2 as a metal sulfide and catalytically reduce NO over the supported metal oxide/metal sulfide to nitrogen or ammonia. The requirements that the solid must be reactive toward both SO_2 and NO, regenerable at a relatively low temperature, have a high surface area per unit weight, have a relatively low rate of attrition, and be reasonably priced were not met by any naturally occurring solid. From the evaluation in section C the solids which had the potential to meet all the criteria established in section B were the oxides of iron, copper, and nickel deposited on a matrix of high surface area alumina or alumina and silica. This section outlines a process meeting these criteria. Iron oxide on alumina is used as the solid to demonstrate the reactions which occur. Following a discussion of the experimental results in Chapter IV, a more precise design discussion is presented in Chapter V.

A simplified diagram of the proposed process is given in Figure i-1. The boiler furnace is to be operated at maximum efficiency. Maximum efficiency is achieved with the minimum net oxidizing atmosphere to completely oxidize the carbon to CO_2, hydrogen to H_2O and sulfur to SO_2. The minimum required excess air over the stoichiometric amount will be a function of the burner design and the type of fuel used. This process is especially applicable to pulverized coal or oil fueled units with front-fired or tangentially-fired furnaces.

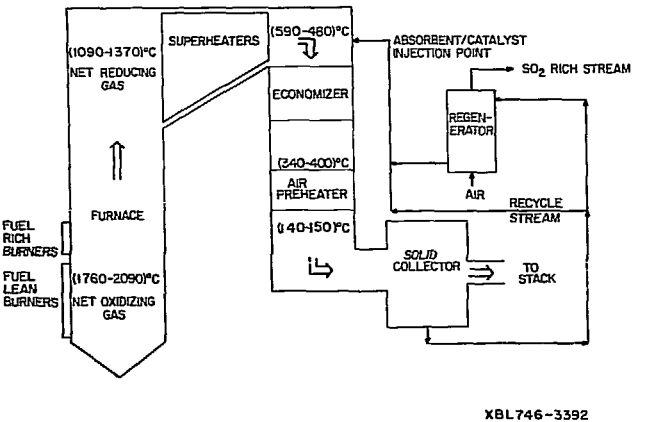

Fig. i-1. Process flow diagram—simultaneous NO_x and SO_x removal.

At a point in the upper part of the furnace, most probably the upper row of burners, a stream of CO and H_2 is added to produce a slightly fuel-rich flue gas at the furnace exit. This does not preclude the presence of O_2 but requires that there be enough CO and H_2 present so that at equilibrium all NO would be converted to N_2, all O_2 to CO_2, and all SO_2 to sulfide. The stream of CO and H_2 could be generated in a moving-grate, coal-fueled stoker unit which was operated with a limited air supply. The main furnace must then burn two fuels, coal and CO + H_2. No furnace modifications are needed.

When the flue gas exits from the superheater section of the boiler, at 480-590°C, it will be contacted with a dispersed phase of catalyst/absorbent particles. The dispersed-phase method of contacting is preferred because it minimized the system pressure drop. The particles will consist of iron oxide deposited on an alumina matrix.

The overall reactions are given in Table 1-9. Nitric oxide is reduced with CO, H_2 or the CO + H_2O combination to N_2 or NH_3. The sulfur compounds will be absorbed as the iron sulfide or sulfate. The major sulfur compound, SO_2, will react with the iron oxide together with a reducing agent to form ferrous sulfide. Any reduced sulfur species H_2S or COS will react directly with reduced iron oxide to form ferrous sulfide. Iron sulfate will result if some O_2 is present in the flue gas at the point of catalyst/absorbent addition.

The original amount of CO and H_2 added to the system will be

above that required to reduce SO_2, NO, and O_2.

Table i-9 OVERALL PROCESS REACTIONS.

ABSORPTION/REDUCTION STEP

$2\ NO + 2\ CO \longrightarrow N_2 + 2\ CO_2$

$2\ NO + 2\ H_2 \longrightarrow N_2 + 2\ H_2O$

$2\ NO + 3\ H_2O + 5\ CO \longrightarrow 2\ NH_3 + 5\ CO_2$

$FeO + SO_2 + 3\ CO \longrightarrow FeS + 3\ CO_2$

$FeO + SO_2 + 3\ H_2 \longrightarrow FeS + 3\ H_2O$

$FeO + H_2S \longrightarrow FeS + H_2O$

$FeS + 2\ O_2 \longrightarrow FeSO_4$

$Fe_2O_3 + CO \longrightarrow 2\ FeO + CO$

$Fe_2O_3 + H_2 \longrightarrow 2\ FeO + H_2O$

REGENERATION STEP

$2\ FeS + 7/2\ O_2 \longrightarrow Fe_2O_3 + 2\ SO_2$

$2\ FeO + \frac{1}{2}\ O_2 \longrightarrow Fe_2O_3$

$2\ FeSO_4 \longrightarrow Fe_2O_3 + SO_2 + SO_3$

The excess CO and H_2 are removed by maintaining an excess of ferric oxide in the catalyst/absorbent feed.

After the contact zone the catalyst/absorbent is separated from the flue gas with cyclones. The major part of these collected solids are returned to the contact zone. A slip-stream diverts a portion of the catalyst/absorbent to the regenerator. Air is added in the regenerator to reoxidize the iron to ferric oxide and to produce a rich SO_2 stream suitable for conversion to concentrated H_2SO_4 or elemental sulfur.

Chapter II

Experimental Program

A. Summary of Phases Planned.

The experimental program was designed to answer two basic questions: 1.) Do the proposed process reactions remove sulfur compounds and nitric oxide when both are present simultaneously? 2.) Are the process rates rapid enough to effect efficient removal of these compounds under typical flue gas conditions?

1. Process chemistry.

a. Overall process confirmation.

The first group of experiments was outlined to provide an initial check on the process feasibility. The reduction of NO over reduced iron oxide and iron sulfide with CO was studied. Simultaneous removal of NO, H_2S and CO was tested with Fe_2O_3. Oxidation of excess CO and H_2 by reaction with Fe_2O_3 was tested. High-temperature catalyst regeneration in a stream of low O_2 concentration was studied.

b. Detailed removal studies.

The second group of experiments studied in detail the removal reactions for sulfur compounds (H_2S, COS, SO_2), oxidizing compounds (NO and O_2), reducing compounds (CO and H_2), and water. Since a multitude of reactions is possible when all of these gases are present, the reaction of each with the catalyst/absorbent was first studied separately. The more complex system of multiple gases was reached by progressively adding these gases to the system. Since

H_2S and SO_2 reacted to produce sulfur in the system feed lines, these two gases were never simultaneously present in the inlet gas. Oxygen was the last gas added to the mixture since the literature (see Chapter I) had reported potential catalyst deactivation with O_2.

The number of gases present in the inlet not only varied from run to run, but also varied within runs. The runs are numbered 1a, 1b, 2a, etc., indicating the actual sequence of reactant addition. Appendix A - 1 is a summary of all experimental runs in chronological order. In Chapter IV the runs are grouped and discussed according to reaction chemistry, since the same reaction may have been studied in several runs. The order in which the reactions were studied was based on their rated importance at that stage of the experimental work. This rating was not only a function of the initial experimental plan, but also of the results obtained in previous runs, literature reviews, and/or calculations made to that date. The reader will note that the experimental results are presented in Chapter IV in a logical order rather than strictly in chronological order.

c. Detailed regeneration studies.

The regeneration studies concentrated on determining the sulfur product from the regeneration and on producing an active catalyst/absorbent. The two potential products are sulfur and sulfur dioxide. As discussed in Chapter I, sulfur is reported to form more readily at low temperature and low oxygen concentration. Sulfur dioxide forms during high temperature regeneration.

The regeneration experiments typically were the last step in a run sequence. Following removal reactions, the catalyst/absorbent bed was purged with the system diluent and then cooled or heated to the selected regeneration temperature. Streams having low O_2 concentrations and air were used for these tests. In some of the low-temperature runs, water was added to see if it could catalyze the formation of sulfur.

2. Process kinetic studies.

a. Temperature, residence time, particle size considerations.

The most likely region in the flue gas path for contacting the flue gas with the catalyst/absorbent is between the inlet of the economizer (about 540°C) and the inlet of the air preheater (about 370°C). The residence time of the flue gas in the region between the economizer and air preheater is about 0.5 seconds.

All of the initial studies of process chemistry were conducted in a fixed bed at about 370°C with a gas residence time in the bed of around 0.50 seconds. The particle size chosen for these studies was the standard 3.2-mm x 3.2-mm pellets of Fe-301-T 1/8 Harshaw Catalyst.

After these studies the results suggested that the experimental conditions should be altered. First, in these experiments some catalyst deactivation was found. This deactivation was predicted to be less of a problem at higher temperatures. Second, the sulfur breakthrough curves for the simultaneous removal runs suggested that the actual reaction times were much less than the gas residence

time in the bed. Third, visual observation of cross-sections of the catalyst/absorbent from the lower temperature runs suggested that there were important diffusion limitations within the 3.2-mm pellets.

These three experimental observations suggested the desirability of runs at higher temperatures with shorter gas residence times and with smaller particles. Consequently, the last part of the simultaneous removal studies was conducted at 540°C with residence times between 0.02 and 0.04 seconds, and with particles-sizes between 0.50-mm and 0.25-mm.

No attempt was made to construct an accurate experimental prototype of the contactor envisioned for an actual plant installation. As described in Chapter I, the actual system would be a dispersed-phase or fluidized-bed type of unit. The experimental approach was to study the process initially in a fixed bed. These experimental data would then be used to predict the expected behavior in the commercial unit. The major differences between the fixed and dispersed-bed systems are related to the bed densities and mass transfer effects. Known correlations, detailed in Chapter V, were used for this purpose. The experimental residence times, gas concentrations, and particle sizes were chosen so that reasonable extrapolations could be made to an actual flue gas contactor to predict the process feasibility.

b. Catalyst/absorbent deactivation.

The other major influence on the process kinetics was the deactivation of the catalyst/absorbent. Studies of this effect

were not planned initially but evolved because this phenomenon occurred in both the lower and the upper temperature ranges. Since the addition of O_2 to the gas mixture first caused the deactivation, the O_2 level and the ratio of oxidizing gas to reducing gas were chosen as the two main variables in this study. An upper gas concentration of 1% O_2 was chosen as as estimate of the potential O_2 in a net reducing flue gas due to incomplete mixing (Johnson, 1972).

B. Experimental Equipment.

1. Overall system.

All of the experimental apparatus was housed in a 3.2-m x 2.1-m x 1.2-m walk-in hood. Hood ventilation was provided with two exhaust fans. An overall sketch of the experimental apparatus is shown in Figure ii-1. This is a straight flow-through system with gas samples taken at the inlet and outlet of the Burrel Tube Furnace which houses the reactor. The discussion of the Gas Chromatographic System and sampling techniques is given in Chapter III.

2. Reactors/Furnace.

a. Fixed-bed reactors.

Fixed-bed, flow-through reactors were used in this study. The first was a 32-mm I.D. 304 stainless steel (SS) reactor. It is shown in Figure ii - 2. Other workers had reported that 304 and 316 SS were active catalysts for NO reduction reactions in the absence of sulfur compounds (Kearby, 1971, and Lamb, 1972). Neither

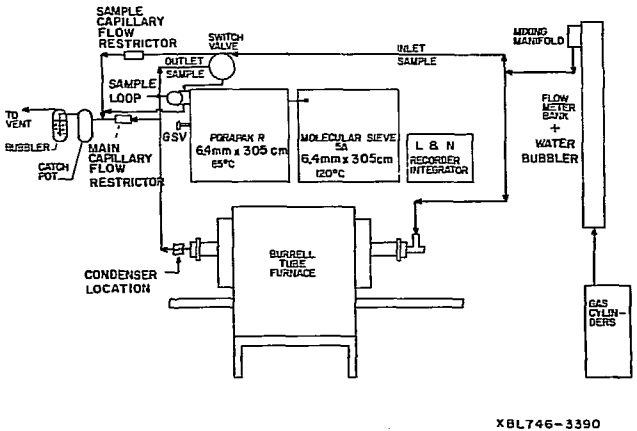

Fig. ii-1. Experimental system.

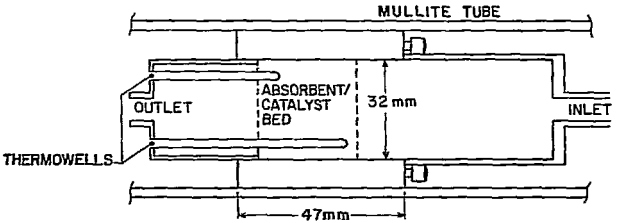

Fig. ii-2. Experimental reactor–32mm.

steel was found significantly reactive in this study. Two other reactors used are shown in Figure ii -3. The 6.4-mm and 9.5-mm reactors were used in the later part of the experimental study to achieve shorter residence times.

The reactions in this study include both gas-metal absorption and gas-metal catalysis. In order to provide a sufficiently high bed capacity for absorption of the sulfur compounds the length of the fixed-bed corresponded to an integral flow reactor for the catalytic reactions. Even in the smaller bed with residence times around 0.02 seconds, the sulfur breakthrough times were greater than 30 minutes. The major disadvantage to working in a fixed-bed reactor is that the removal results must be corrected for both bed-density and mass-transfer effects before they can be directly applied to an actual flue-gas contactor. The influence of both of these effects on the process design can be estimated. This influence is discussed along with the process-design considerations in Chapter V. As mentioned earlier, a more closely analogous reactor would have been a fluidized bed. Since correlations exist which permit extrapolation of data from fixed to dispersed systems, the fixed bed was selected primarily for its simplicity.

b. Reactor furnace.

The reactors were housed in a Burrell Tube Furnace, Model BT-1-9. A 44.4-mm I.D. Mullite tube surrounded the reactor. The 32-mm I.D. reactor rested on the walls of the tube. (See Figure ii - 2). The other two reactors were not in contact with the tube walls. The maximum temperature limit of the furnace was

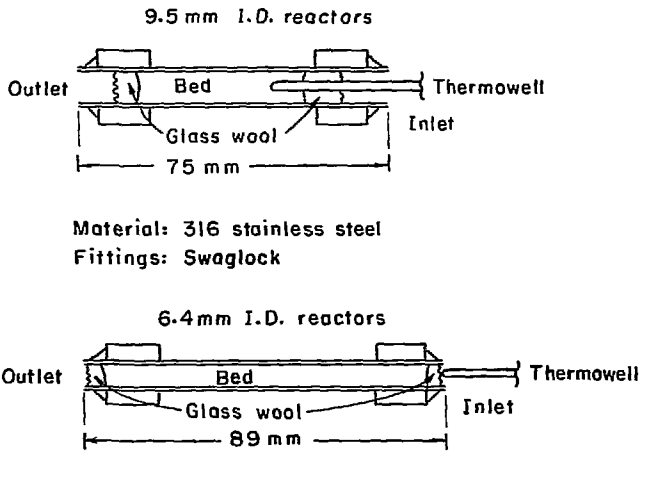

Fig. ii-3. Experimental reactors.

1450°C. A West Instrument Corporation set-point controller, Model J, was used to maintain the desired temperature level. A platinum/platinum - 13% rhodium thermocouple located in the furnace chamber exterior to the Mullite tube was the sensing element for the controller.

c. Fixed-bed temperature measurement.

A more accurate measure of the catalyst/absorbent temperature was obtained from the Chromel/Alumel thermocouples placed in 316 SS thermowells which extended into the inlet and outlet of the 32-mm reactor. Only an inlet thermocouple was used in the smaller reactors. When inert gas was passing through the bed, the inlet temperature was approximately 3°C degrees less than the outlet at an absolute level around 370°C. Figure ii - 4 shows a trace of the furnace and outlet reactor temperatures as a function of time as the reactor heats up to 370°C. The inlet and outlet reactor thermocouples were monitored with the Leeds and Northrup Recorder used to trace the gas chromatograph (G.C.) peaks. The furnace temperature was initially monitored with a modified Varian Aerograph G-10 Recorder. In the latter part of the experimental program this temperature was also monitored with the Leeds and Northrup Recorder. The switching diagram for this circuitry is shown in Figure iii - 6.

3. Heat-traced flow lines.

a. Reactor exit line.

After Run 15 the 6.4-mm exit tube was wrapped with fiber glass sheathing and heat-traced over the last 220-mm to prevent sulfur

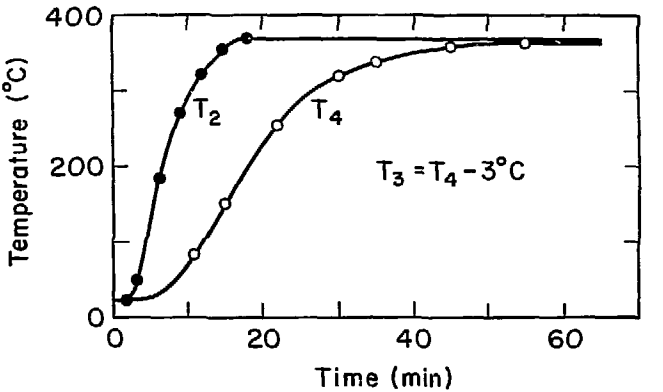

Fig. ii-4. Temperature profiles of furnace chamber and reactor during heat up.
(Data from Run 12)
T_2 = furnace chamber temperature
T_4 = reactor outlet temperature
T_3 = reactor inlet temperature.

precipitation. This section was inside the Mullite tube. The Nichrome wire-fiber glass heat tape was powered with a Powerstat Variac, maximum rating 120 volts, 7.5 amps. A setting of 55 volts was used. This setting gave a temperature of 160°C at the exit end of the 6.4-mm tube. The tape burned out following Run 27. A second heat tape was used for the remainder of the experiments. A setting of 15 volts was used. This gave a temperature of 195°C at the exit end of the 6.4-mm tube with the new tape. These temperatures prevented major sulfur precipitation in the exit reactor line. Since the equilibrium partial pressure of sulfur at 150°C in an inert gas at 1 atmosphere is 230 ppm (Tuller, 1954), only a sulfur concentration greater than this would have produced precipitate in the exit reactor line.

b. Outlet and inlet lines.

The exit lines from the condenser to the bubbler and gas chromatographs were heat-traced with fiber glass tape and Nichrome wire after Run 26. Heating pads of fiber glass and Nichrome wire were also placed over the gas sample valve and switch valve located in the gas chromatographs. The line temperature was around 40°C. The valve temperatures were around 35°C. These temperature levels prevented condensation of water in the exit lines but allowed some condensation of ammonium salts and sulfur which were not condensed in the air-cooled condenser between the reactor exit line and the outlet system line. The Nichrome wire was powered with a Variac, maximum rating 110 volts, 5.0 amps The typical setting to give the above temperture was 90 volts.

The reactor inlet lines, including the gas manifold, were heat-traced in a similar manner after Run 32. The heat tracing was required to prevent slight H_2O condensation in the inlet line noted during earlier runs. This line was powered with a G.R.C. Variac, maximum setting 110 volts, 5.0 amps. A setting of 110 volts gave line temperatures of 35°C.

4. Constant-temperature water bath.

A constant-temperature water bath was made with an insulated 300-ml round bottom, 3-neck flask. The He diluent passed through the bubbler and then into the gas manifold where other gases were added. A contact thermometer and relay controller were used to control the water bath temperature. The Glas-Col heater was powered with a Powerstat Variac, maximum rating 110 volts, 3.0 amps. Typically a setting around 10 volts was used. Water bath temperatures were around 22 - 24°C. Since the water level was only 70-mm above the fritted glass bubbler, the He was only about 60 - 70% saturated with water.

5. Gas-feed system.

Each gas was metered from a gas cylinder through a needle valve and a glass capillary tube and then into the gas manifold mixer. Table ii - 1 lists the source and purity of each gas used. Except for the He, all of the cylinders used a 20 psig feed pressure. Pressure taps leading from the inlet and outlet of the capillary were connected to U - tube manometers. From Runs 1 through 16 water was used in the manometers. After Run 16, Silicone Oil (Dow Corning 704 Fluid) was

used. The capillaries were calibrated with either the specific gas or N_2 at atmospheric pressure and ambient temperature with a soap-bubbler meter. N_2 was used to calibrate the capillaries used for SO_2, H_2S, NH_3, and NO since all were found reactive with the soap solution. The measured pressure drops were corrected for differences in viscosity between the gases. Since the gases were never fed in all together, some flowmeters were calibrated for more than one gas. For all the gases except H_2 and CO, the lines from the gas cylinder to the gas manifold was 316 S.S. Copper was used for H_2 and CO. Stainless steel needle valves (NUPRO "S" Series Fine Metering Valves) with inlet filters (NUPRO "F" Series Inline Filters) were used with the capillary flowmeters. The system diluent, He or N_2, was metered in with a glass-ball rotometer (Manostat Corp. No. 36-541-12). The control on the water feed rate was the water bath temperature. The pressure tap lines from the manometers to the capillaries were Tygon tubing. Catch pots were built in the lines to prevent manometer fluid from contaminating other equipment if a system upset occurred. The gas manifold was a 25-mm x 25-mm X 127-mm block of 316 stainless steel. Hoke valves, attached directly to the manifold, were connected with each flowmeter line. The system diluent entered through the 6.4-mm center bore. All of the tubing in the remainder of the system was 316 S.S. except a short Tygon section connecting the outlet condenser with the outlet system line. The main gas stream tubing 6.4-mm I.D. The sample lines were 3.2-mm I.D. and the tubing around the switch and gas sample valves in the G.C. system was 1.6-mm I.D.

Table ii - 1. Gas-Cylinder Specifications.

GAS	PURITY & SPECIFICATIONS	SOURCE
He	99.99% Min.	Univ. of Calif., Berk., gas.
N_2	99.99% Min.	Univ. of Calif., Berk., gas.
NO	99.0 % Min.	Liquid Carbonics Co.
N_2O	98.0 % Min.	Matheson Gas Co.
NO_2	99.5 % Min.	Baker Chemical Co.
NH_3	98.37% NH_3, 1.00% H_2, 0.57% N_2, 0.06% O_2	Matheson Gas Co.
SO_2	99.98% Min.	Matheson Gas Co.
H_2S	99.6 % Min.	Matheson Gas Co.
COS	99.4 % Min.	K & K Laboratories, Inc.
CO_2	99.5 % Min.	Matheson Gas Co.
CO	99.5 % Min.	Matheson Gas Co.
H_2	99.9 % Min.	Matheson Gas Co.
O_2	99.99% Min.	Univ. of Calif., Berk., gas.

6. Condensers.

a. Removal/regeneration condenser.

A 9.5-mm X 98-mm section 316 S.S. tubing was connected to the 6.4-mm reactor outlet line. Air was blown over this section during the runs. The ammonium salts precipitated primarily in this unit. Also trace amounts of sulfur and water precipitated from the gas stream if they were high in concentration. This unit was installed after Run 15. Prior to this run a section of Tygon tubing served the same function.

b. Water-collection condenser.

At the start of each run after Run 13, the catalyst was dried for 3 hours. The desorbed water was collected in a U - tube emersed in a dry ice-acetone bath. The U - tube was Pyrex glass. It was connected to the reactor outlet line and system outlet line with Tygon tubing. Typically, the glass tube was removed and weighed three times during the drying period to determine the initial catalyst water content.

7. Outlet-line apparatus.

a. Capillary flow restriction.

In order to divert a sample flow from the inlet and outlet gas lines, capillary restrictors were placed in the main flow stream and the sample loop bypass stream. The position of each is shown in Figure ii - 1. This produced a system pressure drop of 25-mm Hg for the 32-mm reactor and 100-mm Hg for the smaller reactors. This provided a split of 2.3/100 for the inlet sample flow/total inlet flow and of 1.8/100 for the outlet sample flow/total outlet flow.

b. Gas scrubber.

After exiting the flow restriction capillary the gases then passed to a 250-ml catch pot and then into a 250-ml fritted-glass bubbler. The bubbler was used to remove wither NH_3 or HCl. This apparatus is discussed in more detail in Chapter III.

CHAPTER III

Analytical Systems

A. Gas Analysis.

A large number of reactive gases were present simultaneously in samples which had to be analyzed in this experimental study. The presence of the following gases was possible: H_2, H_2O, N_2, NH_3, N_2O, NO, H_2S, COS, SO_2, CO, CO_2, and O_2. One approach was to provide a selective analyzer for each species. Although reliable instruments for this purpose can be purchased, their cost was prohibitive for this work. A second approach was to use instruments which detect and quantify all of the gases. Two such instruments are the Mass Spectrometer and the Gas Chromatograph. Gas chromotography was selected for gas analysis because of its simplicity and availability.

1. Detector selection.

Gas chromatographs can be tailored to a wide range of applications. The types of detector and column packing vary with the specific application. The combination of gases listed above can be analyzed best with a thermal conductivity cell (Katharometer), an electron capture detector, or a gas density detector. The gas density detector, although good for corrosive gas analysis, is not recommended for use with helium, the system diluent in this work. The electron capture detector is recommended for gas concentrations less than 10 ppm. It can be modified to work in the range of 10 to 10^4ppm. With this modification its sensitivity decreases to that obtained with the thermal conductivity cell (Mitchell, 1972). Two available

gas chromatographs with thermal conductivity cells were used in this study.

A major deficiency of thermal conductivity detectors is that they react in varying degrees with certain gases. Oxygen and sulfur compounds are especially reactive. Rhenium-tungsten and nickel filaments were used because of their low reactivity toward oxygen and sulfur compounds and their corrosion resistance (Gow-Mac). The rhenium-tungsten filament has the added advantage of a relatively high sensitivity.

2. Column selection.

A literature review and private conversations with technical representatives of Varian Aerograph revealed that no one column packing would produce all of the desired gas separation. Therefore, two packed columns connected in series were required. Polymer packing which has a small degree of polarization is effective for the separation of H_2, CO_2, N_2O, NH_3, H_2S, COS, SO_2, and H_2O, Group I. Molecular Sieve packing effects the separation of H_2, O_2, N_2, NO, and CO, Group II.

In the first third of this work, Runs 1 through 16, Chromosorb 104, a cross-linked polystyrene matrix with no coating, was used for separating the Group I gases. The major reason for selecting Chromosorb 104 was that it reportedly separated NO_2 from CO_2, H_2S, COS, and SO_2. However, it irreversibly adsorbs NH_3 and H_2O. Since the analysis of these two gases was important in the later part of the expermental work, after Run 16, Porapak R packing was substituted for the Chromosorb 104. Porapak R is a porous cross-linked polymer

bead packing made with a small amount of polar monomer. This packing separates all of the gases in Group I, but does not pass NO_2. As expected, NO_2 was not found in the first part of this work, so this is not a major limitation.

Porapak R was selected after screening seven different columns. The hardest criterion to meet was to find a column which gave the desired peak separations with a minimum amout of tailing. The H_2O, SO_2, and NH_3 peaks generally had tailing, NH_3 being the worst in this regard. A qualitative comparison of NH_3 peaks on these columns is given in Table iii-1.

Table iii-1 Qualitative evaluation of low concentration NH_3 peaks on several columns.*

Column	Dimensions cm x cm	Temperature (°C)	Comments
Chromosorb 104	0.635 x 305	120	Tail continued for over 5 min.
Porapak Q	0.318 x 214	110	Tail ended after 5 min.
Porapak R	0.318 x 92	92	Almost no tail after 5 min.
Porapak T	0.318 x 92	120	Significant tail after 4 min.
Porapak Q + Porapak R	0.318 x 214 0.318 x 92	130	Almost no tail after 4 min.
Carbowax	0.635 x 305	155	Tail continued for over 5 min.
Carbowax on Firebrick	0.635 x 153	156	Tail continued for over 5 min.

* NH_3 concentrations ranged from 1-4% in this study.

Only the Porapak R column gave a reasonable peak for NH_3 at these low levels. Although quantification was possible at the 1 to 4% level, lower concentrations produced peaks which were primarily of qualitative value. Wilhite (1968) also reports that tailing of NH_3 occurs at low temperature programming. Landau (1973) reports tailing of NH_3 at low concentrations on a combined Porapak R and polyethyleneimine-coated Porapak R. From the referenced and present work it is obvious that the quantitative analysis of low NH_3 concentrations with a gas chromatograph has not yet been achieved. The NH_3 peaks were primarily used to confirm the presence of NH_3 qualitatively. A bubbler containing an HCl solution collected the NH_3 to give a cumulative quantitative sample. This procedure will be described in section B.1.

Molecular Sieve 5A packing, a synthetic zeolite, separated Group II gases. It was selected for its ability to separate O_2, N_2, NO and CO without giving excessively long tailing patterns for NO. Prior to Run 17, H_2 was also separated with this packing. In the later part of this work, the H_2 peak on the Porapak R column was monitored since this column was connected to the more sensitive rhenium tungsten detector.

3. Column performance.

Gas chromatograms of the two G.C. systems, Chromosorb 104 in series with Molecular Sieve 5A and Porapak R in series with Molecular Sieve 5A, are given in Figures iii-1 and 2.

Since all of the gases were never present in any one chromatogram in either system, these figures are a composite of several samples. A two-pen recorder allowed simultaneous detection of peaks from both

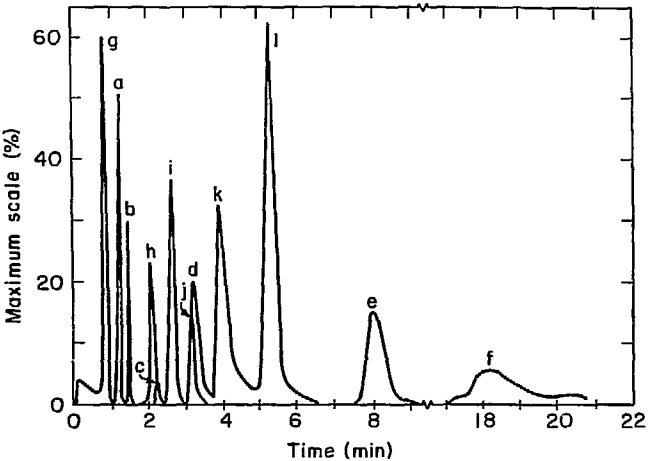

Fig. iii-1. Gas chromatographic trace: Chromosorb 104-molecular Sieve 5A.

	Chromosorb-104					Molecular Sieve 5A			
	Gas	%	Attn.	Span (mV)		Gas	%	Attn.	Span (mV)
a.	CO_2	1.0	8	1	h.	H_2	3.6	1	0.2
b.	N_2O	0.80	8	1	i.	O_2	1.0	1	1
c.	COS	0.34	2	1	j.	N_2	0.05	1	0.2
d.	H_2S	2.0	4	2	k.	NO	0.32	1	0.2
e.	SO_2	0.53	2	1	l.	CO	0.37	1	0.2
f.	NO_2	3.1	2	2					
g.	H_2, O_2, N_2, NO, CO								

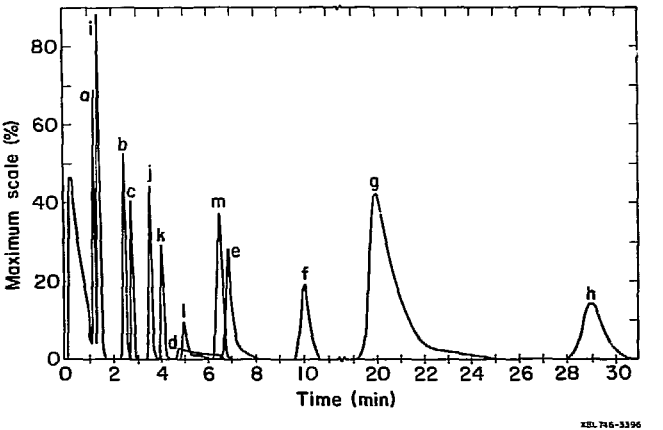

Fig. iii-2. Gas chromatographic trace
Porapak R - molecular sieve 5A.

	Porapak R			
	Gas	%	Attn.	Span (mV)
a.	H_2	2.0	1	0.2
b.	CO_2	2.58	1	10
c.	N_2O	2.0	1	10
d.	NH_3	0.24	1	1
e.	H_2S	0.92	2	1
f.	COS	0.34	1	1
g.	H_3O	1.3	1	1
h.	SO_2	0.71	1	1
i.	O_2, N_2, CO, NO			

	Molecular Sieve 5A			
	Gas	%	Attn.	Span (mV)
j.	O_2	0.52	1	0.5
k.	N_2	0.17	1	0.2
i.	NO	0.25	1	0.5
m.	CO	4.3	2	1

chromatographs. Since the recorder had only one integrator, which could be switched to either pen, it was advantageous to have the peaks eluting at different times. In the first system, Figure iii-1, all peaks except N_2 from the Molecular Sieve, and H_2S from the Chromosorb 104 elute at different times. In this case the N_2 peak area was manually calculated while the H_2S peak area was counted by the integrator. The excessive tailing of NO and CO is both a reflection of noise at the 0.20mv span and some tailing. The tailing of NO_2 even at high concentrations permitted only qualitative analysis. In the second system, Figure iii-2, the NH_3 peak area was either manually calculated or only used for confirming the presence of NH_3. Either the CO or H_2S peak area was manually calculated while the other was counted by the disc integrator. The detailed description of the sampling techniques and equipment arrangement is given in section 5.

4. Column preparation and treatment.

The 305-cm x 6.4-mm Chromosorb 104 column, mesh size 60 to 80 (250-177 μm),316 stainless steel (S.S.) wall, was purchased directly from Varian Aerograph. The packed column was pretreated by heating to 230°C under a helium atmosphere for 12 hours.

The 305-cm x 6.4-mm Porapak R column, mesh size 80 to 100 (177-149 μm) 316, S.S. wall, was made in this laboratory. The steel column was cleaned with the following sequence of solvents:

Table iii-2. Sequence of solvents for cleaning column casing.

Acetone	300 ml
Chloroform	300 ml
Toluene	375 ml
Methanol	175 ml
Acetone	100 ml

The tubing was dried in a helium atomosphere before it was packed. Then while the tubing was still straight, the packing was added. Constant rapping insured even filling. Glass wool plugs held the packing in the column. The column was pretreated by heating to 245°C in a helium atmosphere for 12 hours.

The 305-cm x 6.4-cm Molecular Sieve 5A column, mesh size 30 to 50 (500-250 μm), S.S. wall, was made in this laboratory. The same cleaning and packing procedures described for the Porapak R column were used. The initial column pretreatment was that reported by Dietz (1968). In addition to desorbing all gases, Dietz found that the column must be treated to prevent excessive tailing at low NO concentrations.

Dietz describes his technique as one which first adsorbs NO on very active sieve sites. This adsorbed NO is permanently fixed to these sites by reacting it with O_2 to form NO_2 in situ. This procedure eliminates later adsorption of NO by active adsorbing sites, thereby greatly reducing NO tailing.

The summarized pretreatment described by Dietz is listed below.

1. Activate the sieve by heating to 300°C under vacuum for 20 hours to desorb all gases.
2. Break the vacuum at 300°C with NO, maintaining a low NO flow for 1 hour to saturate the column.
3. Cool the column to 20°C continuing to saturate with NO for another hour.
4. Flush the column with Helium for ½ hour to remove all nonadsorbed NO. Add a stream of O_2 at 25°C to form NO_2 on the active sites.
5. Raise the temperature to 100°C with the O_2 atmosphere and hold for ½ hour to insure that O_2 and NO react.

With this technique Dietz reported NO detection limits of 12 ppm.

The same pretreatment in the present study did little to decrease the NO tailing. Figure iii-3 shows a 7.6% [NO] peak with excessive tailing. A more detailed look at Dietz's work revealed that the column was subjected to temperature programming up to 250°C. In contrast, the operating column temperature in this work was 120°C. Joithe (1972) found that the presence of NO_2 on adsorbed Molecular Sieve 13X aids in the adsorption of NO at 25°C. Similar behavior may occur on the Molecular Sieve 5A if the adsorbed NO_2 is not strongly held. By heating the column to 250°C, Dietz desorbed the majority of the loosely held NO_2. Since the maximum column temperature in this study was only 130°C, the loosely held NO_2 is thought to have been present and partially reactive toward the NO in the sample. Higher temperatures were tested to find the point where loosly held NO_2 would be desorbed and tightly held NO_2 would be retained. The temperature of 250°C gave the best NO peaks.

Figure iii-4 is a trace of an NO peak. This peak is 1.17% and uses the 0.5 mv span yet still has a smaller degree of tailing than the 7.6% [NO] shown in Figure iii-3. The pretreatment for the Molecular Sieve 5A column is therefore that reported by Dietz plus:

6. Heat the column to 250°C under a helium atmosphere for 8 hours.

During Run 14, the NO peaks began to tail and large discrepancies developed between the inlet NO concentrations obtained by G.C. analyses and those obtained from flowmeter reading. The column was

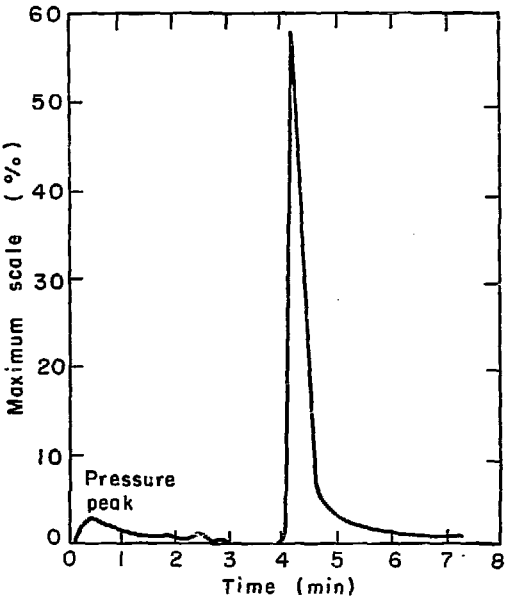

XBL746-3400

Fig. iii-3. NO peak from Molecular Sieve 5A column treated with Dietz method.
[NO] 7.6%
Span 2 mV
Attn. 2
System: Chromosorb 104-Molecular Sieve 5A

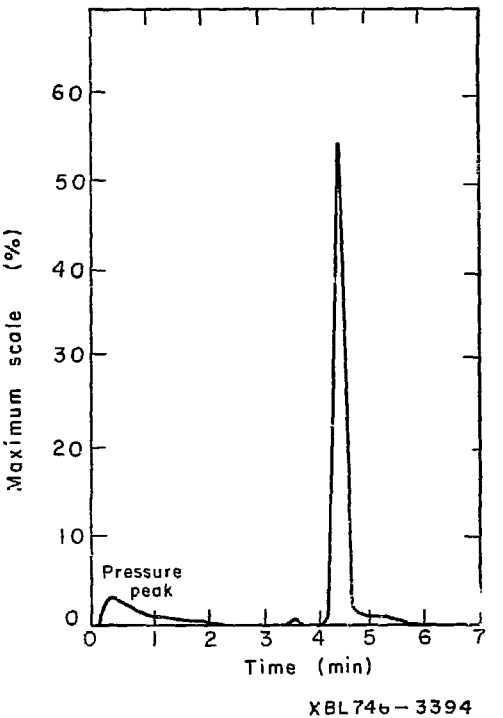

Fig. iii-4. NO peak from Molecular Sieve 5A column treated with 6-step pretreatment.
[NO] 1.17%
Span 0.50 mV
Attn. 1
System: Chromosorb 104-
Molecular Sieve 5A

regenerated following the six-step pretreatment described above, but this did not lead to complete NO sample elution or sharp peaks. Several variations of this procedure failed to regenerate the Molecular Sieve 5A column successfully.

A second, identical column was made. After the six-step pretreatment this column produced good quality NO peaks. This same column-poisoning phenomenon occurred following Run 30. As before a new, identical Molecular Sieve column, pretreated as described, produced good quality NO peaks.

Before Run 14 all of the sulfur compounds were sent directly to Molecular Sieve 5A column where they were irreversiby adsorbed. These adsorbed compounds are suspected of poisoning the Sieve. After Run 16, a bypass valve was installed after the Porapak R column to dump these compounds and water before they entered the second column. This is described in section 5. Several times after installation this valve was not switched at the proper time, allowing the sulfur gases and water to pass into the Sieve causing a poisoning similar to the first case.

5. Chromatographic, recording and integration equipment.

The columns and detectors discussed above were housed in the following specific chromatographs.

Table iii-3. Gas chromatographic equipment.

Position in Sequence	Column 1	Column 2
Manufacturer	Varian Aerograph	Varian Aerograph
Model No.	90-P	A-90-P
Column	Chrom.104 Por R.	Molecular Sieve 5A
Detector	Re/W	Re/W Nickel
Column Temp. (°C)	100	85 120
Detector Temp. (°C)	120	165 155
Filament current (ma)	180	180 180
Helium Carrier (ml/min)	80	80 80
Helium Reference (ml/min)	7.1	7.1 7.1

In the first third of the study, through Run 16, the two machines were connected in series. The entire effluent from the Chromosorb 104 column was fed into the Molecular Sieve 5A column. In the last part of the work the two machines were interconnected to allow both series and parallel operation. The columns were operated in the series mode until the wave of Group I gases had left the first column and entered the Molecular Sieve 5A column. A switch valve arrangement, shown in Figure iii-5 then allowed the other gases which separated on the first column to be discarded before they passed into the Molecular Sieve 5A column. It also provided a separate and parallel helium carrier for the Molecular Sieve 5A column after the gases to be separated on it had eluted from the first column. The 6-port Varian Quad-ring valve was switched at 2 minutes after sample injection, Figure iii-3. The resulting pressure surges in both columns rapidly decayed.

A Leeds and Northrup Speedomax XL Recorder 600 Series with a Series 2000 Disc Integrator was used to record the peaks and their areas. The recorder has two channels one of which is connected to the integrator. A switching arrangement shown in Figure iii-6. enabled the integrated channel to be used on either column. In this way, the output signals from both columns could be monitored simultaneously and the peaks from both columns could be integrated as long as they had different retention times. The channel without

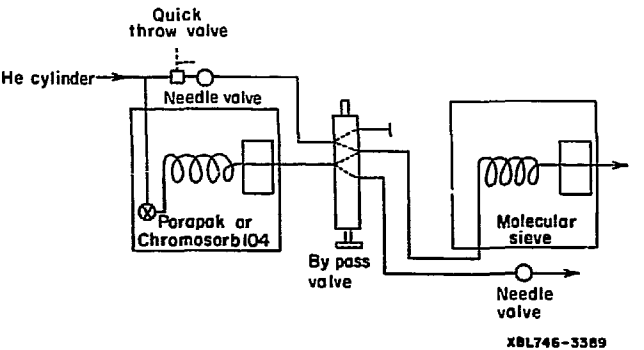

Fig. iii-5. Valve system for chromatographs.

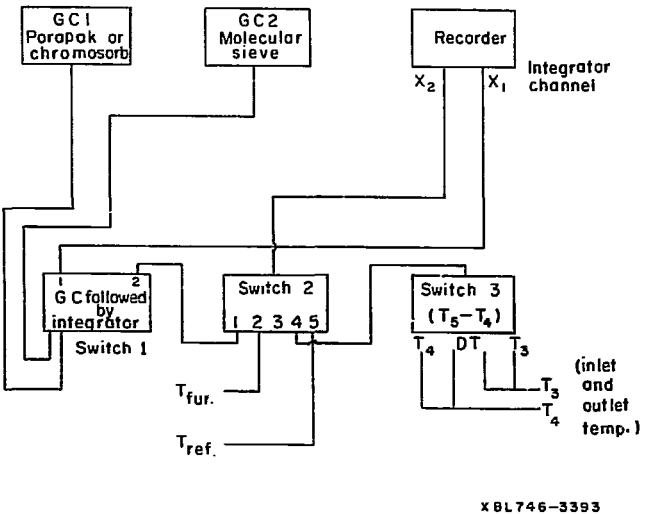

Fig. iii-6. Switch diagram for two-pen recorder.

the integrator was also used for monitoring the voltage output from various thermocouples around the system.

6. Gas sampling.

The gas samples were injected into the column with a 6-port Varian Aerograph Quad-ring valve. Prior to Run 8, all samples were collected in nominal 2-ml pyrex gas sample loops with teflon valves and transferred to the G.C. Prior to purging these loops with the carrier, the connecting lines between the valve and the loops were evacuated and filled with helium. After Run 8, a continuous sample purge was maintained in a 2-ml, 316 stainless steel sample loop. This could be either the inlet or outlet sample. The 6-port valve was again used for the sample injection.

7. Calibration and detection limits for G.C. analyses.

The response of the G.C. columns to gases was determined by passing a stream of a particular gas at atmospheric pressure through the 2-ml sample loop and then to a bubbler. After at least 5 minutes of purging, the response for that gas was recorded several times. In all cases except H_2 and H_2O, 100% gas concentration was used. The number of integrator counts is multiplied by the product of the span and attentuation to give the relative area. The standard areas and their relative standard deviations are given in Table iii-4. The columns were not recalibrated on a regular basis but rather when system changes were made or when large discrepancies developed between the concentrations calculated from the flowmeter readings and the G.C. values for inlet gas samples. The large standard deviation for SO_2 in Table iii-4, 11.6%, represents the difference

between two calibrations 5 months apart.

The calibrations presented in Table iii-4, are for a sample loop temperature of 21.1°C. When the outlet lines and sample loop were heat traced, after Run 26, the temperature was 58.9°C. At this point, the calibrations were adjusted down by the factor 1.128, the ratio of absolute temperatures. A check was made with 0.195% O_2 when the temperatures were 22.8° C & 57.8°C. The predicted ratio was 1.12 and the experimental ratio was 1.17, within 5%.

Table iii-4. Percent standard deviation in gas chromatographic standards.

GAS	COLUMN	PERCENT STANDARD DEVIATION	RELATIVE AREA
CO_2	Porapak R	0.41	142,933
	Chromosorb 104	0.88	148,838
N_2O	Chromosorb 104	0.14	129,408
COS	Porapak R	0.45	161,152
	Chromosorb 104	0.39	185,940
SO_2	Porapak R	12.0	148,304
	Chromosorb 104	2.0	177,152
H_2S	Porapak R	1.1	133,424
	Chromosorb 104	0.60	112,384
H_2O(1%)	Porapak R	7.9	2,695.3
NH_3	Porapak R	0.53	88,062
H_2(1%)	Porapak R	4.4	24.74
	Mol. Sieve 5A	12.0	6.94
N_2	Mol. Sieve 5A	0.34	31,725
O_2	Mol. Sieve 5A	0.34	28,592
CO	Mol. Sieve 5A	0.22	30,387
NO	Mol. Sieve 5A	0.74	28,592
NO_2	Chromosorb 104	(Only qualitative value)	

In addition to the calibration values, the detectable limits of the most important gases were determined. The detection limits of the remaining gases were estimated. In the context of this work, the detection limit is the lowest concentration which can be determined within an accuracy of about 25%. Table iii-5 lists the detection limits and the elution times of the gases. The Molecular Sieve 5A times are for the Porapak R-Molecular Sieve 5A system. The high detection limit for H_2 is a result of the close thermal conductivity of He and H_2. The high limits for NH_3, H_2O and SO_2 on the Porapak R and NO_2 on Chromosorb 104 columns result from the tailing of each gas.

8. Interactions of gases in chromatographic columns.

The discussion in this chapter so far has centered on analysis of individual gases with no mention of samples containing multiple reactive gases. Unavoidable gas interactions were found when multiple gases were analyzed. These interactions resulted in lower concentrations being reported for some gases. This section discusses the interactions and the techniques used to estimate gas concentrations correctly.

In the initial stages of this work multiple gas streams were metered into a helium diluent. This mixture was then sampled and used to determine the conditions necessary for peak separation. During this work it was noted that the gas concentrations calculated from the flowmeter readings did not always correspond to the chromagraphic values. This was noticed especially when there was a combination of H_2S and SO_2 or NO and O_2. These proved to be the two

major interactions. A secondary interaction was the effect of H_2O on the H_2S/SO_2 interactions.

Table iii-5. Detection limits of gases.

GAS	ELUTION* TIME (min)	COLUMN	DETENTION LIMIT(ppm)	ESTIMATION TECHNIQUE
H_2	2.0	Molecular Sieve 5A	6,000	Direct (2/14/73)
	1.15	Porapak R	2,000	Direct (Run 42)
CO_2	1.2	Chromosorb 104	100	Direct (Run 13)
	2.50	Porapak R	100	Direct (Run 28)
N_2O	1.4	Chromosorb 104	100	Estimate from CO_2
	2.70	Porapak R	100	Estimate from CO_2
NH_3	4.7	Porapak R	2,000	Direct (4/10/73)
H_2S	3.2	Chromosorb 104	150	Estimate
	6.5	Porapak R	150	Direct (Run 39)
COS	2.1	Chromosorb 104	100	Direct (Run 13)
	9.7	Porapak R	200	Direct (Run 30)
H_2O	18.8-19.8	Porapak R	2,500	Direct (Run 29)
SO_2	7.7	Chromosorb 104	250	Direct (Run 13)
	27-29	Porapak R	800	Direct (Run 29)
NO_2	17.5	Chromosorb 104	10,000	Estimate (5/5/72)
O_2	3.3	Molecular Sieve 5A	40	Direct (8/18/72)
N_2	3.9	Molecular Sieve 5A	40	Direct (8/18/72)
NO	4.9	Molecular Sieve 5A	200	Direct (8/14/72)
CO	6.2	Molecular Sieve 5A	200	Direct (Run 13)

*Elution time for low-concentration samples. Actual values at 100% level are slightly greater.

In view of the sulfur-formation reaction between H_2S and SO_2, these gases were never used together in the inlet stream. In two of the later runs, 37 and 38, there were outlet samples in which both

were present. In this case, however, one was much greater in concentration than the other and there was no noticeable interaction.

There was approximately a 10% loss in the SO_2 peak area when water was in the same sample. This was caused by a definite broadening of the peak which increased the SO_2 detection limit. The formation of sulfurous or sulfuric acid in the column may have been the cause for the slower desorption. When H_2O and SO_2 were present in the inlet, the SO_2 flowmeter value was used to determine the inlet SO_2. The outlet samples only had SO_2 and H_2O present in those runs in which the catalyst/absorbent was deactivated.

Since the highly detectable H_2S and COS breakthroughs must precede that of SO_2 (Chapter IV, Section E.1.b.), low SO_2 concentrations did not exist in the outlet during the removal steps. After the SO_2 breakthrough, its measured concentration was increased by 10% to compensate for the analytical loss.

Prior to Run 25, NO and O_2 were never present together in either an inlet or an outlet gas stream. In the majority of the following runs, both were present in the inlet gas stream in concentrations of NO from 0.3% to 0.5% and of O_2 from 0.5% to 1.0%. In these runs, the flowmeter readings for each gas were used to obtain their inlet concentrations. Typically the outlet streams from these reactions contained neither NO nor O_2. In some of the runs where the catalyst/absorbent became deactivated, however, the run was continued until both O_2 and NO eluted. In order to determine the extent of interaction of NO and O_2 on the G.C. column a separate study was made.

After Run 30, O_2 (0.22%) and NO (0.56%) were simultaneously

analyzed on what was found later to be a poisoned Molecular Sieve 5A column. Three samples reported an average of only 73% of the O_2 flowmeter level and only 54% of the NO flowmeter level. When the O_2 was cut off, the average NO level in three samples was still only 54%. In this case, the apparent loss of sample was due to the NO_2, H_2O, and sulfur compounds adsorbed to the sieve.

When the new Molecular Sieve 5A column was made and pretreated as described in section 4, simultaneous sampling was still not quantitative. Four separate samples of [NO] from the Molecular Sieve averaged 0.48% for an NO flowmeter level of 0.50%. This 4% loss is within experimental error and confirmed that NO could be analyzed separately. Three inlet samples with both NO and O_2 present in Run 31, the first run following the new column installation, reported losses of both NO and O_2. The ratio of the G.C. to flowmeter concentrations for NO averaged 0.88 and the G.C. to flowmeter concentration for O_2 averaged 0.77. The ratio of the NO concentrations for two inlet samples in Run 33 averaged 0.58, while that for O_2 averaged 0.65. The NO and O_2 concentrations were the same in both runs. Subsequent runs with NO and O_2 in the inlet gas showed the same trend. As with the study on the poisoned column it appears that some NO_2 is formed which is subsequently reactive with later NO samples. An estimate of the final NO and O_2 in the outlet samples was made using the factors of 0.54 for NO, and 0.73 for O_2 mentioned earlier. Since a constant correction factor was not found, the NO and O_2 removals for the runs which resulted in deactivated catalyst are at best only estimates of the actual value. The important runs with active catalysts were not affected. Inlet NO and O_2 values from

all runs were obtained from the flowmeters as discussed earlier.

Joithe (1972) has shown that Molecular Sieve 13X can catalyze the oxidation of NO to NO_2, and that NO_2 can also aid in the adsorption of additional NO. Similar, if not the same, reactions are undoubtedly occurring on the 5A sieve used in this work. Since the NO_2 is irreversibly adsorbed, there is a net loss of nitrogen oxides and O_2 in the column when O_2 is present. Fortunately, this interaction was not significant when both O_2 and NO were present at very low concentration, less that 1000 ppm. The lack of interaction was evidenced by the detection of low NO and O_2 concentration in the effluent streams from the deactivated catalyst/absorbent.

B. Wet-Chemical Gas Analysis.

In addition to the chromatographic gas analyses discussed in section A, a fritted-glass bubbler was used to absorb NH_3 in the removal runs and SO_2 in the regeneration runs. Ammonia collection was necessary since the G.C. was not able to determine accurstely the low concentration present. Sulfur dioxide collection was necessary during regeneration, especially in the runs with short residence times. In these runs, the SO_2 eluted from the entire bed more rapidly than the G.C. sampling could follow.

1. Ammonia collection.

Beginning with Run 19, the effluent gas from all runs in which NH_3 could be formed was passed into a fine fritted-glass bubbler. T^+ solutions in the bubbler ranged from 0.02747 N to 0.05382 N HCl. The liquid height above the bubbler base was 90-mm with 150-ml of

acid and 115 mm with 225 ml of acid. The concentration of acid depended on the total amount of NH_3 expected during a run. At least 150 ml of acid was used. The scrubber efficiency with 225-ml of solutions and 3.6% inlet NH_3 was 93%. This was determined from both G.C. and flowmeter NH_3 measurements. After the run, a 25-ml aliquot of the scrubber solution was titrated with NaOH solution to determine the NH_3 pick-up. The NaOH and HCl solutions were standardized against potassium acid phthalate ($KHC_8H_4O_4$) solutions.

2. Sulfur dioxide collection.

An NaOH solution was used to scrub the regeneration gases in the same way in which the NH_3 was removed. The concentration ranged from 0.08024 to 0.9885 N NaOH. This solution was titrated with HCl and the endpoint determined with a pH meter. The efficiency of the scrubber was 93%. This efficiency was determined by using 3 fritted-glass bubblers in series to remove all of the 0.54% SO_2 from the inlet gas stream.

C. Catalyst/absorbent analysis.

After each run, the catalyst was qualitatively tested for its magnetic properties and color. Intermittent tests were run to determine the presence of iron sulfide. Quantitative tests were made at the end of the experimental series to determine the amount of sulfur in the catalysts.

1. Qualitative tests.

A magnet was passed over the catalyst after the run to detect the presence of Fe_3O_4. Typically all of the catalyst material after

reduction, removal reactions, or regeneration reactions exhibited some Fe_3O_4.

The fresh Fe_2O_3 catalyst was bright red. After either reduction or removal reactions in which no deactivation occurred, the catalyst was black. The Chemical Handbook gives black as t color for FeS, FeO, and Fe_3O_4. When deactivation occurred the catalyst became a dull orange color. In the short-residence-time runs, after Run 36, the black particles were slightly more magnetic than the red.

The presence of FeS was determined by the evolution of H_2S when the catalyst was acidified with HCl.

2. Quantitative Tests.

An oxidation reaction similar to the regeneration runs was used to determine the amount of sulfur in the catalyst. All of the catalyst from each run was ground up and thoroughly mixed. A small sample, about 1 gram, was placed in the 0.95-cm reactor and heated to 677°C. A 1% O_2 stream oxidized the sulfur to SO_2 for 1 hour. The SO_2 was collected in an NaOH scrubber.

Table iii-6 gives a listing of the S to Fe ratio found with this technique. The value of S/Fe from the gas analysis is based on the net loss of sulfur from the gas stream less any sulfur which precipitated. Large discrepancies exist between these two estimates of the sulfur on the solid. The solid analysis reported in this work is that based on the calculated values. This method had less room for error than the stripping technique.

Table iii-6 Comparison of S/Fe ratios

Run	Calculated from Net SO_2 Absorption	Calculated from SO_2 Evolution at 676°C[2]
27	0.51	0.28
29	0.30	0.52
30	0.20	0.29
31, 32	0.57	0.58
35	0.57	0.76
36	0.94	0.76
37	1.01	1.06
38	0.25	--
39	0.96	0.64
40b, 40c	0.91	0.87
40d, 40e	1.00	0.75
41b, 41c	0.48	--
41d, 41e	0.65	--
42	1.30	1.12

D. Precipitate Analysis.

There were two basic types of precipitate which formed in the outlet line, sulfur and ammonia-sulfur salts.

These were first tested for their water solubility. The sulfur was insoluble and the salts were soluble. Some of the sulfur samples were heated to confirm that only a sulfur smell developed. When the salts were heated, an NH_3 smell developed. When an H_2S smell developed in conjunction with the NH_3, the solid was NH_4HS. When an SO_2 smell developed the solid was $(NH_4)_2SO_3$. In some cases, an NH_3 smell developed when the precipitate was dissolved in an NaOH solution, but no sulfur gases eluted upon either heating or acidification. This eliminated NH_4HS or $(NH_4)_2SO_3$ as the precipitate. Precipitation in a $BaCl_2$ solution of the salt confirmed the presence of $SO_4^=$. As much of the precipitate as possible was collected, but because of H_2O adsorption as well as precipitation after the condenser, a quantitative measure of the precipitate was not always possible.

E. Experimental Error.

The experimental error can be separated into six independent areas:

1. Gas chromatographic analysis
2. Integration of effluent gas profiles
3. Catalyst weight measurements
4. Capillary gas flowmeters
5. Condensate and/or precipitate in system lines
6. Effluent gas scrubbing with either HCl or NaOH solutions

1. Gas chromatographic analysis.

The error in the G.C. determinations vary with the gas and the column used. In the first part of this study, through Run 16, a Chromosorb 104 column was used to determine CO_2 and sulfur compounds. In the last part of this work, it was replaced with a Porapak R column which also separated H_2, NH_3 and H_2O. A molecular sieve 5A column was used to analyze the remaining gases. The relative percent error in the standard for each gas was given previously in Table iii-4. Except for H_2 and H_2O all gases were standardized at 100%. The large error in SO_2 and H_2O standarizations on the Porapak R column was due to erratic tailing patterns. The large error in H_2 on the molecular sieve column results because the signal is quite small and is therefore difficult to quantify accurately. The error was significantly lowered when H_2 was separated on the Porapak R column. The remainder of the gases had errors of less than 3%. The assumption of a linear scaling factor of these standards to lower concentration was used. To the extent that this assumption

does not hold, the actual errors will be greater than those presented.

2. Integration of effluent gas Peak Profiles.

Manual plotting and integration of peak profiles with time gave the total change in concentration of each gas for the run. The trapezoidal curve approximation technique was used for the integration. The greatest error in this part was associated with curve estimation, especially in short residence time runs where rapid breakthrough occurred. It is not possible to quantify this error.

3. Catalyst weight measurement

A Mettler balance, accurate to within 0.0001 g., gave negligible error in the actual weighing process. The loss of catalyst in the reactor and or the water content of the catalyst contributed greatly to sample weight error. When 3.2-mm pellets were used there was essentially no sample loss. With 1/4mm to 1/2mm sized particles some material was embedded in the glass wool plugs. Since glass wool looses binder when heated and frays quite readily when removed from the smaller reactors, the exact amount of material lost could not be determined. An estimate of this would be less than 0.5%.

Not until Run 19 was the catalyst dried for 3 hours at 370°C before use. These conditions were necessary to completely remove all of the adsorbed water. Before this run, the drying conditions varied from a vacuum oven at 115°C to drying at 370°C for 1 hour in the reactor. Typical water contents of the catalyst were around 2.5%. The first technique reported values from 1.8% to 2.1%. This would mean that the weight loss in runs before Run 19 were at least 0.5% in error.

Even though these two errors are very small it is of the order of the calculated weight changes from the reactions. This means that greater than 100% error may exist because of the uncertainty in water lost from the catalyst. After Run 19, the error was smaller in the water determination but when the smaller particles were used, the effect of weight loss again became important.

4. Capillary flowmeters.

All gases were metered into the helium diluent with capillary tube flowmeters. Helium was metered with a rotameter.

Maximum and minmum percent deviation of data points from the average straight line approximation for the flow characteristics are given in Table iii-7.

Table iii-7. Percent standard deviation in gas flowmeters.

GAS	Percent Standard Deviation Maximum	Minimum
CO	10	0.81
SO_2	5.5	1.3
H_2	4.1	1.3
H_2S	6.1	1.4
O_2	5.2	0.67
NO	7.3	1.1
NH_3	8.2	1.2
He	0.45	0.30

Maximum deviations reflect lower flows, while minimum deviations reflect higher flows. The lowest flows used in these calculation corresponded to the lowest percentages of each gas used in the study. The large CO error is present only in the first few runs where CO was below 0.5%. In the simultaneous removal runs, the

error would be less than 2%. NH_3 was fed only to check one reaction. The other maximum errors correspond to gas concentrations typically used in the simultaneous runs. Therefore, flowmeters reflect errors ranging from 2 to 7%.

5. Condensation and/or precipitation in system lines.

Appreciable errors in effluent gas concentrations resulted from condensation and/or precipitation in outlet lines. Sulfur precipitate was first noted in the outlet line in Run 1. Between Runs 1 and 12 only trace amounts were noticed. After Run 13, a large build-up of sulfur halfway between the reactor outlet and end of the outlet line was found. Reactions made in Runs 9-12 could have deposited some of this precipitate. Distribution of sulfur between these runs is at best a guess. A secondary heater was added to prevent sulfur condensation deep within the reactor tube. It maintained temperatures between 157°C and 270°C. In later runs, sulfur precipitated in a removable air cooled stainless steel condenser which could be cleaned and weighed. Sulfur-determination errors after Run 13 were about 5%. A second type of precipitate which developed was ammonia-sulfur salts, NH_4HS, $(NH_4)_2SO_3$, and $(NH_4)_2SO_4$. These precipitates were first noticed after Run 22. Collection of these in the air-cooled condenser was not as efficient as sulfur, since their condensation temperatures are lower. These salts sometimes condensed in the outlet sample line and sample loop of the G.C. Outlet lines were heat traced after Run 26. Still some precipi-

tate collected at the switch valve in the G.C. Quantitatively this was a small percentage of the total precipitate. Its effect on the H_2O, SO_2 and NH_3 levels was more pronounced. These gases adsorbed or reacted to form the precipitate.

6. Effluent gas scrubbing.

The HCl and NaOH scrubbers used to collect the SO_2 and NH_3, respectively, were only 93% efficient. A series of 3 bubblers was used to determine the efficiency for both NH_3 and SO_2 Standard solutions and titrations used to determine the amount of gas scrubber were within 5% experimental error.

7. Summary of experimental error analysis.

The main error in these experiments is associated with the measurement of the weight change of the catalyst over the run. In view of this, material balances to estimate the sulfur gained and the oxygen lost from the catalyst were done with the changes in gas composition. Since only an accurate measure of relative gas concentrations was required to calculate the percent removal this value has less than 5% error.

CHAPTER IV

Experimental Results

A. Initial Process Studies.

The initial studies confirmed that the proposed process chemistry was feasible. The 32-mm reactor and 3.2-mm Fe/Al_2O_3 catalyst/absorbent pellets were used in these studies.

1. Reduction of NO with CO over Iron Oxide.

The reduction of NO with CO over iron oxide was studied in seven different runs. N_2 was the only N-product measured. No N_2O was detected. The data are presented in Figure iv-1.

The main influence on the NO removal was the CO/NO ratio. The values of x listed for FeO_x are the arithmetic average of x at the beginning and end of each run. In all cases reported in the figure, except Runs 1a and 4, the catalyst was pre-reduced with CO. Fast (1965) presents equilibrium calculations for the Fe_2O_3, Fe_3O_4, Fe_xO, and Fe systems. Fe_2O_3-Fe_3O_4, Fe_3O_4-Fe_xO, and Fe_3O_4-Fe equilibria are possible. Below 550°C., only the Fe_2O_3-Fe_3O_4 and Fe_3O_4-Fe equilibria are present. Fe_3O_4 is a mixed Fe^{+2}-Fe^{+3} oxide which has an inverse spinel structure (Cotton, 1972). Therefore, under the above experimental conditions, the iron is a mixture of Fe^{+3}, Fe^{+2}, and Fe^0. The actual net valence state appears to have little effect on NO reduction. Similarly, there was no correlation between NO concentration, reactor temperature, or gas residence time and the NO removal within the ranges studied.

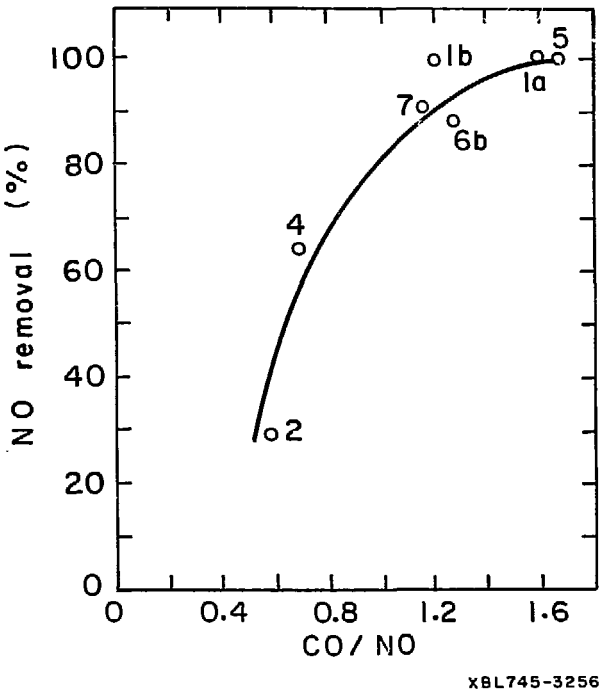

Fig. iv-1. Percent NO removal versus CO/NO over FeO_x.

Run		1a	1b	2b	4	5	6b	7
[NO] (%)		4.1	3.7	1.7	2.6	2.0	0.29	0.30
[CO] (%)		6.6	4.4	1.0	1.8	3.4	0.37	0.35
FeO_x,	x=	1.38	1.01	1.19	1.46	0.92	0.31	<0.10
Temp. (°C)		345	347	365	390	390	380	370
Res. time (sec)		0.88	0.88	0.37	0.40	0.40	0.39	0.39

Fe-301-T 1/8 (3.2mmX3.2mm)

2. Simultaneous removal of NO and H_2S with CO.

The reduced catalyst/absorbent produced after Run 1b was used to test the potential for simultaneous H_2S and NO removal with CO. During the first 120 minutes no H_2S or NO were detected in the effluent gas. Traces of light yellow and white precipitates were noticed close to the bubbler 85 minutes after starting the run. In the last 150 minutes of the run no H_2S or NO were detected. The run was terminated after 270 minutes because sulfur precipitated, plugging the outlet line. The amount of H_2S removed at this point corresponded to 109% of the calculated bed sulfur capacity. Sulfur compounds eluted from the bed because its sulfur capacity had been exceeded. Formation of sulfur is thought to have been by the following reaction:

	$\Delta H_{25°C}$ (kcal)	$\Delta F_{227°C}$ (kcal)	
$2\ H_2S + SO_2 \longrightarrow 2\ H_2O + 3\ S(s)$	-35.0	-13.61	iv-1

Failure of a copper gasket permitted air to leak in, which oxidized some sulfur to SO_2. Had the leak not been present, all of the sulfur would have eluted as H_2S. In subsequent runs either a stainless steel or an aluminum gasket was used. The early traces of light yellow and white precipitates were ignored. Later experiments showed that these were ammonium sulfides and sulfates. The system diluent for this run was N_2, which prevented an accurate closing of the nitrogen material balance. Despite problems in this run, it demonstrated that FeO_x can simultaneously remove H_2S and NO when CO is present.

3. Reduction of NO with CO over Iron Sulfide.

Since the bed capacity for sulfur (as FeS) in Run 1b had been exceeded while maintaining no detectable NO elutions, it was concluded that iron sulfide must also be catalytic for NO reduction. Runs 2d and 32 demonstrated this fact. Figure iv-2 compares these results with those from the FeO_x data. For both low and high CO/NO ratios, FeO_x S_y data are close to the correlation for FeO_x. Run 32 had a slight amount of water present, hence both N_2 and NH_3 were generated. Since NH_3 was only 13% of the nitrogen products, the water effect was small. The conclusion from these runs is that iron sulfide has activity comparable to iron oxide for NO reduction by CO.

4. Oxidation of CO and H_2 with Iron Oxide.

Oxidation of CO and H_2 by reduction of Fe_2O_3 was checked in Runs 8a and 9a. Prior to these runs, reduced iron oxide was produced with net reducing CO and NO streams. Maximum removal of CO in Run 8a was 46% while that for H_2 in Run 9a was only 21% at 370°C in 0.67 seconds. A detailed discussion of these oxidation reactions is given in section H. This cursory look confirmed that both CO and H_2 can be oxidized by Fe_2O_3, CO reacting more readily than H_2.

5. Oxidation of FeS to Iron Oxide and SO_2.

The final process stage to check was the catalyst/absorbent regeneration. Runs 2e and 10b confirmed the regeneration reactions. In Run 2e at 444°C the initial concentration of SO_2 was 0.066%

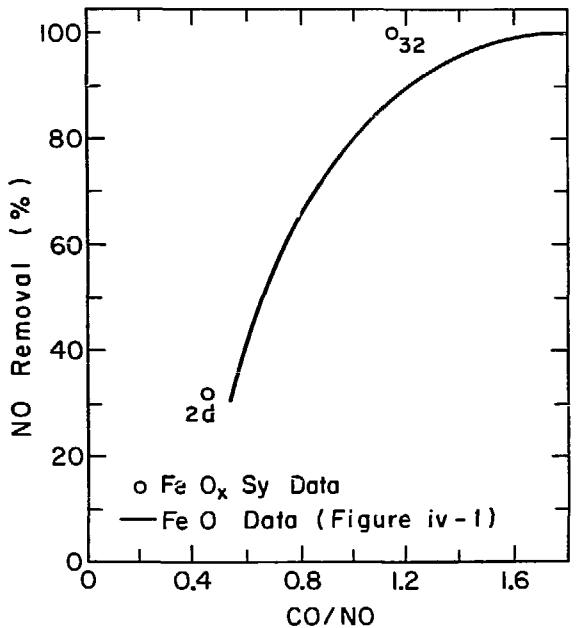

XBL 745-214

Fig. iv-2. Percent NO removal versus CO/NO. Comparison of FeO_x data to FeO_xS_y data.

Run	2d	32
[NO]	1.8%	0.89%
[CO]	0.80%	1.02%
FeO_xS_y (avg)	x=.40, y=1.1	x=.63, y=.63
temp. (C)	356	378
res. time (sec)	0.38	0.41

Fe-301-T1-8
(3.2mm-0.2mm)

over FeS when [O_2] was 0.75%.At 518°C the maximum [SO_2] was 1.4% when [O_2] was 0.78%. A quantitative sulfur balance was not obtained. However, the relative product distribution, based on gas chromatograph (G.C.) and precipitate analyses, showed that approximately 95% of the product was SO_2 and 5% was sulfur.

In Run 10b, SO_2 began to evolve rapidly from $FeSO_4$ at a temperature around 670°C. The iron sulfate gave an SO_2 concentration oi 0.47% at 560°C. This increased dramatically to 16% at 670°C. Lowell (1971) reports decomposition of $FeSO_4$ between 603-810°C and of $Fe_2(SO_4)_3$ between 781-810°C. The National Bureau of Standards (1966) reported slightly lower temperature levels of 550°C and 680°C, respectively. NBS also state that in the range of 680°C to 730°C, the decomposition pressure of $FeSO_4$ is greater than that of $Fe_2(SO_4)_3$. Yost and Russell (1944) support the lower decomposition temperatures. They report an SO_3 concentration at one atomosphere of 26% over $Fe_2(SO_4)_3$ at 670°C. Since the run continued until the SO_2 concentration was 0.86%, most of the sulfates had already decomposed. The pellets from both Runs 2e and 10b were visually similar to fresh pellets. A sulfur balance was not possible.

6. Summary of initial studies.

The initial process studies confirmed the following:

a. NO can be reduced to N_2 by CO over either iron oxide or iron sulfide at 370°C.

b. NO and H_2S can be simultaneously removed by reactions with reduced iron and CO at 370°C.

c. Both CO and H_2 can be oxidized by Fe_2O_3 at 370°C.

d. Catalyst regeneration can be accomplished at temperatures around 670°C. to yield iron oxide and SO_2.

B. Removal of Sulfur Compounds.

Normal power plants emit sulfur in the form of either SO_2 or SO_3. SO_2 accounts for more than 98% of the total sulfur (Levy, 1970). The proposed removal process requires that a net reducing flue gas be generated. This means that in addition to SO_2, other potential sulfur compounds will be produced - H_2S, COS and S_2. Under reducing conditions, essentially no SO_3 will be present (Reese, 1965).

1. Removal of H_2S with Iron Oxide.

The following reaction was studied in five different runs.

	$\Delta H_{25°C}$ (kcal)	$\Delta F_{370°C}$ (kcal)	$\Delta F_{538°C}$ (kcal)	
$FeO + H_2S \longrightarrow FeS + H_2O$	-11.9	-9.25	-9.57	iv-2

These runs had approximate conditions of 2% H_2S, 370°C. and a gas residence time of 0.50 seconds. Figure iv-3 is a plot of the percent H_2S removal as a function of run time. All runs gave essentially complete H_2S removal during the first 3 minutes. The rate of departure from 100% removal appears to be a function of the initial amount of FeO in the solid. Run 16b, with $FeO_{1.35}$, departs at 3 minutes. Runs 19c and 24c, with $FeO_{1.27}$ and $FeO_{1.26}$, depart at about 18 minutes. Run 2c, with $FeO_{1.19}$, deviates from this trend due to a lower residence time and reaction temperature. Surprisingly Run 24e, with $FeO_{1.23}S_{.14}$ gives the longest time until departure, 30 minutes. The oxidation state of the iron would predict that the

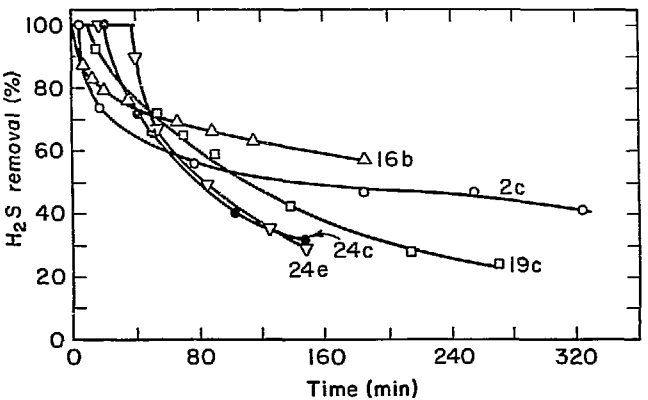

XBL 745-3253

Fig. iv-3. Removal of H_2S by reduced iron oxide.

Run	2c	16b	19c	24c	24e
T(°C)	360	381	376	371	373
θ (sec)	0.37	0.50	0.47	0.45	0.45
$[H_2S]$%	1.9	2.1	1.85	2.1	2.0
Solid(I)	$FeO_{1.19}$	$FeO_{1.35}$	$FeO_{1.27}$	$FeO_{1.26}$	$FeO_{1.23}S_{.14}$
Solid(F)	$FeO_{.10}S_{1.1}$	$FeO_{.57}S_{.80}$	$FeO_{.50}S_{.78}$	$FeO_{.50}S_{.76}$	$FeO_{.71}S_{.65}$
Symbol	O	△	□	●	▽

Fe-301-T 1/8
(3.2mmX3.2mm)

breakthrough time for Run 24e should be similar to that for Run 16b. No explanation has been found for this discrepancy. Based on equation iv-2, the hydrogen material balance in Run 16b closed to within 8.5%, supporting the contention that one sulfur is exchanged for one oxygen. The qualitative lead acetate test for the presence of sulfide was positive for the catalyst/absorbent from Run 1c.

2. Removal of COS with Iron Oxide.

Similar results were obtained for the reaction:

	$\Delta H_{25°C}$ (kcal)	$\Delta F_{370°C}$ (kcal)	$\Delta F_{538°C}$ (kcal)	
$FeO + COS \longrightarrow FeS + CO_2$	-20.2	-17.3	-17.5	iv-3

Percent removal of COS as a function of run time for Run 9b is shown in Figure iv-4. Departure from 100% removal occurs at 5 minutes, somewhat sooner than expected based on the H_2S work. Fifty percent removal of COS occurs after 65 minutes for COS, while for Run 24c with comparable initial FeO_x, 50% removal of H_2S occurs after 80 minutes. It appears from these two comparisons that H_2S is the more reactive species.

The overall carbon balance on Run 9b closed within 7.3%. CO_2 was the primary product of the reaction. It decreased with time as the COS removal decreased. CO was the other product. After the first 20 minutes, CO eluted at a constant concentration of 0.20%. This concentration corresponds to 5.3% of the inlet COS which is far greater than could be expected from the 0.32% CO in the COS feed cylinder. The constant elution rate for CO implies that it is generated independent of the extent of the main reaction.

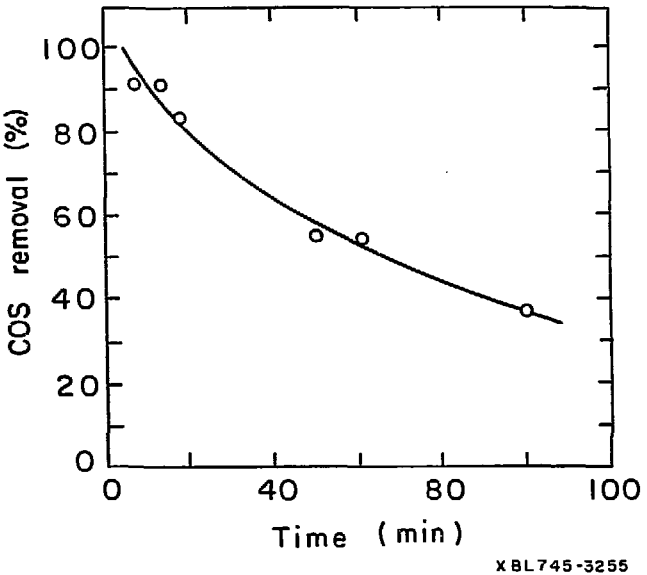

Fig. iv-4. Removal of COS with reduced iron oxide.

Run	96	Fe-301-T 1/8
T(°C)	370	(3.2mmX3.2mm)
θ (sec)	0.60	
[COS]	3.75%	
Solid(I)	$FeO_{1.25}$	
Solid(F)	$FeO_{.76}S_{.49}$	

The following decomposition reactions are thermodynamically unfavorable:

	$\Delta H_{25°C}$ (kcal)	$\Delta F_{370°C}$ (kcal)	$\Delta F_{538°C}$ (kcal)	
$COS \longrightarrow CO + \frac{1}{2} S_2(g)$	+21.8	+9.46	+6.27	iv-4
$COS \longrightarrow CO + S(s)$	+ 6.38	+5.75(227°C)		iv-4a

This next reaction is thermodynamically favorable.

	$\Delta H_{25°C}$ (kcal)	$\Delta F_{370°C}$ (kcal)	
$FeS + COS \longrightarrow FeS_2 + CO$	-13.42	-6.50	iv-5

Haas (1973) has confirmed the presence of both FeS and FeS_2 by x-ray diffraction analysis under similar conditions. He studied the following reaction at a temperature of 400°C over an iron/alumina catalyst.

	$\Delta H_{25°C}$ (kcal)	$\Delta F_{370°C}$ (kcal)	$\Delta F_{538°C}$ (kcal)	
$SO_2 + 2\ CO \longrightarrow 2\ CO_2 + \frac{1}{2} S_2$	-48.9	-33.4	-29.3	iv-6

COS was identified as the raction intermediate.

Since CO was formed and the presence of FeS_2 was implied, reactions iv-3 and iv-5 undoubtedly have occurred in Run 9b. With this interpretation, 8.8% of the sulfided iron was FeS_2 and 91.2% was FeS. No independent determination of FeS_2 was made in this work.

3. Formation and removal of sulfur vapor.

If sulfur is present in the flue gas it should be decreased to a very low value over the catalyst/absorbent in view of the following equilibria:

	$\Delta H_{25°C}$ (kcal)	$\Delta F_{370°C}$ (kcal)	$\Delta F_{538°C}$ (kcal)	
$CO + \frac{1}{2} S_2(g) \longrightarrow COS$	-21.8	- 9.46	- 6.27	iv-7
$H_2 + \frac{1}{2} S_2(g) \longrightarrow H_2S$	-20.2	-13.7	-11.7	iv-8

Querido (1973) reported that above 327°C. reaction iv-7 proceeded to a significant extent in less than 0.20 seconds over a CuS/Al_2O_3 catalyst. Haas (1971) reported that reaction iv-7 occurs above 300°C. over an FeS/Al_2O_3 catalyst. In these investigations COS was the final product. In the present work COS and H_2S would subsequently react with FeO to form FeS, resulting in a lower potential S_2 level than in either of the cited references. In view of these facts, no experimental work was done specifically with S_2.

4. Removal of SO_2.

a. Removal with Iron Oxide.

The final sulfur compound considered was SO_2. Direct contact of SO_2 with either oxidized or reduced iron oxide resulted in negligible SO_2 removal. Figure iv-5 shows that SO_2 removal is greatest for reduced iron oxide. Even with reduced oxide, however, only 7% of the potential sulfur absorption was realized.

b. Removal with CO or H_2 over Iron Oxide.

In the presence of either CO or H_2, SO_2 was substantially removed over the Fe/Al_2O_3 catalyst/absorbent. Figure iv-6 presents results of these studies. The major reactions included the following:

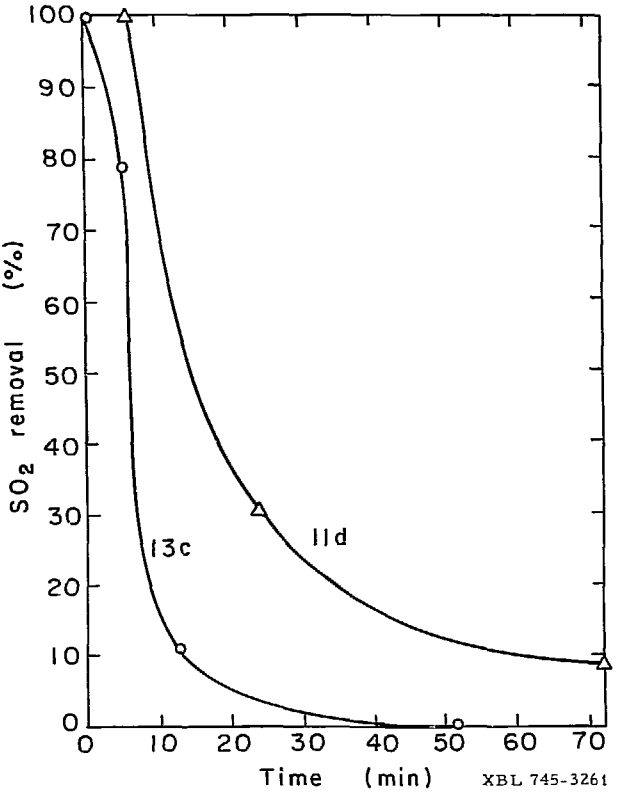

Fig. iv-5. Removal of SO_2 with oxidized and reduced iron oxide.

Run	13c	11d
T(°C)	377	382
θ (sec)	0.56	0.54
$[SO_2]$ in	1.46%	1.40%
Solid(I)	$FeO_{1.5}$	$FeO_{1.26}$
Solid(F)	$FeO_{1.5}(SO_2)_{.03}$	$FeO_{1.26}(SO_2)_{.07}$

Fe-301-T 1/8
(3.2mmX3.2mm)

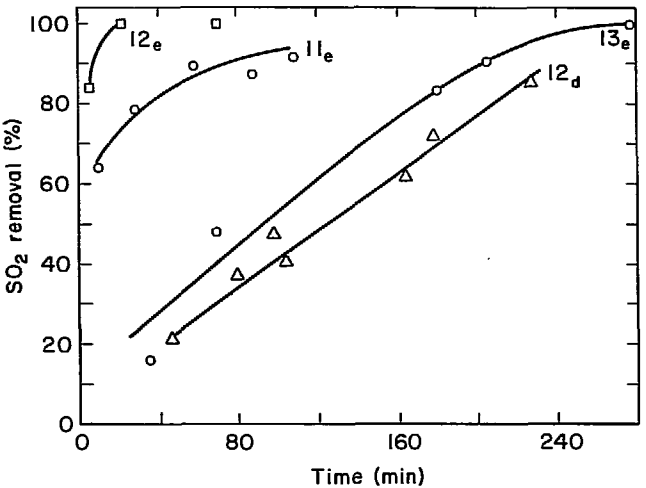

Fig. iv-6.

Sulfur removal with time as a function of solid and gas compositions.
T = 370-379°C, θ = 0.5-0.7 sec
Fe-301-T 1/8 (3.2mmX3.2mm)

Run	$\frac{[CO]}{[SO2]}$	$\frac{[H2]}{[SO2]}$	$\frac{\Delta[H2]}{\Delta[SO2]}$	$\frac{\Delta[CO2]}{\Delta[SO2]}$	Solid Initial (I)	Solid Final (F)
11e	0	3.5	2.8	0	$FeO_{1.3}S_{.074}$	$FeO_{.86}S_{.40}$
12d	1.9	0	0	-2.8	$FeO_{1.5}S_{.018}$	$FeO_{1.5}S_{.50}$
12e	3.1	0	0	-2.5	$FeO_{1.5}S_{.50}$	$FeO_{1.4}S_{.68}$
13e	2.1-2.6	0	0	-2.8	$FeO_{1.5}S_{.023}$	$FeO_{1.2}S_{.43}$

	$\Delta H_{25°C}$ (kcal)	$\Delta F_{370°C}$ (kcal)	$\Delta F_{538°C}$ (kcal)	
$\frac{1}{3} Fe_2O_3 + 7/2\ CO + SO_2 \longrightarrow FeS + 7/2\ CO_2$	-90.1	-64.5	-57.9	iv-9
$FeO + 3\ CO + SO_2 \longrightarrow FeS + 3\ CO_2$	-90.8	-60.2	-53.1	iv-10
$2\ CO + SO_2 \longrightarrow 2\ CO_2 + \frac{1}{2} S_2$	-48.9	-33.4	-29.3	iv-11
$\frac{1}{3} Fe_2O_3 + 7/2\ H_2 + SO_2 \longrightarrow FeS + 7/2\ H_2O$	-55.7	-50.3	-48.4	iv-12
$FeO + 3\ H_2 + SO_2 \longrightarrow FeS + 3\ H_2O$	-61.4	-48.7	-45.8	iv-13
$2\ H_2 + SO_2 \longrightarrow 2\ H_2O + \frac{1}{2} S_2$	-29.2	-25.7	-24.4	iv-14

In Run 11e reduced iron oxide was contacted with a net reducing gas stream. The gradual increase of SO_2 removal with time is a result of continual surface reduction as well as sulfidation. The overall ratio of the change of $[H_2]$ to the change of $[SO_2]$ ($\Delta[H_2]/\Delta[SO_2]$) was 2.8. This would imply that all three reactions iv-12, 13, and 14 could be important, based on reaction stoichiometry.

Oxidized iron and a reducing atmosphere relative to reaction iv-11 were used in Runs 12d and 13e. A significantly longer time was required for these runs to achieve the same SO_2 removal as in Run 11e. In both cases, the overall change of product CO_2 to reactant SO_2 ($\Delta[CO_2]/\Delta[SO_2]$) was -2.8, even through the inlet reactant ratio ($[CO]/[SO_2]$) only ranged from 1.9 to 2.6. SO_2 removals up to 100% were achieved in the later part of Run 13e. The negative signs only reflect product/reactant ratio changes. This apparent anomaly is explained by realizing that at the beginning of these runs, the majority of the reducing agent was consumed in reducing Fe_2O_3. As more reduced iron became available, the CO + SO_2 reaction became dominant. Therefore, the initial ($\Delta[CO_2]/\Delta[SO_2]$) will be greater

than 3.5 and the final absolute ratio will be between 2.0 and 3.5. Figure iv-7 illustrates this point. The initial $\Delta[CO_2]/\Delta[SO_2]$ is much greater for Runs 12d and 13e than for Runs 12e of 11e. After sufficient time, Runs 11e, 12e, and 13e approach a $\Delta[CO_2]/\Delta[SO_2]$ of between -2.5 and -2.7. Run 12d, with a lower inlet $[CO]/]SO_2]$ ratio, drops to about 2.0. These limiting values, plus sulfur precipitate in the lines, verify that reactions iv-11 and iv-14 do proceed to some extent.

Because sulfur precipitate was not anticipated, only a combined measure of sulfur from Runs 9b, 11e, 12d, and 12e was obtained. Measured precipitate accounted for 15% of the total sulfur removed in these runs. In Run 13e sulfur precipitate was anticipated but it accounted for only 4.8% of the total change in SO_2. A weighted average of $\Delta[CO]/\Delta[SO_2]$ calculated according to equation iv-10 and iv-11 to give the experimentally found value of 2.5 would predict that 50% of the total change of SO_2 could be accounted for by the sulfur precipitate. This value predicts a much greater amount of sulfur than was found. In keeping with earlier findings that FeS_2 may form, the following overall reactions should be considered:

	$\Delta H_{25°C}$ (kcal)	$\Delta F_{370°C}$ (kcal)	$\Delta F_{538°C}$ (kcal)	
$4/3\ FeO + 6\ CO + 7/3\ SO_2 \longrightarrow$				
$FeS_2 + 1/3\ FeS + 6\ CO_2$	-205	-130	-111	iv-15
$4/3\ FeO + 6\ H_2 + 7/3\ SO_2 \longrightarrow$				
$FeS_2 + 1/3\ FeS + 6\ H_2O$	-146	-107	- 95.8	iv-16

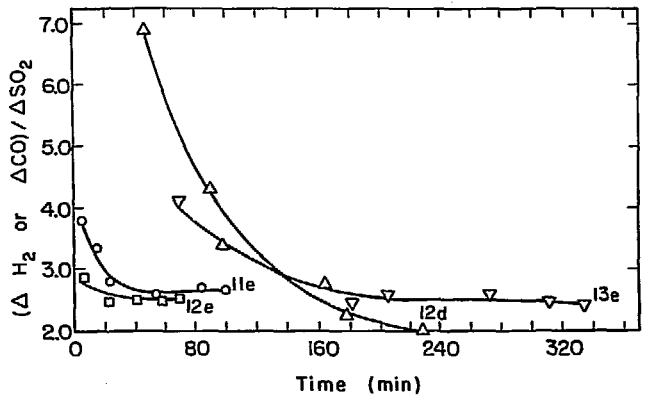

XBL 745-3221

Fig. iv-7. Variation of reaction stoichiometry with time for both H_2 and CO reduction of SO_2.

	Run	T (°C)	θ (sec)	$[SO_2]$ (%)	$[H_2]$ (%)	[CO] (%)
O	11e	382	0.54	1.35	4.8	0
Δ	12d	370	0.59	1.1	0	2.1
□	12e	370	0.59	1.08	0	3.4
▽	13e	377	0.56	0.72→0.77		1.5→1.8

Fe-301-T 1/8
(3.2mmX3.2mm)

For these reactions, the $\Delta[CO]/\Delta[SO_2] = \Delta[H_2]/\Delta[SO_2] = 2.57$, which is within the experimentally determined range. Since sulfur precipitate alone cannot account for deviation from a stoichiometric ratic below 3.0, some FeS_2 may have formed.

In addition to S_2 which eluted from the bed, small amounts of H_2S (Run 11e) and COS (Runs 12d, 12e, and 13) were detected. H_2S eluted in Run 11e during the entire sulfidation. It increased from 2.8% to 14% of the inlet SO_2 value as the bed became sulfided. In Runs 12d-12e and 13e, COS was detected during the majority of each run. The highest COS measured was 10% of the inlet SO_2. COS formation is in agreement with the theory proposed by Haas (1973) that COS is the reaction intermediate in the reduction of SO_2 to sulfur by CO. By analogy H_2S may also serve this function in the $SO_2 + H_2$ reaction.

c. Removal with CO and H_2 over Iron Oxide.

A comparison of the simultaneous reaction kinetics of CO and H_2 with SO_2 was made in Run 27d. In the first 110 minutes a stream of CO and H_2 passed over reduced and partially sulfided catalyst. Figure iv-8 shows only 15% H_2 removal and 2% CO removal. Introduction of SO_2 resulted in 100% SO_2 removal and increased the CO removal to 33%. No change in H_2 removal was noted. Both the CO and H_2 removals gradually dropped off with time, H_2 removal decreasing more rapidly. Measured $\Delta[CO]/\Delta[SO_2]$ was 2.70, which is what would be expected with an excess of reducing agent, based on Figure iv-7. Thus, the sulfided catalyst promotes reduction of SO_2 with CO in preference to reduction of SO_2 with H_2.

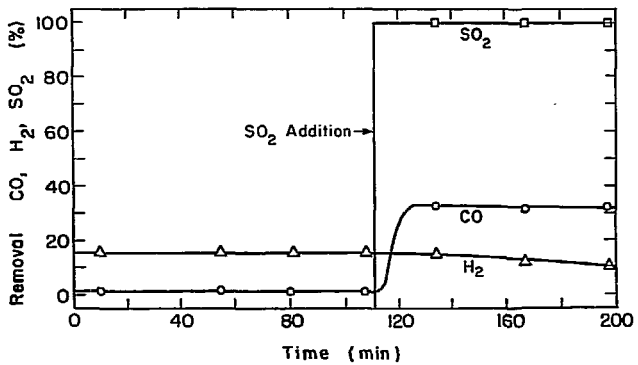

XBL 745-3220

Fig. iv-8. Reduction of SO_2 in a combined CO and H_2 stream.

Run	27d
T(°C)	374
θ (sec)	0.43
$[H_2]$	3.7%
[CO]	4.0%
$[SO_2]$	0.45%
Solid(I)	$FeO_{1.1}S_{0.15}$
Solid(F)	$FeO_{0.85}S_{0.26}$

Fe-301-T 1/8
(3.2mm×3.2mm)

5. Reduced catalytic activity.

Absence of a reducing agent for SO_2 not only results in the incomplete removal of SO_2 but also inhibits the catalyst with respect to reduction reactions. In Figure iv-9, the upper line, Run 13a, represents CO removal over fresh Fe_2O_3, while the middle line, Run 13d, shows CO removal over Fe_2O_3 which had been exposed to a stream of 1.46% [SO_2]. The fresh catalyst exhibits a rate roughly 3.3 times that of the inhibited catalyst. This rate decrease is more than can be explained by the CO concentration difference. The catalyst was inhibited for surface reduction in Run 13d by adsorbed SO_2. Introduction of SO_2 into the inlet gas line resulted in an immediate increase in CO_2 formation and an equivalent SO_2 reduction. In this case, the catalyst was still active for the CO + SO_2 reaction. The lower line, Run 12b, is CO removal from a system containing both absorbed and gas-phase SO_2. In this case, neither Fe_2O_3 nor SO_2 reacted with CO for over one hour. The CO removal rate is nearly 35 times slower than that over the fresh catalyst in Run 13a. The only significant differences between the bottom two lines was the SO_2 present in Run 12b. After treating this catalyst in Run 12b with CO at 370°C for 38 minutes, introduction of SO_2 resulted in stoichiometric conversion of CO to CO_2 and SO_2 reduction as noted above following Run 13d.

6. Summary of sulfur compound removal.

This work confirms that both H_2S and COS react with reduced iron oxide to give, primarily, FeS. Rapid decline of both H_2S and

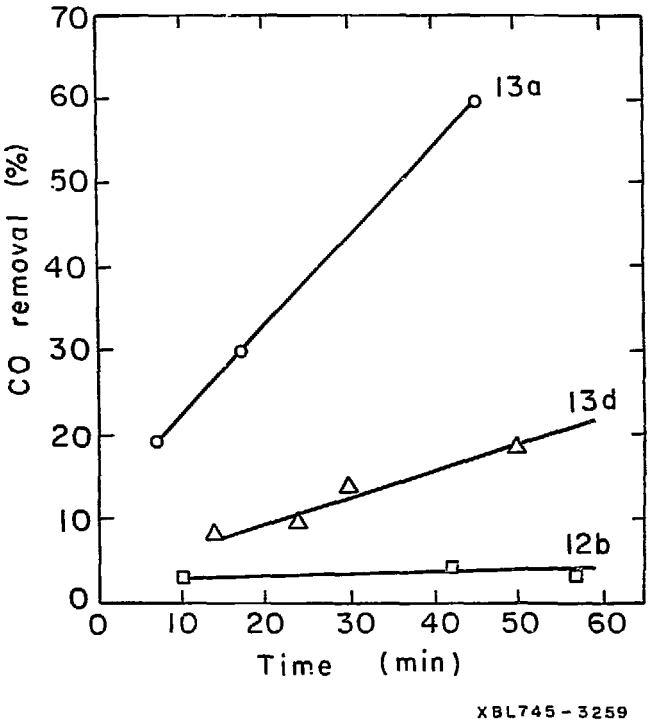

XBL745-3259

Fig. iv-9. The effect of absorbed SO_2 on Fe_2O_3 and SO_2 reaction by CO.

Run	12b	13a	13d
T(°C)	371	377	377
θ (sec)	0.59	0.51	0.51
[CO]%	2.2	1.94	1.28
[SO_2]%	1.2	0	0
Solid(I)	$FeO_{1.5}(SO_2)_{.028}$	$FeO_{1.5}$	$FeO_{1.5}(SO_2)_{.023}$

Fe-301-T 1/8 (3.2mmX3.2mm)

COS percent removals could be slowed by higher temperatures and smaller catalyst/absorbent pellets. These changes should also increase the total amount of sulfur absorbed per mole of iron.

Almost complete removal of SO_2 with CO or H_2 is possible at 370°C and a residence time of approximately 0.6 seconds over the 3.2-mm Fe/Al_2O_3 catalyst/absorbent. The problem of sulfur elution before complete bed sulfidation requires further study. Higher temperature and small particles should help solve this problem. For effective SO_2 removal, the gas stream needs to contain a reducing agent. Exposure of the catalyst/absorbent at 370°C to SO_2 without reducing agent results in partial deactivation for both SO_2 and Fe_2O_3 reduction. The original activity can be restored by treating the catalyst at this temperature with CO. Experimental results of Run 11b indicated that H_2 is also effective for this reactivation.

7. Sulfur compound distribution in a net reducing flue gas.

The form in which sulfur will be present in reduced flue gas is a function of the equilibrium conditions at the temperature where reaction kinetics essentially freeze. Initially, sulfur will be completely oxidized to SO_2 with excess oxygen. At the point of addition of the rich CO and H_2 stream, SO_2 could be reduced to H_2S COS, or S_2 depending upon conditions in the flue gas. Thermodynamic calculations show that these reduced sulfur species predominate at lower temperatures. Since no useful information was located on the homogeneous kinetics of SO_2 reduction, runs were made to determine

an approximate lower temperature limit.

a. Thermodynamic equilibria of sulfur compounds in reduced flue gas.

Thermodynamic equilibrium calculations for a typical oil-fired power plant flue gas under reducing conditions indicate that as the temperature decreases, H_2S, COS, and S_2 increase while SO_2 decreases. Table iv-1 lists flue gas compositions and the corresponding reactions considered. Results are shown in Figure iv-10.

Table iv-1. Gas composition and reactions for plant equilibrium Calculations.

Flue Gas Composition (before reaction):

	(%)	Reactions Considered:
$[N_2]$	73.90	$2\ COS + SO_2 \longrightarrow 2\ CO_2 + 3/2\ S_2$
$[CO_2]$	13.96	$2\ H_2S + SO_2 \longrightarrow 2\ H_2O + 3/2\ S_2$
$[H_2O]$	10.16	$CO + H_2O \longrightarrow CO_2 + H_2$
[CO]	0.817	$3\ H_2 + SO_2 \longrightarrow H_2S + 2\ H_2O$
$[H_2]$	0.817	$3\ CO + SO_2 \longrightarrow COS + 2\ CO_2$
$[O_2]$	0.195	$H_2 + \frac{1}{2} S_2 \longrightarrow H_2S$
$[SO_2]$	0.154	$CO + \frac{1}{2} S_2 \longrightarrow COS$
		$COS + H_2O \longrightarrow H_2S + CO_2$

$$\frac{\text{Oxidizing Equivalents}}{\text{Reducing Equivalents}} = \frac{2[O_2] + 3[SO_2]}{[CO] + [H_2]} = 0.521$$

$$\frac{[CO_2]}{[H_2O]} = 1.37$$

At temperatures below 800°C, H_2S is the primary equilibrium sulfur species when the CO_2 to H_2O ratio is 1.37, which is typical

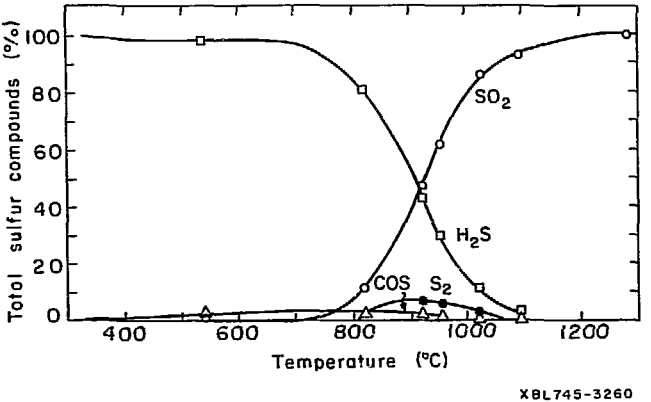

Fig. iv-10. Equilibrium distribution of sulfur compounds in a typical power plant flue gas. (See Table iv-1 for data.)

of oil-fired power plant conditions. Coal-fired plants have a higher $[CO_2]/[H_2O]$, typically around 2. As long as reaction kinetics are rapid at 800°C or below, neither SO_2, S_2, nor COS will be present to a significant extent. The next section will discuss a case where the CO_2 to H_2O ratio is much less than one. Under these conditions, sulfur is the main reduced product at lower temperatures.

b. Homogeneous kinetics of SO_2 reduction.

A non-catalytic experiment, Run 28, was made to determine the lowest temperature at which these reactions would proceed. The inlet gas was 0.5% SO_2, 1.6% CO, 1.6% H_2, and 1.7% H_2O in a helium diluent. The stream was fed directly into the 44.4-mm ID Mullite furnace tube. This substantially increased the gas residence time in the reactor to a value about 10 times that found in normal coal-fired furnaces above 1090°C, 2.4 sec. compared to 0.24 sec.

Results of this work are shown in Figure iv-11 and indicate that reaction did not occur at a significant rate at temperatures up to 950°C. In tests run above 1093°C, reaction took place. When reaction occurred, large amounts of sulfur precipitated, preventing any quantitative estimation of the gas composition at high temperatures after reaction. Qualitatively, there must have been some COS or H_2S present which, cooled, reacted with SO_2 to form sulfur.

The equilibrium calculations of Figure iv-9 are based on a $[CO_2]/[H_2O]$ ratio of 1.37. Run 28 had $[CO_2]/[H_2O]$ equal to 0.088 for 1094°C and 0.37 for 1260°C. The low CO_2 level allowed small changes

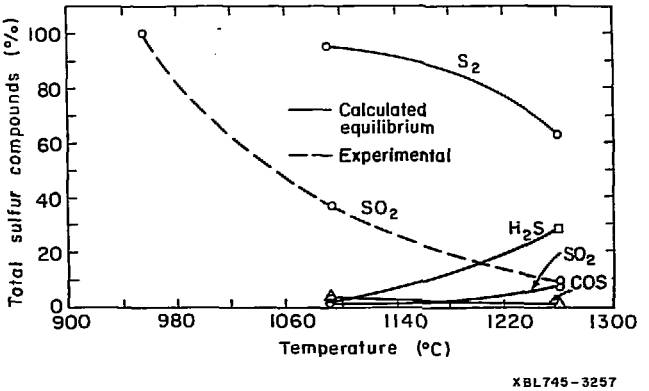

Fig. iv-11. Equilibrium distribution of sulfur compounds under Run No. 28 conditions. Experimental SO_2 distribution.

Expt.		
	$[H_2O]$	1.95%
	$[CO]$	1.5%
	$[H]$	1.6%
	$[SO_2]$	0.5%

in CO_2 indicative of reaction progress, to be detected. From an equilibrium point of view, this lower value favors the reduction reactions over that in the actual flue gas.

The effect of this lower $[CO_2]/[H_2O]$ ratio on the experimental system equilibria is to make S_2 the predominant species at lower temperatures. Figure iv-11 is a plot of the calculated equilibria and the experimental SO_2. Only at temperatures above 1094 C°does the experimental SO_2 value begin to approach equilibrium value.

These results show that reaction kinetics should freeze at around 1094°C or higher in normal flue gases. Figure iv-10 illustrates a typical sulfur compound distribution at 1094°C:

SO_2 -- 95.3%

H_2S -- 3.8%

S_2 -- 0.63%

COS -- 0.29%

Freezing the equilibria at a higher temperature would result in a higher SO_2 level. Therefore, the primary sulfur species in flue gas will be SO_2 even though it contains an excess of CO and/or H_2.

Okay and Short (1973) report equilibrium calculations for a net reducing flue gas with $[CO_2]/[H_2O] = 1.17$. As in the present study they report H_2S as the predominant sulfur species at low temperatures. In their kinetic studies, as in the present work, no effort was made to maintain CO_2 in the inlet feed or $[CO_2]/[H_2O]$ in the outlet. At their highest SO_2 removal and lowest water concentration the CO_2 formed from reaction would yield only a $[CO_2]/[H_2O]$ ratio of about 0.2. The previous discussion of Figures iv-10 and

iv-11 has shown that at high $[CO_2]/[H_2O]$ H_2S is the prime lower temperature sulfur species while at low $[CO_2]/[H_2O]$ S_2 is the prime species. Therefore, even though S_2 was the primary reduced sulfur species in the experimental system it will not necessarily be so under power plant conditions. A catalyst promoting these reactions at lower temperatures (below 800°C) with a typical flue gas ratio of $[CO_2]/[H_2O]$ under reducing conditions will form primarily H_2S.

C. Removal of Nitric Oxide.

Nitric oxide forms in the primary combustion zone of the furnace. A small amount of the NO is oxidized during flue gas cooling. This results in the effluent NO_x being 90 - 95% NO and 5 - 10% NO_2. (Bartok, 1969). Rosser, (1956) reports homogeneous thermal decomposition rates for NO_2 above 540°C, which imply negligible NO_2 in the flue gas above this temperature. Since the flue gas entering the contact zone will not only be at 540°C but also reducing, essentially all the NO_x will be NO. The experimental work studied only the reduction of NO.

1. Reduction of NO with Iron Oxide.

Removal of NO by catalytic reduction with a reducing agent over iron oxide and iron sulfide was reported in part A. At that time, no attempt was made to understand the removal mechanism. Klimisch (1972) has proposed an oxidation-reduction mechanism for the iron oxide system. Experiments were run to confirm this mechanism by demonstrating that NO could be reduced by reaction with either reduced iron oxide or iron sulfide. Figure iv-12 shows the percent

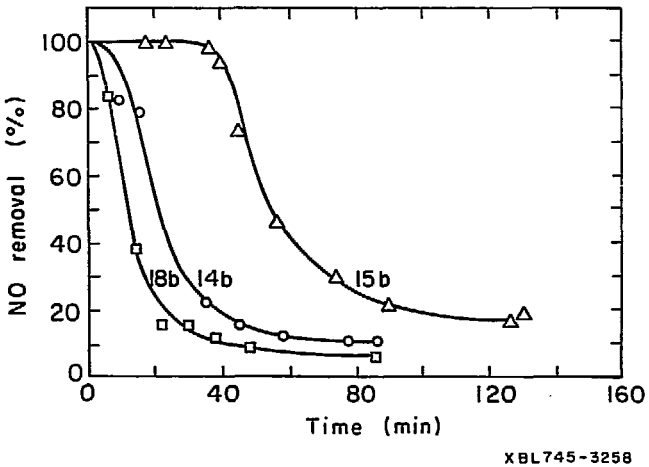

Fig. iv-12. Oxidation of reduced iron oxide with NO.

Run	14b	15b	18b
T(°C)	374	377	377
θ (sec)	0.55	0.51	0.48
[NO]%	2.17	0.98	1.34
Solid(I)	$FeO_{1.34}$	$FeO_{1.19}$	$FeO_{1.42}$

Fe-301-T 1/8
(3.2mmX3.2mm)

	$\Delta H_{250°C}$ (kcal)	$\Delta F_{370°C}$ (kcal)	$\Delta F_{538°C}$ (kcal)	
7 NO + 2 FeS ⟶				
$Fe_2O_3 + 7/2\ N_2 + 2\ SO_2$	-444	-392	-377	iv-19
3 NO + FeS ⟶				
$FeO + 3/2\ N_2 + 3O_2$	-177	-162	-157	iv-20

The overall $\Delta[N_2]/\Delta[SO_2]$ was 2.42 for this run. The ratio of $\Delta[N_2]/\Delta[SO_2]$ for individual samples ranged from 3.85 for the first sample to 1.84 for the last sample. If the mechanism of oxidation required $FeSO_3$ first to form and subsequently to decompose, initially $[N_2]$ would be greater than $1.5x[SO_2]$. Figure iv-13 shows that this is what occurred experimentally . Since Lowell (1971) reports $FeSO_3$ decomposition at 382°C to form SO_2 and FeO, this mechanism is probably what occurred. The $\Delta[N_2]/\Delta[SO_2]$ for reactions iv-19 and iv-20 are 1.75 and 1.50 respectively. Based on these reactions, the surface is still undergoing oxidation at 160 minutes. Quantitative sampling for NO on the Molecular Sieve 5A column was not possible in the first 65 minutes. However, the Chromosorb 104 column, indicated qualitatively that large NO concentrations were present. Absence of N_2 on the Molecular Sieve 5A column in the first 65 minutes also concurred with this fact. Gradual increase of NO removal with time is opposite to the effect noticed for reduced iron oxide in Figure iv-12. This suggests that the oxidation of FeO by NO proceeds more rapidly than that of FeS. As fresh FeO is formed from FeS the overall rate of NO removal gradually increases for the bed. Initially

NO removal by reduced iron oxide as a function of run time for three different runs. The following reactions may occur:

	$\Delta H_{25°C}$ (kcal)	$\Delta F_{370°C}$ (kcal)	$\Delta F_{538°C}$ (kcal)	
$2\ Fe_3O_4 + NO \longrightarrow$				
$3\ Fe_2O_3 + \frac{1}{2}\ N_2$	-76.4	-53.6	-46.8	iv-17
$2\ FeO + NO \longrightarrow$				
$Fe_2O_3 + \frac{1}{2}\ N_2$	-90.8	-67.1	-62.2	iv-18

Run 15b exhibits a higher removal of NO because the solid was more strongly reduced and the NO concentration was lower than in other runs. The gradual decrease with time is caused by depletion of reduced iron on the outer surface of the catalyst pellets.

In Runs 14b and 15b, the catalyst had been initially reduced with CO to levels reported in Figure iv-12. In Run 18, H_2 was used. Oxidation of FeO in Run 15b produced not only N_2 but also CO_2. This result was probably caused by desorption of CO_2 or oxidation of adsorbed CO remaining after reduction. The N_2 generated from reaction with CO was 18% of the total. In Run 14b, CO_2 was not monitored, but it must also have been present since reduction conditions for 14a and 15a were similar. The analytical system, at this time, was not set up to monitor water, so adsorption of H_2 was not checked.

2. Reduction of NO with Iron Sulfide.

Oxidation of iron sulfide not only produces N_2 but also liberates SO_2. Figure iv-13 presents the results from Run 16c. Possible overall reactions include the following:

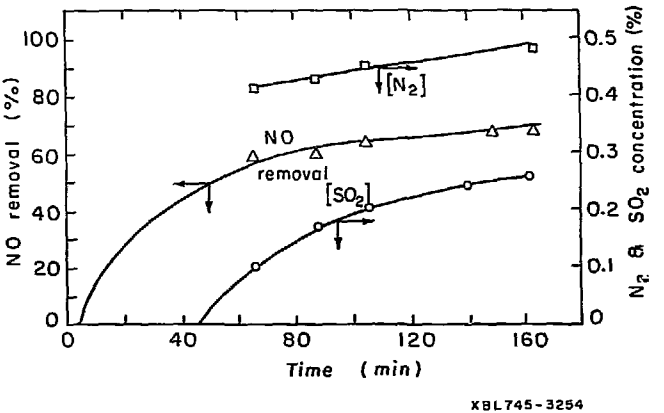

Fig. iv-13. Oxidation of iron sulfide with NO.

Run	16c
T(°C)	373
θ (sec)	0.50
[NO]	1.44%
Solid(I)	$FeO_{.57}S_{.80}$

Fe-301-T 1/8
(3.2mmX3.2mm)

the decomposition of $FeSO_3$ prevents major pore blocking that may have caused the rapid decrease in NO removal over Fe_2O_3. Fresh FeO formed from decomposition of $FeSO_3$ may also be a very active reducing agent for NO. When a reducing gas is present, reduction of $FeSO_3$ back to FeS, will occur instead of its decomposition, preventing SO_2 evolution.

3. Reduction of NO with H_2 over Iron Oxide.

In addition to CO, H_2 is also an active reducing agent for NO over both reduced iron oxide and iron sulfide. In Runs 18c and 19a, fresh catalyst was reduced to $FeO_{1.41}$ and $FeO_{1.27}$ and then used to catalyze the following reactions:

	$\Delta H_{25°C}$ (kcal)	$\Delta F_{370°C}$ (kcal)	$\Delta F_{538°C}$ (kcal)	
$NO + H_2 \longrightarrow \frac{1}{2} N_2 + H_2O$	-79.4	-70.3	-67.7	iv-21
$NO + 5/2\ H_2 \longrightarrow NH_3 + H_2O$	-90.4	-65.3	-58.0	iv-22

$$NH_3 \text{ selectivity} = \frac{[NH_3]}{2[N_2]+[NH_3]} \times 100$$

Figure iv-14 shows results of those runs in which there was complete NO removal. The final value of the NH_3 selectivity was 23% and 30%, respectively. NH_3 selectivity is the percent reduced N formed from NO in the form of NH_3. Determinations of instantaneous NH_3 selectivities were based on N_2 gas chromatographic (G.C.) peaks. The material balances for H_2 and N_2 had 18% and 22% error in run 18d; 8% and 12% in Run 19b. The large error in Run 18d was cause by H_2O and NH_3 adsorbing to an appreciable extent on catalyst pellets at 370°C. This adsorption produced a chromatographing effect of H_2O

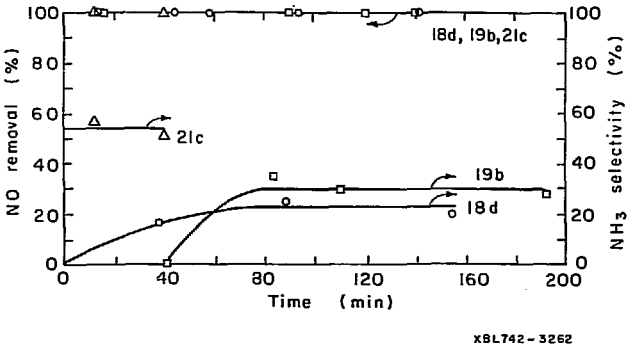

Fig. iv-14. Reduction of NO with H_2 over reduced iron oxide and sulfide. Percent NH_3 selectivity and percent removal.

Run	18d	19b	21c
T(°C)	379	377	372
θ (sec)	0.49	0.47	0.51
[NO]%	0.50	0.42	0.33
[H_2]%	2.44	2.3	0.43
Solid(I)	$FeO_{1.41}$	$FeO_{1.27}$	$FeO_{.14}S_{.60}$
Symbol	O	□	△

Fe-301-T /8 (3.2mmX3.2mm)

and NH_3 through the bed. In Run 18d, sampling and material balances were terminated when inlet gases were cutoff, while in Run 19b, sampling and material balances continued until NH_3 and H_2O peaks were negligible. This procedure required an additional sampling time of 30 minutes.

4. Reduction of NO with H_2 over Iron Sulfide.

Run 21c was conducted after the reduced oxide had been sulfided. These results are presented in Figure iv-14. As before, complete NO removal was obtained. NH_3 selectivity was noticeably higher even though there was a lower stoichiometric ratio between H_2 and NO. The 54% NH_3 selectivity measured corresponds to all the H_2 forming NH_3. The N_2 formed was probably from excess NO oxidizing the surface. Had more H_2 been present, a higher NH_3 selectivity might have resulted.

5. Reaction of NO and H_2O with Iron Oxide or Iron Sulfide.

Since both reduced iron oxide and iron sulfide were found to be capable of reducing NO to N_2 without any other reducing agent, their ability to form NH_3 from a stream of NO and H_2O was tested in Run 24. Both substances were capable of forming NH_3. Figure iv-15 shows the percent removal NO and the NH_3 selectivity for each trial. Higher NO removals and higher NH_3 selectivity obtained in Run 24d implies that regardless of the reducing agent present in the gas phase, iron sulfide will reduce most of the NO to NH_3 if H_2O is present. The decrease in sulfur content of the solid in Run 24d was determined from the quantity of the precipitate, NH_4HS, in the outlet line. NH_3 and H_2S were not detected in the G.C. sample. NH_3 and H_2S elutions were close to the same values since no NH_3

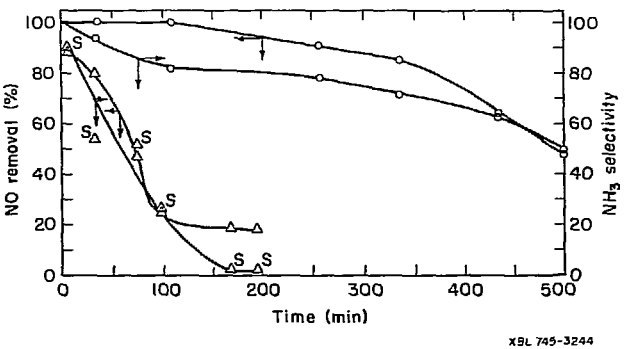

Fig. iv-15. Reaction of NO+H_2O with either iron oxide or iron sulfide.

Run	24b	24d
T(°C)	372	372
θ (sec)	0.45	0.45
[NO]	0.45%	0.47%
[H_2O]	1.3%	1.5-2.5%
Solid(I)	$FeO_{1.13}$	$FeO_{.5}S_{.76}$
Solid(F)	$FeO_{1.26}$	$FeO_{1.23}S_{.14}$
Symbol	△	○

Fe-301-T 1/8 (3.2mmX3.2mm)

Δ^S = NH_3 selectivity

collected in the HCl scrubber and no H_2S was detected in the G.C. samples.

NH_4HS is formed by reaction of equivalent amounts of NH_3 and H_2S. The decomposition temperature of NH_4HS is 118°C (Handbook Chemistry & Physics). Ammonium sulfide, $(NH_4)_2S$, is formed in an excess of NH_3. It is stable only below -18°C (Kirk, 1963). At ambient conditions, it loses NH_3 and changes to NH_4HS. There are also a number of ammonium polysulfides possible but their definite compositions are rather uncertain.

6. Reduction of NO with CO and H_2O over Iron Sulfide.

The presence of CO in the NO-H_2O-FeS system gave NH_3 selectivities over 90%. Figure iv-16 shows data from two runs with a sulfided catalyst. In both cases complete NO removal was achieved. Because N_2 evolutions were very small in both cases, there is no real difference between the apparent 91% and 96% NH_3 selectivities. At 204 minutes into Run 24f, the H_2O feed was terminated. Immediately, N_2 was generated as seen by the decreased NH_3 selectivity. A significant difference between these two runs is that no sulfur was removed from the catalyst in Run 22d while a significant amount was stripped off in Run 24f. Removal was evident by the absence of NH_3 in the gas sample and precipitation of ammonium salts in the lines.

An important parameter in these runs was the reducing or oxidizing character of the gas stream. Reduction of 1 mole of NO to form ½ mole of N_2 requires either 1 mole of H_2 or CO. To form NH_3 from NO requires 2.5 moles of H_2 or CO per mole of NO. Formation of a

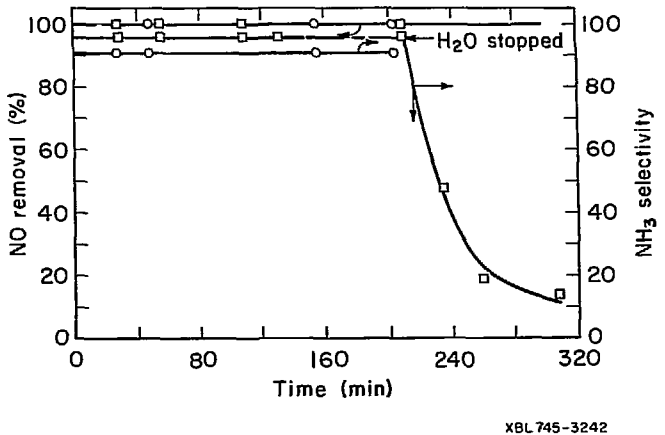

Fig. iv-16. Reduction of NO with CO+H_2O over iron sulfide.

Run	22d	24f
T(°C)	374	373
θ (sec)	0.49	0.44
[NO]	0.58%	0.46%
[CO]	1.1%	0.40%
H_2O%	3.4	2.2-2.8
Solid(I)	$FeO_{.27}S_{.97}$	$FeO_{.71}S_{.65}$
Solid(F)	$FeO_{.17}S_{.97}$	$FeO_{.68}S_{.46}$

Fe-301-T 1/8
(3.2mmX3.2mm)

sulfide from SO_2 requires 3 moles of H_2 or CO per mole of SO_2. Reduction of O_2 requires 2 moles of H_2 or CO per mole of O_2. The following definitions are used in the remainder of the text:

$$\frac{\text{Oxidizing Equivalents}}{\text{Reducing Equivalents}} \approx \frac{O}{R}$$

$$(O/R)N_2 = ([NO] + 3[SO_2] + 2[O_2])/([H_2] + [CO])$$

$$(O/R)NH_3 = (2.5[NO] + 3[SO_2] + 2[O_2])/([H_2]+[CO])$$

Run 24f was made under oxidizing conditions, $(O/R)NH_3 = 2.88$, which could have enabled SO_2 to escape and form $(NH_4)_2SO_3$ with effluent NH_3. After the H_2O was cut off there was no H_2 source for NH_3 formation. The system was then close enough to stoichiometric with respect to N_2 formation, $(O/R)N_2 = 1.15$, so that no SO_2 eluted and no precipitate formed.

7. Summary NO removal reactions.

This series of studies showed that H_2, CO, FeO, and FeS can act either in combination or independently as reducing agents for NO. When either H_2 or H_2O is present, both N_2 and NH_3 will be the products of NO reduction. NH_3 selectivity is greatest for a sulfided catalyst under reducing conditions with either H_2 or CO and H_2O as the reducing agents. When a source of hydrogen is available, the system must be net reducing with respect to NH_3 formation to prevent sulfur compounds from being stripped from the catalyst/absorbent.

D. Simultaneous Removal of Sulfur Compounds and Nitric Oxide at Low Temperatures.

The last section studied removal of NO over sulfided catalysts. In this section, the simultaneous removal of NO and the sulfiding of the catalyst/absorbent are discussed.

1. Reduction of NO with H_2S over Iron Sulfide.

The potential for the catalytic reduction of NO by H_2S over iron sulfide was studied first. Sulfur formation and sulfide formation reactions which are possible include the following:

	$\Delta H_{25°C}$ (kcal)	$\Delta F_{370°C}$ (kcal)	$\Delta F_{538°C}$ (kcal)	
$NO + H_2S \longrightarrow$				
$\frac{1}{2} N_2 + H_2O + \frac{1}{4} S_2$	- 59.2	- 56.7	- 56.0	iv-23
$FeO + H_2S \longrightarrow$				
$FeS + H_2O$	- 11.9	- 9.25	- 9.57	iv-2
$NO + 5/2\ H_2S \longrightarrow$				
$NH_3 + 5/4\ S_2 + H_2O$	- 39.8	- 31.1	- 28.6	iv-24
$NO + 3/2\ H_2O + 5\ FeO \longrightarrow$				
$NH_3 + 5/2\ Fe_2O_3$	-119	- 57.0	- 44.3	iv-25
$\frac{1}{2} S_2 + 2\ NO \longrightarrow$				
$SO_2 + N_2$	-130	-115	-111.0	iv-26
$FeO + NO + 2\ H_2S \longrightarrow$				
$\frac{1}{2} N_2 + 2\ H_2O + FeS_2$	-106.3	- 81.8	- 76.0	iv-27

In Run 22c, 1.1% H_2S and 0.55% NO were passed over iron sulfide. Complete NO and H_2S removal resulted. NH_3, N_2, H_2O, and precipitate

were present in the outlet line. The precipitate indicated that some H_2S possibly eluted from the bed. The precipitate was yellowish-white in color with a crystalline appearance suggesting a mixture of ammonium salts and sulfur. Data for this run are given in Figure iv-17. Since the catalyst was almost completely sulfided at the start of the run, reactions iv-2 and iv-27, (surface sulfiding) probably did not occur to any significant extent. The reported loss of S from the surface is within the experimental error. Reactions generating N_2 and NH_3 occur at the start of the run with reactions generating NH_3 predominating after the first hour. All of the collected precipitate was water soluble and had a significant partial pressure of NH_3. As noted earlier, NH_4HS has a high NH_3 partial pressure. If reaction iv-26 occurred, another possibility would be $(NH_4)_2SO_3$, which also decomposes giving NH_3. Since essentially 100% H_2S removal was found there must have either been some sulfur which precipitated upstream of the condenser or ammonium polysulfides formed in the low temperature precipitates.

As noted in the change of solid composition in Figure iv-17, the surface was oxidized, possibly by a reaction such as iv-25. Net surface oxidization implies that even with sulfur present as H_2S, a reducing agent will be needed to maintain an active reduced catalyst.

2. Removal of NO and H_2S with H_2 over Iron Oxide.

In Run 21a, H_2 was used as the reducing agent to remove H_2S and NO over fresh Fe_2O_3. Figure iv-18 presents the results. In this

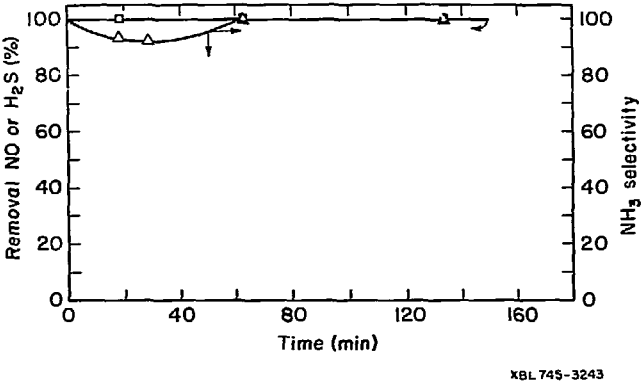

Fig. iv-17. Reduction of NO with H_2S.

Run	22c
T(°C)	366
[NO]	0.55%
[H_2S]	1.1%
Solid(I)	$FeO_{.40}S_{1.0}$
Solid(F)	$FeO_{.57}S_{.97}$

O H_2S removal
□ NO removal
△ NH_3 selectivity

Fe-301-T 1/8
(3.2mmX3.2mm)

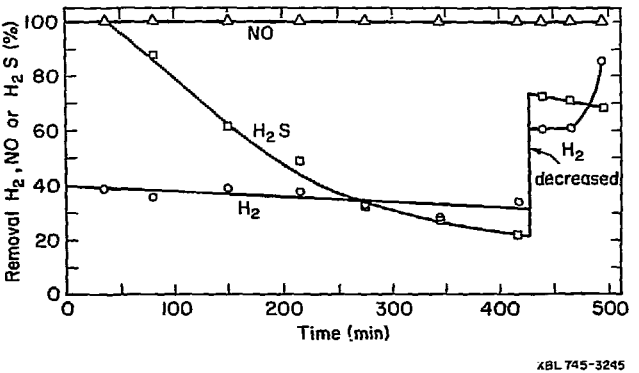

Fig. iv-18. Simultaneous removal of NO and H_2S with H_2. Part a, 0-428 minutes. Part b, 428-495 minutes.)

Run	21a	21b
T(°C)	372	372
θ (sec)	0.49	0.50
[NO]	0.33%	0.33%
[H_2]	3.1%	0.43%
[H_2S]	1.97%	1.97%
Solid(I)	$FeO_{1.5}$	$FeO_{.23}S_{.76}$
Solid(F)	$FeO_{.22}S_{.96}$	$FeO_{.23}S_{1.2}$

Fe-301-T 1/8
(3.22mmX3.2mm)

run there was a large excess of H_2, 3.8 times the stoichiometric amount for NH_3 formation. This large H_2 excess and the presence of H_2S resulted in 100% NH_3 selectivity over the entire run. The solid was not only sulfided but also reduced. In Run 21b, H_2 was decreased to 0.52 times the stoichiometric amount for NH_3 formation. The reactivity of H_2S with NO was seen immediately by the large increase in H_2S removal. Although H_2 removal increased, the absolute amount of H_2 reacting in the system decreased.

3. Removal of NO and H_2S with both CO and H_2 over Iron Oxide.

Run 22a used both CO and H_2 to remove H_2S and NO. Figure iv-19 reports the data. In this run the NO removal was 100% and the NH_3 selectivity was 100%. CO reacts to a greater extent in the system than H_2, reporting about 90% removal while the H_2 removal was about 30%.

4. Removal of NO and H_2S with CO over Iron Sulfide.

After Run 22a H_2O and H_2 were cut off and the [CO] increased. Figure iv-20 shows the data for Run 22b. As before, all NO was converted to NH_3. The H source in this run was H_2S causing the initial increase in H_2S removal. As the bed is sulfided H_2S removal decreases back to the level in Run 22a. Excess CO with respect to the NH_3 reaction slightly reduced the solid. Figures iv-18 and 19 show 50% H_2S removal at 193 and 115 minutes, respectively. These times are within those reported in Figure iv-3 for sulfidation of reduced iron in the absence of NO and reducing agents. The longer time above 50% H_2S removal in Figure iv-18 is probably due to the

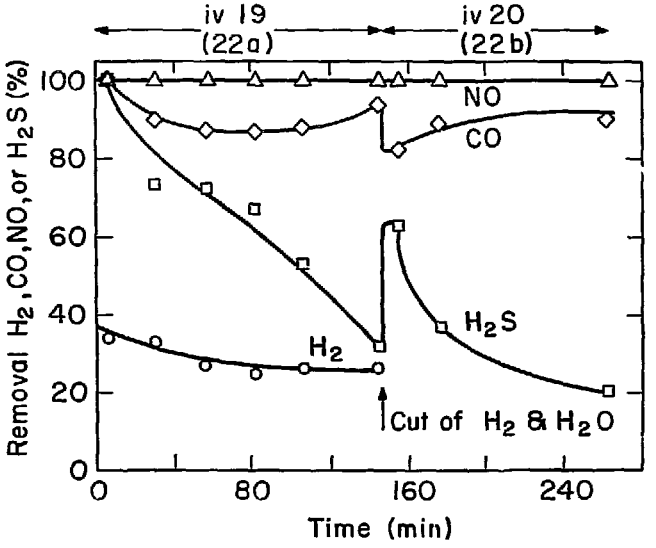

Fig. iv-19. Simultaneous removal of NO and H_2S with CO and H_2.

Fig. iv-20. Simultaneous removal of NO and H_2S with CO.

Run	22a	22b
T(°C)	371	371
θ (sec)	0.48	0.48
[NO]	0.52%	0.50%
[H_2]	1.2%	0
[CO]	0.96%	2.0%
[H_2S]	2.0%	2.0%
[H_2O]	6.3%	0
Solid(I)	$FeO_{1.5}$	$FeO_{.92}S_{.61}$
Solid(F)	$FeO_{.92}S_{.61}$	$FeO_{.40}S_{1.0}$

Fe-301-T 1/8 (3.2mmX3.2mm)

stronger reducing atmosphere, i.e. Figure iv-18 $(O/R)N_2 = 0.106$ and Figure iv-19 $(O/R)N_2 = 0.238$.

5. Removal of NO and COS over Iron Sulfide.

The second sulfur compound tested for removal with NO was COS. A short test confirmed that this system also removed all of the NO as NH_3. The potential reactions in this system would be:

	$\Delta H_{25°C}$ (kcal)	$\Delta F_{370°C}$ (kcal)	$\Delta F_{538°C}$ (kcal)	
$3\ H_2O + 5\ COS + 2\ NO \longrightarrow$				
$5\ CO_2 + 5/2\ S_2 + 2\ NH_3$	-121.0	-102	- 97.0	iv-28
$COS + H_2O \longrightarrow H_2S + CO_2$	- 8.27	- 8.05	- 7.95	iv-29

Since both S_2 and H_2S can form, reactions iv-24 and iv-26 could also occur. In Run 22e [COS] was 0.23%; [NO], 0.56%; $[H_2O]$, 4.0%. Complete removal of NO and COS resulted. The NH_3 selectivity was 100%. The same type of precipitate developed in this run as in the H_2S + NO reactions, Section D.1. Final catalyst/absorbent analysis could not be calculated because the COS feed to the system was erratic. Since there was more NO than COS, the surface of the catalyst/absorbent was probably oxidized.

6. Removal of NO and SO_2 with CO and H_2 over Iron Oxide.

Simultaneous removal of NO and SO_2 with CO and H_2 over iron sulfide was studied in Runs 27e and 27f. Data from these runs are plotted in Figure iv-21 with the last 35 minutes from Run 27d, removal of SO_2 with CO and H_2. Introduction of 0.53% NO caused an increase in both CO and H_2 removals. NH_3 selectivity is about 80%. Complete

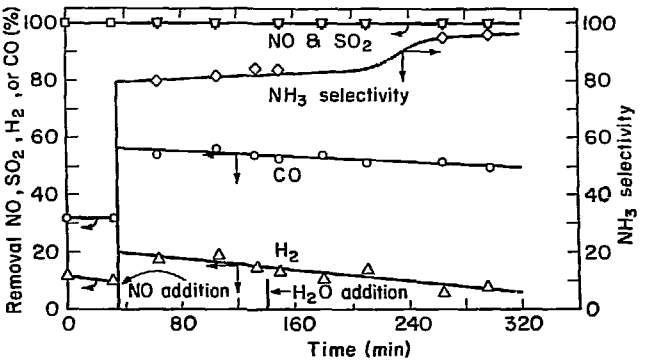

XBL 745-3246

Fig. iv-21. Simultaneous removal of NO and SO_2 with H_2 and CO over iron sulfide. (Part f, 35-131 minutes; part g, 131-320 minutes.)

Run	27f	27g
T(°C)	374	374
θ (sec)	0.43	0.43
[NO]	0.53%	0.58%
[SO_2]	0.45%	0.44%
[CO]	3.9%	3.8%
[H_2]	3.7%	3.7%
[H_2O]	0%	1.0%
Solid(I)	$FeO_{.85}S_{.26}$	$FeO_{.72}S_{.26}$
Solid(F)	$FeO_{.92}S_{.26}$	$FeO_{1.06}S_{.26}$

Fe-301-T 1/8
(3.2mmX3.2mm)

NO and SO_2 removal were obtained. SO_2 did not sulfide the catalyst but was converted to COS and H_2S which eluted from the bed. H_2S reacted with eluted NH_3 to precipitate as NH_4HS. In Run 27f, H_2O was added to the inlet gases. There was no immediate effect on the effluent gas. Toward the end of the run, though, the NH_3 selectivity had increased to 95%. This suggests that H produced from the water-gas shift reaction may be more reactive than molecular H_2 in NH_3 formation. Klimisch (1972) reported this result for the Cu-Cr oxide system. COS and H_2S eluted in this run. There was slight oxidation of the catalyst surface when H_2O was present.

7. Removal of NO, H_2S, and O_2 with CO and H_2 over Iron Oxide.

Experimental work reported to this point was done in the absence of O_2. Since there may be some O_2 present in the flue gas, experiments were run to determine its effect on NO and sulfur-compound removal. Runs 25a and 25b studied the effect of O_2 on the removal of H_2S and NO. Figure iv-22 reports the results. Almost immediately after starting the run, precipitate deposited in the outlet lines. The precipitate was NH_4HS and S_2. This was a much quicker breakthrough of H_2S and COS than had previously occurred. Because some of the effluent H_2S reacted to form the precipitate, actual H_2S removal is only about 75% of that shown in the figure. At 160 minutes H_2S in the inlet gas was cut down, resulting in a higher percent removal of H_2S and a lower percent removal for H_2. The [COS] eluted was roughly constant at 0.08%. At 288 minutes both [CO] and [H_2] were increased. This increase produced higher removals of H_2 and lower removals of H_2S. CO removal remained

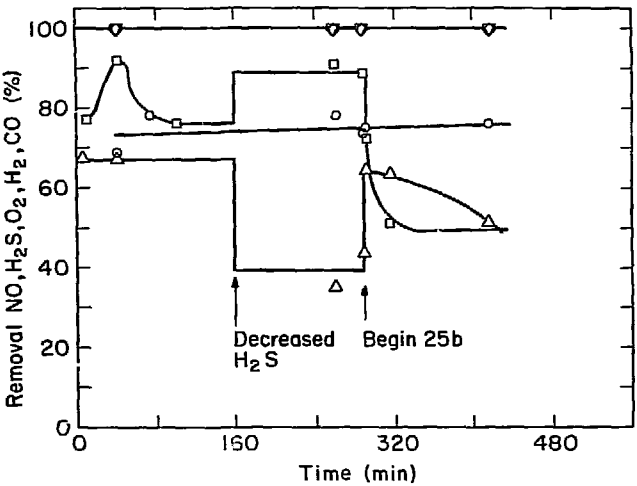

Fig. iv-22. Simultaneous removal of NO, H_2S, O_2 with H_2 and CO.

Run	25a	25b
T(°C)	368	374
θ (sec)	0.45	0.45
[NO]	0.51%	0.56%
[CO]	1.1%	1.4%
[O_2]	0.55%	0.62%
[H_2S]	2.0-1.0%	2.1%
[H_2O]	1.7%	1.4%
[H_2]	1.1%	1.3%
Solid(I)	$FeO_{1.5}$	$FeO_{.6}S_{.87}$
Solid(F)	$FeO_{.6}O_{.87}$	$FeO_{.04}S_{1.3}$

O CO removal
△ H_2 removal
◇ O_2 removal
▽ NO removal
□ H_2S removal

Fe-301-T 1/8
(3.2mmX3.2mm)

constant. The NH_3 collected in both the HCl scrubber and in the precipitate corresponded to a selectivity of 80%. This is only slightly less than the 100% selectivity reported in the absence of O_2, over iron sulfide in Run 22a. Throughout this run, the catalyst remained active for reduction of NO and O_2. The early elution of sulfur compounds suggests that oxygen inhibits sulfidation. The ratio, $(O/R)NH_3$, was 1.08 and 0.98 for Runs 25a and 25b, respectively. This proximity to the stoichiometric ratio in the gas stream and the initially unreduced catalyst both contributed to the system oxygen.

8. Removal of NO, SO_2, and O_2 with CO and H_2 over Iron Oxide.

When SO_2 and higher O_2 levels were tested, Run 26a, the catalyst became inactive for reduction of NO and SO_2. The only reactions which continued were O_2 and Fe_2O_3 reduction. Figure iv-23 shows the deactivation with respect to all reactions followed by reactivation of all but the NO and SO_2 reduction. In this run, $(O/R)N_2$ was 1.02, oxidizing with respect to even the N_2 formation reactions. Since no NH_3 was formed, there was no precipitate in this run. A significant difference in this run is that H_2 removal is substantially greater than CO removal, even though both have the same concentration. When O_2 was absent, the reverse was noted.

A final system variable which was studied under these conditions was particle size. Simultaneous removal of NO, O_2, and SO_2 with CO was tested with 3.2-mm pellets and with particles .50-mm to .25-mm in size. In both cases, catalyst deactivation was noted. In Run 29b, the catalyst initially removed all the NO, SO_2, and O_2. After 80

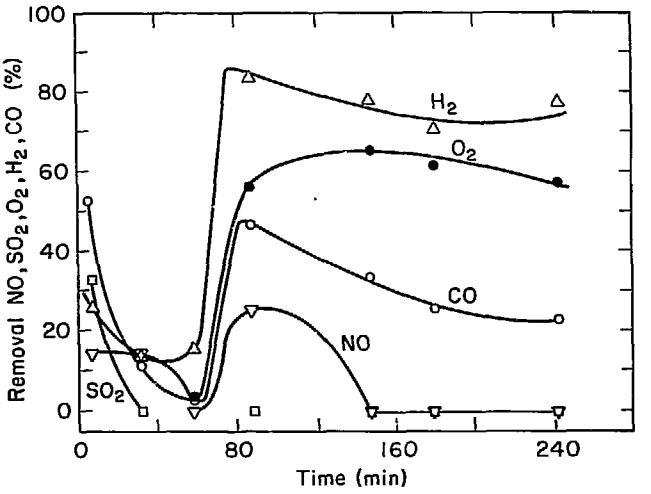

Fig. iv-23. Simultaneous removal of NO, SO_2, O_2 with H_2 and CO.

Run	26a
T(°C)	368
θ (sec)	0.45
[CO]	2.2%
[H_2]	2.2%
[O_2]	2.0%
[NO]	0.5%
[SO_2]	0.37%
Solid(I)	$FeO_{1.5}$
Solid(F)	$FeO_{1.3}S_{.01}$

Fe-301-T 1/8 (3.2mmX3.2mm)

minutes on stream, it was eluting 6% and 12% of inlet NO and SO_2, respectively. O_2 was removed over the entire run. These data are presented in Figure iv-24. The NH_3 selectivity was about 30%, much lower than previously noted. In Run 29b $(O/R)NH_3$ was 1.10, slightly oxidizing with respect to total NH_3 product. If the 30% NH_3 selectivity is accounted for, the ratio is 0.98, slightly reducing. The outer layer of the catalyst near the bed exit was reduced. Had the run continued, the oxidation front would undoubtedly have passed through the entire bed.

In Run 30c there was a net oxidizing atmosphere and the entire bed of particles was oxidized. The 0.50-mm to 0.25-mm particles were exposed to a stream with $(O/R)N_2$=1.16, net oxidizing with respect to N_2 formation. As Figure iv-25 shows, all removals rapidly drop to zero. The order of decrease is the same as in Run 29b, SO_2 first, NO second, and O_2 third. This suggests a relative order of oxidizing power, O_2 being the most powerful. The specific effect of the smaller particle size at this temperature was masked by the deactivation. At the end of this run, the entire bed was oxidized. The particles were completely oxidized, exhibiting no reducing inner core as was seen in Run 29b.

9. Summary of Simulaneous Removal of NO and sulfur compounds.

Simultaneous removal of NO and sulfur compounds at 370°C is best accomplished with reduced iron oxide in a net reducing atmosphere which has no O_2 present. If O_2 is present, rapid catalyst deactivation will occur when the gas is net oxidizing. Even under net reducing conditions, slow catalyst oxidization will occur when O_2 is present in the gas stream. Smaller particles do not appear to slow or

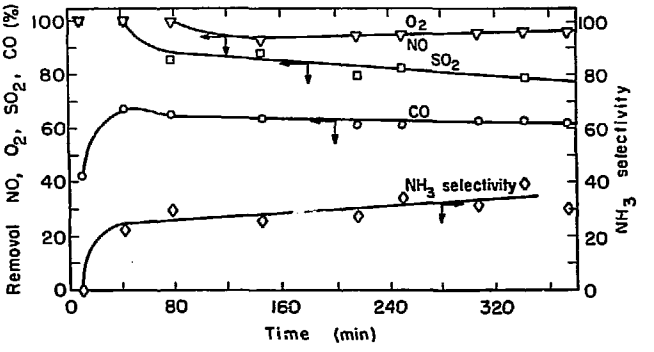

XBL 745-3223

Fig. iv-24. Simultaneous removal NO, O_2, SO_2 with CO.
Run 29b [CO] 4.2-4.6% [SO_2] 0.51% Solid(I) $FeO_{1.23}$
T(°C) 374 [NO] 0.53% [H_2O] 1.14% Sclid(F) $FeO_{2.5}S_{.43}$
θ (sec) 0.44 [O_2] 1.0% Fe-301-T 1/8 (3.2mmX3.2mm)

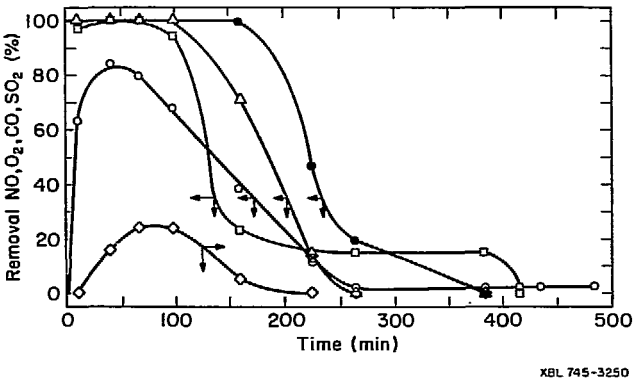

Fig. iv-25. Simultaneous removal of NO, O_2, SO_2 with CO.
Fe-301-T 1/8 (0.50mm-0.25mm)

Run	30c	Symbol
T(°C)	371	
θ (sec)	0.28	
[CO]	4.95%	○
[NO]	0.61%	△
[O_2]	1.1%	●
[SO_2]	0.98%	□
[H_2O]	0.7-1.2%	
Solid(I)	$FeO_{1.18}$	
Solid(F)	$FeO_{2.2}S_{.29}$	
NH_3 selectivity		◇

prevent catalyst deactivation.

The capability of NO to oxidize FeS forming SO_2 was shown. Since O_2 is a stronger oxidizer, it is capable of oxidizing FeS at least to the same extent and probably continuing to form sulfate. If $FeSO_4$ forms, as is expected thermodynamically, it can be reduced as follows:

	$\Delta H_{25°C}$ (kcal)	$\Delta F_{370°C}$ (kcal)	$\Delta F_{538°C}$ (kcal)	
$FeSO_4 + 4\ CO \longrightarrow FeS + 4\ CO_2$	-72.7	-74.1	-76.4	iv-30
$FeSO_4 + 4\ H_2 \longrightarrow FeS + 4\ H_2O$	-33.4	-58.7	-66.5	iv-31

Kinetic limitations at 370°C may inhibit these reactions even under net reducing conditions. The upper temperature of 538°C may allow these reactions to proceed.

E. Simultaneous Removal of SO_2 and NO at High Temperatures.

Experiments reported in all previous sections are run at temperatures close to 370°C. In power plants this corresponds to the temperature of the flue gas at the inlet of the air preheater. The upper limit on the reaction zone is the inlet to the economizer. Temperatures here are about 540°C. Runs discussed in this section were at this temperature level.

1. Removal of NO, SO_2, and O_2 with CO and H_2O over Iron Oxide.

a. Long residence time runs.

Simultaneous removal of NO, SO_2, and O_2 with CO and H_2O over reduced iron oxide was studied in Runs 31b and 35b. The catalyst/

absorbent size was 3.2-mm pellets. The data are presented in Figures iv-26 and iv-27. Both runs maintained complete removal of NO and O_2 over the entire run. SO_2 was not completely removed. Estimation of SO_2 removal with time was not possible because eluted sulfur compounds formed ammonia salts. The average SO_2 removal is plotted starting when precipitate was first seen. The precipitate which formed was white and released NH_3 when heated. Tests confirmed that is was $(NH_4)_2SO_3$. NH_3 was also collected in th HCl scrubbers. These two sources gave average NH_3 selectivities for the runs of 64% and 69%, respectively. The precipitate formed most heavily toward the end of the run in both cases. The NH_3 selectivity increased with time in both runs. In Run 31b and 35b (O/R)NH_3 was 0.956 and 1.00. Both runs were thus net reducing, with Run 35b being slightly less so. The pellets at the end of each run were solid black and reflected no tendency to poison. The high removals achieved for all compounds over the entire bed suggest that the actual reaction time is less than the gas residence time in the bed. The CO removal begins to drop off only after 75% of the iron has been sulfided. This behavior suggests reaction times of the order of 0.10 second or less, 36,000 hr^{-1} space time.

b. Short residence time runs

Runs 36b and 37b confirmed that reaction does occur in less than 0.10 second. A 6.4-mm ID. 316 stainless steel reactor gave residence times about 0.04 to 0.02 seconds, depending on the catalyst charge. In this smaller reactor 2 grams of catalyst corresponded to

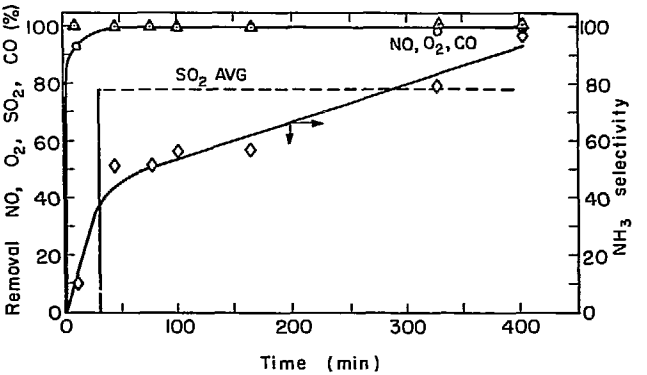

XBL 745-3218

Fig. iv-26. Simultaneous removal of NO, O_2, SO_2 with CO and H_2O.

Run	31b
θ (sec)	0.33
T(°C)	538
[NO]	0.58%
[O_2]	0.50%
[SO_2]	0.65%
[CO]	4.6%
[H_2O]	1.6%
Solid(I)	$FeO_{1.18}$
Solid(F)	$FeS_{0.78}$
○ CO removal	
△ NO removal	
• O_2 removal	Fe-301-T 1/8
–– SO_2 avg. removal	(3.2mmX3.2mm)
◇ NH_3 selectivity	

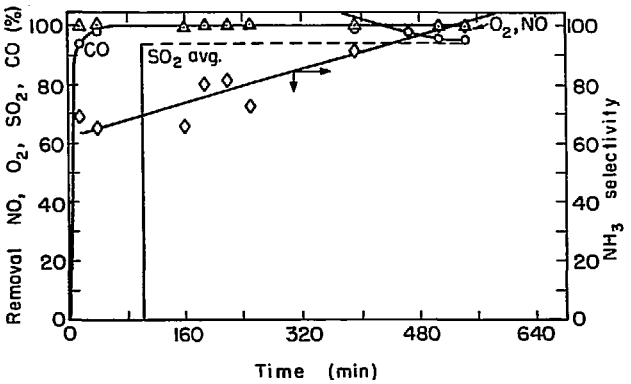

Fig. iv-27. Simultaneous removal of NO, O_2, SO_2 with CO and H_2O.

Run	35b
θ (sec)	0.34
[NO]	0.50%
[O_2]	0.49%
[SO_2]	0.48%
[CO]	3.7%
[H_2O]	1.8%
Solid(I)	$FeO_{1.17}$
Solid(F)	$FeS_{0.96}$
O CO removal	
Δ NO removal	
• O_2 removal	
-- SO_2 avg. removal	Fe-301-T 1/8
◇ NH_3 selectivity	(3.2mmX3.2mm)

a residence time of about 0.034 seconds. This smaller volume cuts the sulfur breakthrough time 10-fold from that in the 3.2-mm reactor. With the SO_2 feed rates in Runs 36b and 37b, the calculated sulfur breakthrough times were 78 and 56 minutes, respectively. Figures iv-28 and 29 report the actual breakthrough times close to these values. Exact determination of the breakthrough curve was not possible with the existing analytical system.

In Figure iv-28, Run 36b, sulfur eluted in the form of H_2S and COS. Ammonia was collected both as precipitate and in the HCl scrubber. The average NH_3 selectivity for Run 36b was 48%. The oxidation level for this run was $(O/R)N_2 = 0.81$ and $(O/R)NH_3 = 1.01$. If 100% NH_3 selectivity had occurred anywhere in the bed, the atmosphere would have been net oxidizing. Although the bed remained reactive for the entire run, the catalyst at the end of the run was oxidized in the first half of the bed; both Fe_2O_3 and $FeSO_4$ were found to be present.

In Run 37b, Figure iv-29, the average NH_3 selectivity was 68%. The oxidation levels at the start were $(O/R)N_2 = 0.84$ and $(O/R)NH_3 = 1.05$. Producing 100% NH_3 locally would result in a net oxidizing atmosphere. This apparently occurred after 80 minutes, since all removals went below 10%. At 160 minutes the O_2 level was decreased to make $(O/R)NH_3 = 0.85$. Removals immediately increased. The $[O_2]$ was cycled again, and the same results occurred. When the system had a net reducing atmosphere with respect to NH_3 generation, the catalyst was active. It is significant to note that even though the catalyst was substantially sulfided in the first cycle, sulfur compounds

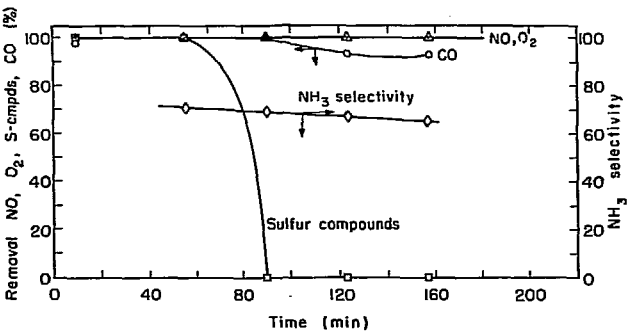

Fig. iv-28. Simultaneous removal of NO, O_2, sulfur compounds and CO.

Run	36b	
T(°C)	370	
θ (sec)	0.34	
[NO]	0.50%	
[O_2]	0.45%	
[SO]	0.50%	Fe-301-T 1/8
[CO]	3.6%	(0.50mm-0.25mm)
[H_2O]	1.4%	
Solid(I)	$FeO_{1.34}$	
Solid(F)	$FeS_{0.76}$	

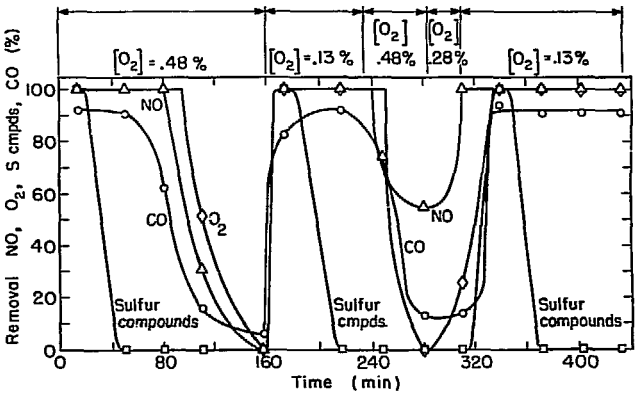

XBL 745-3215

Fig. iv-29. Simultaneous removal of NO, O_2, sulfur compounds and CO.

Run	37b
T(°C)	378
θ (sec)	0.031
[NO]	0.49%
[O_2]	Varied
[SO_2]	0.50%
[CO]	3.5%
[H_2O]	1.3%
Solid(I)	$FeO_{1.30}$
Solid(F)	$FeO_{0.63}S_{1.06}$

Fe-301-T 1/8
(0.50mm-0.25mm)

stopped eluting immediately after the O_2 level was decreased. As in Run 36b, when the run was complete, the last half of the bed had remained active while the entrance had been oxidized during the run.

The sulfur compound elution pattern is shown in Figure iv-30. H_2S initially breaks through followed by COS then SO_2. NO elutes at about the same time as SO_2, followed by O_2. This pattern was repeated twice. The third pattern appears to be the same, only slower. This suggests that the level of O_2 or the O/R ratio has a direct influence on the bed capacity.

In normal operating conditions, the catalyst/absorbent would not be used after complete sulfidization. Run 37b continued after complete sulfidization. Another extended run was made, Run 38, in which the CO level was varied at a constant O_2 level of 0.98%. Even under net reducing conditions, the sulfided catalyst rapidly deactivated. Reactivation only occurred when O_2 was removed from the inlet gases. This emphasizes the importance of maintaining reduced iron oxide in the catalyst/absorbent. Ferrous oxide is required both for the absorption of sulfur compounds and to prevent rapid catalyst deactivation.

2. Removal-Regeneration Cycles for NO,SO_2, and O_2 with CO over Iron Oxide.

In Runs 39 and 40, a cyclic removal/regeneration procedure was used to provide a high level of FeO when testing the catalyst activity. A larger, 9.5-mm reactor was used in this study to give longer breakthrough times for sulfur compounds. The charge of 2.6 grams of

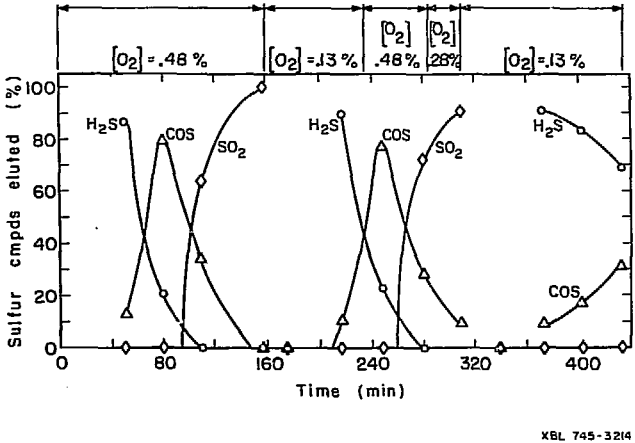

XBL 745-3214

Fig. iv-30. Distribution of sulfur compounds eluted in Run 37b.
O H_2S △ COS ◇ SO_2 (Detailed data, see Fig. iv-29.)

catalyst gave a residence time of 0.040 seconds. Calculated breakthrough times for sulfur compounds for Runs 39 and 40 were 69 minutes and 75 minutes, respectively. This longer time enabled at least two samples to be taken prior to breakthrough.

In Run 39 the actual breakthrough of H_2S below 90% removal occurred between 50 and 70 minutes for the four trials. The data are presented in Figure iv-31. Complete O_2 and NO removal were achieved for all trials. The average NH_3 selectivity for these trials ranged between 53 and 64%. The $(O/R)N_2$ was 0.758 and $(O/R)NH_3$ was 0.896, reducing with respect to both NH_3 and N_2 formation.

The catalyst was regenerated in situ between each trial. The temperature was first raised to 670°C. The $[O_2]$ in the regeneration gas stream in Run 39 was varied from 2% to 21%. The regeneration conditions are given in Figure iv-31. Air regeneration gave the catalyst with the highest sulfur capacity. All removal steps, however, appear comparable to the first.

Run 40 had removal conditions, parts b and e, similar to Run 39. The data are presented in Figure iv-32. The regeneration conditions, parts c,d and f,g were altered to determine sulfate levels in each half of the bed. Run 40b was with fresh catalyst and Run 40e was with the regenerated catalyst from Run 40d. After the removal steps, the black particles (reactor exit) were separated from the red (reactor entrance). Each half was heated to 693°C for one hour under stream of a He. Any $FeSO_4$ would decompose under these conditions. A stream with 1% O_2 was then introduced for one hour to oxidize the sulfide to SO_2. The SO_2 generated in steps c,d and f,g was collected in

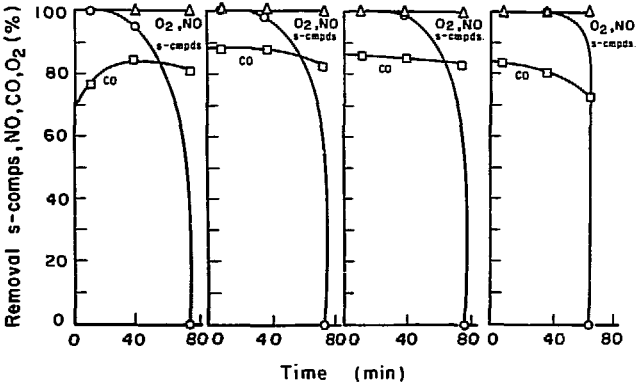

Fig. iv-31. Percent removal of S-compounds, NO, CO versus run time with four successive removals. Run No. 39.

Removal conditions

[NO] = 0.50%	[CO] = 5.5%	Removal at:
[SO_2] = 0.56%	[O_2] = 1.9%	T = 560°C
[H_2O] = 1.7.		θ = 0.04 sec

Fe-301-T 1/8 (0.50mm-0.25mm)

Regeneration conditions

1st 4% [O_2] for 66 min.	Regeneration at:
2nd 2% [O_2] for 129 min.	T = 670°C
3rd 21% [O_2] for 63 min.	θ = 0.038 sec

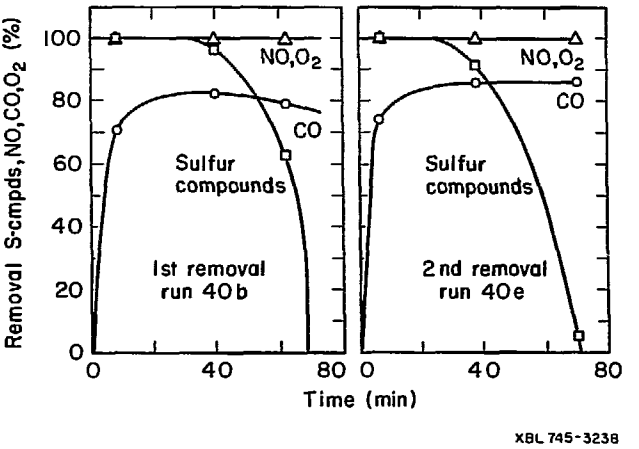

Fig. iv-32. Removal of S-compounds, NO, CO versus run time.

Removals:

[NO]	0.53%
[O_2]	1.0%
[CO]	5.55%
[SO_2]	0.53%
[H_2O]	1.7%

θ = 0.038 sec
T = 599°C

Fe-301-T 1/8
(0.50mm-0.25mm)

Regenerations:

T = 693°C 1%[O_2] for 65 minutes
T = 675°C 0%[O_2] for 60 minutes

NaOH scrubber solutions. Sulfate was found in both reduced and oxidized particles. The two bed sections were then combined and recharged to the reactor for the second removal step. The results are summarized below:

Table iv-2. Sulfate level in reacted catalyst/absorbent.

	Reduced, Black (Bed Exit)		Oxidized, Red (Bed Entrance)		Overall	
Run	40b-c,d	40e-f,g	40b-c,d	40e-f,g	40b-c,d	40e-f,g
S as $SO_4^=$ (%)	11.6	13.3	64	48.1	23.0	18.4
S as $S^=$ (%)	88.4	86.7	36	52.9	77.0	81.6

The O_2 in the sulfate corresponded to only 17 and 21% of the total O_2 in the feed for Runs 40b and 40e, respectively. Removal of the remaining O_2 was by reaction with CO. Integration of the curve area and solid analysis from the second regeneration show about the same capacity. Both trials had an NH_3 selectivity of 45%. In Run 40 the $(O/R)N_2$ was 0.80 and $(O/R)NH_3$ was 0.94, both net reducing.

In Run 39, each trial resulted in an S/Fe ratio of around 0.60 to 0.70. In Run 40, the S/Fe ratio was between 0.90 and 1.0. Comparision of the O/R ratios would suggest that Run 39 should have been more strongly sulfided. The increased temperature of Run 40, 39°C higher than Run 39, may account for the higher sulfidation level.

These two runs have demonstrated the activity and regenerability of the catalyst even when 1% O_2 is present in the inlet stream. This oxygen level results in between 15 to 25% of the sulfur forming sulfate. The oxygen consumed in this sulfate formation is only 15 to 20% of the inlet O_2 feed.

F. Ammonia Generation

Numerous runs have been discussed in which either NH_3 or ammonia-sulfur salts were formed. Jones (1971) and Klimisch (1972) have shown that the presence of oxygen will decrease ammonia selectivity during NO reduction. A correlation between both this effect and the effect of the oxidizing or reducing nature of the catalyst/absorbent on NH_3 selecticity was found. Figure iv-33 shows the effect on the NH_3 selectivity of the product of the ratio of the moles of oxide to moles of sulfide in the solid with the ratio of oxidation to reduction equivalents in the inlet gas. The ratio for the oxide to sulfide is an average of initial and final conditions. This procedure is not strictly correct since initially no sulfide is present and at the end there is a large amount of sulfide. The qualitative trend on this graph is important: the greater the reducing equivalents in the gas or the more sulfide on the solid, the greater will be the NH_3 selectivity. This correlation is for runs between 370° and 590°C. NH_3 is unstable relative to N_2 and H_2 at and above 370°C for the concentrations used in this experiment. Shelef (1972) reports NH_3 decomposition at the upper temperature limit with an iron oxide catalyst. There is no apparent decomposition in these runs since all runs have about the same dependence on the combined factor. Runs with copper and nickel, reported in the next two sections, were made to test the potential of these metals to produce lower NH_3 selectivities.

G. Simultaneous Removal of SO_2, NO and O_2 with Copper Oxide and Nickel Oxide.

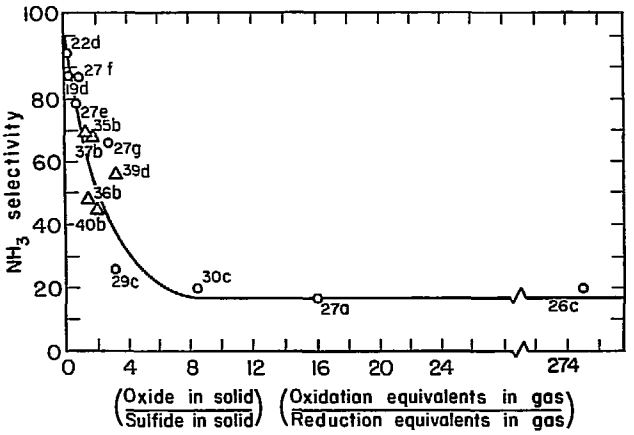

XBL 745-3212

Fig. iv-33. NH_3 selectivity as a function of solid and gas composition.

Run	Gas composition (%) [NO]	[SO_2]	[CO]	[H_2]	[O_2]	[H_2O]
19d	0.38	0	0	2.5	0	0
22d	0.58	0	1.1	0	0	3.4
26c	0.50	0.95	3.7	3.6	2.0	4.9
27a	0.50	0.41	3.6	3.6	2.0	1.4
27e	0.53	0.44	3.9	3.7	0	0
27f	0.55	0.44	3.8	3.7	0	1.0
27g	0.53	0.45	3.7	3.6	1.3	1.0
29c	0.53	0.50	4.6	0	1.0	1.·
30c	0.61	0.98	4.9	0	1.1	1.0
35b	0.50	0.48	3.7	0	0.49	1.8
36b	0.50	0.50	3.6	0	0.45	1.3
37b	0.49	0.50	3.5	0	0.13-0.48	1.3
39d	0.49	0.56	5.5	0	1.0	1.7
40b	0.53	0.53	5.6	0	1.0	1.7

O T = 370-380° C, θ = 0.5-0.7 sec
△ T = 538-590° C, θ = 0.02-0.04 sec

(Fe-301-T 1/8)

1. Removal with Copper Oxide.

Copper Oxide was reported to accomplish simultaneous SO_2 and NO removal by forming S_2 and N_2 (Quinlan, 1973 and Ryason, 1967). A similar copper catalyst was tested for its ability to remove SO_2 as a sulfide and NO as N_2 and NH_3. The catalyst was Harshaw Cu-0803T1/8 which has 10% CuO deposited on activated Al_2O_3. The 3.2-mm pellet size was used. The catalyst was first reduced with CO to $CuO_{0.15}$. Calculated breakthrough time for the sulfur compounds is 129 minutes assuming Cu_2S formation. Figure iv-34 presents the data. NO, O_2, and SO_2 were completely removed. CO removal dropped at first then increased to about 100% toward the end of the run. Sulfur compound removal reflects elution of COS during the first 150 minutes. The large breakthrough after 150 minute is H_2S. NH_3 selectivity constantly increased over the run. The average value from the HCl scrubber and precipitate was 73%. In this run $(O/R)N_2$ was 0.714 and $(O/R)NH_3$ was 0.95, net reducing. If all NO had been converted locally to NH_3, a condition close to stoichiometric, within experimental error, may have occurred. Quinlan (1973) assumed that the water-gas shift reaction did not proceed and hence no NH_3 could be formed. They could have missed generated NH_3 since they did not analyze for it. At the start of Run 33b, when O was being removed from the catalyst, the system may have gone slightly oxidizing, causing elution of CO and COS. With iron oxide in Runs 31b and 35b, SO_2 eluted throughout the runs instead of COS. This fact implies that copper has higher catalytic activity for SO_2 reduction but that iron is more reactive with the H_2S or COS which are produced.

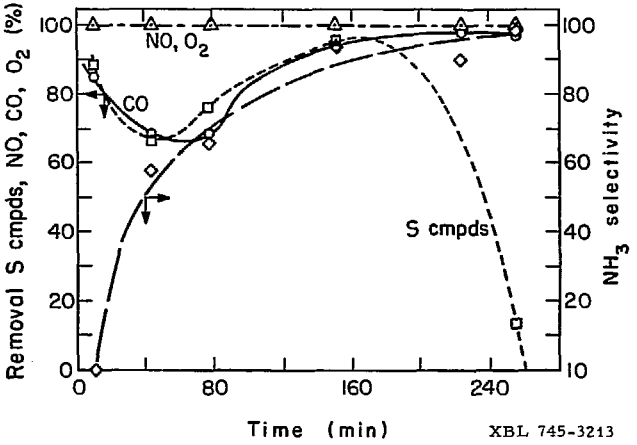

Fig. iv-34. Simultaneous removal of SO_2, NO, CO, and O_2 over copper oxide catalyst.

Run	33b
T(°C)	538
θ (sec)	0.33
[NO]	0.50%
[O_2]	0.50%
[SO_2]	0.50%
[CO]	4.2%
[H_2O]	1.9%
Solid(I)	$CuO_{.15}$
Solid(F)	$CuS_{.59}$

△ NO removal
● O_2 removal
□ Sulfur compounds
○ CO removal
◇ NH_3 selectivity

Cu-0803-T 1/8
(3.2mmX3.2mm)

2. Removal with Nickel Oxide.

A combination of nickel and iron oxides was tested to see if the amount of NH_3 produced could be decreased. Klimisch (1973) has demonstrated the ability of Ni to decompose NH_3 on a Pt-Ni-Al catalyst at 500°C. The iron was to function as it had in previous runs while the nickel was to decompose the NH_3 which formed.

Run 41 was identical with Run 40 except that the first half of the bed was Fe-0301 and the second half was Ni-301 catalyst. Both catalysts were ground to 0.50-0.25-mm in size, NH_3 selectivities for the two parts were 27% and 41%, respectively. These values are only slightly lower than for the iron oxide runs. The data are presented in Figure iv-35. Calculated breakthrough times for parts a and c are 65 minutes and 75 minutes, respectively. The two-step regeneration was used separately on the iron and nickel portions after each trial. The reported S/Ni values were 1.29 and 1.26 while the S/Fe values were 0.48 and 0.65. The overall sulfate level was 26%, most of which was in the iron. Contamination of the nickel portion of the catalyst bed with some of the iron probably caused the high S/Ni ratio.

3. Summary of Copper and Nickel runs

These runs show that although both nickel and copper catalysts are active for the proposed removal reactions neither significantly lowers the NH_3 selectivity or inhibits the formation of sulfate. The reactions forming the copper and nickel sulfides and sulfates are:

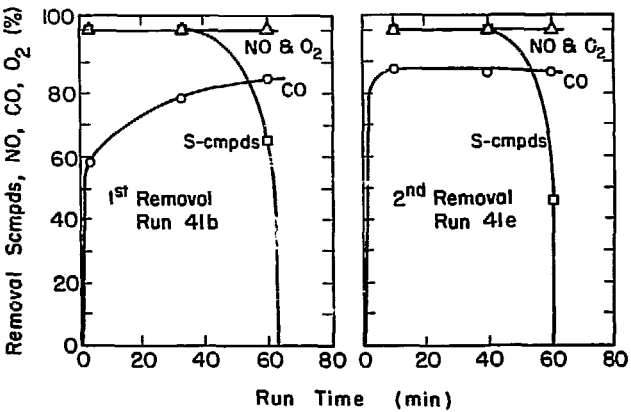

XBL 745-3222

Fig. iv-35. Removal of sulfur compounds, NO, O_2 and CO. Two successive cycles. Run No. 41.

Removals:
[NO] 0.53%
[O_2] 1.0%
[CO] 5.6%
[SO_2] 0.58%
[H_2O] 1.7%
θ = 0.043 sec
T = 600°C

Regeneration:
T = 671°C [O_2] = 0 %
T = 695°C [O_2] = 1 %

	$\Delta H_{25°C}$ (kcal)	$\Delta F_{25°C}$ (kcal)	$\Delta F_{370°C}$ (kcal)	$\Delta F_{676°C}$ (kcal)	
$2\ CuO + CO \longrightarrow$					
$Cu_2O + CO_2$	-32.8	-----	-36.2	-36.9	iv-32
$Cu_2O + SO_2 + 3\ CO \longrightarrow$					
$Cu_2S + 3\ CO_2$	-110.5	-----	-97.1	-81.1	iv-33
$NiO + SO_2 + 3\ CO \longrightarrow$					
$NiS + 3\ CO_2$	-92.1	(Not Known)		-----	iv-34
$CuSO_4 \longrightarrow$					
$CuO + SO_2 + \frac{1}{2}\ O_2$	+75.64	+54.72	-----	+13.37	iv-35
$NiSO_4 \longrightarrow$					
$NiO + SO_2 + \frac{1}{2}\ O_2$	+84.74	+61.52	-----	-----	iv-36

Lowell (1971) lists the decomposition temperatures of $CuSO_4$ and $NiSO_4$ as 840-935°C and 730-890°C, respectively. In the regeneration runs, 1% O_2 was used at 675°C. These conditions only partially regenerated copper oxide. A comparison of SO_2 collected in the scrubber with that on the solid showed that CuO was only 50% regenerated. The dark greenish color present is characteristic of $CuSO_4$. The same comparison for nickel showed that it was almost completely regenerated. The catalyst was a faint green color which is the characteristic color of NiO.

H. Oxidation of CO and H_2.

One of the process requirements is that the flue gas have a net

reducing atmosphere. Excess CO or H_2 needs to be removed by oxidation with oxidized catalyst to prevent discharge into the atmosphere. Reactions for the iron oxide system include the following:

	$\Delta H_{25°C}$ (kcal)	$\Delta F_{370°C}$ (kcal)	$\Delta F_{538°C}$ (kcal)	
$Fe_2O_3 + CO \longrightarrow$				
$2\ FeO + CO_2$	+ 1.57	- 6.96	- 7.77	iv-37
$3\ Fe_2O_3 + CO \longrightarrow$				
$2\ Fe_3O_4 + CO_2$	-12.83	-20.42	-23.28	iv-38
$Fe_2O_3 + H_2 \longrightarrow$				
$2\ FeO + H_2O$	+11.4	- 3.28	- 5.50	iv-39
$3\ Fe_2O_3 + H_2 \longrightarrow$				
$2\ Fe_3O_4 + H_2$	- 3.0	-16.8	-20.9	iv-40

1. CO Oxidation.

Oxidation of CO was studied in more detail than that of H_2, since a greater percentage of the reducing agent will be CO, see Chapter V. The data are presented in Figure iv-36. A 60% maximum CO removal was achieved with the 3.2-mm pellets of Fe/Al_2O_3 in Runs 14a, 15a, and 24a. When the CO level was decreased and the particles were sized 0.50-0.25-mm, close to 100% CO removal was initially achieved. As in other runs, CO removal drops off rapidly. Higher removals with smaller particles suggests that diffusion limits the extent of reaction in the larger particles. Raising the temperature to 538°C with the larger pellets also produced removals close to 100%. In all runs

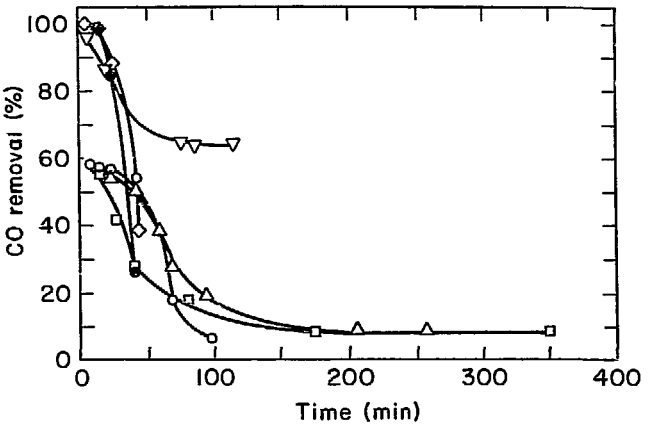

Fig. iv-36. Oxidation of CO with iron oxide. Long residence time.

Run	14a	15a	24a	30a	31a	35a
T(°C)	378	368	407	370	538	538
θ (sec)	0.55	0.52	0.43	0.29	0.33	0.34
[CO] (%)	1.7	1.6	2.0	0.50	2.9	3.0
Solid(I)	$FeO_{1.5}$	$FeO_{1.5}$	$FeO_{1.5}$	$FeO_{1.5}$	$FeO_{1.5}$	$FeO_{1.5}$
Solid(F)	$FeO_{1.34}$	$FeO_{1.25}$	$FeO_{1.13}$	$FeO_{1.18}$	$FeO_{1.18}$	$FeO_{1.19}$
Symbol	○	△	□	▽	◇	•
Size(mm)	3.2	3.2	0.5-0.25	3.2	3.2	3.2

Fe-301-T 1/8

where CO removal was 100% in the first sample, the outlet CO_2 did not equal inlet CO flow. As the run progressed, the total CO_2 + CO did equal the inlet CO within the experimental error. It is suspected that adsorption of CO or CO_2 occurs. This phenomenom was briefly discussed in connection with Run 15, Section C.1. The initial high removal for the low CO . is in part due to CO adsorption.

Another set of with a much shorter residence time is illustrated in Figure iv-37. These runs were with 0.50-0.25-mm sized particles. A rapid drop-off of CO removal is shown for the 1% CO runs. Run 38a with CO 0.38% shows a much slower drop-off with time.

CO removals in both Runs 30a and 38a remained high since the time required to reduce the surface is longer with the low CO concentration. If diffusion or first-order kinetic limitations predominated, the percent removal should be uneffected by the CO concentration. The variation can be explained by an initially active surface followed by a progressively less active surface species. This fact would suggest that, in order of decreasing activity toward CO, the iron oxides would rank Fe_2O_3 > Fe_3O_4 > FeO.

Some of the excess CO may also be oxidized by unreacted O_2 in the gas stream. In Run 8 the CO + O_2 reaction was studied over both reduced and oxidized iron. The data are present in Figure iv-38. O_2 removal was 1 % in the two cases. In the net reducing system, the solid was reduced in both cases. After 100 minutes, both Runs 8b and 8d had CO removals which corresponded to only the O_2 oxidation, demonstrating the catalytic ability of iron oxide.

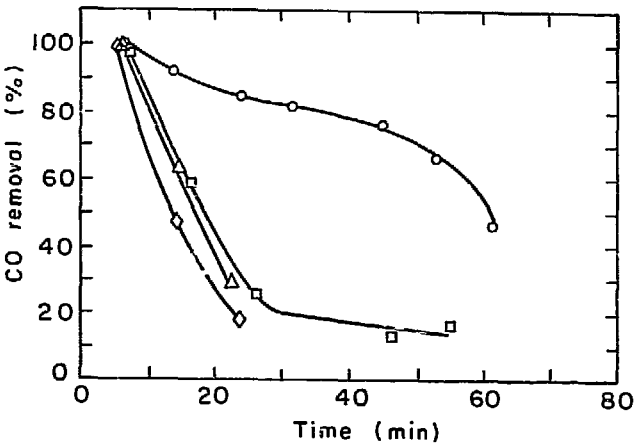

XBL 745-3263

Fig. iv-37. Oxidation of CO with iron oxide. Short residence time.

Run	38a	39a	40a	42a
T(°C)	538	560	566	571
θ (sec)	0.022	0.040	0.040	0.045
[CO] (%)	0.38	0.94	1.0	1.0
Solid(I)	$FeO_{1.5}$	$FeO_{1.5}$	$FeO_{1.5}$	$FeO_{1.5}$
Solid(F)	$FeO_{1.20}$ ○	$FeO_{1.16}$ △	$FeO_{1.13}$ ◇	$FeO_{.99}$ □

Fe-301-T 1/8
(0.50mm-0.25mm)

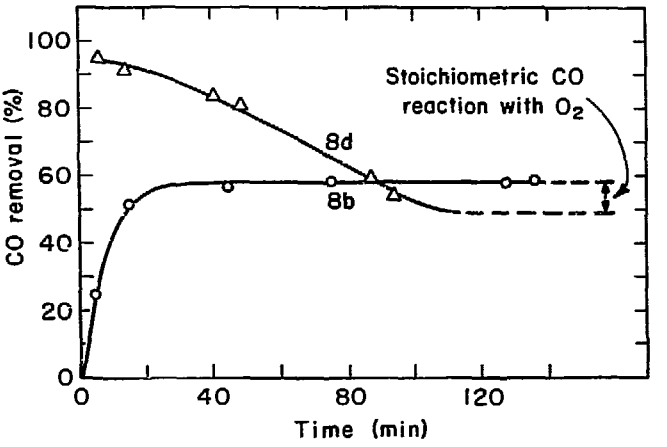

XBL 745-3239

Fig. iv-38. Oxidation of CO with O_2 over oxidized and reduced iron oxide.

Run	8b	8d
T(°C)	436-377	377
θ (sec)	0.61-0.66	0.67
[CO]	3.0%	3.1%
[O_2]	0.87%	0.78%
Solid(I)	$FeO_{1.14}$	$FeO_{1.50}$
Solid(F)	$FeO_{1.09}$	$FeO_{1.35}$
Symbol	O	Δ

Fe-301-T 1/8
(3.2mmX3.2mm)

2. H_2 oxidation.

The H_2 oxidation study was conducted only with the large, 3.2-mm pellets. The data are presented in Figure iv-39. The highest H_2 removal for these tests was about 25%. This result is some 35 percent units lower than the CO removal under comparable conditions. The rise in the curve for Run 9a is a result of the temperature increase to 453°C. If diffusion limitations within the pellets were the rate-determining step, H_2 oxidation should proceed faster than CO oxidation. The reverse is the actual case, implying that H_2 oxidation kinetics are slower than combined CO oxidation diffusion and kinetic rates.

I. Other Reactions Studied.

1. Water-gas shift reaction.

In experiments on NO reduction, NH_3 was formed when H_2O and CO were the reducing agents. This fact suggested that the water-gas shift reaction proceeds in the presence of either iron oxide or iron sulfide. Run 42 showed that both H_2 and CO_2 were produced, confirming this prediction. The data are presented in Figure iv-40. The H_2O removal was determined by the H_2 produced. The percent water removal is much lower than that of CO because it is in excess. The discrepancy between the $[CO_2]$ and $[H_2]$ produced is due to error in the H_2 measurement and oxidation of the surface by CO. There is very little significant difference between the two catalysts. Since the water-gas shift reaction does proceed, H_2 may be an important intermediate not only for the NH_3, but also for the H_2S seen in runs containing SO_2, H_2O and CO. Okay (1973) reports that with a CuS

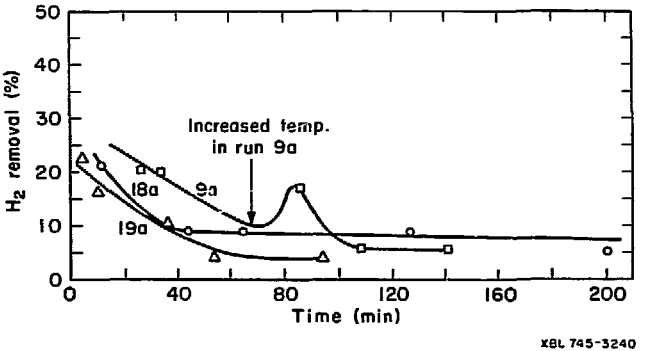

Fig. iv-39. Oxidation of H_2 with iron oxide.

Run	9a	18a	19a
T(°C)	378-453	385	374
θ (sec)	0.60-0.53	0.49	0.49
$[H_2]$ %	4.45	1.40	3.1
Solid(I)	$FeO_{1.5}$	$FeO_{1.50}$	$FeO_{1.36}$
Solid(F)	$FeO_{1.25}$	$FeO_{1.42}$	$FeO_{1.29}$

Fe-301-T 1/8
(3.2mmX3.2mm)

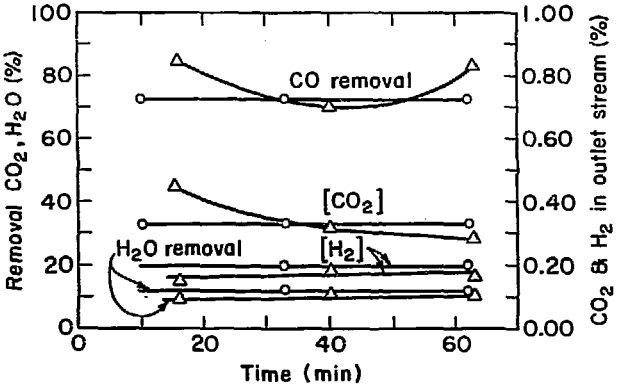

XBL 745-3241

Fig. iv-40. Progress of water-gas shift reaction over iron oxide and iron sulfide.

Run	42b	42d
T(°C)	571	571
θ (sec)	0.045	0.045
[CO]	0.50%	0.50%
$[H_2O]$	1.7%	1.7%
Solid(I)	$FeO_{.77}$	$FeS_{1.1}$
Solid(F)	$FeO_{.55}$	$FeS_{1.1}$
	O	△

Fe-301-T 1/8
(0.50-0.25mm)

catalyst the water-gas shift reaction does not occur. He based this claim on the fact that neither H_2 nor H_2S were produced when H_2O was added to a system of CO and SO_2. This is not an adequate test for the water-gas shift reaction.

2. High temperature, short residence time sulfidation.

The discussion in part B on sulfidation of iron oxide presented data collected at 370°C. The sulfidation step in Run 42c was carried out at 570°C with a gas residence time in the bed of 0.045 seconds. This run showed that COS did not break through until 85% to 98% of the bed was sulfided. This fact implies that the actual reaction time was much less than 0.045 seconds. The data are presented in Figure iv-41. The COS breakthrough curve is extrapolated from one point. Breakthrough occurred to rapidly to obtain more intermediate samples.

The calculated COS breakthrough, assuming only FeS formation, is 82 minutes, somewhat less than the actual. Under similar conditions, except that O_2 and NO were present, breakthrough was in 60 to 65 minutes, Run 39 (Figure iv-31). These results suggest that some FeS_2 may have formed in this run and that NO and O_2 may inhibit sulfidization.

3. NH_3 oxidation.

The potential of Fe_2O_3 to oxidize NH_3 at 368°C was studied in Run 23 over 3.2-mm pellets. No reaction which produced N_2 occurred. A slight adsorption of NH_3 resulted in some NH_3 loss from the 2.1% NH_3 inlet stream. When O_2 (1.4%) was added, 20% of the NH_3 was

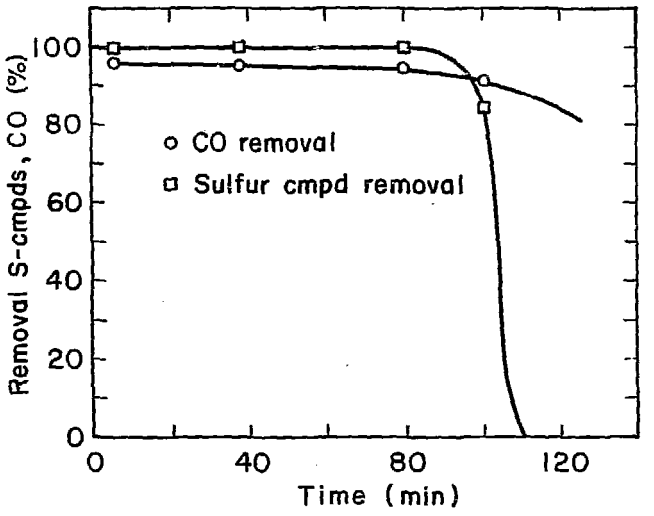

XBL 745-3237

Fig. iv-41. Sulfidation of iron oxide. High temperature, short residence time.

Run	42c
T(°C)	571
θ (sec)	0.045
$[SO_2]$	0.53%
Solid(I)	$FeO_{.55}$
Solid(F)	$FeS_{1.3}$

Fe-301-T 1/8
(0.50mm-0.25mm)

initially oxidized. After 10 minutes the amount of NH_3 oxidized dropped to 5%. The oxidization was short-lived. Therefore, if NH_3 forms at 368°C, it will not decompose or oxidize to N_2 over iron oxide. Following this run, H_2 and H_2S were successively passed over the catalyst. Neither H_2 nor H_2S reacted, which indicated that adsorbed NH_3 deactivated the catalyst for reductions at 368°C. Peri (1965) reports a 5% monolayer coverage of NH_3 on activated alumina at 400°C.

4. Activity of Activated Alumina.

Run 34 tested the activity of activated alumina for the proposed reactions. Activated Alumina No. LA-6173 from the Norton Company was tested. The alumina was 3.2-mm extruded pellets with a surface area of 250 m^2/gm. Adsorbed water on the alumina reacted with CO at 538°C. to produce some CO_2. The reaction rapidly decreased. Similarily, when a gas mixture of 4% CO, 0.48% NO, 0.54% SO_2, 0.48% O_2 and 1.7% H_2O was passed over the catalyst at 538 C only a small amount of the gases reacted. The solid somposition corresponded to $Al_2O_{3.09}S_{.008}$. This run showed that the Al_2O_3 matrix is relatively inactive. Lowell (1971) reports that $Al_2(SO_4)_3$ decomposes to the oxide at 650°C. Thus, if any does form, it will decompose in the regeneration step, 677°C.

J. Iron Sulfide Oxidation.

Oxidation of FeS to form Fe_2O_3 and to liberate SO_2 or S_2 is required to regenerate the spent catalyst/absorbent. The desired sulfur product will depend on the specific plant location. In general, sulfur would be preferable to sulfuric acid. The initial

regeneration work discussed in section A yielded almost exculsively SO_2. The regeneration process was studied in more detail to determine if S_2 could be generated. The important reactions include the following:

	$\Delta H_{25°C}$ (kcal)	$\Delta F_{227°C}$ (kcal)	$\Delta F_{676°C}$ (kcal)	
$2\ FeS + 7/2\ O_2 \longrightarrow$ $Fe_2O_3 + 2\ SO_2$	-293.3	-262.2	-232	iv-41
$2\ FeS + 3/2\ O_2 \longrightarrow$ $Fe_2O_3 + S_2(g)$	-120.5	-106	- 91.9	iv-42
$2\ FeS + 3/2\ SO_2 \longrightarrow$ $Fe_2O_3 + 7/4\ S_2(g)$	+ 9.05	+ 10.2	+ 12.8	iv-43
$2\ FeS + 3/2\ SO_2 \longrightarrow$ $Fe_2O_3 + 7/2\ S(s)$	- 44.92	- 10.3	-------	iv-44
$2\ FeSO_4 \longrightarrow$ $Fe_2O_3 + 2\ SO_2 + \frac{1}{2}\ O_2$	+102.2	+ 49.9	- 6.8	iv-45

Thermodynamics shows that sulfur is favored at low temperatures and SO_2 is favored at high temperatures. Reaction kinetic limits may prevent low temperature formation of sulfur, while S_2 oxidation may prevent S_2 production.

1. High temperature, low O_2 concentration.

a. Large pellets.

Runs 11f and 12 were conducted at temperatures between 538°C

and 720°C to see if sulfur could form at low O_2 levels. O_2 ranged from 1.5% to 2.8% with residence times between 0.36 and 1.0 seconds. The 3.2-mm pellets were used. Trace amounts of sulfur collected in outlet lines, but by far the majority of sulfur from these runs eluted as SO_2. In Run 12 a mixture of 1.7% SO_2 and 0.5% O_2 was fed to see if SO_2 formation reactions could be inhibited. The same results were noted: only trace amounts of sulfur formed.

b. Small particles.

Low O_2 levels and high temperatures were used in Runs 39 and 42 with the 0.50-0.25-mm sized particles to check on the sulfur product. In these runs, only SO_2 eluted. No traces of sulfur were detected even though the O_2 level ranged from 0 to 1.9% and residence times varied from 0.02 to 0.04 seconds.

The initial regeneration period (677°C and 1% O_2) in Run 42 lasted for 65 minutes. A second regeneration period (677°C and 1% O_2) of 210 minutes for this same catalyst showed that only 84% of the bound sulfur had been evolved in the initial period. A closer look at the three different O_2 regeneration steps in Run 39 is shown in Table iv-3.

Table iv-3 O_2 concentration effect on regeneration.

Run 39 (677°C)	2%O_2		4%O_2		21%O_2	
	t=37	t=69	t=5	t=35	t=5	t=34
% SO_2 after t(min.)	0.88	0	1.2	0	0.51	0
% O_2 after t(min.)	0	1.1	0	2.3	18	21
Regeneration time (min.)	129		66		63	
SO_2 collected in scrubber (ml)	89		86		93	

Even after 129 minutes with 2% O_2 and 66 minutes with 4% O_2 there was still a substantial O_2 removal over the bed. With air there was no detectable O_2 removal after 34 minutes. In both the 4% and 21% O_2 case SO_2 elution ceased after 5 to 35 minutes. In the 2% O_2 case some SO_2 still eluted. The SO_2 collected by the NaOH scrubbers for each step differ by only 7.8%. This is within the experimental error. The O_2 breaks through only after most of the SO_2 has eluted in the low concentration cases. The remaining O_2 removal is caused by iron oxide oxidation.

Additional regeneration tests at 677°C and 1%O_2 were conducted on samples from selected runs. The particles tested were ground to less than 0.25-mm. The comparison of the S/Fe ratio determined by the sulfur picked up in the removal step to that determined by SO_2 evolution in the regeneration step for each run is given in Table iii-6. There is no consistent pattern in the reported deviation. The major error is caused by the inability to predict the extent of oxidation of the surface with the 1% O_2.

From this study it was concluded that air is the best regeneration gas at 677°C. Actual residence times for the 0.50-0.25-mm particles should be between 5 and 35 minutes. The 100 micron particles used in a power plant with air as the regeneration gas should require the lower limit, 5 minutes.

2. Low temperature-low O_2 concentration.

Low-temperature regeneration runs were made with 3.2-mm pellets. In Runs 13f, 16d, and 21d, temperatures were 260-288°C, and the O_2 level was 1.5-1.3%. Run 21d also had 1.9% H_2O. In both Runs, 13f

and 16d, there was an initial large SO_2 elution which decreased rapidly to zero. No O_2 reacted after this step. When the catalyst was heated to 374°C more SO_2 eluted. The catalyst bed showed that only a few of the pellets at the bed entrance had been oxidized. The remainder of the bed was not oxidized. No S_2 was collected. SO_2 evolution may have been from $FeSO_3$ decomposition. Evolved SO_2 may have poisoned the remaining pellets for oxidation, explaining why only partial bed oxidation resulted. No SO_2 or S_2 eluted from Run 21d. Lower temperatures were used in Run 19e, 71°C, and Run 24g, 104°C. H_2O was present in the air mixture used in Run 24g. Oxygen at 1.3% was used in Run 19. Neither run produced any S_2 or SO_2, either at these temperatures or when the catalyst was heated to 370°C.

3. Summary of regeneration results.

Regeneration of iron sulfide with oxygen to give iron oxide and sulfur directly does not appear possible. High temperature (677°C) regeneration to give iron oxide and SO_2 is a practical reaction.

CHAPTER V. Process Design

A. Overall Rate Analysis.

1. Removal process.

a. Defining equation for reactors.

In order to translate the experimental results obtained in a small, fixed-bed contactor to an operating system with a large, dispersed-phase contactor, a model describing the system behavior must be developed. The general expression which governs NO and SO_2 removal in both fixed and dispersed contactors is the following:

$$\frac{Cag}{Cag_o} = \exp\,[-K_1 \theta \rho_B] \qquad v - 1$$

where:
- Cag = gas concentration after residence time θ.
- Cag_o = gas concentration at inlet conditions.
- K_1 = overall reaction coefficient.
- θ = residence time of gas in the contactor.
- ρ_B = solid density within the contactor.

The development and assumptions of this equation are given in Appendix A - 2. K_1 is a composite function involving both mass transfer and kinetics. The value of K_1 will be calculated for both fixed-bed and dispersed contactors in section B.b.1. The variables θ and ρ_B are set by experimental conditions in the fixed-bed work. In the dispersed contactor design θ and ρ_B will be adjusted to give the required Cag/Cag_o.

As will be discussed in section B.1.b.ii., although Cag/Cag_o is the same for both contactors, the absolute values of Cag and Cag_o for the experimental work were slightly higher than the concentrations found in practice.

b. Key process variables.

The important process variables identified in the experimental study are listed below.

1. Reaction temperature.
2. Gas residence time.
3. Particle size.
4. Gas concentration.
5. Gas composition.
6. Solid composition.

From the design equation, v - 1, two additional variables when scaling up will include:

7. Mass-transfer effects.
8. Bed density.

These variables are discussed in section B.1. of this chapter in a slightly different order.

2. Regeneration process.

a. Defining equations for regenerator.

The experimental study showed that high-temperature regeneration of the sulfide was needed to produce an active catalyst. The model will therefore be similar to that developed by Guha (1972) for the oxidation of FeS_2. Expressing the extent of regeneration as the percent of FeS reacted to give Fe_2O_3 and SO_2 the model becomes

$$\% \text{ Solid reacted} = 100 - \frac{[r - 7/4(1-\varepsilon')\frac{K_2}{\rho_{SM}} Cag_o t]^3 100}{r^3} \qquad v\text{-}2$$

where:

r = radius of particles.
Cag_o = O_2 concentration.
K_2 = overall reaction coefficient.
t = time of solids reaction.
$1-\varepsilon'$ = volume fraction of particle which is FeS
ρ_{sm} = molar density of FeS.

The development and assumptions of this equation are given in Appendix A-3. K_2 is a composite function involving both mass transfer and kinetics.

b. Key process variables.

The important regeneration variables found in the experimental study include the following:

1. Regeneration temperature.
2. O_2 concentration.
3. Particle size.
4. Solids residence time in regenerator.
5. Solid composition.

From equation v-2, the mass transfer effects, as they influence K_2, will also be a variable of the process. These variables will be discussed in Section B.2. of this chapter.

B. Discussion of the Variables.

1. Removal reactions.

a. Reaction temperature.

All of the removal reactions occurred in the desired temperature region of 370°C - 540°C. The upper level (540°C) is the recommended temperature of operation. At this temperature, catalyst deactivation due to sulfate formation is inhibited, reaction kinetics are more rapid, and large differences between the temperature for removal and that for regeneration are avoided.

b. Kinetic and mass transfer effects.

The overall reaction coefficient, K_1, is a function which includes both kinetic and mass transfer effects. This is shown in the following relationship:

$$K_1 = \left(\frac{1}{V_p k_r \eta} + \frac{1}{S_{ex} k_m}\right) \qquad v\text{-}3$$

where:
k_m = overall mass transfer coefficient.
k_r = overall kinetic rate coefficient.
S_{ex} = specific external surface area of particles.
V_p = specific volume of particles.
η = kinetic effectiveness factor.
(See Appendix A-2 for development.)

This expression, like equation v-1, assumes first-order dependence of the gas concentration on both the kinetic and mass-transfer rates. In order to estimate the required density of solids in the dispersed contactor as well as the gas residence time in the contactor, K_1 must be evaluated for both the fixed and dispersed contactor.

i. Fixed-bed contactor.

(a.) Required residence time.

Sulfur dioxide removal in a fixed-bed contactor proceeds until the bed has been almost completely sulfided. During sulfidation there is an oxide/sulfide reaction zone which moves through the bed. Since breakthrough of sulfur compounds in the runs at 540°C did not occur until the bed was almost completely sulfided, this reaction zone is much smaller than the bed length. The

sulfidation of iron oxide with SO_2 and CO in Run 42, Figure iv-41, resulted in sulfur compound elution only after 85% to 98% of the bed had been sulfided. Since the nominal gas residence time in the bed was 0.045 seconds, the gas phase removal process went to completion in the fixed bed in 0.0068 to 0.001 seconds.

Nitric oxide removal is catalytic and will proceed until the bed becomes deactivated. The deactivation of catalyst/absorbent results when the catalyst is partially oxidized by O_2. Runs 36b and 37b reported simultaneous removal of SO_2 and NO when the gas residence time was 0.030 - 0.034 seconds. Examination of the catalyst from both of these runs showed that only the last half of the bed was active. This meant that the reactive residence time for NO removal was less than 0.015 seconds in the fixed-bed reactor. A more definitive residence time can be obtained from Figure iv-30 with the gas concentration profiles of Run 37b. In this run, the catalyst was poisoned, first eluting H_2S then COS, SO_2, NO, and O_2. If it is assumed that the bed was poisoned for NO removal when the first outlet NO was measured, at 110 minutes, then the extrapolated NO breakthrough, between 80 - 90 minutes, occurs after 73 - 82% of the bed is inactive. Therefore the residence time in the reaction zone is estimated at 0.005 - 0.008 seconds.

These results confirm that in the experimental fixed-bed reactor the maximum required residence time for simultaneous NO and SO_2 removal is about 0.003 seconds. This is with at least 99%

removal of both NO and SO_2. The minimum residence time for 99% removal was not obtained in this study. The reason for this apparent lack of data is given in the next few paragraphs. Data extrapolation, which was discussed in the previous paragraphs, suggests that times as fast as 0.001 seconds may be the minimum.

(b) External mass transfer rate estimation.

The reaction residence times measured in the fixed-bed are for processes in which both kinetic and mass transfer rates are important. The gas phase mass transfer rates in the fixed-bed can be estimated from empirical correlations and then used to calculate the kinetic contribution to K_1.

Sherwood (1974) presents an empirical correlation for external mass transfer in fixed-beds when the particle Reynolds Number (Re_p) is greater than 1.0.

$$J_D = 1.17\ (Re_p)^{-.415} \qquad v - 4$$

Since the experimental Re_p in the present work is less than 1.0, this expression, representing an upper bound, and the correlation based on one experimenter's data, (Sherwood, 1974) representing the lower bound, were used for obtaining the value of J_D, the mass transfer j-factor. The mass transfer coefficient is related to J_D by the following equation:

$$k_m = \left[\frac{J_D}{(S_c)^{2/3}}\right] U_{AVE} \qquad v - 5$$

where: J_D = mass-transfer j factor.
k_m = external mass transfer coefficient.
S_c = Schmidt Number
U_{AVE} = Interstitial velocity past particles.
(Sherwood, 1974)

In addition to k_m, the Sherwood Number for mass transfer, Sh, is also calculated. Table v-1 presents the calculated k_m and Sh for the listed conditions.

Table v-1 Calculated k_m and Sh for the fixed-bed contactor.

Bed Density = 1.172 g/cm^3
Diluent, Helium 400 cm^3/min @ 23°F, 1 Atm.
Temperature = 538°C

Diameter, d_p (mm)	0.250		0.500	
Re_p	0.304		0.608	
	high	low	high	low
J_D	1.92	0.22	1.44	0.60
k_m (cm/sec)	225	25.8	169	70.3
Sh = ($k_m d_p$/D)	1.63	0.187	2.44	1.02

The expected range for k_m for the 0.250-mm particles is 25 - 255 cm/sec and for the 0.500-mm particles is 70 - 169 cm/sec. The lack of more experimental data below a Re_p of 1.0 prevents the narrowing of these ranges.

The reaction kinetics, to be discussed in section B.1.b.i.(c), were significantly influenced by the external mass transfer limitations. The NO and SO_2 removal reactions rates were so rapid that it was impractical to design an experimental unit which would

be free of external mass transfer limitations. In order to have such a system, the feed velocity would have to be substantially increased. This would mean, at a constant SO_2 concentration and bed volume, that bed sulfidation would occur much more rapidly, hence limiting the amount of sampling before sulfur compound breakthrough. As it was, in the runs with the shortest residence time and with the lowest possible inlet SO_2 (about 0.5%), only two samples could be taken before breakthrough. Increasing the bed volume would not help since the total feed of SO_2 to the bed would have to be increased proportionately to maintain the same residence time. Continuous gas monitors with a higher sensitivity would have allowed operation of a small scale system which was free of external mass transfer limitations.

(c.) Reaction rate estimation.

Equation v-3 has presented the model for the overall reaction coefficient K_1. The values of $S_{ex}k_m$ can be estimated based on the previous section. The value for K_1 can be calculated from equation v-1 using the experimental data obtained in this work. Given these two parameters, the value of the solids rate constant, $V_p k_r n$, can be estimated in equation v-3. These values are given in Table v-2.

Table v - 2. Estimation of solids rate constants for removal reactions in the fixed-bed contactor.

(Run 42. Discussed section i.(a.) & Figure iv - 41)

Bed Density = 1.172 g/cm^3
Diluent, Helium 400 cm^3/min @ 25°C, 1 Atm.
Temperature = 538°C
C_{ag}/C_{ag_o} = 0.010
Residence time = 0.008 sec (max); 0.001 sec (min)

Particle Size (mm)	0.250				0.500			
	high		low		high		low	
$k_m S_{ex}$ (cm^3/g-sec)	30,150		3,457		11,323		4,710	
	(max)	(min)	(max)	(min)	(max)	(min)	(max)	(min)
K_1 (cm^3/g-sec)	3,929	491	3,929	491	3,939	491	3,929	491
$Vpk_r\eta$ (cm^3/g-sec)	4,518	499	*	572	6,017	513	23,695	548

* K_1 & $k_m S_{ex}$ combination not possible.

A range for $V_p k_c n$ is reported instead of one number for each particle size since neither $k_m S_{ex}$ nor K_1 could be determined accurately. For all cases except one, the particle rate appears to be the rate controlling step.

ii. Dispersed-bed contactor.

(a.) External mass transfer rate estimation.

Dispersed-bed contactors can range from a fluidized bed with void fractions close to 0.60 up to highly dispersed systems with void fractions very close to 1.0 (Reh, 1971). Separate mass transfer correlations have been developed for dense-phase and dilute-phase contactors. Kunii and Levenspiel (1969) present correlations for fluidized beds:

$$Sh = 0.374\ Re_p^{1.18} \qquad 0.1 < Re_p < 15 \qquad v\text{-}6$$

$$Sh = 2.01\ Re_p^{0.5} \qquad 15 < Re_p < 250 \qquad v\text{-}7$$

and for a single shpere,

$$Sh = 2.0 + 0.6\ S_c^{1/3}\ Re_p^{1/2} \qquad v\text{-}8$$

At a Re_p of 1.0 the Sh for a fluidized bed would be lower than that for a single sphere. The theoretical value for Sh for a single sphere in an infinite stagnant medium is 2.0. Since equation v-6 would predict lower values, the validity of equation v-6 is questionable when studying anything but dense-phase fluid beds. In dense fluid beds, as in fixed beds, the interaction of concentration gradients may result in the Sh being less than 2.0. However, the proposed type of contactor is a dilute dispersed-

phase system. As a conservative estimate of the mass transfer under these conditions the last terms in equation v-8 will be deleted. Therefore,

$$Sh = 2.0 \qquad \text{v-9}$$

will be used to estimate the mass transfer coefficients. Since the value of $k_m S_{ex}$ is used in the rate equations, Table v-3 lists the values of both k_m and $k_m S_{ex}$ for several candidate particle sizes.

Table v-3. Estimation of mass transfer coefficients for a dispersed-phase contactor.

T = 538°C, Diluent = N_2, Sh = 2.0

Diameter, d_p (mm)	0.050	0.075	0.100	0.150
k_m (cm/sec)	459	306	229	153
$k_m S_{ex}$ (cm^3/g-sec) x 10^5	3.18	1.37	.792	0.325

Section B.1.b.ii.(c.) will give a discussion of the reason for selection of these particle sizes.

(b.) Reaction rate estimation.

In the discussion of the fixed-bed data above, an estimate of the solids rate parameter was made for the catalyst tested. The catalyst used in the dispersed contactor will be slightly different than the one on the fixed-bed case. It will still have 20% ferric oxide but will have an alumina-silica matrix instead of only alumina. The latest commercial alumina-silica matrix cracking catalysts have surface areas (S_v) around 200 m^2/g (Gussow, 1972).

The experimental catalyst had an S_v of 41 m^2/g. This means that an increase in the specific volume can be expected in going from the fixed-bed unit to the dispersed phase contactor with the newer catalyst. The increase in V_p will not be proportional to the increase in S_v. A comparison of two commercial Harshaw catalysts was used to estimate the new V_p. Table v-4 presents the data.

Table v-4. Estimation of specific pore volume of high surface area catalyst (Harshaw, 1973).

Catalyst	$S_v(m^2/g)$	$V_p(cm^3/g)$	$x = \frac{\ln (V_{p1}/V_{p2})}{\ln (S_{v1}/S_{v2})}$
1. Fe-0301T 1/8	41	0.31	0.4878
2. Fe-0303P	105	0.49	

The logarithmic proportionality constant, x, is used to calculate the new V_p of 0.67 cc/g. The ratio V_{p2}/V_{p1} is then 2.16, where 1 denotes experimental catalyst and 2 denotes new catalyst.

Predicting the effectiveness factor for the reactions with the solid in a dispersed phase is somewhat more difficult. Petersen (1965) presents an equation for the effectiveness factor for a first-order reaction developed for a spherical pellet:

$$\eta = \frac{3}{h_s}\left[\frac{1}{\tan h_s} - \frac{1}{h_s}\right] \qquad \text{v-10}$$

where: h_s = thiele modulus = $\frac{r}{3}\left[\frac{\rho_p S_v k_r}{De}\right]^{\frac{1}{2}}$

ρ_p = particle density.

S_v = specific surface area.

$$De = \text{effective diffusivity} = \left(\frac{1}{D_{ke}} + \frac{1}{D_{12,e}} \right)^{-1}$$

k_r = reaction rate coefficient.

r = particle radius.

When intraparticle diffusion is controlling, the asympotic solution to equation v-10 becomes:

$$\eta = 3/h_s \qquad \text{v-11}$$

$$\text{for} \quad \eta = h_s/3 > 3 \qquad \text{v-12}$$

The effectiveness factor is a ratio of the average rate of reaction or adsorption in the pellet to the maximum rate if intraparticle diffusion were absent. Since the maximum rate is unknown, one way to determine whether intraparticle diffusion is rate controlling is to calculate the ratio of the rate predicted by intraparticle diffusion and compare that with the overall rate measured. This ratio is simply the effectiveness factor using the rate coefficient determined from experiments instead of the actual kinetic rate coefficient. The values of K_1 (Table v-2), divided by the catalyst specific surface area (41×10^4 cm^2/g) give the pseudo k_r for the conditions of that run. At 538°C in He with a calculated De of 0.0293 cm^2/sec (see eqn. v-10), the ratio of the calculated diffusion rate to the overall rate is 0.95. Since this value is close to 1.0, the overall particle rate is strongly diffusion controlled. This implies that the variation of η will be represented by the following equation:

$$\eta \propto \frac{1}{h_s} \approx \frac{3}{r} \left[\frac{De}{\rho_p S_p k_r} \right]^{1/2} \qquad \text{v-13}$$

The largest contribution to De was the Knudsen diffusion coefficient which varies with $\varepsilon^2/(S_v\rho_p)$ (Satterfield, 1963). The apparent density can be expressed as

$$\rho_p = \rho_s(1-\varepsilon) \qquad \text{v-14}$$

where: ρ_s = absolute solid density.

ε = particle porosity.

With the above proportionalities for η, De, and ρ_p and with $\varepsilon_2 = 0.74$ and $\varepsilon_1 = 0.567$, the new effectiveness factor for the 200 m^2/g catalyst can be expressed as a function of the original.

$$\eta_2 = 0.44\eta_1(r_1/r_2) \qquad \text{v-15}$$

where: subscript 1 denotes experimental conditions.

subscript 2 denotes dispersed conditions.

The new product $k_r V_p \eta$ will be

$$(V_p\eta k_r)_2=(V_p\eta k_r)_1(2.16)(0.44)^{r_1}/_{r_2}=0.957(^{d_1}/_{d_2})(V_p\eta)_1 \qquad \text{v-16}$$

The factor 0.957 in equation v-16 shows that the reaction rate will be essentially the same for both the experimental and the new catalyst matrix. The calculated values for $(V_p\eta k_r)_2$ are given in Table v-5 for various particle sizes. Table v-2 is used to obtain conditions for case 1. An average particle size, d_1 = 0.375 mm is used. Two values for $(V_p\eta k_r)_1$ are used, 4518 and 533 cm^3/g-sec. These are the values of the lowest maximum value of $(V_p\eta k_r)_1$ and the average of the minimum $(V_p\eta k_r)_1$ values. This analysis assumes that η will be much less than 1 at the new conditions.

Table v-5. Estimation of dispersed phase solids rate coefficient.

d_2 (mm)	0.050		0.075		0.100		0.150	
	max	min	max	min	max	min	max	min
$(V_p n \kappa_r)_2$ (cm/g-sec) x 10^3	32.4	3.83	21.6	2.55	16.2	1.91	10.8	1.28

(c.) Solids concentration.

The estimates of the mass-trasfer and solids rate coefficients for the dispersed phase are combined by way of equation v-3 into a value for K_1. K_1 can then be used in equation v-1 to determine the required dispersed phase concentration as a function of particle size and residence time. Table v-6 summarizes these results.

Table V-6. Required dispersed-phase density as a function of residence time and particle diameter.

Temperature = 538°C
C_{ag}/C_{ag_o} = 0.10

Diameter (mm)	0.050		0.75		0.100		0.150	
$k_m S_{ex}$ (cm^3/g-sec) x 10^5	3.18		1.37		0.792		0.325	
	max	min	max	min	max	min	max	min
$V_p n k_r$ (cm^3/g-sec) x 10^3	32.4	3.83	21.6	2.55	16.2	1.91	10.8	1.28
K_1 (cm^3/g-sec) x 10^3	29.4	3.78	18.6	2.50	13.4	1.87	8.11	1.23
θ (sec)	0.500	0.500	0.500	0.500	0.500	0.500	0.500	0.500
ρ_B (g/cm^3) x 10^{-3}	0.157	1.22	0.248	1.84	0.344	2.46	0.568	3.74
θ (sec)	1.00	1.00	1.00	1.00	1.00	1.00	1.00	1.00
ρ_B (g/cm^3) x 10^{-3}	0.0785	0.610	0.124	0.920	0.172	1.23	0.284	1.87
θ (sec)	2.00	2.00	2.00	2.00	2.00	2.00	2.00	2.00
ρ_B (g/cm^3) x 10^{-3}	0.0393	0.305	0.062	0.460	0.086	0.615	0.142	0.935

With a catalyst/absorbent size distribution between 0.050 - 0.150 mm and a 0.5-second residence time, the required bed density will be between 0.16 x 10^{-3} and 3.7 x 10^{-3} g/cm^3. With a 1.0-second residence time for this same size distribution, the range of the bed density would be between 0.079 x 10^{-3} and 1.87 x 10^{-3} g/cm^3. Existing power plant duct work allows for about 0.5-second residence time. Duct modifications could increase this time to 1.0-seconds if necessary. The 1-second residence time is chosen for the design basis. This criterion will be discussed in the next section. Therefore, the required bed density will be between 0.079 x 10^{-3} and 1.87 x 10^{-3} g/cm^3. With a catalyst particle density of 1.79 g/cm^3, the void fraction, ε, ranges between 0.99996 and 0.99895. Since the ε for normal fluid bed operation is less than 0.70, the contactor required for the entire range of void fractions would have the solids highly dispersed (Reh, 1971). The specific design presented in Section D.4. of this chapter has a catalyst/absorbent loading of 0.185 x 10^{-3} g/cm^3 (1.14 x 10^{-3} lbs/ft^3), which is 2.3 times as concentrated as the minimum and 0.10 times as concentrated as the maximum. This concentration lies within the acceptable, experimentally determined range.

The MnO_2 dry absorption process for SO_2 removal (Uno, 1971) uses a dispersed phase of MnO_2 at 100 to 180°C to absorb and remove SO_2 from oil-fired power plant stack gases. The concentration of solids in this process has a range, 0.15 x 10^{-3} g/cm^3 to 0.20 x 10^{-3} g/cm^3, roughly the same as that used in the proposed process.

An SO_2 removal of 90% is claimed. Since the proposed process will operate at 540°C, mass transfer and kinetic rates should increase substantially over the MnO_2 process. In view only of these considerations, the proposed solids concentration should be quite adequate.

(d.) Residence time in contactor.

The initial discussion of residence time was the time that it took the flue gas to pass from the economizer inlet (540°C) to the air preheater inlet (370°C). The experimental studies showed that the best operation would be obtained at 540°C. The residence time normally available at 540°C will vary with the unit. Heil (1972) reports that the flue gas velocity in this region varies from 22.9 m/sec (75 ft/sec) for high volatile eastern coals to 13.7 m/sec (45 ft/sec) for coals with highly abrasive tendencies. An average value of 15.2 m/sec (50 ft/sec) is selected for design purposes. Typical distances in coal-fired units at 540°C correspond to residence times around 0.20 seconds (Stevens , 1974). Table v-6 shows that to achieve nearly complete reaction at low solid densities, higher residence times are needed. The reaction constants presented in this table show that 90% removal can be achieved in 1 second with low solids density. Typical velocities in this region would require then that about 15.2 m (50 ft) of ducting be added. This would be a reasonable addition to a unit. Additional residence time may also be obtained. First, the gas and solids must pass

through a solids separator at this temperature. Second, the 15.2 m/sec velocity is typically that within the economizer section. In the free duct it would be reduced to about 13.4 m/sec. This additional residence time (possibly 0.20 seconds) provides some margin of safety.

Equation v-1 showed that the residence time and bed density can be adjusted to give a constant removal, i.e., increasing the bed density by a factor of 2 would enable the residence time to be cut by one half. Therefore, the actual amount of removal for a given residence time can be controlled by the solids density, i.e., the recycle solids rate, within the contractor.

(e.) Particle size.

Mass transfer and kinetic effects were shown to require a catalyst/absorbent size distribution between 0.050 - 0.150 mm. Sizes smaller than this range would tend to enhance the reaction rates and hence the overall rate, since the particle rates are the rate-limiting step. The difficulty with smaller particles is that they would be more difficult to collect in either cyclones or electrostatic precipitators and they would also be more difficult to separate from the flyash in pulverized coal-fired units.

A typical flyash size distribution for pulverized coal-fired furnaces is given in Table v-7. The average size is 20 microns. Table V-7 also lists the size distribution for a typical commercial fluid-bed cracking catalyst to illustrate the range of particle

sizes when the average size is 58 microns.

Table v-7. Particle size distribution of P.C. flyash and Si - Al cracking catalyst.

Flyash (USDHEW, 1969)		Catalyst (Gussow, 1972)	
Size (microns)	Wgt % less than	Size (microns)	Wgt % less than
10	30		
20	50	20	<2
40	70	40	13 - 20
60	80	80	78 - 85
80	85	105	93 - 97
100	90	149	99+
200	96		

With a catalyst/absorbent of this size distribution, there is definitely significant overlap. If an average size of 75 microns is used, a better separation of catalyst/absorbent and flyash will be possible without significantly effecting the mass transfer and kinetic rates. Table v-8 presents a size distribution for such a catalyst.

Table v-8. Size distribution for catalyst/absorbent with average size 75 microns.

size (microns)	Wgt % less than
10	<0.2
20	0.9
40	6
60	28
80	56
100	77
200	100

This distribution was obtained by extrapolating the data of Gussow

(1972) on a log/probability plot of particle size versus cumulative percent. Although there is still some overlap between this distribution and normal flyash, it is not as significant. That is, flyash has 70% less than 40μ while the catalyst/absorbent has 6% less than 40μ.

In addition to the kinetic and mass transfer limits on larger sized particles, the influence of particle size on catalyst attrition is also important. Zenz (1971, 1974) reports that catalyst attrition results primarily from high velocity impact. He found that attrition occurred mainly from breakdown of coarse particles: fines (less than 44 microns) do not get finer. In fluid-bed catalytic cracking units he found that essentially all of the attrition occurred in the cyclones. Thermal cycling (between 500°C and 650°C) as well as attrition in the dense phase fluid beds contributed little to the overall attrition rate of Si/Al catalysts. In laboratory experiments, Tanaka (1968), found that below a critical particle size, the rate of particle breakup drops essentially to zero. The critical particle size decreased with impact velocity and increased with material strength. However, in all cases the critical size was in the vicinity of 50 microns. Therefore attrition considerations would require particles with an average diameter around 50 microns.

Flanders (1974) has reported that a commercially operating SiO_2/Al_2O_3 cracking catalyst with an average particle size of 60 microns has an attrition loss of about 0.004% of the material sent into the cyclones. High-velocity, 22.3 m/sec (75 ft/sec), cyclones

are used in the proposed process. The catalyst has a Moh hardness of 6. Forsythe (1949), Gwyn (1969), and Gussow (197ℓ) all discuss relative rates of attrition between various catalysts tested but do not give any absolute value for the attrition rates.

Since an average particle size of 75 microns is desired from the standpoint of particle separation and collection, an estimate of the expected attrition rate needs to be made. The data of Flanders (1974) is used as the starting point and the relationship between particle-size distribution and attrition rate found by Gwyn (1969) is used to predict the rate with an average size of 75 microns. Unlike previously quoted investigators, who found that in this size range the attrition rate increased with increasing particle size, Gwyn's correlations indicate a 14% decrease in the rate. This would predict an attrition loss of 0.0034%. Since there appears to be some uncertainty as to the validity of this decrease, the attrition rate is taken as 0.004% of the material entering all the cyclones in the process.

(f.) Gas concentrations.

The removal rates presented in section A.1.a. assumed first-order kinetics for all reactions. Equation v-1 shows that with this assumption the level of concentration of the reactants does not effect the percent removal. Therefore, if this assumption holds, even though most of the experiments were carried out at NO and SO_2 concentrations 10 times and 2 times, respectively, those encountered in practice, the results will still be applicable.

Shelef (1972) found that when the NO concentration was decreased from 4000 ppm to 250 ppm, NO conversion actually increased from 80% to 100 %. Copper chromite catalyst at 305°C with 1.4% H_2 was used. With this large excess H_2, the NH_3 selectivity increased from 20% to 95% when the inlet NO was decreased. The major effect of a lower NO concentration would possibly be an increase in the NH_3 formed. The extrapolation of the SO_2 data over a factor of 2 is reasonable and should present no difficulties.

(g.) Gas and solid composition.

Experiments summarized in Figure iv-33 have shown that the solid and gas composition are both important variables in determining NH_3 selectivity. Increasing the sulfide content of the solid or the amount of CO + H_2 in the gas stream increases the NH_3 selectivity. Increasing the oxide content of the solid or the amount of O_2 in the gas stream decreases the NH_3 selectivity. To have a low NH_3 selectivity would require high oxygen levels in both the solid and the gas. These trends go counter to the requirements for effective NO and SO_2 removal. The balance of these variables is such that the minimum NH_3 selectivity is about 50%. This results in acceptable sulfur loadings on the solid and reducing agents in the gas to allow self-sustained regeneration and effective removal reactions. Solid and gas compositions cannot practically be selected to minimize NH_3. Ammonia emitted from this process is well below current allowable levels, and is not

considered an environmental detriment. This is discussed in more detail in Chapter VI. The important consideration for the gas composition is that it be at least net reducing. This means that the ratio

$$\frac{O}{R} = \frac{2[O_2] + [NO] + 3[SO_2]}{[CO] + [H_2]} \qquad \text{V-17}$$

should be equal to or less than 1. Values greater than 1 may result in eventual catalyst deactivation.

The allowable solid composition will be determined by both the removal and regeneration processes. In the fixed-bed experiments only an averaged solids composition, at the end of the run, could be estimated. The range of compositions within the bed varied from highly sulfided at the bed entrance to slightly sulfided at the bed exit. In tests with the smaller particles the reaction rates , discussed in section B.1.b.i., were so rapid that apparently the percent sulfidation of the solid had no significant effect on the removal rate of sulfur compounds, as long as the solid was less than about 85% sulfided. The biggest influence of the solid composition on NO removal was the level of sulfate. The experimental work showed that for active catalyst/absorbent the sulfate level could reach 15% of the total sulfur reacted.

Excess Fe_2O_3 will also be needed in the catalyst/absorbent

to remove the excess CO and H_2. The amount required is arbitrarily set at 110% of the stoichiometric requirement for reduction of the excess CO and H_2.

The level of sulfide in the solid is also important from the standpoint of regeneration. In the regenerator a net exothermic reaction is desired to maintain the high temperature. Exothermic reactions are the oxidation of FeS to SO_2 and Fe_2O_3 and the oxidation of FeO to Fe_2O_3. The decomposition of any $FeSO_4$ formed in the removal process and heating requirements for the solids and air are endothermic loads. Given the limits for $FeSO_4$ and Fe_2O_3 in the removal step, the minimum amount of FeS necessary can be calculated from an energy balance. From an operational standpoint, the amount of FeS should be substantially higher than this minimum to allow for system fluctuations. Any excess heat generated will be removed and used in another part of the process or in the power plant.

2. Regeneration reactions.

a. Regeneration temperature.

High temperature regeneration, producing SO_2 and Fe_2O_3, was found in the experimental work to produce an active catalyst. The lowest temperature suitable was 680°C. The upper temperature limit will depend on catalyst sintering effects and materials of construction. Harnsberger (1974) reported sintering of SiO_2/Al_2O_3 catalytic cracking catalysts around 760°C. The upper limit for

castable-lined stainless steel is also about 760°C. Therefore, acceptable regeneration temperatures range between 680 - 760°C. The temperature level attained will be a function of the solid composition and the heat either removed or added to the system.

b. Kinetic and mass transfer effects.

i. Fixed-bed regenerator.

(a.) Required residence time.

In the experimental study the required regeneration time for the 0.250 - 0.500 mm particles was between 300 - 2100 seconds when air was used as the regeneration gas.

(b.) Mass transfer and reaction rate estimation.

In section B.1.b.i. the gas phase mass transfer in the removal study was found in all practical cases to be more rapid than the estimate of the particle reaction kinetics. Since higher gas reaction temperatures were used in the regeneration study than in the removal study, the gas phase mass transfer was probably not rate-limiting in the former case. Higher temperatures will also increase the reaction kinetics to a greater extent than intraparticle diffusion. This means that, as in the removal step, the regeneration step will probably be controlled by the intraparticle diffusion rate.

Equation v-2 expresses the extent of regeneration as a function of particle kinetics, residence time, and particle radius. The overall rate coefficient, K_2, can be estimated from experimental

data. This is shown in Table v-9. The range of K_2 presented results from the uncertainty in the % solid reacted and in the time required. The maximum range of K_2 is expected to be between 0.0669 and 0.00326 cm/sec.

Table v-9. Overall coefficient for fixed-bed regeneration.

$\rho_{sm} = 4.58 \times 10^{-3}$ g moles FeS/cm^3 cat.

$1-\epsilon = 0.950$

$Cag_o = 2.69 \times 10^{-6}$ g moles/cm^3

Diameter (cm)	0.0250				0.0500			
% solid reacted	90		99		90		99	
time (sec)	300	2100	300	2100	300	2100	300	2100
$K_2 \times 10^{-2}$ (cm/sec)	2.29	.326	3.34	.478	4.57	.653	6.69	.956

ii. Fluidized bed regenerator.

The regenerator will be a fluidized bed which will function as a reactor to oxidize the solid to Fe_2O_3 and as a classifier to separate the flyash and the catalyst/absorbent. The catalyst/absorbent size distribution will range between 50 - 100 microns. The reasons for this range are given in section B.1. The main design parameters to be determined are the residence time at tempeature necessary to regenerate the catalyst/absorbent and the air velocity in the bed.

The entrmt. velocity of small particles in a continuous fluid bed is reported to be higher than the terminal velocity of an isolated particle. Lewis (1949) found this effect for particles less

than 0.25 mm. Table v-10 presents entrmt. velocities for both flyash and catalyst/absorbent at regeneration conditions.

Table v-10. Entrmt. velocities of flyash and catalyst/absorbent under conditions of continuous fluidization. (Correlation of Lewis, 1949).

$\rho_{CAT/ABS}$ = 1.79 g/cm^3 (Entrmt. = Entrainment)
$\rho_{F.A.}$ = 0.84 g/cm^3
T = 538°C in N_2

	Flyash		Catalyst/Absorbent	
Diameter (mm)	.020	.100	.020	.040
Terminal velocity (mm/sec)	5.08	127	10.8	43.3
Entrmt. velocity (mm/sec)	66	293	140	333

Based on the flyash distribution in Table v-7, and the catalyst/absorbent distribution in Table v-8, a bed velocity of 333 mm/sec (1.09 ft/sec) would result in eluting at least 90% of the flyash and only 6.0% of the catalyst/absorbent. The cyclone banks would be arranged so that the primary cyclones collect the majority of the catalyst/absorbent and the secondary cyclones collect the flyash. The solids stream from the primary cyclones is sent back into the system. The solids stream from the secondary cyclones is discarded.

The necessary residence time for the catalyst in the regenerator can be estimated from equation v-2. The values for ρ_{sm}, 1-ε' and C_{ago} used in these calculations are typical of an actual design case. Since a range for K_2 was found experimentally, (Table v-9), a corresponding range for t will be given with each particle size.

Table v-11. Estimated catalyst/absorbent regeneration time under continuous fluidization conditions.

$\rho_{sm} = 1.414 \times 10^{-3}$ gmoles FeS/cm^3 Cat.

$1-\epsilon' = 0.9863$

$Cag_o = 2.69 \times 10^{-6}$ gmoles/cm^3

Diameter (cm)	.0050		.0100		.0150	
K_2 (cm/sec)	.00326	.0669	.00326	.0669	.00326	.0669
$t_{99\%}$ (sec)	367	17.9	732	35.7	1098	53.6
$t_{99.9\%}$ (sec)	421	20.5	840	41	1260	61

The ranges of acceptable residence times for 99.9% regeneration from Table v-11 for the catalyst/absorbent is 20 - 421 seconds and 61 - 1260 seconds depending on the particle size. The upper limit in both of these ranges is high only because rapid gas sampling during experimentation was not possible. One would expect that the regeneration time and sulfidation time would be at least similar in magnitude since both are controlled by intraparticle diffusion. The regeneration rate could be higher than the sulfidation rate since the O_2 concentration during regeneration will be about 80 times the SO_2 concentration used in the experiments.

In Run 42, Figure iv-41, the sulfidation of the solid was reported to occur very rapidly. The elution of sulfur compounds in Run 42 occurred only after 85 - 98% of the bed had been sulfided. Since the calculated COS breakthrough (assuming FeS formed) was 4920 seconds, the sulfidation time of the solid was 100 - 740 seconds. With a higher concentration of reactant in the gas, 21% instead of

0.53%, the time would be between 2.5-18.7 seconds. This discussion shows that the lower range of residence times for regeneration presented in Table v-11 correspond more closely to the actual case than the upper range. For design considerations a solids hold-up time of 300 seconds will be provided to ensure complete regeneration.

C. CO and H_2 Generator.

1. Practical considerations.

The discussion in Chapter I showed that an excess of CO and H_2 can be produced when fossil fuels are burned in an O_2-deficient environment. The first requirement is that the fuel used to produce the CO/H_2 mixture be the same as the fuel used in the plant. This minimizes fuel, storage, handling and conveying equipment. The second requirement is that the heat of the gasification be recovered in the boiler cycle. The third requirement is that carbon and soot formation be minimized in the gasifier.

2. Type of generator.

Recent restrictions on the use of natural gas have essentially eliminated the construction of new natural gas-fired power plants. New fossil-fueled power plants will burn almost exclusively oil or coal. The generator for $CO + H_2$ must also be designed to be fueled by oil or coal. A fluidized bed of limestone (EPA, 1971) could be used in the case of oil and a coal-fired stoker unit could be used in the case of coal. In either case the unit should operate

adiabatically, the heat of reaction being recovered in the boiler convection pass.

Under reducing conditions, both oil and coal have the potential to form soot. In the detailed design, the considerable experience in the production of producer gas will be drawn upon to minimize soot formation in the gasifier. Once the carbon has been oxidized, equation v-18 shows that the CO combination reaction to give C and CO_2 is unfavorable at operating conditions.

	$\Delta H_{25°C}$ (kcal)	$\Delta F_{727°C}$ (kcal)	$\Delta F_{1093°C}$ (kcal)	
$2\ CO \longrightarrow CO_2 + C$	-41.2	-0.81	+14.2	v-18

In order to minimize the amount of carbon formation in the main flue gas when coal or oil is burned, the main combustion zone of the furnace will be operated under oxidizing conditions. At roughly 1100°C, a rich stream of CO/H_2 produced in a fuel gasifier will be added to convert the flue gas to net reducing stoichiometry. This pregasification of a portion of the fuel will prevent carbon formation in the main flue gas stream. The amount of fuel gasified will depend on the CO/H_2 requirements to accomplish the removal reactions. Since the design presented in section D.is for a coal-fired plant, only the chain grate stoker design will be discussed in detail.

The gasifier will operate with an amount of air just sufficient to convert the carbon to CO and the sulfur to SO_2. In actual practice, with high CO levels, the sulfur will probably be in the form of H_2S. Designing for SO_2 formation provides for a conservative

design since this requires more CO and H_2. The conversion of fuel N to NO was assumed to be 20%. Under the actual reducing conditions in the gasifier this value may be much lower. The H_2 content of the gasifier streams is taken as the amount of H_2 in the fuel. The actual amount of H_2 present after the gasifier stream has mixed with the flue gas will be a function of the equilibrium established by the water-gas shift reaction. Figure v-1 shows the H_2/CO established when this gasifier stream is mixed with a typical coal flue gas, where CO_2/H_2O is 2.14. Above 1100°C, the H_2/CO ratio is around 0.20. Therefore, the major reducing agent will be CO. With oil-fired units there will be slightly more H_2 present but still the major reducing agent will be CO.

D. Design Bases.

1. Process flow sheet.

To obtain an evaluation of the merit of the proposed process, the conceptual design discussed in Chapter I is combined with the experimental results of Chapter IV to produce the detailed design of a system to remove SO_x and NO_x from a 1000-Mw coal-fired power plant. The flow sheet for this design is presented in Figure v-2. The stream flows and temperatures are presented in Table v-12. This version of the process uses a sulfuric acid plant for sulfur recovery.

In the discussion of the experimental work in Chapters II, III, and IV, the metric system of units has been used. In the discussion

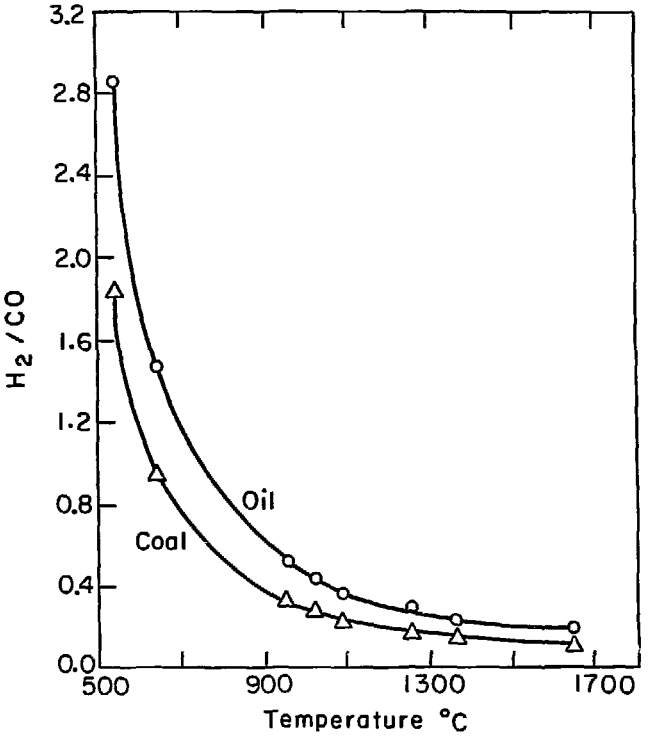

Fig. v-1. Equilibrium H_2/CO ratio in flue gas for oil and coal units.

Oil: $(CO_2/H_2O)_{avg.}=1.38, \frac{H_2+CO}{H_2O+CO_2} = 0.0004082$

Coal: $(CO_2/H_2O)_{avg.}=2.14, \frac{H_2+CO}{H_2O+CO_2} = 0.0004545$

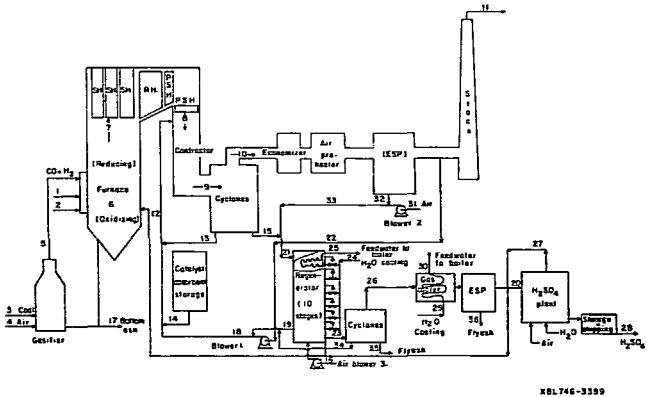

Fig. v-2. Simultaneous NO and SO_2 removal process.

TABLE V-12 PROCESS FLOWS

SOLID STREAMS	1	3	9	10	11	12	13	14	15	17	18	19	20	21	23	25	32	33	34	35	36
COAL (Tph) x 10^2	2 736	0120	0	0	0	0	0	0	0	0	0	0	0	0	0	0	0	0	0	0	0
FLYASH (Tph) x 10^2	0	0	0700	07039	001320	0640	0400	0	2134	00027	07384	07384	001013	2384	2146	02146	02507	02507	0	1931	07039
CAT/ABS (Tph) x 10^2	0	0	14 32	004354	000218	14 32	10 74	000716	3 870	0	3 883	3 368	0	3 883	2160	0	004130	004130	2149	000143	0
FeS (lbmph) x 10^2	0	0	10 33	00585	00070	14 42	14 42	0	4 81	0	0	0	0	4 010	0	0	005658	005658	0	0	0
FeO (lbmph) x 10^2	0	0	45 70	01377	00010	33 97	33 97	0	11 37	0	0	0	0	11 33	0	0	01308	01300	0	0	0
Fe_2O_3 (lbmph) x 10^2	0	0	1 185	00057	000020	10 30	1 414	001701	4713	0	8 875	7 600	0	4718	1 0403	0	000542	000547	1 040	000336	0
$FeSO_4$ (lbmph) x 10^2	0	0	3 303	00103	00005	2 548	2 548	0	8483	0	0	0	0	0403	0	0	000070	000078	0	0	0
Al_2O_3 (lbmph) x 10^2	0	0	224 7	0413	0034	224 7	168 0	01127	60 17	0	56 18	57 65	0	50 73	3 678	0	06409	06400	3 670	00224	0
Temp (°F)	260	77	1000	1000	300	1000	1000	77	1000	77	1000	1250	760	800	1250	1250	300	160	1260	1250	760
Gas Flow (acfm) x 10^6	--		42 02	42 02	21 07	1507	0	0	0	0	1507	0	7745	04020	1 093	1 093	0	02102	0	0	0
Den. CAT/ABS $\frac{lb}{ft^3}$ x 10^{-3}	-		11 30	00346	000337	3040	70347	70347	84075	0	102 1	03404	0	2471	4 657	0	11007	6 31	04075	027	0
Den. F.A. $\frac{lb}{ft^3}$ x 10^{-3}	-		607	0709	00701	141	2 22	2 23	0	30411	5 07	277	0401	104	0 64	0196	33079	38 3	0	30120	30410

GAS STREAM FLOWS	2	4	5	6	7	8	9	10	11	16	20	22	26	27	31
N_2 (lbmph) x 10^4	16 12	1 347	1 354	10 11	17 40	17 40	17 40	17 48	17 49	4854	4060	00513	4060	1098	00039
O_2 (lbmph)	42,050	3 670	0	3 095	104 8	104 8	0	0	0	1,211	123	0	123	100 2	0
CO_2 (lbmph) x 10^4	0	0	0	3 297	3 196	3 196	4 030	4 030	4 030	0	0	01503	0	0	00181
H_2O (lbmph) x 10^2	43 35	3 021	6 063	103 8	213 7	213 7	213 6	213 6	213 6	1,276	0	7060	0	0	00546
CO (lbmph) x 10^2	0	0	73 76	0	23 50	23 50	1065	1065	1055	0	0	0	0	0	0
H_2 (lbmph) x 10^2	0	0	70 17	0	5 340	5 340	4335	4335	4336	0	0	0	0	0	0
SO_2 (lbmph) x 10^2	0	0	1 149	5 13	6 203	6 203	0203	0203	0203	0	4 01	0	4 01	104	0
NO (lbmph) x 10^2	0	0	2607	1 455	1 717	1 717	1717	1717	1717	0	0	0	0	0	0
NH_3 (lbmph)	0	0	0	0	0	0	77 70	71 70	71 70	0	0	0	0	0	0
Total Gas (lbmph) x 10^4	20 04	1 741	2 455	21 70	23 80	23 80	23 07	23 07	23 07	6008	5266	0003	6266	2713	0704
Temp (°F)	300	300	2000	2700	2300	1000	1000	1000	300	300	750	300	1260	160	77

LIQUID FLOWS	24	25	29	30
Feed H_2O (gpm)	2 400	2 400	600	600
Temp (°F)	700	305	700	305

	28
H_2SO_4 (Tph)	210

acfm = actual cubic feet per minute

lbmph = pound moles per hour

Tph = Tons per hour

of the plant design and throughout the remainder of this chapter, the English system of units will be used because of its greater ease of interpretation by most engineers. The removal reactions reported between 370 - 538°C are between 700 - 1000°F. The regeneration reaction at 677°C is at 1250°F. Equipment dimensions are given in inches and feet. Flow rates are given in pound moles per hour (lbmphr) or tons per hour (Tph). Densities and concentrations are given in pounds per cubic foot (lbs/ft^3).

2. Materials flow.

The bases for the design are presented in Appendix A - 4. Table v-13 gives a listing of the calculations used to develop this design. The gas compositions at key points in the process are given in Table v-14.

Table v-13. Calculation flowsheet.

Select	Calculate
1. Furnace	
Coal composition.	Thermal value of coal.
Excess air level	Total coal rate
Inlet air humidity.	Furnace flue gas composition.
Power plant efficiency.	Rate of flue gas and required CO/H_2 flow per wgt furnace-fired-coal.
% fuel N to NO	
% thermal NO of total NO	
ash split between flyash and bottoms.	
2. Gasifier	
Coal composition.	Adiabatic operating temperature.
Excess air level	Gasifier gas composition.
Inlet air humidity.	Thermal value of coal.
% fuel N to NO.	Rate of flue gas per wgt. gasifier-fired coal.
% thermal NO of total NO.	Coal split between gasifier and furnace.
Ash split between flyash and bottoms.	
3. Total flue gas	
% O_2 removed in flue gas when CO/H_2 added.	Temperature wher CO/H_2 added
Maximum temperature of superheater inlet.	Flue gas composition.
	Flue gas rate.
4. Contactor	
% Removal ($CO + H_2$), SO_2, NO.	Flow of FeS, FeO, Fe_2O_3, $FeSO_4$.
% SO_2 removed as S^{-2}.	Flow of catalyst in contactor.
% SO_2 removed as SO_4^{-2}.	Flue gas composition after contactor.
Temperature.	Exit gas from regenerator.
Fraction of solids sent to regenerator.	
Amount of excess Fe_2O_3.	
Composition of original solid.	
5. Regenerator	
% Inlet solid regenerated.	Catalyst/absorbent exit composition.
Temperature.	Solids exit flow rate.
Stoichiometric air requirement.	Exit gas rate.
	Exit gas composition.

Table V-14. Gas compositions in the process.

	Contactor Entrance	Contactor Exit	Regenerator Exit
N_2 (%)	73.44	73.86	88.5
CO_2 (%)	15.95	17.02	0
H_2O (%)	8.98	9.02	0
O_2 (ppm)	819	0	2.35
NO (ppm)	721	72.5	0
SO_2 (ppm)	2247	265	91,450
CO (ppm)	9900	82.6	0
H_2 (ppm)	2247	183	0
NH_3 (ppm)	0	326	0
$(O/R)_{NH_3}$	0.93	---	---

3. Heat balance.

The process has been designed to minimize heat losses. The heat generated in the gasifier is recovered in the boiler convection pass. The exit flue gas contains no excess air, which minimizes sensible heat losses. The excess heat produced by the exothermic regeneration reactions is recovered in heating coils containing boiler feedwater. The regeneration exit gas is cooled with a heat exchanger containing boiler feedwater. In both cases the boiler feedwater transfers the heat back into the steam boiler cycle. The solids, exiting from the regenerator, also transfer sensible heat back to the flue gas where it can be recovered in either the

economizer or the air preheater. The combustion potential of CO, H_2, and NH_3 and the sensible heat of the regenerator gas and disposed flyash represent process heat losses. The next paragraphs will give the details of the energy balance.

The heat liberated during combustion of coal in the furnace was estimated from the following formula (Steam, 1963):

$$\frac{BTU}{lb\ Coal} = 14{,}544\ C + 62{,}028\ (H_2 - \frac{O_2}{8}) + 4{,}050\ S. \quad \text{v-19}$$

where: C, H_2, O_2, and S are the weight fractions of each element in coal.

The heat liberated from the partial combustion of coal in the gasifier unit was first calculated from the ΔH_f for CO and SO_2 formation. This value was increased slightly (2.4%) to be consistent with the bases of equation v-19.

The heat liberated when the CO/H_2 stream reduces 95% of the excess O_2 was calculated from ΔH_f data for CO_2 and H_2O. The final value for H_2/CO in the flue gas stream was taken as the equilibrium value from the water-gas shift reaction at 2200°F. With this assumption the amount of CO_2 and H_2O formed and the amount of heat released can be calculated. Table v-15 summarizes the heat generated during combustion.

Table v-15. Heat released in combustion reactions.

(1000-Mw coal-fired unit.)
334.92 Tons coal/hr.

	% of Coal	BTU/hr ($\times 10^9$)	% of heat
Oxidizing furnace	81.70	7.168	85.32
Gasifier	18.30	0.374	4.45
O_2 Removal reaction	---	0.859	10.23
Total		8.401	100.00

If the same amount of coal were burned in an oxidizing furnace to CO_2, H_2O, and SO_2, the heat liberated would be 8.774×10^9 BTU/hr. This implies a potential heat loss of around 4%. A more accurate estimate of the loss is obtained by calculating the amount of heat liberated if the excess CO and H_2 were reacted to CO_2 and H_2O. This calculation shows a potential loss of 0.342×10^9 BTU/hr, which is 3.9% of the total heat liberated.

Some of the apparent loss in this step of the process is offset by the fact that instead of the usual 20% excess air there is essentially 0% excess air in the effluent gas from the plant. Heating this excess air from 77°F, an average inlet temperature, to 300°F, an average stack-gas temperature, requires approximately 0.072×10^9 BTU/hr, which is 0.82% of the total energy.

The removal reactions in the contactor are also exothermic. Appendix A - 5 lists the reactions considered and their $\Delta H_{25°C}$ values. Table v-16 lists the heat evolved during the removal reactions. This heat is recovered in the economizer and air preheater.

Table v-16. Energy released in removal reactions.

a. 90% removal ($CO + H_2$), NO, SO_2
b. Reduction: 43.7% by H_2, 56.3% by CO

Reactant	Assumptions	ΔH BTU/hr (x 10^9)
NO	50% NH_3 selectivity	0.0204
SO_2	15% sulfur removed as SO_4^{-2} 95% sulfur as SO_2 in gas 5% sulfur as H_2S	0.0776
$CO + H_2$	% Red H_2/% Red CO = 0.776	-0.00598
Fe_2O_3	Iron reduced to FeO for FeS formation reaction	-0.00332
O_2	97.6% O_2 formed SO_4^{-2} (Amount to give required SO_4 = level)	0.0000478
	Total Release	0.0887

All of the reactions except the reduction of Fe_2O_3 and the oxidation of CO and H_2 are exothermic. The selected split of the reduction between CO and H_2 was based on an average of the H_2/CO ratios between 1000°F and 2200°F. If more of the reduction were by CO, the reactions would all be more exothermic. The role of H_2 in the reduction is not expected to increase above the assumed value.

Heat is also produced in the process external to the furnace. The two main reactions occurring in the regenerator, which are the last three reactions in Appendix A - 5, are exothermic. As stated earlier, the amount of heat liberated in the regeneration will depend upon the solids composition and inlet temperature, the inlet air flow rate and its temperature, and the temperature level required for regeneration. In order to operate the regenerator at

a constant temperature, this heat must be removed by cooling coils (using boiler feedwater) immersed in the fluidized bed. The heat release for this design is given in Table v-17.

Table v-17. Energy generation in regeneration reactions.

(1000-Mw coal-fired unit)

Conditions:

Solid: 0.05899 lbs FeS/lb Catalyst
0.1136 lbs FeO/ " "
0.01799 lbs $FeSO_4$/lb "
0.01051 lbs Fe_2O_3/ " "
0.7989 lbs Al_2O_3/ " "

1000°F Inlet Temperature

Regenerator: 1250°F; Contactor: 1000°F

Air: 110% of stoichiometric for complete oxidation to Fe_2O_3 and SO_2
300°F Inlet Temperature

H_2O: Inlet 280°F, Outlet 365°F

Sensible heat recovered in regenerator coils:	0.1057 x 10^9 BTU/hr.
Sensible heat transferred by solids to contactor:	0.0258 x 10^9 BTU/hr.
Heat recovered in regenerator gas cooler:	0.0212 x 10^9 BTU/hr.

Adding both of the heat sources from the process reactions and the heat recovered from the solids and gas gives a total of 0.2684 x 10^9 BTU/hr. With the potential loss of 0.342 x 10^9 BTU/hr from the excess CO + H_2 and the gain of 0.2684 x 10^9 BTU/hr the percentage heat loss as a result of the process is 0.839% of the total liberated in the power plant. This loss is approximately the same as that calculated for the savings gained by the decreased amount of excess air used. Reducing the excess air effectively to zero would result in a significant reduction in the loss of sensible heat in the stack gas.

If this is in fact found operationally possible, there would be a definite incentive for the process from the standpoint of energy conservation. In the operating cost section it is assumed that there will be a 0.839% energy loss. This gives a conservative design estimate.

4. Equipment description.

a. Contactor.

The contactor is basically an extension of the duct between the primary superheater and the economizer sections. It is to be fabricated of 3/16-in carbon steel lined with 3 inches of 85% MgO/$CaSiO_3$ castable insulation. The duct length of 50 feet provides the required residence time. The contactor cross section is 32.6 ft x 83.6 ft. The catalyst/absorbent is sprayed into the contactor entrance by pneumatic conveying lines. The solids and the flue gas are in concurrent flow. Within the contactor, the catalyst/absorbent concentration for this design in 1.14×10^{-2} lb/ft^3. This concentration corresponds to a dilute-phase contactor and is within the experimental range required. Flyash will also be present in the contactor at a concentration of 0.070×10^{-2} lb/ ft^3. This gives a flyash to catalyst/absorbent ratio of 0.061. The concentration of flyash used in this design is expected to be a maximum. The large amount is a result of overlap in catalyst/absorbent and flyash distribution. Either smaller flyash or larger catalyst/absorbent particles would result in a better separation, decreasing the amount of flyash recycled..

b. Regenerator.

The regenerator is a series of ten fluidized beds stacked vertically. The inlet solids are pneumatically conveyed to the top of the regenerator and pass through the series of beds, exiting at the regenerator base. Solids pass between beds in downcomers. The basis for ten fluid beds instead of one is to conserve construction area. If plant space were available, a single fluidized bed could be constructed. In the 10-unit design the regeneration air enters a manifold on one side of the tower. One-tenth of the inlet air passes to each fluid bed. The effluent gas and solids are collected in a manifold on the opposite side of the regenerator and pass to the high efficiency cyclones. Sectional views of the regenerator are shown in Figure v-3. The interior cross section is 13.7 ft x 13.7 ft. The plates are 6 feet apart, with a bed height of about 1 foot. The beds were designed with a void fraction of 0.60. Given the feed of both catalyst/absorbent and flyash, the bed density ranges from 43.3 lb/ft^3 at the top to 44.6 lb/ft^3 at the bottom.

The interior of the regenerator and the exit manifold are 1/4-inch 316 SS. The entrance air manifold is 3/8-inch carbon steel. The outside area is insulated with 3 inches of 85% $MgO/CaSiO_3$. The gas distributor plates and the bed separation plates are 1/8-inch 316 SS. A 3/8-inch, 8-ft carbon steel skirt is provided.

The inlet air temperature to the bed is 300°F. The beds are kept at 1250°F by cooling coils in which boiler feedwater is circulated. These coils are 1.66-inch Sch 40 316 SS pipe having 0.25-inch fins with 10 fins/inch. A total of 165.3 ft^2 of surface area per bed is

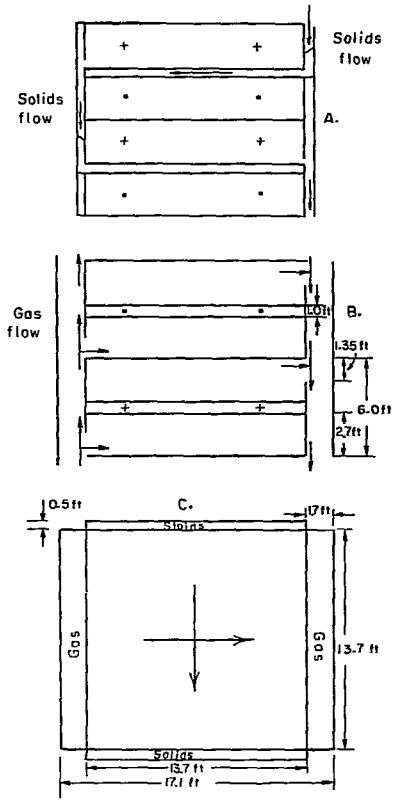

Fig. v-3. Regenerator schematic.
A. Solids flow.
B. Gas flow.
C. Plan view.

provided. Ten control values in the lines remove heat as needed from each bed.

c. Gasifier.

The design of the gasifier is based on the design of a continuous feed, rectangular construction incineration system. The fuel is burned on a moving chain grate. Niessen (1970) reports that a 250-Tpd municipal incinerator generates about 1.7×10^5 acfm of flue gas at 1600°F. The required gasifier gas rate at 1600°F is 6.51×10^5 acfm. With linear extrapolation of the gas volumes this implies that a municipal incinerator capable of handling 957 Tpd would be roughly the size of the gasifier. The furnace would have refractory walls with no heat-transfer surface provided. All of the heat generated would be removed in the convection zone of the boiler. The air supplied to the gasifier will come from the normal F.D. fan system for the inlet air. The coal burned in this unit will typically be between 1/8-inch and 1-inch in size (Steam, 1963). The larger size allows about 85% of the ash to be collected in the bottoms.

d. Cyclones and electrostatic precipitators.

The main cyclone bank which collects the solids immediately after the contactor are medium-efficiency cyclones found on normal coal-fired units. EPA (August, 1973) and Benson (1974) report that such cyclones are 85% efficient on flyash. The typical pressure drop is 3 inches of H_2O. The material of construction is carbon steel. Popper (1970) reports the collection efficiency as a function of particle size from 2.5 up to 150 microns for this type cyclone

bank on coal flyash. With the catalyst/absorbent size distribution given in Table v-8 these cyclones would be expected to give an overall efficiency of 98.876%. Even though this is relatively high it still would allow a large loss of catalyst/absorbent. A second similar bank of cyclones was therefore added to the design. This gives a total pressure drop across the cyclones of 6.0 inches. The second bank of cyclones will be 80% efficient for flyash removal and 97.293% for catalyst/absorbent. The overall efficiency of the cyclone banks will thus be 97% for the flyash and 99.9696% for the catalyst/absorbent.

The electrostatic precipitator (ESP) for the main flue gas is not considered a part of this design since most plants either have one or will have to have one regardless of the installation of this process. The ESP will provide an efficiency of 95% for both the flyash and catalyst/absorbent. The large amount of iron on the catalyst should give resistivities similar to the flyash. With the ESP in the system the overall efficiencies become 99.85% for the flyash and 99.998% for the catalyst/absorbent.

The cyclones on the regenerator are operated at 1250°F. These are high efficiency cyclones made of 316 SS and lined with castable insulation to prevent high erosion rates. Flanders (1974) discussed cyclones of this design which had removal efficiencies of 99.996% on Si/Al catalyst/absorbent with an average size of 60 microns. The units discussed had primary and secondary cyclones which developed a pressure drop of 30 inches of H_2O. The units handled a gas flow

from a fluid bed catalytic cracking regenerator, which was 2.93 times the rate required in the present regenerator. The specifications for the cyclone bank required for the regenerator will be similar to these. The catalyst/absorbent removal efficiency is taken as 99.933%. The flyash removal efficiency is taken at 90%. The catalyst/absorbent will primarily be collected in the first bank of cyclones whi'e the second bank will collect the flyash and the remainder of the catalyst/absorbent.

An electrostatic precipitator is added before the H_2SO_4 plant to remove 95% of the flyash remaining after the cyclones. This unit is sized by scaling up from the TVA data reported by Benson (1974). Since the precipitator operates at 750°F, it is classed as a "hot" precipitator. The material of construction to be used is 316 SS.

e. Blowers and motors.

The centrifugal blowers used for the regenerator air supply and the pneumatic conveying lines are capable of moving gas up to pressure differentials greater than 1000 inches H_2O but are operated at the required level. (See Table v-18). This high pressure capability is obviously more than is required under normal conditions but may be needed if solids plug up in any part of the system.

The motors used were all 3-phase, enclosed-fan-cooled electric motors operating at a nominal 1,800 rpm.

f. Catalyst storage tank.

A carbon-steel storage tank with manholes and ladders is provided

for storage for the catalyst/absorbent. The size is 1100 gallons, 8257 ft^3. This would give a 90-day supply at a net consumption of 143 lbs/hr.

g. Regenerator gas cooler.

After the regenerator cyclones a SS-U-tube exchanger is used to cool the flue gas from 1250°F to 752°F. The 1-inch tubes had boiler feedwater flowing in them;the total surface area provided was 3225 ft^2. An overall U of 10 BTU/hr ft^2 °F was used for the design. This is a conservative design since finned tubes could be used to decrease the tubing length.

h. Pumps and motors.

The pumps required to circulate the regenerator bed coolant and the regenerator gas coolant will be the same as those used to circulate water to and from the economizer. Control valves will be used to regulate the flow to each bed. Only the control valves are considered as a process cost.

i. Piping and Ductwork.

Solids conveyance in the process is by means of fluidized transport. The gas used to accomplish the fluidization is taken from a gas stream at approximately the same temperature as the solids. The fluid density in the transport lines ranges from 3.05 to 0.0063 lb/ft^3. The piping and ductwork required are designed for a transport velocity of 50 ft/sec. This velocity was selected to achieve the smallest cross-section possible without having excessive erosion

(Flanders, 1974). All bends should be 90° to minimize solids attrition (Flanders, 1974). The lengths of piping selected were estimated to be reasonable for the design presented. The details are given in the Cost Summary, Table v-18. The transport reference was Zenz (1960).

j. H_2SO_4 plant.

The sulfuric acid plant design was taken from Sittig (1971). The plant is an integrated contact plant with 3-stage contacting. The overall conversion efficiency for the unit was 96.8%. The product can range from 93% H_2SO_4 to various grades of oleum. Total production from this plant is 210 Tpd as 100% H_2SO_4. The regenerator exit gas, the feed to the H_2SO_4 plant, has 9.1% SO_2 in it. The tail gas from the H_2SO_4 plant can be mixed with the air to the furnace so that the remaining SO_2 can be recovered. Facilities are provided for 30 days storage and for shipping of the acid.

E. Economic Analysis.

1. General discussion.

In order to estimate the economic feasibility of the proposed process a cost model was developed for both the fixed capital investment (FCI) and the operating cost (OC). This model includes all of the added equipment required by the removal process. The FCI and OC for the H_2SO_4 plant were obtained directly from Sittig (1971).

The basic reference for constructing the cost model was Peters (1968). The FCI was separated into direct costs and indirect costs. Table v-19 shows the breakdown of the items within each group. The

TABLE V 10 REMOVAL PROCESS — EQUIPMENT SUMMARY.

EQUIPMENT	DESCRIPTION	SIZE UNIT	COST UNIT	DATED COST $	OCTOBER 1973 PURCHASE COST $	REFERENCE
1 Contactor						
Steel (carbon)	2 @ 3/16 in x 32.6 ft x 50 ft 2 @ 3.16 in x 83.6 ft x 50 ft	88,035 lbs	0.13 $/lb	11,502 (I) 1/67	10,077	Peters, 1968, p. 854
Insulation ($MgO \cdot CaSiO_3$)	3 in x 11,020 ft^2	11,020 ft^2	.081 $/$ft^2$ (cost) .335/ft^2 (labor)	16,234 11/62	21,094	Dorning, 1963, p. 180
2 Regenerator						
Steel (stainless, 316)						
Shell	1/4 in x 13.66 ft x 17.1 ft x 66 ft	60,700 lbs	1.106 $/lb			
Plates	1/8 in x 13.65 ft x 14.3 ft x 10 ft	10,278 lbs		100,625 (I) 1/67	105,015	Peters, 1968, p. 854
Steel (carbon)	3/8 in x 8 ft x 17.1 ft 3/8 in x 13.66 ft x 66 ft	24,030 lbs	0.23 $/lb	5,734 (I) 1/67		
Insulation	3 in $MgO/CaSiO_3$	4,630 ft^2	.081 $/$ft^2$ (cost) 33 $/$ft^2$ (labor)	5,051 1962	8,591	
3 Gasifier	7.772 x 10^5 cfm @ 2000 °F	957 TPD equiv. Incinerator	1,000 $/TPD	2.218 x 10^6 (I) 1968	1,564,000	Nielsen, 1970, p. VII, 93 111
4 Cyclone (contactor)	(scale factor 0.80) 2 Cyclone Banks identical	4.205 x 10^5 cfm @ 1000 °F	606,010 cfm / $112,000	762,700 1970	866,700	Benson, 1974, Popper, 1970, p. 99
Insulation + Struct	Estimated at 15%				130,014	
5 Cyclone (regenerator) (ss)	(scale factor 0.80) High Efficiency @ 1250 °F	1.224 x 10^5 cfm	368,700 cfm / $407,000	172,107 1973	172,107	Flanders, 1974, *Popper, 1970, p. 99*
6 ESP (regenerator) (ss)	(ss construction) (scale factor 0.80) 86% Efficient @ 760 °F	8.070 x 10^4 cfm	606,010 cfm / $1,231,000	630,610 1972	502,032	Benson, 1974 Oglesby, 1971
8 Fans and Blowers						
Reg. Air Blower #3	Centrifugal @ 300 °F	5.44 x 10^4 cfm	- - - -	70,000 1/67	92,100	Peters, 1968, p. 470
Reg. Solids Blower #2	Centrifugal @ 77 °F	1.02 x 10^3 cfm	- - - -	9,000 1/67	11,854	Peters, 1968, p. 470

TABLE V 10 (continued)

EQUIPMENT	DESCRIPTION	SIZE UNIT	COST UNIT	DATED COST $	OCTOBER 1973 PURCHASE COST $	REFERENCE
Cont Solids Blower 1	Centrifugal @ 300 °F	8 150 x 10^3 cfm	----	21,000 1/67	27,050	Peters, 1968, p. 470
8 Motors for Fans and Blowers	(3 phase, enclosed fan cooled)					
Reg Air Blower Motor #3	Δp = 1 50 psi, E_f = 70, E_m = 94 0	630 bhp	----	30,000 1/67	52,225	Peters, 1968, p. 474,480
Reg Solids Blower Motor	Δp = 1 48 psi, E_f = 70, E_m = 88	21 bhp	----	950 1/67		
Cont Solids Blower Motor	Δp = 4 04 psi, E_f = 70, E_m = 92	250 bhp	----	9,000 1/67		
9 Heat Exchange Area in Reg	Sch 40, 316 ss, 1 66 in O D pipe 0 25 in fins, 10 fins/in	10 i= 165 3 ft^2	----	14,600 1/67	19,000	Peters, 1968, p. 571, 580
Control Valves	10 gate, 316 ss	5600		0,000 1/67	7,803	Peters, 1968, p. 462
Carbon SteelPiping	Sch 40, 1 66 in O D pipe	1040 ft	$0.40/ft	410 1/67	546	Peters, 1968, p. 436
10 Flue Gas Cooler from Reg	3225 ft^2 (1250 °F - 752 °F) (ss)	- -	$60,000	60,000 1/67	66,857	Peters, 1968, p. 560
11 Catalyst Storage Tank	Carbon Steel, 90 day	0267 ft^3 1104 gal.	----	1,440 1/67	1,007	Peters, 1968, p. 477
12 Piping and Duct						
Piping	O.D 1 07 ft Sch 40	204 ft	$40/ft	11,760 1/67	22,001	Peters, 1968, p. 436
Duct Work	2 28 ft x 2 28 ft x 1/8 in x 400 ft	10,710 lbs	$ 10/lb	3,300 1/67		Peters, 1968, p. 864
Duct work	4 26 ft x 4 26 ft x 1/8 in x 100 ft	0,020 lbs	5.23/lb	2 020 1/67		Peters, 1968, p. 864
Remainder	(Estimated at 50% other)				11,300	
			TOTAL:	Insulation = 100,599 (I)		
				Piping = 34,440 (P)		
				Major Equip. = 3,600,081		
				Pur. Eq. = 63,775,120 (E)		

TABLE V-19. PROCESS FIXED CAPITAL INVESTMENT (FCI).

DIRECT COSTS	METHOD CALCULATED	OCTOBER 1973 COST		
Purchased Equipment (E)	Itemized Equipment Costs	$3,775,129	Total ($)	Percent of Total
Installation (Labor, Found., Const.)	40% (E)	1,510,052		
Instrumentation	13% (E)	490,767		
Instrumentation Installation and Accessories	8% (E)	302,010		
Pipe Costs (P)	Itemized Pipe Costs	34,449		
Pipe Labor Installation	46% (P)	15,846		
Pipe Insulation Material and Labor	25% (P)	8,612		
Electrical Installation	7.5% (FCI)	1,265,603		
Building and Service	5% (FCI)	843,735		
Insulation Major Equipment (I)	Itemized Insulation Costs	160,599		
Startup Expense	8% (FCI)	1,349,977		
		9,756,779	9.756×10^6	57.8%
INDIRECT COSTS				
Engineering and Supervision	35% (E)	1,321,295		
Construction Expenses	34% (E)	1,283,644		
Contractor's Fee	3.75% (FCI)	632,802		
Contingencies	8% (FCI)	1,349,977		
Working Capital	15% (FCI)	2,531,206		
		7,118,824	7.118×10^6	42.2%
SUMMARY		Removal	FCI = $16.87 x 10^6	
	FCI = 4.36 (E) + 3.24 (P) + 1.69 (I)	H_2SO_4	FCI = $1.67 X 10^6	
		Total	FCI = $18.54 X 10^6	

items were estimated as a function of the total purchased equipment cost (E), piping and duct costs (P), insulation costs (I), and FCI. The piping and insulations costs were calculated from the amount required instead of as a percentage of E. The cost model used for the removal process is

$$FCI = 4.36(E) + 3.24(P) + 1.89(I) \qquad v\text{-}20$$

The operating costs were divided into direct costs and fixed costs. Table v-20 shows the breakdown of the items for each group. Only the maintenance and fixed costs are estimated as a percentage of FCI. The royalties are calculated as a percentage of the total operating cost. The fixed operating costs are taken as 14.67% of FCI. This assumes depreciation over a 15 year period as suggested by Buchard (1972). It is assumed that all of the capital will be borrowed for the removal process at an average interest of 5% over the 15 years.

2. Cost Basis.

The costs required for the model are non-installed equipment costs. In some cases only the installed equipment costs were available. The equipment cost was estimated by dividing these costs by 1.4, which assumes a 40% installation charge. Those costs which were treated this way have a superscript I in the dated cost column of Table v-18. The equipment cost sources are given in this table. In order to standardize all costs the Chemical Engineering plant cost index was used. All costs were updated to October 1973. The CE plant index for the pertinent years is given in Table v-21.

TABLE V-20. REMOVAL PROCESS OPERATING COSTS.

DIRECT COSTS	METHOD CALCULATED	OCTOBER 1973 COSTS		TOTAL COSTS	
Energy Loss Charge	Lost heat value (.0084) (8.77 x 10^9 BTU/hr) @ 30¢/MMBTU	245,040	$/yr.	$/yr.	Mills/kwhr
	from pressure loss across 2nd cyclone @ 1¢/kwhr	201,400			
Catalyst Make up	143.2lb/hr @ 30¢/lb	376,330			
Operating Labor and Supervision	SF0,000/yr shift pos. 4 equiv.	200,000			
Utilities	848 bhp + 20% adj. + ESP @ .00026 kw/acfm	68,237			
Maintenance	8% FCI	1,340,078			
Royalties	4% (Total Operating Costs)	237,070			
Laboratory Charges	10% (Labor and Supervision)	20,000			
Plant Overhead	50% (Labor and Maintenance)	774,000			
		3,473,050	$/yr	3.473×10^6	0.452
FIXED COSTS					
Depreciation (15 years)	6.67% FCI	1,126,643			
Taxes and Property	2% FCI	337,404			
Insurance	1% FCI	168,747			
Interest	5% FCI	843,735			
		2,476,519	$/yr	2.476×10^6	0.322
				55.949×10^6/yr.	0.774 mills/kwhr
					(Increasing cat. make-up by factor of 10 gives total cost of 1.23 mills/kwhr

Table v-21. CE Plant cost index.

Year	1957	1962	1967	1968	1969
Index	100	101.5	109.1	113.7	119.0

Year	1970	1971	1972	1973
Index	125.7	132.2	137.2	143.7

The items costed from Peters (1968) were generally obtained from correlations of equipment cost versus size. The items obtained elsewhere were generally only listed in one size. The scaling factors for specific equipment types suggested by Popper (1970) were used to obtain the cost of specific size equipment.

3. Process Costs.

The total purchase equipment cost for the process comes to \$3.78 x 10^6. The three most costly items are the gasifier, the contactor cyclones, and the electrostatic precipitator on the regenerator effluent gas stream. These items account for \$3.14 x 10^6 or 83% of the total. The gasifier alone represents 42% of the cost. The gasifier cost, stated above, is based on a 957 Tpd municipal incinerator plant. The cost data presented by Niessen (1970) for the municipal incinerator furnace includes the costs for a crane, primary chamber, secondary chamber, FD fans, associated ducting, ash removal system, gas cooling by water spray, stack, piping, instrumentation and controls. The gasifier unit obviously does not require all of this equipment, but since a further breakdown of furnace costs was not found this cost was used, giving a conservative value. Niessen (1970) reports that above 300 Tpd the furnace cost will average around \$1,900/Tpd. More accurate cost data on the gasifier would probably result in a lower

cost.

The total FCI for the removal process is 16.87×10^6. Direct costs represent 57.8% of the total. The two largest costs are the purchased equipment, 3.78×10^6, and the working capital, $2,53 \times 10^6$. Since in equation v-20 E is multiplied by 4.36 to give its contribution to FCI, it is by far the most sensitive item in the analysis.

The operating costs listed in Table v-20 show 58.4% as direct process costs. The energy loss is that due to the net heat lost by the process and the energy needed to overcome the added 3-inch pressure drop in the second bank of cyclones. The fuel charge for the heat requirement is $38¢/10^6$ BTU. The electrical charge for the power is 1¢/kwh.

Catalyst costs are about 30¢/lb, Harnsberger (1974). The high charge for maintenance (8% FCI) is used since there may be material erosion problems in the solid transport lines. The overall operating cost is 0.774 mills/kwh. With a catalyst attrition rate of 10 times that used in Table v-20 the operating cost would be 1.23 mills/kwh.

The process costs for the H_2SO_4 plant were taken directly from Sittig (1971). This report gives both FCI and operating costs for the H_2SO_4 plant. For a 210 Tpd plant the FCI is 1.55×10^6. Storage and shipping facilities were estimated from EPA (May, 1973) to be 1.23×10^5. This gives the total investment of 1.67×10^6. The operating cost for the plant is $101/hr. With a 20% increase for distribution and marketing costs the H_2SO_4 cost would be $121/hr (0.138 mills/kwh). If the H_2SO_4 were sold at $25/Ton, a credit of

$219/hr would be realized. This credit corresponds to about 0.25 mills/kwh.

The total process costs with and without H_2SO_4 credit are given in Table v-21.

Table v-21. Process costs for 1000-Mw coal-fired power plant.

	Removal Process	H_2SO_4 Plant	Credit	Total Process
FCI ($/Kw)	16.87	1.67	----	18.54
OC (mills/ kwh)	0.77	0.14	-0.25	0.66

Even if the acid were not sold the operating cost would be only around 0.90 mills/kwh.

CHAPTER VI

Discussion and Recommendations

A. Process Evaluation.

1. Description of the process.

A dry process operating at relatively high temperatures (1000°F) has been developed for the simultaneous removal of NO and SO_2 from power plant stack gases. A catalyst/absorbent consisting of 20% ferric oxide supported on alumina contacts the flue gas under reducing conditions in a dispersed-phase reactor. Reactions occur which effect the absorption of SO_2 as either ferrous sulfide or sulfate and the reduction of NO to either N_2 or NH_3 (Section IV.E.). In the high temperature (1250°F) fluidized bed regenerator, the catalyst/absorbent is reoxidized by air to ferric oxide and produces an effluent gas containing about 9% SO_2, which is a suitable feed for a H_2SO_4 plant. The flow sheet for the process is shown in Figure V-2.

The removal reactions for both SO_2 and NO require a net reducing flue gas. A coal gasification unit produces the required amount of CO and H_2 (Section V.C.), while most (81%) of the coal is burned under oxidizing conditions in the furnace. Since the rich CO/H_2 stream is added prior to the superheater section, the heat generated in the coal gasifier is recovered in the convection pass of the boiler. The CO/H_2 concentration in the effluent stack gas is controlled by maintaining an excess of ferric oxide in the catalyst/

absorbent recycle stream.

A process flow sheet applicable to a 1000-Mw coal-fired power plant and designed to remove 90% of the NO and SO_2 in the flue gas is presented in Chapter V. Since the process equipment and reactant transport techniques are similar in scale and throughput to those in fluidized bed catalytic cracking units, the technology required for implementing this process is considered to be established. The economic analysis of the process is based on October 1973 dollars. The process requires a fixed capital investment of $18.5/kw and has operating costs of 0.91 mills/kw-hr. The investment cost includes $1.67/kw for the H_2SO_4 plant. With a $25/Ton credit for the concentrated H_2SO_4, the operating cost would be reduced to 0.66 mills/kw-hr.

2. Comparison with other processes.

Princiotta (1974) has evaluated the six leading processes for SO_2 removal. All of these processes, except the low-sulfur fuel alternative, involve cooling the flue gas and contacting it with an aqueous stream. The investment and operating costs for these processes are presented in Table vi-1. The costs for the proposed process are reported at 100% load factor and fixed operating charges at 14.67% of the capital costs per year, whereas the basis in Table iv-1 is an 80% load factor and an 18% rate for fixed charages. The operating cost for the proposed process on this basis is still 0.91 mills/kw-hr. The decrease in direct charges is almost compensated for by the increase in fixed costs. The capital investment charge

TABLE iv-1. COMPARISONS OF SO_2 CONTROL PROCESS SYSTEMS FOR COAL-FIRED POWER PLANTS (Princiotta, 1974)

	Reactant input requirements	Throwaway or recovery	Approx. invest. costs[a] for coal-fired boilers $/kw	Approx. (annual) costs,[b] mills/kw-hr: No credit for S recovery	Approx. (annual) costs,[b] mills/kw-hr: With credit for S recovery	SO_2 removal efficiency,%
Coal-fired power plant	N. A.	N. A.	200	8.0[c]	N. A.	N. A.
Low-sulfur fuel increment (coal and oil)	N. A.	N. A.	N. A.	2.0 - 4.0	N. A.	N. A.
Wet lime/limestone/ $Ca(OH)_2$ slurry scrubbing	Lime (100-120% Stoich.); limestone (120 -150% Stoich.)	Throwaway $CaSO_3$/ $CaSO_4$	35 - 52	1.5 - 2.4	N. A.	80 - 90
Magnesium oxide scrubbing	MgO alkali; carbon and fuel for regeneration and drying	Recovery of conc. H_2SO_4 or elem. sulfur	36 - 66	1.6 - 3.0	1.4 - 2.8	90
Monsanto catalytic oxidation (add-on)	Catalyst V_2O_5 (periodic replacement) and fuel for heat	Recovery of dilute H_2SO_4	43 - 67	1.6 - 2.7	1.5 - 2.6	85 - 90
Wellman-Lord process (soluble sodium scrubbing with regeneration)	Sodium make-up and heat for regeneration	Recovery of conc. H_2SO_4 or sulfur	40 - 68	1.5 - 3.2	1.2 - 2.8	90
Double alkali process	Sodium make-up plus lime/limestone (100-130% Stoich.)	Throwaway $CaSO_3$/ $CaSO_4$	26 - 47	1.2 - 2.2	N. A.	90

(a) Generally, where a cost range is indicated, the lower end refers to a new unit (1000 Mw); the high end refers to a 200 Mw retrofit unit. Costs include particulate removal and are in 1973 dollars.
(b) Assumptions: Costs calculated at 80% load factor, fixed charges per year ~18% of capital costs.
(c) Includes environmental controls to minimize land and water pollution.

remains unchanged.

If the maximum retrofit factor of 1.25 is applied to the capital charge cost, as suggested by Burchard (1972) for existing installations, the cost would be \$23.1/kW including the H_2SO_4 plant. Based on both efficient removal of pollutants and on the process economics, the process definitely shows potential for practical application.

3. Reasons for economy.

The strikingly lower costs predicted for this process are due to several advantages inherent to the design which has been developed. These are enumerated below.

a. Equipment size and complexity.

The contacting zone in the proposed process is at 1000°F and has a gas velocity around 50 ft/sec. A residence time around 1 second is required. The wet scrubbing processes cited by Princiotta (1974) operate around 130°F with maximum gas velocities of 8 - 13 ft/sec (Nannen, 1974; EPA, 1973). The flue gas residence time in the scrubbers is around 1.5 - 2.5 seconds. In spite of the high temperature, and the resulting high specific volume of the flue gas, the shorter residence time results in similar volumes for the high temperature contactor and scrubbers for a given flow rate. More explicitly, the higher contactor temperature results in a specific gas volume increase of 2.47. Therefore, the contactor volume needs to be increased by this amount over the scrubber volume to achieve

the same residence time. Since the required gas residence time in the scrubber is between 1.5 to 2.5 times that in the contactor, the contactor volume needs to be increased by only 1 to 1.6 times that of the scrubber. The faster allowable gas velocities in the contactor result in its cross-section being between 3.8 to 6.3 times smaller than that in a scrubber for the same gas volume. This means less duct expansion and gas distribution equipment at the contactor entrance. It also allows for a more compact design since at power plant sites vertical distance in one unit is less expensive than horizontal area in several units. The higher temperatures also result in more rapid diffusion and kinetic rates in the contactor than in the scrubbers. The faster rates are reflected in shorter required residence times.

Other considerations which combine with a smaller required cross-section to give a relatively low capital investment for the process are related to the process simplicity. In this process no large holding tanks are required for reaction or settling of reactants. All of the blowers are operated at 300°F or below with negligible solids in the gas streams passing through them. The contactor has no complicated internal structure. The contactor can be made of carbon steel. The regenerator and the solids recycle line temperatures are within the service range for normal stainless steels.

b. Improved thermal efficiency.

With the flue gas exiting the power plant stack very close to stoichiometric composition, the thermal efficiency of the plant will be improved by about 0.82% relative to operation with 20% excess air. The fuel requirements for removing the SO_2 and NO are estimated to be roughly this same amount (Section V.D.3.). If there are no thermal losses in the process, there are indications that a slight increase in thermal output over normal operating conditions may actually result. Finally, the fuel required for reheating the stack gas, necessary for plume buoyancy in wet-scrubbing processes, is of course avoided in this case.

c. Make-up cost.

The size distribution of the catalyst/absorbent (average size 75 microns) has been selected to allow highly efficient (99.998%) collection in a series of low-pressure-drop cyclones and an electrostatic precipitator in the main gas stream. The high-efficiency cyclones in the regenerator collect 99.933% of the inlet solids. The net result is first, a low catalyst/absorbent make-up requirement. Second, no solids disposal problem is created since the catalyst/absorbent is regenerated and almost totally recycled.

B. Potential Process Problems.

1. Ammonia emissions.

The catalytic reduction of NO forms both N_2 and NH_3, although it would be desirable to produce only N_2. Since the latter was not found possible, the process is expected to emit 300 - 400 ppm NH_3.

NH_3 is not reactive in the photochemical smog cycle. However, it will react with H_2SO_4 or HNO_3 present in the air to form ammonium salts. These will be in the form of aerosols which limit visibility. NH_3 emissions will not increase the aerosol problem, however, since the H_2SO_4 or HNO_3 would already be present as aerosols. In fact, the addition of NH_3 to the atmosphere will tend to neutralize the acid aerosols present, making them less objectionable.

The only NH_3 emissions standard which has been established is that for the San Francisco Bay Area. For large industrial stacks the limit is 2500 ppm (BAAPCD, 1972). Since the proposed emissions are only 13% of this standard, the ammonia emission is considered acceptable at present.

2. Accuracy of process design.

The prediction of dispersed-phase behavior from fixed-bed data is based on a model correlating the gas phase mass transfer rates for the two cases. As discussed in section V.B.1.ii., the prediction of these rates at low Reynolds numbers is not well established. At worst, the rates might be about one-tenth of those used in the design (Kunni, 1969). The dispersed-phase kinetics were estimated from the fixed-bed data. Due to the uncertainties in the experimental work, a range was given for the reaction rate constant. If the *minimum* reaction time required were 0.01 second, instead of 0.001 second as stated in section V.B.1.b., the reaction rate in the dispersed-phase contactor would be one-tenth of that discussed. A decrease in both the mass transfer rate and the reaction rate by a

factor of 10 would still result in the reaction rate controlling. Hence, the overall rate would be decreased by 10. The effect on the design would be to require 10 times the solids density within the contactor to effect the same removal. Streams to and from the regenerator would not be affected. If the solids density in the contactor were increased by 10 and the amount of solids lost from the process were increased by 10, then the operating costs would increase to about 1.31 mills/kw-hr. If the size of the solids blower, motor, and ductwork were increased to provide the same solids density with this added load, the capital investment would increase to a maximum of $20.5/Kw. Thus, the uncertainty in the experimental data has little potential effect on the process economics.

3. Flyash separation from catalyst/absorbent.

The separation of flyash from the catalyst/absorbent is important for the process. In the design the following collection efficiencies were used:

	Flyash	Cat/Abs
Contactor cyclone	97%	99.9696%
Main flue gas ESP	95%	95%
Regenerator (by elution)	10%	94%
Regenerator cyclones	90%	99.933%
Regenerator ESP	95%	95%

The difference in these efficiencies will provide adequate separation of the flyash and catalyst/absorbent. This assumes that the flyash particles will break up while cycling around the process. If this does not occur, large particles of flyash will build up in the system until the attrition rate equals the rate of flyash collection. Un-

fortunately there are no available data to predict the attrition characteristics of flyash. If the flyash built up to 10 times the present level assumed for the contactor, the ratio of flyash to catalyst/absorbent would rise to about 0.60. The effect on the economics would probably be something less than the effect of increasing the recycle of catalyst/absorbent by a factor of 10. The latter effect was shown earlier to be quite small in comparison with other process economics.

C. Recommendations.

The next step in the process development would be to determine the reaction kinetics in a dispersed-phase contactor. This contactor would probably be a fluidized bed at first, moving later to a unit with highly dispersed solids. The dispersed-phase contactors will not only give some idea of the gas phase mass transfer limitations expected, but also will allow the reactions to proceed in a bed with a more uniform solids composition. The experimental data showed qualitative evidence that under this uniform condition less ferrous sulfate and ammonia would form.

At several points in the experimental work, the number of samples taken was limited by the batch gas sampling technique used. In the dispersed contactor tests, continuous monitors on at least SO_2 and NO should be used. Sensitivity should also be improved in the gas monitoring system to allow analysis of all reactant gases at levels below 100 ppm.

The addition of silica to the alumina matrix has been suggested to decrease catalyst attrition. Tests are needed to confirm that this does not decrease the solids activity for NO and SO_2 removal. Any new catalyst matrix developed should also be tested for attrition. The most reasonable way would be to compare the new catalyst's attrition rate with that of a known commercial catalyst whose plant-scale attrition rate is known. Zenz (1974) discusses the technique for such tests. Samples of flyash tested in such an apparatus may give an estimate of flyash attrition relative to catalyst/absorbent attrition which could be used to establish better the level of flyash in the contactor.

The activity of the catalyst/absorbent as a function of time needs also to be tested. In these tests the solids should be cycled between removal and regeneration steps. The effect of flyash on the catalyst activity needs to be determined.

These suggested studies should produce sufficient data to obtain design values with substantially narrower ranges for the process variables. The process effectiveness and costs could then be stated with more certainty.

NOMENCLATURE

a = radius of FeS/Fe_2O_3 interface in particle during regeneration.

C_{ag} = bulk gas concentration at a particular time.

C_{ago} = bulk gas concentration at inlet conditions.

C_{as} = gas concentration at external surface of particle.

d_p = particle diameter.

D = gas phase diffusivity.

D_e = effective diffusivity in particles.

D_{ke} = effective Knudsen diffusivity in particles.

D_{12e} = effective gas phase bulk diffusivity.

E = total equipment cost.

F_{ao} = reactant flowrate.

FCI = fixed capital investment.

ΔF_T = thermodynamic free energy of reaction at temperature T.

h_s = Thiele modulus for a sphere.

ΔH_T = thermodynamic heat of reaction at temperature T.

I = insulation costs.

j_D = mass transfer j-factor.

k_m = overall mass transfer coefficient.

k_r = overall kinetic rate coefficient.

K_1 = overall reaction coefficient for removal reactions.

K_2 = overall reaction coefficient for regeneration reactions.

lbmph = pound moles per hour.

N_a = moles of reactant.

NH_3 selectivity (%) = percent reduced nitrogen compounds formed from NO in the form of NH_3.

OC = process operating costs.

$(O/R)_{NH_3} = (2.5[NO] + 3[SO_2] + 2[O_2])/([H_2] + [CO])$

$(O/R)_{N_2} = ([NO] + 3[SO_2] + 2[O_2])/([H_2] + [CO])$

P = piping costs.

r = catalyst/absorbent radius.

r_a = reaction rate.

R_{ep} = particle Reynolds number.

Sc = Schmidt number.

S_{ex} = specific external surface area of particles.

S_v = total specific surface area of particles.

t = residence time of solid in regenerator.

T = temperature.

Tph = tons per hour.

u_{ave} = average interstitial velocity past particles.

V = reactor volume

V_p = specific volume of particles.

W_m = molar amount of FeS in particles.

X_a = fractional conversion of reactant a.

z = amount of solid in contactor.

ϵ = particle porosity.

$1-\epsilon'$ = volume fraction of particle which is FeS.

η = kinetic effectiveness factor.

θ = residence time of gas in contactor.

ρ_B = bulk solids density.

ρ_p = particle density.

ρ_{sm} = molar density of FeS in solids.

[ ] = gas concentrations.

REFERENCES

1. BAAPCD, Amendment to Regulation 2, Division 15-Odorous Substances, Bay Area Air Pollution Control District, December 6, 1972.

2. Bagwell, F. A., et al., "Utility Boiler Operating Modes for Reduced Nitric Oxide Emission," Journal of the Air Pollution Control Association, 21 (11), p. 702, 1971.

3. Ball, J. S., Am. Petroleum Inst. Proc. 42 (VIII) (1962).

4. Baranski, A., et al., "Kinetics of Reduction of Iron Catalysts for Ammonia Synthesis," Journal of Catalysis, 26, p. 286, 1972.

5. Bartok, W., et al., "Systems Study of Nitrogen Oxide Control Methods for Stationary Sources-Volume II," NAPCA PB 192789, November, 1969.

6. Bartok, W., et al., "Systematic Investigation of Nitrogen Oxide Emissions and Combustion Control Methods for Power Plant Boilers," from Air Pollution and its Control by Coughlin, R. W., et al., AIChE Symposium Series No. 126, Volume 68, p. 66, 1972.

7. Beavon, D. K., "A Method for Removing Sulfur from Gases," French Patent Application 69 28844, August 22, 1969.

8. Benson, J. R., and Corn, M., "Costs of Air Cleaning with Electrostatic Precipitators at TVA Steam Power Plants," J. of Air Poll. Cont. Assoc., 24 (4), p. 340, 1974.

9. Bienstock, D., et al., "Formation of Oxides of Nitrogen in Pulverized Coal Combustion," J. of Air Poll. Cont. Assoc., 16 (8), p. 442, August 1966.

10. Burchard, J. K., et al., "Some General Economic Considerations of Flue Gas Scrubbing for Utilities," CSD-EPA, Research Triangle

Park, October, 1971.

11. Chilton, T. H., "Reducing SO_2 Emission from Stationary Sources," from Sulfur and SO_2 Developments ed. by CEP, p. 115 New York, 1971.

12. Cotton, F. A., Wilkinson, G., Advanced Inorganic Chemistry. A Comprehensive Text. 3rd edition, 1972.

13. Davis, J. C., "Desulfurization-Part 2 ...SO_2 Removal Still Prototype," Chemical Engineering, p. 52, June 12, 1972.

14. Dietz, R. N., "Gas Chromatographic Determination of Nitric Oxide on Treated Molecular Sieve," Analytical Chemistry, 40 (10) p. 1576, 1968.

15. Dinning, T. N., "Guide to Insulation Cost for Vessels," Chemical Engineering, 70 (8) p. 186, 1963.

16. EPA, "Conceptual Design and Cost Study Sulfur Oxide Removal From Power Plant Stack Gas. Magnesium Scrubbing-Regeneration: Production of Concentrated Sulfuric Acid," EPA-R2-73-244, May, 1973.

17. EPA, "Full-Scale Desulfurization of Stack Gas by Dry Limestone Injection. Volume II,", EPA-650/2-73-019-b, August, 1973.

18. EPA, "Evaluation of the Fluidized Bed Combustion Process, Volume II." EPA PB-211-494, November, 1971.

19. Fast, J. D. Interaction of Metals and Gases, pgs. 50 - 70, Academic Press, New York, 1965.

20. Feinman, J., Drexler, T. D., "Kinetics of Reduction of Ferrous Oxide with Hydrogen in a Fluidized Bed at Steady State," AIChE Journal, 7 (4), p. 584, 1961.

21. Feinman, J., "Kinetics of Hydrogen Reduction of Iron Ore in a Batch-Fluidized Bed," I&EC Process Design and Development 3 (3), p. 241, 1964.

22. Flanders, R , Process Engineer Chevron Research Company, private communication, 1974.

23. Forsythe, W. L., Hertwig, W. R., "Attrition Characteristics of Fluid Cracking Catalysts, Laboratory Studies," Industrial and Engineering Chemistry, 41 (6), p. 1200, 1949.

24. Gandhi, H. S., Shelef, M., "The Adsorption of Nitric Oxide and Carbon Monoxide on Nickel Oxide," Journal of Catalysis, 24, p. 241, 1972.

25. Gandhi, H. S., Shelef, M., "The Adsorption of Nitric Oxide on Copper Oxides," Journal of Catalysis, 28, p. 1, 1973.

26. Gidaspow, D., Onischak, M., "Regenerative Sorption of Nitric Oxide. A Concept for Environmental Control and Kinetics for Ferrous Sorbents," presented 22nd Canadian Chm. Engr. Conf. on "Catalysis and Sorption in Air Pollution Control", Sept. 20, 1972.

27. Glaubitz, F., "Economic Combustion of Sulfur-Containing Fuel Oil-A Means of Avoiding Dew-Point Difficulties in Boiler Operation," Mitt. VGB, no. 68, p. 338, 1960.

28. Glaubitz, F., "Operating Experience with Oil-Fired Boilers in the Combustion of Sulfur-Containing Fuel Oil with the Lowest Possible Excess Air," Mitt. VGB, no. 73, p. 289, 1961.

29. Glaubitz, F., "Experience of Three Years Operation of Oil-Fired Boilers with Extremely Low Excess Air," Energie, vol. 14, p. 459, 1962.

30. GOW-MAC Instrument Co. Bulletin SB-13.

31. Guha, B. K., Narsimhan, G., "Control Regimes and Particle Temperature Gradients during Decomposition of Pyrites," The Chemical Engineering Journal, 3, p. 145, 1972.

32. Gussow, S., Higginson, G. W., "Crack with New Zeolitic Catalyst," Hydrocarbon Processing, p. 116, June 1972.

33. Gwyn, J. E., "On the Particle Size Distribution Function and the Attrition of Cracking Catalysts," AIChE Journal, 15 (1), p. 35, 1969.

34. Haas, L. A., et al., "Removing Sulfur Dioxide by Carbon Monoxide Reduction," US Bureau of Mines RI 7483, 1971.

35. Haas, L. A., Khalafalla, S E.; "Kinetic Evidence of a Reactive Intermediate in Reduction of SO_2 with CO," Journal of Catalysis, 29, p. 264, 1973.

36. Hammons, G. A., Skopp, A., "NO_x Formation and Control in Fluidized Bed Combustion Processes," Trans. ASME. Paper No. 71-WA/APC-3, presented Nov. 1971.

37. Harnsberger, H. F., Research Physical Chemist Chevron Research Company, private communication, 1974.

38. Harshaw Chemical Co., "Harshaw Catalysts for Industry," Catalogue No. 500, 1973.

39. Hazard, H. R., Fellow ASME, Columbus Laboratories Battelle Memorial Institute, private communication, 1974.

40. Heil, T. C , Supervisor Performance Analysis Babcock & Wilcox Co., private communication, 1972.

41. Hopton, G. U., "The Purification of Coal Gas," from Chemical Engineering Practice by Cremer, H. W. and Davies, T., Vol. 2

Chpt. 12, Butterworth Scientific Publications, London, 1956.

42. Johnson, M. L., Essenhigh, R. H., "The Potential of Industrial Furnaces for CO Emission," from Air Pollution and its Control by Coughlin, R. W. No. 126 Vol. 68, p. 311, 1972.

43. Joithe, W., et al., "Removal and Recovery of NO_x from Nitric Acid Plant Tail Gas by Adsorption on Molecular Sieves," Ind. Eng. Chem. Des. Develop., 11 (3), p. 434, 1972.

44. Jonke, A. A., et al., Argonne National Lab. Monthly Report No. 8, March 1969; Monthly Report No. 16, January 1970.

45. Jones, J. H., et al., "Selective Catalytic Reaction of Hydrogen with Nitric Oxide in the Presence of Oxygen," Environmental Science & Technology, 5 (9), 790, 1971.

46. Jordan, C W., et al., "Gum Deposits in Gas Distribution Systems," Industrial and Engineering Chemistry, 27 (10), 1180, 1935.

47. Kasaoka, S., et al., "Catalytic Reduction of Sulfur Dioxide with Carbon Monoxide," International Chemical Engineering, 13 (4), p. 762, 1973.

48. Kearby, K. K., et al., "Catalytic Conversion of Exhaust Gas Impurities," US Patent 3,565,574, February 23, 1971.

49. Khalafalla, S E., et al., "Catalytic Reduction of Sulfur Dioxide on Iron-Alumina Bifunctional Catalysts," Ind. Eng. Chem. Res. Develop., 10 (2), p. 133, 1971.

50. Kirk, R. E., Othmer, D. F., Encyclopedia of Chemical Technology, John Wiley & Sons, 1963.

51. Klimisch, R. L., Barnes, G. J., "Chemistry of Catalytic Nitrogen Oxide Reduction in Automotive Exhaust Gas," Environmental Science

& Technology, 6 (6) p. 543, 1972.

52. Klimisch, R. L., Taylor, K. C., "Ammonia Intermediacy as a Basis for Catalyst Selection for Nitric Oxide Reduction," Environmental Science & Technology, 7 (2), p. 127, 1973.

53. Kokes, R. J., Journal of Physical Chemistry, 70, p. 296, 1966.

54. Kunii, D., Levenspiel, O., Fluidization Engineering, John Wiley & Sons, New York, 1969.

55. Lamb, A., Tollefson, E. L., "Catalytic Reduction of Nitric Oxide in Low Concentration High Velocity Gas Streams," presented at 22nd *Canad. Chm. Eng. Conf. on* "Catalysis and Sorption in Air Pollution Control" September 1972.

56. Landau, J. I., "The Catalytic Reactions of Nitric Oxide: Construction of an Apparatus and Preliminary Studies," Masters Thesis Univ. of Calif., Berkeley, 1973.

57. Lange, H. B., "NO_x Formation in Premixed Combustion: A Kinetic Model and Experimental Data," presented at 64th AIChE Mtg. San Francisco, November 1971.

58. Levenspiel, O., Chemical Reaction Engineering, John Wiley & Sons, New York, 1962.

59. Lewis, G. N., Randall, M., Thermodynamics, Rev. by Pitzer, K. S., Brewer, L., McGraw-Hill, New York, 1961.

60. Lewis, W. K., et al., "Characteristics of Fluidized Particles," Industrial and Engineering Chemistry, 41 (6), p. 1094, 1949.

61. Lowell, P.S., et al., "Selection of Metal Oxides for Removing SO_2 from Flue Gas," Ind. Eng. Chem. Process Des. Develop., 10 (3), p. 384, 1971.

62. Lundsford, J. H., J. Chemical Physics, 52 p. 2141, 1968.

63. Martin, G. B., Berkau, E. E., "An Investigation of the Conversion of Various Fuel Nitrogen Compounds to Nitrogen Oxides in Oil Combustion," from Air Pollution and its Control by Coughlin, R. W., et al., AIChE Symposium Series No. 126, Volume 68, p. 45, 1972.

64. McCann, J. J., et al., "NO_x Emissions at Low Excess-Air Levels in Pulverized-Coal Combustion," Trans. of ASME. Paper No. 70-WA/APC-3, presented Nov. 1970.

65. Mitchell, B., Applications Chemist at Varian Aerograph, private communication, 1972.

66. Nannen, L. W., Kreith, F., "Removal of SO_2 from Low Sulfur Coal Combustion Gases by Limestone Scrubbing," J. of Air Poll. Cont. Assoc., 24 (1), p. 29, 1974.

67. National Bureau of Standards, "High Temperature Properties and Decomposition of Inorganic Salts. Part 1. Sulfates, "NSRDS-NBS 7, 1966.

68. Niessen, W. R., et al., "Systems Study of Air Pollution From Municipal Incineration. Volume I," EPA PB-192 378, March 1970.

69. Nonhebel, G., Gas Purification Processes for Air Pollution Control, Newnes-Butterworths London, 1972.

70. Oil Paint & Drug Reporter, October 18, 1971.

71. Okay, V. C., Short, W. L., "Effect of Water on Sulfur Dioxide Reduction by Carbon Monoxide," Ind. Eng. Chem. Des. Develop., 12 (3), p. 291, 1973.

72. Otto, K., Shelef, M., "The Adsorption of Nitric Oxide on Iron Oxides," Journal of Catalysis, 18p. 184, 1970.

73. Peri, J. B., "Infrared Study of Adsorption of Ammonia on Dry Gamma-Alumina," The Journal of Physical Chemistry, 69 (1), p. 231, 1965.

74. Peters, M S., Timmerhaus, K. D., Plant Design and Economics for Chemical Engineers, 2nd ed. McGraw-Hill, New York, 1968.

75. Petersen, E. E., Chemical Reaction Analysis, Prentice-Hall, New Jersey, 1965.

76. Pierce, J. A , "A Study of the Reaction Between Nitric Oxide and Hydrogen Sulfide," J. Phys. Chem. 33, p. 22, 1929.

77. Popper, H., ed., Modern Cost-Engineering Techniques, McGraw-Hill Co., New York, 1970.

78. Princeton Chemical Research, Contract No. PH 86-68-48 with NAPCA, 1968.

79. Princiotta, F. T., Ponder, W. H., "Current Status of SO_2 Control Technology," Presented at the Lawrence Berkeley Laboratory Seminar entitled Sulfur, Energy and Environment, April 4, 1974.

80. Querido, R., Short, W. L., "Removal of Sulfur Dioxide from Stack Gases by Catalytic Reduction to Elemental Sulfur with Carbon Monoxide," Ind. Eng. Chem. Process Des. Develop., 12 (1), p. 10, 1973.

81. Quinlan, C. W., et al., "Simultaneous Catalytic Reduction of Nitric Oxide and Sulfur Dioxide by Carbon Monoxide," Ind. Eng. Chem. Process Des. Develop., 12 (3), p. 360, 1973.

82. Reh, L., "Fluidized Bed Processing," Chem. Eng. Progress, 67 (2), p. 58, 1971.

83. Reman, G. H., Verkoren, H., "A High-Intensity Combustor for Liquid Fuels," from Future of Fuel Technology by Critchley, G. N., ed. 1963.

84. Reese, J. T., et al., "Prevention of Residual Oil Combustion Problems by Use of Low Excess Air and Magnesium Additive," Trans. of ASME-Journal of Engineering for Power, p. 229, April 1965.

85. Riesz, C. H., et al., "Catalytic Decomposition of Nitric Oxide," Air Pollution Foundation of Los Angeles Report No. 20, 1957.

86. Robson, F. L., et al., "Technological and Economic Feasibility of Advanced Power Cycles and Methods of Producing Nonpolluting Fuels for Utility Power Stations," NAPCA Contract No. CPA 22-69-114, December 1970.

87. Rosser, W. A., Wise, H., J. Chem. Physics, 24, p. 493, 1956.

88. Ryason, P. R., Harkins, J., "Studies on a New Method of Simultaneously Removing Sulfur Dioxide and Oxides of Nitrogen from Combustion Gases," J. of Air Poll. Cont. Assoc., 17 (12), p. 796, 1967.

89. Satterfield, C. N., Sherwood, T. K., The Role of Diffusion in Catalysis, Addison-Wesley, Massachusetts, 1963.

90. Sax, I.N., Dangerous Properties of Industrial Materials, 3rd ed., Reinhold Book Co., New York, 1968.

91. Shah, I. S., "MgO Absorbs Stackgas SO_2," Chemical Engineering, p. 80, June 26, 1972.

92. Shelef, M., Otto, K., "Appearance of N_2O in the Catalytic Reduction of NO by CO," Journal of Catalysis, 10, p. 408, 1968.

93. Shelef, M., et al., "The Oxidation of CO by O_2 and by NO on

Supported Chromium Oxide and Other Metal Oxide Catalysts," Journal of Catalysis, 12, p. 361, 1968.

94. Shelef, M., et al., "The Heterogeneous Decomposition of Nitric Oxide on Supported Catalysts," Atmospheric Environment, 3, p. 107, 1969.

95. Shelef, M., Kummer, J. T., "The Behavior of Nitric Oxide in Heterogeneous Catalytic Reactions," AIChE Symposium Series No. 115, Vol. 67, p. 74, 1971.

96. Shelef, M., Gandhi, H. S., "Ammonia Formation in Catalytic Reduction of Nitric Oxide by Molecular Hydrogen. I. Base Metal Oxide Catalysts." Ind. Eng. Chem. Prod. Res. Develop., 11 (1), p. 2, 1972.

97. Sherwook, T. K., Pigford, R. L., Mass Transfer, Chpt. 6, To be published, McGraw-Hill, 1974.

98. Sittig, M., Sulfuric Acid Manufacture and Effluent Control, Noyes Data Corporation, New Jersey, 1971.

99. Slack, A V., "Removing SO_2 from Stack Gases," Environmental Science & Technology, 7 (2), p. 110, 1973.

100. Steam its Generation and Use, The Babcock & Wilcox Co. New York, 1963.

101. Stevens, W. A., Power Construction Division Bechtel Corporation, private communication, 1974.

102. Stollery, J. L., "Fundamentals of Fluid Bed Roasting of Sulphides," Engineering and Mining Journal, 165 (10), p. 96, 1964.

103. Tanaka, T., Suzuki, A., "Crushing Efficiency in Relation to Some Operational Variables and Material Constants," I&EC Process Design & Development, 7 (2), p. 161, 1968.

104. Thomas, A. D., et al., "Applicability of Metal Oxides to the Development of New Processes for Removing SO_2 from Flue Gases - Volume I," NAPCA PB 185562, July 1969.

105. Tomany, J. P., et al., "A Survey of Nitrogen-Oxides Control Technology and the Development of a Low NO_x Emissions Combustor," Transactions of the ASME-Journal of Engineering for Power, Paper No. 70-WA/Pwr-2, 1971.

106. Tuller, W. N., The Sulphur Data Book, McGraw-Hill, Book Co., New York, 1954.

107. Turner, D. W., et al., "Influence of Combustion Modification and Fuel Nitrogen Content on Nitrogen Oxides Emissions from Fuel Oil Combustion," from Air Pollution and its Control by Coughlin, R. W., et al., AIChE Symposium Series No. 126, Volume 68, p. 55, 1972.

108. Uno, T., et al., "Scale-up of a SO_2 Control Process," from Sulfur & SO_2 Developments ed. by CEP, p. 73, New York, 1971.

109. USDHEW, "Air Quality Criteria for Particulate Matter," NAPCA, Washington, D. C , January 1969.

110. USDHEW, "Control Techniques for Sulfur Oxide Air Pollutants," NAPCA, Washington, D. C., January 1969.

111. USDHEW, "Control Techniques for Nitrogen Oxides from Stationary Sources," NAPCA, Washington, D. C., March 1970.

112. Welty, A. B., "Flue Gas Desulfurization Technology," Hydrocarbon Processing, p. 104, October 1971.

113. Wilhite, W F., "The Use of Porous-Polymer Beads for Analysis of the Martian Atmosphere," Journal of Gas Chromatography, 6, p. 84, February 1968.

114. Winter, E R.S., "The Catalytic Decomposition of Nitric Oxide by Metallic Oxides," Journal of Catalysis, 22, p. 158, 1971.

115. Yost, D M., Russell, H., Systematic Inorganic Chemistry of the Fifth-and Sixth-Group Nonmetallic Elements," Prentice-Hall, New York, 1944.

116. Zenz, F. A., "Find Attrition in Fluid Beds," Hydrocarbon Processing, p. 103, February, 1974.

117. Zenz, F. A., "Help from Project E-A-R-L," Hydrocarbon Processing, p. 119, April 1974.

118. Zenz, F. A., Othmer, D. F., Fluidization and Fluid-Particle Systems, Reinhold Publishing Co., New York, 1960.

APPENDIX

APPENDIX A-1

EXPERIMENTAL SUMMARY

DATE	RUN	REACTION	CONDITIONS FOR RUN: T (°C)	[illegible]	[illegible]	Diluent	INLET GAS CONC (%)	SOLID INITIAL / FINAL	OVRL. MAT. BALANCE: C	H	N	Surface	PARTICLE SIZE (mm)	REF. FIG. IN TEXT	COMMENTS
5/20-21/[illegible]	1a	$NO + CO \longrightarrow \frac{1}{2}N_2 + CO$	345	105	0.88	N_2	NO 4.1, CO 4.6	[illegible] / [illegible]	—	X	—	X	3.2	iv-1	
"	1b	" "	347	205	"	"	NO 3.4, CO 4.4	" / [illegible]	—	X	—	X	"	"	
"	1c	$NO + CO + H_2S \longrightarrow$	347	290	"	"	NO 2.4, CO 4.1, H_2S 2.0	" / FeS_x	—	—	—	—	"		Noted ppt
5/[illegible]-6/[illegible]	2a	$Fe_2O_3 + CO \longrightarrow FeO, Fe_3O_4$	360 / 420	323 / 185	0.31 / 0.35	N_2 / "	CO = 11.8, CO = "	[illegible] / [illegible]	15%	X	X	X	3.2		
"	2b	$NO + CO \longrightarrow \frac{1}{2}N_2 + CO_2$	365	271	0.37	"	NO 1.7, CO 1.0	" " / " "	12%	X	—	X	"	iv-1	
"	2c	$FeO + H_2S \longrightarrow FeS + H_2O$	360	582	"	"	H_2S 1.9	" " / [illegible]	X	—	X	X	"	iv-3	
"	2d	$NO + CO \longrightarrow \frac{1}{2}N_2 + CO_2$	356	158	0.38	"	NO 1.8, CO 0.90	" " / " "	2%	X	11%	X	"	iv-2	
"	2e	$2FeS + \frac{7}{2}O_2 \longrightarrow Fe_2O_3 + 2SO_2$	444 / 515	102 / 636	0.21 / 0.19	"	O_2 [illegible]	——	X	X	X	—	"		
	3	ABORTED													Leaky Sample Valve
7/[illegible]-[illegible]	4	$NO + CO \longrightarrow \frac{1}{2}N_2 + CO_2$	390	1152	0.40	He	NO [illegible], CO [illegible]	[illegible] / [illegible]	1%	X	20%	—	3.2	iv-1	
6/[illegible]-30/[illegible]	5	$NO + CO \longrightarrow \frac{1}{2}N_2 + CO_2$	390	1416	0.40	He	NO 3.0, CO [illegible]	[illegible] / [illegible]	8%	X	10%	—	3.2	iv-1	
9/1-2/[illegible]	6a	$NO + CO \longrightarrow \frac{1}{2}N_2 + CO_2$	387	129	—	He	NO [illegible], CO [illegible]	[illegible] / [illegible]	—	X	—	X	3.2		
"	6b	$NO + CO \longrightarrow \frac{1}{2}N_2 + CO_2$	380	1620	0.39	"	NO [illegible], CO [illegible]	[illegible] / [illegible]	3%	X	25%	—	"	iv-1	
7/3/[illegible]	7	$NO + CO \longrightarrow \frac{1}{2}N_2 + CO_2$	370	1086	0.39	He	NO 0.30, CO [illegible]	[illegible] / [illegible]	3%	—	40%	X	3.2	iv-1	
9/[illegible]-[illegible]	8a	$Fe_2O_3 + CO \longrightarrow Fe_3O_4, FeO$	371 / 436	135 / 159	[illegible] / 0.41	N_2 / "	CO = 3.0, CO = 3.1	[illegible] / [illegible]	9%	—	—	—	3.2		Initial run at 215°C

EXPERIMENTAL SUMMARY

DATE	RUN	REACTION	CONDITIONS FOR RUN: T (°C)	Flow (cc/min)	Pres. (atm)	Diluent	Inlet gas conc. (%)	SOLID: Initial / Final	OVR. MAT. BALANCE: C	H	N	Surface	PARTICLE SIZE (nm)	REF. FIG. NO.	COMMENTS
[illegible]	8b	$CO + \frac{1}{2}O_2 \longrightarrow CO_2$	[illegible]	104 / [illegible]	[illegible]	N_2	CO = [illegible], O_2 = [illegible]	[illegible]	56%	X	X	X	32	IV-38	
"	8c	$2Fe_3O_4 + \frac{1}{2}O_2 \longrightarrow Fe_2O_3, Fe_2O_3$	[illegible]	[illegible]	[illegible]	"	O_2 = [illegible]	[illegible]	—	X	X	X	"		
"	8d	$CO + \frac{1}{2}O_2 \longrightarrow CO_2$	377	107	[illegible]	"	CO [illegible], O_2 [illegible]	[illegible]	16%	X	X	—	"	IV-38	
10/4/[illegible]	9a	$Fe_2O_3 + H_2 \longrightarrow Fe_3O_4, FeO$	[illegible]	[illegible]	[illegible]	[illegible]	H_2 = [illegible]	[illegible]	X	—	X	X	32	IV-39	
"	9b	$FeO + COS \longrightarrow FeS + CO_2$	370	90	0.60	"	COS = [illegible]	[illegible]	73%	X	X	—	"	IV-4	
10/[illegible]	10a	$FeSO_4 \longrightarrow FeO + SO_3$	[illegible]	255	15	He	No other gases	[illegible]	X	X	X	X	32		
"	10b	$2FeS + \frac{7}{2}O_2 \longrightarrow Fe_2O_3 + 2SO_2$	470	200	40	"	" " "	[illegible]	X	X	X	X	"		
"	10c	" " " "	"	260	15	"	O_2 = [illegible]	[illegible]	X	X	X	—	"		
[illegible]	11a	$Fe_2O_3 + SO_2 \longrightarrow (SO_4)_{[illegible]}$	374	[illegible]	0.54	He	SO_2 1.5	[illegible]	X	X	X	X	32		
"	11b	$3Fe_2O_3 + H_2 \longrightarrow Fe_3O_4, FeO$	378	200	0.48	"	H_2 [illegible]	[illegible]	X	—	X	X	"		
"	11c	" " " "	95	215	4.9	"	H_2 [illegible]	—	X	—	X	X	"		
"	11d	$FeO + SO_2 \longrightarrow FeO(SO_4)_{[illegible]}$	382	78	0.54	"	SO_2 [illegible]	[illegible]	X	X	X	X	"	IV-5	
"	11e	$FeO + SO_2 + 3H_2 \longrightarrow FeS + 3H_2O$	"	154	"	"	SO_2 [illegible], H_2 [illegible]	[illegible]	X	—	X	X	"	[illegible] IV-6	
"	11f	$FeS_2O_7 \longrightarrow SO_3 + Fe_2O_3$	[illegible]	200 / 150	[illegible]	"	No other gases	— —	X	X	X	—	"		Reactor reactive at high temp.
[illegible]	12a	$Fe_2O_3 + SO_2 \longrightarrow Fe_2O_3(SO_4)_{[illegible]}$	371	40	0.59	He	SO_2 [illegible]	[illegible]	X	X	X	X	32		
"	12b	$Fe_2O_3 + 7CO + 2SO_2 \longrightarrow 2FeS + 7CO_2$	"	90	"	"	CO [illegible], SO_2 [illegible]	[illegible]	—	X	X	X	"	IV-9	Noted S_2 ppt
"	12c	$Fe_2O_3 + CO \longrightarrow Fe_3O_4, FeO$	"	40	"	"	CO [illegible]	[illegible]	—	X	X	X	"		
"	12d	$Fe_2O_3 + 7CO + 2SO_2 \longrightarrow 2FeS + 7CO_2$	"	260	"	"	CO [illegible], SO_2 [illegible]	[illegible]	—	X	X	X	"	[illegible] IV-6	Noted S_2 ppt

EXPERIMENTAL SUMMARY

DATE	RUN	REACTION	CONDITIONS FOR RUN: T (°C)	Run time	[illegible]	Diluent	Inlet gas conc. (%)	SOLID: Ending [illegible]	OVERALL MAT. BALANCE: C	H	N	Surface	PARTICLE SIZE (μm)	REF. FIG.	COMMENTS
11/10-11/11	12e	$Fe_2O_3+7CO+2SO_2 \rightarrow 2FeS+7CO_2$	370	72	0.49	He	CO 8.4, SO₂ 1.88	[illegible]	—	X	X	X	32	IV-7, IV-6	
"	12f	$FeS+SO_2+O_2 \rightarrow S_2, SO_3$	688	120	0.55	"	O₂ [illegible], SO₂ [illegible]	" " — —	X	X	X	X	"		
"	12g	$2FeS+\frac{7}{2}O_2 \rightarrow Fe_2O_3+2SO_2$	"	"	0.36	"	O₂ [illegible]	— —	X	X	X	—	"		
11/11-11/12	13a	$3Fe_2O_3+CO \rightarrow Fe_3O_4, FeO$	377	49	0.51	He	CO 1.99	[illegible]	—	X	X	X	32	IV-9	
"	13b	$2FeO+\frac{1}{2}O_2 \rightarrow Fe_2O_3, Fe_3O_4$	380 "	31 480	0.71 9.1	"	O₂ 1.95	" [illegible]	X	X	X	X	"		SO₂ rapidly dropped off
"	13c	$Fe_2O_3+SO_2 \rightarrow Fe_2O_3(SO_4)_{0.11}$	377	48	0.56	"	SO₂ 1.99	[illegible]	—	X	X	X	"	IV-5	
"	13d	$3Fe_2O_3+CO \rightarrow 2Fe_3O_4+CO_2$	"	32	0.51	"	CO 1.38	[illegible]	—	X	X	X	"	IV-9	
"	13e	$Fe_2O_3+7CO+2SO_2 \rightarrow 2FeS+7CO_2$	"	836	0.56	"	CO 1.49-1.82, SO₂ [illegible]	[illegible]	—	X	X	X	"	IV-8, IV-6	
"	13f	$2FeS+\frac{7}{2}O_2 \rightarrow Fe_2O_3+2SO_2$	260	153	0.41	-	O₂ 1.5	— —	X	X	X	—	"		
1/9/13	14a	$Fe_2O_3+CO \rightarrow Fe_3O_4, FeO$	370	97	0.55	He	CO 1.1	[illegible]	67%	X	X	X	32	IV-38	
"	14b	$NO+2FeO \rightarrow \frac{1}{2}N_2+Fe_2O_3$	379	87	-	"	NO 1.11	" [illegible]	X	X	78%	—	"	IV-12	
2/1/13	15a	$Fe_2O_3+CO \rightarrow Fe_3O_4, FeO$	368 400	271 70	0.61 0.50	He "	[illegible]	[illegible]	19%	X	X	X	32	IV-38	
"	15b	$NO+2FeO \rightarrow \frac{1}{2}N_2+Fe_2O_3$	377	125	0.81	"	NO 0.98	[illegible]	X	X	16%	—	"	IV-12	
2/19-19/13	16a	$Fe_2O_3+H_2 \rightarrow Fe_3O_4, FeO$	392	193	0.48	He	H₂ 1.8	[illegible]	X	—	X	X	32		Began measuring H₂O on GC
"	16b	$FeO+H_2S \rightarrow FeS+H_2O$	378	199	0.50	"	H₂S 3.1	[illegible]	X	0.5%	X	X	"	IV-2	
"	16c	$3NO+FeS \rightarrow SO_2+\frac{3}{2}N_2+FeO$	"	167	"	"	NO 1.48	[illegible]	X	X	X	X	"	IV-13	
"	16d	$2FeS+\frac{7}{2}O_2 \rightarrow Fe_2O_3+2SO_2$	288	660	0.58	"	O₂ 1.9	— —	X	X	X	X	"		
"	16e	$SO_{2(ads)} \rightarrow SO_{2(g)}$	375	708	0.51	"	No other inlet gas	— —	X	X	X	X	"		

EXPERIMENTAL SUMMARY

DATE	RUN	REACTION	CONDITIONS FOR RUN: T (°C)	Run Time (min)	P_{H_2} (atm)	Diluent	Inlet Gas Comp (%)	SOLID Initial / Final	OVERALL MAT. BALANCE: C	H	N	Surface	PARTICLE SIZE (nm)	REF. FIG. in Text	COMMENTS
1/18-19/81	16f	$FeSO_4 + 3H_2 \rightarrow FeS + H_2O$	371	115	0.80	He	H_2 1.8	[illegible]	X	—	X	—	8.1		
[illegible]	17a	$Fe_2O_3 + H_2 \rightarrow Fe_3O_4, FeO$	395	449	0.49	He	H_2 1.5	[illegible]	X	—	X	X	3.2		
"	17b	$2FeO + NO \rightarrow \frac{1}{2}N_2 + Fe_2O_3$	380	127	0.48	"	NO 0.[illegible] – 0.81		X	X	27%	X	"		
"	17c	$Fe_2O_3 + H_2 \rightarrow Fe_3O_4, FeO$	452	142	—	"	H_2 [illegible]		X	—	X	X	"		
"	17d	$NO + H_2 \rightarrow N_2, NH_3$	382	167	0.47	"	NO 0.31, H_2 2.0		X	—	—	—	"		
[illegible]	18a	$Fe_2O_3 + H_2 \rightarrow Fe_3O_4, FeO$	385	203	0.48	He	H_2 1.9	[illegible]	X	—	X	X	3.2	IV-59	
"	18b	$NO + 2FeO \rightarrow \frac{1}{2}N_2 + Fe_2O_3$	377	90	"	"	NO 1.3	[illegible]	X	X	14%	X	"	IV-13	
"	18c	$Fe_2O_3 + H_2 \rightarrow Fe_3O_4, FeO$	379	162	0.49	"	H_2 1.3	[illegible]	X	—	X	X	"		
"	18d	$NO + H_2 \rightarrow N_2, NH_3$	"	156	"	"	NO 0.30, H_2 3.9	[illegible]	X	18%	22%	—	"	IV-14	
[illegible]	19a	$Fe_2O_3 + H_2 \rightarrow Fe_3O_4, FeO$	374	121	0.49	He	H_2 [illegible]	[illegible]	X	3%	X	X	3.2	IV-59	Began quantifying H_2O on G.C.
"	19b	$NO + H_2 \rightarrow N_2, NH_3$	377	190	0.47	"	NO 0.42, H_2 7.3	[illegible]	X	84%	12%	X	"	IV-14	
"	19c	$FeO + H_2S \rightarrow FeS + H_2O$	"	296	"	"	H_2S 1.[illegible]	[illegible]	X	131%	X	X	"	IV-3	Noted S ppt
"	19d	$NO + H_2 \rightarrow N_2, NH_3$	390	188	0.46	"	NO 0.[illegible], H_2 [illegible]	[illegible]	X	5%	—	X	"	IV-33	
"	19e	$FeS + O_2 \rightarrow FeS, FeSO_4$	54-90	138	0.86	"	O_2 4.6		X	X	X	X	"		
"	19f	$SO_{2(ads)} \rightarrow SO_{2(g)}$	280	240	0.86	"	No other gases		X	X	X	—	"		
	20	ABORTED													H_2S leak
[illegible]	21a	$NO + H_2 + H_2S + Fe_2O_3$	372	428	0.49	He	NO [illegible], H_2S [illegible], H_2 [illegible]	[illegible]	X	7%	—	X	3.2	IV-18	

EXPERIMENTAL SUMMARY

DATE	RUN	REACTION	T (°C)	Run Time (min)	Bed Wt (gm)	Diluent	INLET GAS CONC (%)	SOLID Initial / Final	C	H	N	Surface	PARTICLE SIZE (mm)	REF. NB PAGE	COMMENTS
8/11-15/73	21b	$NO + H_2 + H_2S + FeS_xO_y$	372	75	0.80	He	NO 0.33, H_2 0.93, H_2S 1.93	[illegible] / [illegible]	X	—	—	X	3.2	IV-18	
"	21c	$NO + H_2 \longrightarrow NH_3, N_2$	"	45	"	"	" "	" " / " "	X			X	"	IV-14	
"	21d	$FeS + O_2 + H_2O \longrightarrow SO_2, S_2$	260	390	0.60	"	O_2 0.8, H_2O 13	" " / — —	X	—	—	—	"		
8/18-20/73	22a	$NO + CO + H_2O + H_2S + Fe_xO_y$	371	174	0.48	He	NO [illegible], H_2O 2.0, H_2S [illegible], H_2 [illegible], CO .96	[illegible] / [illegible]	37%	12%	—	X	3.2	IV-19	
"	22b	$NO + CO + H_2S + FeS_xO_y$	"	134	"	"	NO [illegible], H_2S 2.0, CO 1.0	" " / [illegible]	—	—	—	X	"	IV-20	
"	22c	$NO + H_2S + FeS_xO_y$	365	130	0.51	"	NO [illegible], H_2S 1.1	" " / [illegible]	X	—	—	X	"	IV-17	Noted ppt
"	22d	$NO + CO + H_2O + FeS_xO_y$	374	210	0.49	"	NO [illegible], CO 1.1, H_2O [illegible]	" " / [illegible]	30%	—	—	X	"	IV-35 IV-16	
"	22e	$NO + COS + H_2O + FeS_xO_y$	371	150		"	NO [illegible], COS [illegible], H_2O [illegible]	" " / — —	X	—	—	—	"		Noted ppt
9/1-2/73	23a	$NH_3 + Fe_2O_3 \longrightarrow (NH_3)_{ADS}$	368	167	0.44	He	NH_3 2.1	[illegible] / [illegible]	X	—	—	X	3.2		
"	23b	$Fe_2O_3 + H_2 \longrightarrow FeO, Fe_3O_4$	418 374	48 490	0.43 0.44	" "	H_2 7.0	" " / [illegible]	X	—	—	X	"		
"	23c	$NO + FeO + H_2O \rightarrow N_2, NH_3$	"	94	"	"	NO [illegible], H_2O [illegible]	" " / —	X	—	X	X	"		
"	23d	$FeO + H_2S$	"	30	"	"	H_2S 7.0	[illegible] / —	X	—	X	—	"		
9/6-10/73	24a	$Fe_2O_3 + CO \longrightarrow Fe_3O_4, FeO$	407	402	0.43	He	CO 3.0	[illegible] / [illegible]	1%	X	X	X	3.2	IV-36	
"	24b	$FeO + NO + H_2O \rightarrow NH_3, N_2$	372	174	0.45	"	NO [illegible], H_2O 11	" / [illegible]	X	—	—	X	"	IV-16	
"	24c	$FeO + H_2S \longrightarrow FeS + H_2O$	371	204	"	"	H_2S 2.1	" / [illegible]	X	73%	X	X	"	IV-5	
"	24d	$NO + H_2O + FeS \rightarrow NH_3, N_2$	373	354	"	"	NO [illegible], H_2O [illegible]	" " / [illegible]	X	—	21%	X	"	IV-15	
"	24e	$FeO + H_2S \longrightarrow FeS + H_2O$	"	144	"	"	H_2S 2.0	" " / [illegible]	X	34%	X	X	"	IV-3	
"	24f	$NO + CO + H_2O + FeS$	"	214	0.44	"	NO 0.44, CO 0.40, H_2O [illegible]	" " / [illegible]	7%	—	X	X	"	IV-16	Noted ppt.
"	24g	$FeS + O_2 + H_2O$	105	240	0.88	"	O_2 21, N_2 79	— / —	X	—	X	—	"		

EXPERIMENTAL SUMMARY

DATE	RUN	REACTION	CONDITIONS FOR RUN: T (°C)	Bed Vol.	Bed Wt.	Diluent	Inlet Gas Conc. (%)	SOLID Initial / Final	OVRL. MAT. BALANCE: C	H	N	Surface	PARTICLE SIZE (mm)	REF. FIG. IN TEXT	COMMENTS
[illegible]	25a	$Fe_2O_3+H_2+H_2S+CO+NO+O_2+H_2O$	368	290	0.45	He	O_2 .33, NO .51, CO 11, H_2S [illegible], H_2O [illegible], H_2 11	Fe_2O_3 / [illegible]	8.8%	16%	—	X	.32	IV-22	Noted ppt
"	25b	"	374	165	"	"	.42 .51 1.4 .31 1.4 1.3	" / [illegible]	10.9%	3%	—	X	"	"	" "
"	25c	"	"	163	"	"	.45 .51 1.1 .20 1.4 1.1	" / [illegible]	8.5%	—	—	4.4%	"		" "
[illegible]	26a	$Fe_2O_3+H_2+SO_2+CO+NO+O_2+H_2O$	368	242	0.45	He	O_2 1.0, NO .05, CO 2.3, SO_2 [illegible], H_2O 4.9, H_2 [illegible]	[illegible] / [illegible]	2.3%	—	—	X	.32	IV-28	
"	26b	"	"	172	"	"	" " " 1.0 " "	" / [illegible]	3.4%	—	—	X	"		
"	26c	"	374	300	"	"	" " .39 " " 3.6	" / [illegible]	5.5%	—	—	7.4%	"	IV-33	
[illegible]	27a	$Fe_2O_3+H_2+CO+SO_2+O_2+NO+H_2O$	379	293		He	CO [illegible], H_2 [illegible], SO_2 [illegible], NO [illegible], H_2O 1.4, O_2 2.0	[illegible] / [illegible]	2.3%	—	—	X	.32	IV-33	
"	27b	$CO+FeS_xO_y$	374	240		"	CO 4.1	" / [illegible]	—	X	X	X	"		
"	27c	$CO+H_2+FeS_xO_y$	"	110	0.43	"	CO 4.0, H_2 3.9	" / [illegible]	—	—	X	X	"		
"	27d	$CO+H_2+SO_2+FeS_xO_y$	"	90	"	"	CO [illegible], H_2 3.9, SO_2 .45	" / [illegible]	9.3%	10%	X	X	"	IV-8	
"	27e	$CO+H_2+SO_2+NO+FeS_xO_y$	"	98	"	"	CO [illegible], H_2 3.9, SO_2 .45, NO .31	" / [illegible]	9.7%	20%	—	X	"	IV-31, IV-21	
"	27f	$CO+H_2+SO_2+NO+H_2O+FeS_xO_y$	"	189	"	"	CO [illegible], H_2 [illegible], SO_2 .44, NO .58, H_2O 1.0	" / [illegible]	8.5%	45%	99%	X	"	"	
"	27g	$CO+H_2+SO_2+NO+H_2O+O_2+FeS_xO_y$	379	202		"	CO [illegible], H_2 [illegible], SO_2 .44, H_2 [illegible], H_2O [illegible], O_2 1.5	" / [illegible]	13.8%	17.4%	2.7%	23%	"	IV-33	
[illegible]	28a	$SO_2+CO+H_2+H_2O$	957	40		He	SO_2 .52, CO 1.9, H_2 1.6, H_2O 1.9	No Catalyst	—	—	X	X	1.3 Catalyst	IV-11	
"	28b	"	1094	174 / 105		"	.50 1.6 1.6 1.5	" "	8.2%	21%	X	X	"	"	Noted ppt
"	28c	"	1174	62		"	.52 1.7 1.6 1.9	" "	—	—	X	X	"	"	"
"	28d	"	1260	75		"	.52 1.3 1.6 1.5	" "	—	—	X	X	"	"	"

EXPERIMENTAL SUMMARY

DATE	RUN	REACTION	CONDITIONS FOR RUN: T (K)	Run time (min)	P (kPa)	Diluent	Inlet gas conc (%)	SOLID: Initial / Final	OVRL. MAT. BALANCE: C	H	N	Surface	PARTICLE SIZE (nm)	REF. FIG. IN TEXT	COMMENTS
9/1–8/73	29a	$Fe_2O_3 + CO \rightarrow FeO, Fe_3O_4$	374	[illegible]	0.45	He	[illegible]	$FeO_{1.5}$ / $FeO_{1.13}$	3.6%	X	X	X	3.2		
"	29b	$FeO + CO + O_2 + NO + SO_2 + H_2O$	"	194	0.44	"	O_2 1.0, NO .99, CO 4.1, SO_2 .81, H_2O 1.11	"	9.8% (29b–29c)	8.6% (29b–29c)	—	X	"	IV-34	
"	29c	" " " " " "	"	215	"	"	1.0, .83, 4.6, .60, 2.1(?)	$FeO_{1.13}$ [illegible]			—	227%	"	IV-35	
9/11–11/73	30a	$Fe_2O_3 + CO \rightarrow Fe_3O_4, FeO$	370	98	0.29	He	CO 0.8	$FeO_{1.5}$	12%	X	X	X	.25–50	IV-36	
"	30b	" " " "	"	108	"	"	CO 5.0	$FeO_{1.18}$	15%	X	X	X	"		
"	30c	$FeO + CO + O_2 + NO + SO_2 + H_2O$	"	350	0.28	"	O_2 1.1, NO .41, CO 4.93, SO_2 .48, H_2O .9–1.2	" / $FeO_{1.1}S_{.19}$	3%	—	2.8%	15%	"	IV-33, IV-25	All pellets red
10/13/73	31a	$Fe_2O_3 + CO \rightarrow Fe_3O_4, FeO$	538	49	0.35	He	CO 7.9	$FeO_{1.5}$ / $FeO_{1.18}$	0.5%	X	X	X	3.2	IV-36	
"	31b	$FeO + CO + O_2 + NO + SO_2 + H_2O$	"	460	"	"	O_2 .60, NO .58, CO 4.4, SO_2 .15, H_2O very	" / $FeO_{1.0}$	4.2%	—	3.7%	13%	"	IV-24	All pellets black
10/11/73	32.	$NO + CO \rightarrow N_2, NH_3$	379	208	0.41	He	CO 1.0, NO 0.89		7.4%	X	—	>300%	3.2	IV-2	A slight amount of H_2O present
10/10/73	33a	$2CuO + CO \rightarrow Cu_2O + CO_2$	535	40	0.55	He	CO 3.0	CuO / $CuO_{.19}$	1%	X	X	X	3.2		
"	33b	$Cu_2O + O_2 + H_2O + SO_2 + CO + NO$	"	257	0.53	"	O_2 0.5, NO 0.5, CO 4.3, SO_2 0.8, H_2O 1.9	" / $CuS_{.53}$	5.4%	19%	22%	38%	"	IV-34	Noted ppt
11/4/73	34a	$Al_2O_3(H_2O) + CO$	560	60	0.53	He	CO 8.0	Al_2O_3 / Al_2O_3	—	X	X	X	3.2		
"	34b	$Al_2O_3 + CO + NO + SO_2 + O_2 + H_2O$	"	230	0.51	"	O_2 .48, NO .48, CO 4.0, SO_2 .54, H_2O 1.9	" / $Al_2O_3S_{.01}$	34%	—	6%	53%	"		
11/14/73	35a	$Fe_2O_3 + CO \rightarrow Fe_3O_4, FeO$	538	44	0.34	He	CO 3.0	$FeO_{1.5}$ / $FeO_{1.17}$	6.8%	X	X	X	3.2	IV-36	
"	35b	$FeO + CO + O_2 + NO + SO_2 + H_2O$	"	536	"	"	O_2 .49, NO .60, CO 3.4, SO_2 .48, H_2O 1.5	" / $FeS_{.14}$	9.0%	1.3%	13%	67%	"	IV-37, IV-33	

EXPERIMENTAL SUMMARY

DATE	RUN	REACTION	CONDITIONS FOR RUN: T (°C)	Run Time (min)	Age (secs)	Diluent	Inlet Gas Conc (%)	SOLID: Initial / Final	OVRL. MAT. BALANCE: C	H	N	Surface	PARTICLE SIZE (µm)	REF. FIG. IN TEXT	COMMENTS
11/20/73	36a	$Fe_2O_3 + CO \rightarrow Fe_3O_4, FeO$	538	64	0.15	He	CO .48	FeO1.5 / FeO1.14	70%	X	X	X	.25–.50		6.4 mm reactor
"	36b	$FeO + CO + O_2 + NO + SO_2 + H_2O$	"	225	0.054	"	O2 NO CO SO2 H2O / .45 .50 .66 .60 1.5	" / FeS[illegible]	16%	—	6.4%	270%	"	IV-18, IV-33	" "
11/19/73	37a	$Fe_2O_3 + CO \rightarrow Fe_3O_4, FeO$	370 to 538	72	0.011 to 0.011	He	CO 0.18	FeO1.5 / FeO1.39	—	X	X	X	.25–.50		6.4 mm reactor
"	37b	$FeO + CO + O_2 + NO + SO_2 + H_2O$	"	435	0.051	"	O2 NO CO SO2 H2O / .13-.18 .49 1.8 .5 1.5	" / FeO[illegible]S[illegible]	11%	13%	14%	79%	"	IV-29, IV-30, IV-33	" "
12/8-10/73	38a	$Fe_2O_3 + CO \rightarrow Fe_3O_4, FeO$	538	61	0.022	He	CO .38	FeO1.5 / FeO1.30	—	X	X	X	.25–.50	IV-37	6.4 mm reactor
"	38b	$FeO + CO + O_2 + NO + SO_2 + H_2O$	"	1446	"	"	O2 NO CO SO2 H2O / 1.0 .83 [illegible] .54 1.3	" / —	—	—	—	—	"		" "
11/16/73	39a	$Fe_2O_3 + CO \rightarrow Fe_3O_4, FeO$	560	25	0.040	He	CO .44	FeO1.5 / FeO1.11	5%	X	X	X	.25–.50	IV-37	9.5 mm reactor
"	39b	$FeO + CO + O_2 + NO + SO_2 + H_2O$	"	75	"	"	O2 NO CO SO2 H2O / 1.0 .49 5.5 .56 1.3	" / FeO[illegible]S[illegible]	9%	20%	8%	X	"	IV-31	" "
"	39c	$FeS + O_2 \rightarrow FeO_x, SO_2$	671	66	0.038	"	O2 4.0	" " / FeO[illegible]	X	X	X	X	"	"	" "
"	39d	$FeO + CO + O_2 + NO + SO_2 + H_2O$	560	74	0.040	"	O2 NO CO SO2 H2O / 1.0 .49 5.5 .50 1.3	" / FeO[illegible]S[illegible]	15%	9.6%	13%	X	"	IV-[illegible], IV-35	" "
"	39e	$FeS + O_2 \rightarrow FeO_x, SO_2$	671	129	0.038	"	O2 4.0	" " / FeO[illegible]	X	X	X	X	"	IV-31	" "
"	39f	$FeO + CO + O_2 + NO + SO_2 + H_2O$	560	76	0.040	"	O2 NO CO SO2 H2O / 1.0 .49 5.5 .54 1.3	" / FeO[illegible]S[illegible]	34%	28%	19%	X	"	"	" "
"	39g	$FeS + O_2 \rightarrow FeO_x, SO_2$	671	55	0.038	"	O2 21.0	" " / FeO1.5	X	X	X	X	"	"	" "
"	39h	$FeO + CO + O_2 + NO + SO_2 + H_2O$	560	63	0.040	"	O2 NO CO SO2 H2O / 1.0 .49 5.5 .86 1.3	" / FeO[illegible]S[illegible]	1.5%	14%	14%	300%	"	"	" "
1/6/74	40a	$Fe_2O_3 + CO \rightarrow Fe_3O_4, FeO$	565	27	0.040	He	CO 1.0	FeO1.5 / FeO1.13	36%	X	X	X	.25–.50	IV-37	9.5 mm reactor
"	40b	$FeO + CO + O_2 + NO + SO_2 + H_2O$	600	72	0.038	"	O2 NO CO SO2 H2O / 1.0 .53 5.6 .63 1.3	" / FeO[illegible]S[illegible]	—	—	20%	X	"	IV-33, IV-32	"
"	40c	$FeSO_4 \rightarrow FeO_x, SO_2$	670	60 "	0.018 0.011	" "	No other gases " " "	— / —	X	X	X	X	"	IV-52	" Black pellets Red pellets
"	40d	$FeS + O_2 \rightarrow FeO_x, SO_2$	694	" "	[illegible]	"	O2 - 1.0 " "	FeO[illegible] / FeO[illegible]	X	X	X	X	"	"	" Black pellets Red pellets

EXPERIMENTAL SUMMARY

DATE	RUN	REACTION	CONDITIONS FOR RUN: T (°C)	Run Time (min)	W/F	Diluent	Inlet Gas Conc (%)	SOLID Initial / Final	OVR. MAT. BALANCE: C	H	N	Surface	PARTICLE SIZE (mm)	REF. FIG. in Text	COMMENTS
1/4/79	40c	$FeO + CO + O_2 + NO + SO_2 + H_2O$	600	70	0.038	He	O_2 1.0, NO .85, CO 9.6, SO_2 .65, H_2O 1.9	$FeO_{1.5}$ / $FeO_{1.0}S_{1.0}$	—	—	96%	X	.35–.50	IV-31	9.5mm reactor
"	40f	$FeSO_4 \rightarrow FeO_x, SO_2$	670	56 / 60	0.018 / 0.012	" / "	No other gases / " " "	— / —	X	X	X	—	"	"	" Wash pellets / Red pellets
"	40g	$FeS + O_2 \rightarrow FeO_x, SO_2$	695	60 / 60	0.018 / 0.012	" / "	O_2 = 1.0 / " "	$FeO_{1.5}$ / $FeO_{1.5}$	X	X	X	—	"	"	" " " / " "
1/8/79	41a	$NiO + Fe_2O_3 + CO$	560	28	0.045	He	CO 1.0	NiO/$FeO_{1.5}$ / 45% O removed	5%	X	X	X	.35–.50		9.5mm reactor
"	41b	$Ni + FeO + O_2 + H_2O + SO_2 + CO + NO$	600	66	"	"	O_2 1.0, NO .85, CO 9.6, SO_2 .68, H_2O 1.9	—	—	—	11%	X	"	IV-35	"
"	41c	$NiSO_4 + FeSO_4 \rightarrow Fe_2O_3 + NiO + SO_2$	670	60 / 60	0.018 / 0.010	" / "	No other gases / " " "	—	X	X	X	X	"	"	"
"	41d	$NiS + FeS + O_2 \rightarrow Fe_2O_3 + NiO + SO_2$	695	64 / 60	0.018 / 0.020	" / "	O_2 = 1.0 / " "	—	X	X	X	X	"	"	"
"	41e	$NiO + FeO + O_2 + H_2O + SO_2 + CO + NO$	600	69	0.045	"	O_2 1.0, NO .85, CO 9.8, SO_2 .68, H_2O 1.9	—			18%	X	"	"	"
"	41f	$NiSO_4 + FeSO_4 \rightarrow Fe_2O_3 + NiO + SO_2$	670	60 / 60	0.018 / 0.010	" / "	No other gases / " " "	—	X	X	X	—	"	"	" Ni pellets / Fe pellets
"	41g	$NiS + FeS + O_2 \rightarrow Fe_2O_3 + NiO + SO_2$	695	60 / 60	0.018 / 0.010	" / "	O_2 = 1.0 / " "	—	X	X	X	—	"	"	" Ni pellets / Fe pellets
1/15/79	42a	$Fe_2O_3 + CO \rightarrow Fe_3O_4, FeO$	570	56 / 19	0.045 / "	He	CO = 1.0 / CO = 0.8	$FeO_{1.5}$ / $FeO_{1.??}$	6.3%	X	X	X	.35–.50	IV-57	9.5mm reactor
"	42b	$H_2O + CO \rightarrow H_2 + CO_2$	"	84	"	"	CO 0.8, H_2O 1.9	" / $FeO_{1.33}$	8.6%	—	X	X	"	IV-40	" "
"	42c	$FeO + 3CO + SO_2 \rightarrow FeS + 3CO_2$	"	123	"	"	CO 1.8, CO_2 0.85	" / $FeS_{1.1}$	—	X	X	X	"	IV-41	" "
"	42d	$H_2O + CO \rightarrow H_2 + CO_2$	"	69	"	"	CO 0.8, H_2O 1.9	" / "	10.9%		X	X	"	IV-40	" "
"	42e	$FeS + O_2 \rightarrow Fe_2O_3, SO_2$	695	65	0.039	"	O_2 1.9	—	X	X	X	—	"		" "
"	42f	" " " "	"	210	"	"	" / "	—	X	X	X	—	"		" "

APPENDIX A-2

Overall Reaction Rate Analysis

A. Kinetic Rate:
(Levenspiel, 1962)

1. Assumptions: First-order reaction kinetics.

Effectiveness factor can account for effect of intraparticle diffusion.

2. Rate per unit volume of catalyst/absorbent (p. 446):

$$(1/V_p z)(dN_a/dt) = - k_r \eta C_{as}$$

where: V_p = specific volume (cm^3/g).

z = amount of catalyst (g).

N_a = moles of reactant A (g moles).

t = time (sec).

k_r = reaction rate constant (sec^{-1}).

η = effectiveness factor (dimensionless).

C_{as} = gas concentration at exterior surface of solid (g moles/cm^3).

3. Since the reactor volume is a more useful quantification than the amount of catalyst, z, the relationship: $V = z/\rho_B$ is used to eliminate z. Where: V = reactor volume (cm^3).
ρ_B = solids density in the contactor (g/cm^3).

Therefore: $(1/V)(dN_a/dt) = - \rho_B V_p k_r \eta C_{as}$ (A2-1)

B. External Mass Transfer:
(Levenspiel, 1962)

The value of C_{as} in the above equation may differ from C_{ag}, bulk concentration since there may be gas-film resistance. The relationship given on p. 445 (Levenspiel):

$$(-1/S_{ex})(dN_a/dt) = k_m(C_{ag} - C_{as}) \qquad (A2-2)$$

assumes: Linear concentration gradients.

No interaction of diffusing species.

In this expression: S_{ex} = external particle surface area (cm^2/g).

k_m = mass transfer coefficient (cm/sec).

C. Overall Rate:
(Levenspiel, 1962)

Since the kinetics and mass transfer rates are in series they can be combined as follows:

kinetic: $[1/(VV_p\rho_B k_r \eta)]\ (dN_a/dt) = - C_{as}$

mass transfer: $[1/(S_{ex} k_m z)]\ (dN_a/dt) = - (C_{ag} - C_{as})$

overall: $r_a = (dN_a/dt)\,[1/(VV_p\rho_B k_r \eta) + 1/(S_{ex} k_m z)] = - C_{ag}$

where: r_a = overall rate (g moles/cm^3-sec).

Substituting the relationship for V to eliminate z, the expression becomes:

$$r_a = (1/V)\ (dN_a/dt)\,[1/(V_p\rho_B k_r \eta) + 1/(\rho_B S_{ex} k_m)] = - C_{ag}$$

$$r_a = (1/V)\ (dN_a/dt) = - (1/V_p k_r \eta + 1/S_{ex} k_m) C_{ag} \rho_B \qquad \text{(A2-3)}$$

$$K_1 = (1/V_p k_r \eta + 1/S_{ex} k_m)^{-1}.$$

Then: $$r_a = (1/V)\ (dN_a/dt) = - K_1 \rho_B C_{ag}. \qquad \text{(A2-4)}$$

D. Packed-Bed Reactor Equation:
(Levenspiel, 1962)

1. Levenspiel presents the analysis of a differential section of a packed-bed reactor as: $F_{ao}\, dX_a = (-r_a)\, dV$

Where: F_{ao} = inlet rate of reactant (g moles/sec).

X_a = fractional conversion of reactant (dimensionless).

C_{ag} can be eliminated in equation (A2-4) by the relationship:

$$C_{ag} = C_{ago}\,(1 - X_a)$$

where: C_{ago} = inlet gas concentration (g moles/cm^3).

Then: $F_{ao}\, dX_a = K_1 C_{ago} (1-X_a)\rho_B dV.$ (A2-5)

2. The above equation is now integrated over the entire reactor volume.

$$\int_0^{X_a} \frac{dX_a}{(1-X_a)} = \int_0^{V} \frac{\rho_B K_1 C_{ago}}{F_{ao}}\, dV$$

$$1 - X_a = \exp\left[- \frac{C_{ago} V}{F_{ao}} K_1 \rho_B\right]$$

Since the residence time $\theta = C_{ago} V / F_{ao}$

$$C_{ag}/C_{ago} = \exp[-K_1 \theta \rho_B] \quad \text{(A2-6)}$$

APPENDIX A-3

Regeneration-Rate Analysis

A. The main regeneration reaction is:

$$FeS + 7/4\ O_2 \longrightarrow 1/2\ Fe_2O_3 + SO_2$$

Guha (1972) presented an equation representing the oxidation of FeS_2.

The development here is analogous to his work.

1. Assumptions: First-order reaction.

   Mass transfer resistance in bulk fluid is negligible.

2. Rate of particle oxidation can be given as:

$$(-1/4\pi a^2)\ (dW_m/dt) = (7/4)\ (1-\epsilon')\ K_2\ C_{ago} \qquad (A3-1)$$

where: a = radius of particle at FeS/Fe_2O_3 interface. (cm).

W_m = molal amount of FeS. (g moles FeS)

t = time (sec)

$1-\epsilon'$ = volume FeS/volume particle ($cm^3 FeS/cm^3$ particle).

K_2 = overall reaction coefficient (cm/sec).

C_{ago} = $)_2$ bulk concentration (g moles/cm^3).

The factor 7/4 is the stoichiometric coefficient. With a redefinition of K_2 this could be incorporated into K_2.

3. The molal amount of FeS, W_m, can be expressed as a volume times a density:

$$dW_m/dt = d(4/3\pi a^3 \rho_{sm})/dt = 4\pi a^2 \rho_{sm}\, da/dt$$

where: ρ_{sm} = molal density of FeS (g moles/cm^3).

Equation (A3-1) can thus be expanded as:

$$-\rho_{sm} da/dt = (7/4)\,(1-\epsilon')\,K_2\,C_{ago}.$$

Separating variables:

$$da = -\,7/4\,(1-\epsilon')\,(1/\rho_{sm})\,K_2\,C_{ago})\,dt.$$

Integrating from the outer surface a = r, t = 0 to the center a = 0,

t = t, where r is the particle radius.

$$a - r = (-7/4)\,(1-\epsilon')\,(K_2/\rho_{sm})\,C_{ago}\,t. \qquad \text{(A3-2)}$$

4. The percent solid reacted is $100[(r^3-a^3)/r^3] = 100[1-(a/r)^3]$.

Combining with (A3-2);

$$\%\ \text{solid reacted} = 100\left\{1-[r-7/4\,(1-\epsilon')(K_2/\rho_{sm})C_{ago}t]^3/r^3\right\}$$

(A3-3)

5. The required time for a given % solid reacted is then:

$$t = r[1-(1-\%\ \text{solid reacted}/100)^{1/3}]\,/[7/4(1-\epsilon')(K_2/\rho_{cm})C_{ago}]$$

(A3-4)

APPENDIX A-4

Design Bases - 1000-Mw Power Plant

1. Furnace- Pulverized coal, tangentially fired.

   a. Coal Analysis:

	wgt fraction	
Carbon (C)	0.7220	
Hydrogen (H)	0.0476	
Oxygen (O)	0.0615	
Nitrogen (N)	0.0149	
Sulfur (S)	0.0300	
Water H_2O	0.0347	
Ash	0.0893	(Steam, 1963)

   b. Ten percent excess air at 60% relative humidity.

   c. Power plant efficiency 38.9% (Robinson, 1970).

   d. Twenty percent fuel N converted to NO.

   e. Thermally formed NO is 20% of total NO.

   f. Ash - 15% bottoms and 85% flyash.

2. Gasifier- chain grate stoker.

   a. Coal analysis: same as in furnace.

   b. Stoichiometric air for conversion of all carbon to CO and sulfur to SO_2; 60% relative humidity in inlet air.

   c. Twenty percent fuel N converted to NO.

   d. No NO is formed thermally.

   e. Ash - 85% bottoms and 15% flyash.

3. Total flue gas.

   a. Ninety-five percent of the excess O_2 removed when CO/H_2 added.

   b. Inlet temperature to superheaters 1260°C (2300°F).

4. Contactor.

   a. Ninety percent removal of excess ($CO + H_2$), SO_2, NO.

   b. Eighty-five percent of SO_2 removed as S^{-2}.

   c. Fifteen percent of SO_2 removed as SO_4^{-2}.

   d. Removal reactions occur at 1000°F.

   e. Twenty-five percent of solids stream leaving contact sent to regenerator; 75% is recycled.

   f. Ten percent excess Fe_2O_3 in solids feed to contactor from regenerator.

   g. Composition and properties of catalyst/absorbent:

      20% Fe_2O_3, 80% ($Al_2O_3 + SiO_2$), $S_v = 200\ m^2/g$, $V_p = 0.67 cm^3/g$.

5. Regenerator.

   a. All inlet iron converted to Fe_2O_3.

   b. Regeneration reactions occur at 1250°F.

6. Solids Collectors.

   a. Contactor Cyclones and Electrostatic Precipitator for main flue gas.

	Collection Efficiency (%)		
	Cyclones	ESP	Overall
Flyash	97	95	99.85
Cat./Abs.	99.9696	95	99.9980

(Solids collected in ESP are sent to the regenerator while those collected in the cyclones are sent to the contactor (75%) or to the regenerator (25%).

b. Regenerator Cyclones.

	Collection Efficiency (%)		
	Primary	Secondary	Overall
Flyash	0	90	90
Cat./Abs.	99.933	100	100

(Solids collected in the primary cyclones are sent to the contactor while those collected in the secondary cyclones are sent to ash disposal)

c. Regenerator ESP. This unit collects 95% of the inlet flyash.

APPENDIX A-5

Heat effects in the removal and regeneration reactions.

	REACTIONS	ΔH 25° C (kcal)
1.	$2\,NO + 2\,CO \rightarrow N_2 + 2\,CO_2$	-89.23
2.	$2\,NO + 2\,H_2 \rightarrow N_2 + 2\,H_2O$	-79.40
3.	$2\,NO + 3\,H_2O + 5\,CO \rightarrow 2\,NH_3 + 5\,CO_2$	-230.10
4.	$NO + 5/2\,H_2 \rightarrow NH_3 + H_2O$	-90.40
5.	$FeO + SO_2 + 3\,CO \rightarrow FeS + 3CO_2$	-90.90
6.	$FeO + SO_2 + 3\,H_2 \rightarrow FeS + 3H_2O$	-61.36
7.	$FeO + H_2S \rightarrow FeS + H_2O$	-11.91
8.	$Fe_2O_3 + CO \rightarrow 2\,FeO + CO_2$	+ 1.57
9.	$Fe_2O_3 + H_2 \rightarrow 2\,FeO + H_2O$	+11.40
10.	$FeO + SO_2 + \frac{1}{2}\,O_2 \rightarrow FeSO_4$	-85.40
11.	$CO + H_2O \rightarrow H_2 + CO_2$	- 9.83
12.	$CO + \frac{1}{2}\,O_2 \rightarrow CO_2$	-67.64
13.	$H_2 + \frac{1}{2}\,O_2 \rightarrow H_2O$	-57.80
14.	$2\,FeS + 7/2\,O_2 \rightarrow Fe_2O_3 + 2SO_2$	-243.30
15.	$2\,FeO + \frac{1}{2}\,O_2 \rightarrow Fe_2O_3$	-69.21
16.	$2\,FeSO_4 \rightarrow Fe_2O_3 + SO_2 + SO_3$	-78.-